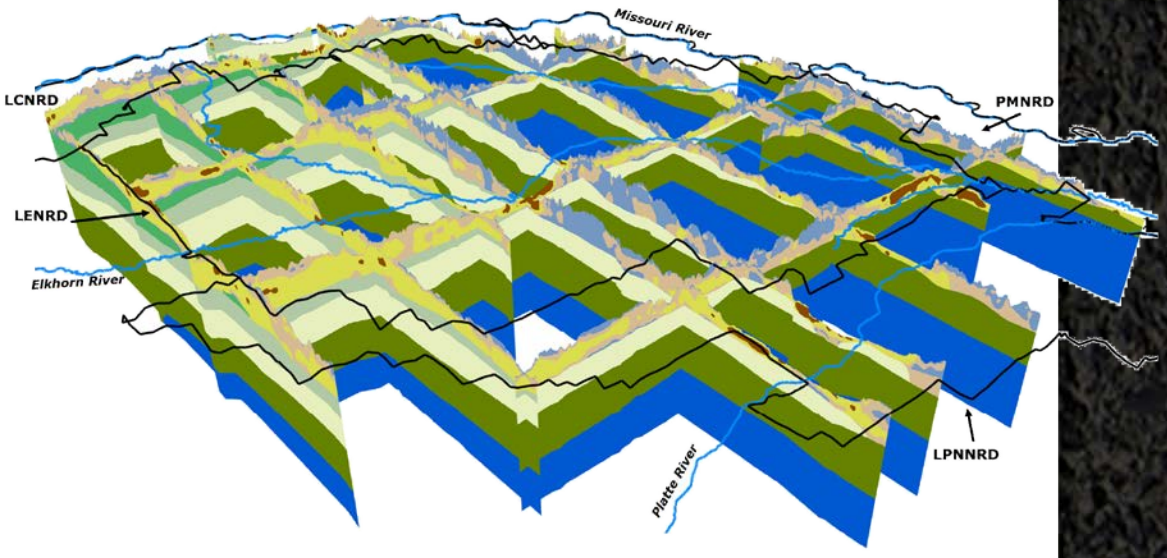
Final Report on Airborne Electromagnetic Geophysical Surveys and Hydrogeologic Framework Development for the Eastern Nebraska Water Resources Assessment

Volume I – Including the Lewis & Clark, Lower Elkhorn, and Papio-Missouri Natural Resources Districts



Prepared for:

Eastern Nebraska Water Resources Assessment
3125 Portia Street
Lincoln, NE 68521

July 20, 2015

EXPLORATION RESOURCES INTERNATIONAL

July 20, 2015

Final Report on Airborne Electromagnetic Geophysical Surveys and Hydrogeologic Framework Development for the Eastern Nebraska Water Resources Assessment – Volume I, including the Lewis and Clark, Lower Elkhorn, and Papio-Missouri River Natural Resources Districts

Prepared for:
Eastern Nebraska Water Resources Assessment

Submitted by:
Exploration Resources International Geophysics, LLC
6207 Hwy 80 East
Vicksburg, MS 39180
Phone: (866) 974-6867

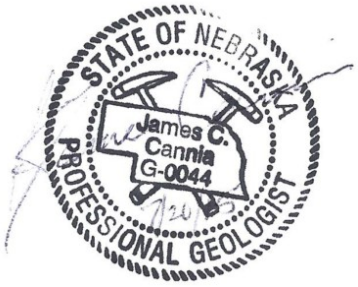
Clint P. Carney, P.G.
Clint.Carney@xrigeo.com

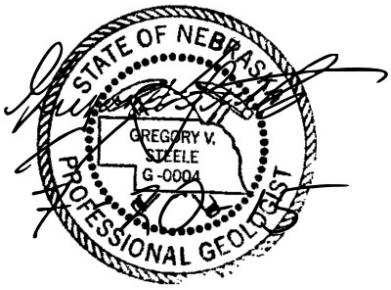
Jared D. Abraham
Jared.Abraham@xrigeo.com

James C. Cannia, P.G.
Jim.Cannia@xrigeo.com

Gregory V. Steele, P.G.
Greg.Steele@xrigeo.com







Executive Summary

Exploration Resources International (XRI) is pleased to submit our report to the Eastern Nebraska Water Resources Assessment (ENWRA) titled "*Final Report on Airborne Electromagnetic Geophysical Surveys and Hydrogeologic Framework Development for the Eastern Nebraska Water Resources Assessment - Volume I, including the Lewis and Clark, Lower Elkhorn, and Papio-Missouri River Natural Resources Districts.*" The final report of this investigation is separated into two volumes. Volume I describes the methods, background information, and findings of the airborne survey conducted in the Fall of 2014 that covered approximately the northern half of the ENWRA area, and included the Lewis and Clark, Lower Elkhorn, and Papio-Missouri River Natural Resources Districts. Volume II describes the methods, background information, and findings from the Spring 2015 airborne survey that covered the southern half of the ENWRA area, including the Lower Platte North, Lower Platte South, and Nemaha Natural Resources Districts. This project was conducted to address ENWRA's water resource concerns by completing reconnaissance flight lines in the glacial terrain of eastern Nebraska. This hydrogeologically complex area has undergone increased groundwater development in recent years which prompted ENWRA to seek additional information on the aquifers underlying the region. XRI entered into an agreement with ENWRA to undertake this study on September 15, 2014.

The scope of work for this project was as follows:

1. SCOPE OF WORK

1.1 An Airborne Electromagnetic (AEM) survey was flown in 2 phases over a specified area in eastern, NE within the ENWRA area to support creation of a regional hydrogeological framework of this area. This framework will be provided both as preliminary AEM data and as a final product in an Interpretative Report. Approximately 1,298 line miles of AEM and magnetic data will be collected in the two (2) phases.

1.2 Phase 1 commenced on Oct. 11, 2014. The Contractor entered into a contract with a subcontractor to fly 750 line miles over the specified area of the ENWRA to obtain the data for Phase 1 of the Survey, which was then used by XRI to provide the hydrogeological framework contained in the interim report presented on April 9, 2015. XRI provided status reports to the ENWRA group, concerning the progress of the flights on a daily basis including the areas flown, production rates, and flight plan for the following day. The ENWRA group was updated on a regular basis on progress of the interim report.

1.3 XRI contracted with a subcontractor to fly approximately 550 flight miles over the specified area of the ENWRA to obtain the data for Phase 2 of the Survey, which was then used by XRI to provide the hydrogeological framework for the Interpretative Report for the Phase 2 area. XRI provided status reports to the ENWRA concerning the progress of the flights on a daily basis which included the areas flown, production rates, and flight plan for the following day. The ENWRA group was updated on a regular basis on progress of the interim report.

1.4 XRI processed and performed quality assure and quality control protocols on all of the

data collected from the Survey and ground system.

1.5 XRI inverted the AEM data and derived a 3D electrical model of the surveyed area. These inverted georeferenced data will be delivered to the ENWRA and incorporated into the Interpretative Report.

1.6 XRI shall provide an Interpretative Report that will include locations of aquifer(s), and a hydrogeologic framework that includes the AEM relationship to geologic test holes, as well as delineation of potential recharge areas along two-dimensional profiles ("the Data Report'). The Interpretative Report will also include all data and metadata files and will be delivered to the ENWRA in PDF digital format.

1.7 XRI subcontracted with a qualified aircraft company to complete the flights of the area in order to acquire the data necessary to complete the Survey, the cost of which is included in the Compensation provided for below.

2. SCHEDULE

2.1 Upon completion of data acquisition of each phase of the Survey, XRI began the geophysical processing, including numerical inversions to create a preliminary and final datasets to be shared with the ENWRA.

2.2 Post geophysical processing, XRI began development of the hydrogeologic framework. At times during its development, XRI interacted with ENWRA staff to keep the ENWRA group apprised of progress. After completion of the framework for Phase 1, an interim Interpretative Report was produced and delivered to the ENWRA on April 9, 2015 (Completion of Phase 1). The final Interpretative Report for both phases will be delivered no later than July 30, 2015 (Completion of Phase 2).

For organizational purposes, this report (Volume I) formally discusses the findings of the AEM survey for the LCNRD, LENRD, and the PMRNRD, although some inclusion of the Lower Platte North (LPNNRD) occurs due to the southern extent of the phase I flight lines. A small portion of the flight lines in the PMRNRD were collected in the Spring 2015 survey and are included in Volume I. Volume II of this report includes the assessments of the LPNNRD, as well as the Lower Platte South and Nemaha NRDs.

As summarized above, the AEM data for Phase 1 of the project were successfully collected on October 11-19, 2014, including all quality control, quality assurance, and initial inversions of the data. In total, 889 line-miles of data were collected during Phase 1 of the survey. All contracted activities within the scope and schedule of work were met or exceeded.

Interpretation of the AEM data collected in 2014 provides a subsurface characterization of the principal aquifer that correlated with pre-existing geologic information. The AEM provided detailed verification and quantification of the geology that underlies the flight lines within the project area and also provided an improved understanding of the glacial and bedrock features present in the subsurface. Lithologic descriptions from test holes (University of Nebraska-Conservation and Survey Division) and oil and gas records (Nebraska Oil and Gas Conservation Commission) provided useful historical information in the

development of the new hydrogeologic framework. Additional supporting data included historic cross sections and a limited number of geophysical logs from the Conservation and Survey Division.

The nature of the AEM reconnaissance line flight pattern (i.e. a large distance between flight lines) limits the analysis of the subsurface to two-dimensional (2D) sections along the flight lines, which results in an insufficient amount of information that is required for estimation of aquifer volumes or the amount of groundwater in storage provided from this survey. However, the 2D sections do provide the location, orientation, groundwater levels (from the 1995 CSD water table map), and connectivity between the deposits comprising the principal aquifer and the local streams that were crossed by flight lines in the project area. Also revealed in the hydrogeologic framework are locations at the land surface where the potential for recharge to the principal aquifer along the flight is likely the greatest. The 2D sections of the glacial till and loess areas provide limited insight into the confined and unconfined nature of the groundwater system and where water quality management could be impacted by the presence or absence of these materials.

Within the project area, the principal aquifer is made up of Quaternary deposits and the underlying Tertiary Ogallala Group. Often aquifer materials of these formations are in hydrogeologic connection with each other. Within the Quaternary deposits and the Tertiary Ogallala Group, the aquifer materials were divided into marginal and principal aquifer materials, with a third subcategory of the principal materials defined as coarse, sand-rich intervals that displayed the highest resistivities of all Quaternary materials detected in the AEM survey. These aquifer material types were located mostly in the western and southern thirds of the project area. The marginal aquifer is the predominant groundwater source in the eastern one-third of the project area. Aquitard materials occur mostly in the central and eastern extents of the project area. Potential Cretaceous Dakota Formation bedrock aquifers are detected only as areas of high resistivity because of limited test hole information available in the area. This lack of supporting information limits the ability to fully characterize aquifer conditions based on resistivity values alone. Paleozoic strata are detected in the AEM survey, but minimal information on water quality and test hole logs again limited conclusive hydrogeologic and stratigraphic interpretation on these units. In the LENRD, brackish and saline groundwaters are known to exist in the bedrock strata. While these groundwater types can be mapped by AEM methods, there are limited historical data or new supporting data available to confirm that these waters are present beneath the project area. The body and appendices of this report contain the information used in the AEM interpretation and development of the hydrogeologic framework for the Phase 1 areas.

Key findings include:

1) Aquifer resources beneath the survey area vary considerably within the Quaternary and Tertiary system, with most of the extensive principal aquifer materials located in the western half of the northern ENWRA project area and beneath the valleys of the major surface water drainages.

2) LCNRD - The aquifer resources beneath the LCNRD vary from thick sequences of principal and marginal aquifer materials beneath the western half of the district to minimal thickness in Quaternary deposits mantled atop Cretaceous bedrock in the north-central section of the district. Beneath the

western half of the district is a continuous body of principal aquifer material interlayered with marginal aquifer material that sit atop basal aquitard material. The surficial deposits in this area range from 150 ft thick sequences of aquitard material to marginal aquifer material. In the south central area of the district, the AEM survey revealed numerous locations of pronounced surface topography underlain by sand-rich principal aquifer material. The eastern half of the district is underlain by predominately marginal aquifer and aquitard materials approaching 300 ft in thickness, with isolated pockets of principal and sand-rich principal aquifer materials. The *To* is present beneath nearly the western two-thirds of the district. The full sequence of Cretaceous strata is present beneath the district, with each formation at least 200 ft thick beneath the western half of the LCNRD. The *Kd* ranges from 400 to over 500 ft in thickness, with much of the eastern half of the district underlain by intervals with resistivities ranging from 20-40 ohm-m. The undifferentiated Paleozoic strata ranges in depth from over 1,500 ft beneath the west side of the district to approximately 600 ft near the district's eastern boundary.

3) LENRD - The LENRD hosts the most extensive sequences of continuous principal aquifer material in the northern half of the ENWRA project area, primarily in the western half of the district. Several distinct bodies of sand-rich principal aquifer (>50 ohm-m) ranging from 100-200 ft thick were identified in this area of the survey. The *To* is present beneath the western one-third of the LENRD and comprises nearly half of the principal aquifer at some locations in this area. East of flight lines 200801 and 201001, however, the Quaternary system is comprised primarily of marginal aquifer and aquitard materials. At some locations, the entire Quaternary sequence consists of aquitard materials, which can approach 400 ft in thickness. The contrast in subsurface conditions between the western and eastern halves of the district is evident in the distribution of irrigation wells. Principal aquifer resources are also present in the southern LENRD, mostly associated with alluvium of the Elkhorn River and Morgan Creek valleys. The entire Cretaceous sequence is present beneath the district, ranging in thickness from over 1,600 ft beneath the northern half of the district to approximately 1,000 ft below the southern half of the LENRD. The *Kd* is present beneath the entire district, ranging in thickness from nearly 600 ft in the west to approximately 100 ft in the far southeast corner of the LENRD. Beneath much of the eastern half of the LENRD, intervals of resistivity ranging from 20-40 ohm-m are common in the *Kd*, some approaching 400 ft in thickness, and at some isolated locations, intervals greater than 40 ohm-m are present.

4) PMRNRD - The PMRNRD is underlain by predominately marginal aquifer and aquitard material, with discontinuous areas of principal and sand-rich principal aquifer material scattered across the district. This pattern of Quaternary material distribution is apparent along flight line 202001 that traces north to south along much of the district's extent. In this area, basal principal aquifer deposits area underlain by over 200 ft of marginal aquifer and aquitard deposits. In the northern area of the district southwest of South Sioux City, NE, most of the Quaternary sequence consists of aquitard material. South of the Omaha metropolitan area in Sarpy County, extensive sand-rich principal aquifer deposits are present beneath the Platte River valley, as well as in an isolated corner of the district near Ashland, NE. *Kd* is present beneath the entirety of the district. Most of the *Kd* beneath the PMRNRD contains intervals ranging from 20-40 ohm-m that are typically 200 ft or greater in thickness. South of the Omaha metropolitan area, the *Kd* ranges from 100 to 200 ft in thickness, but consists primarily of strata with resistivity ranging from 20-40 ohm-m, with extensive intervals greater than 40 ohm-m. Along the

district's southern edge, the AEM survey revealed the presence of the Humboldt Fault beneath the Platte River valley.

5) The Tertiary *To* material under much of the western half of the northern ENWRA project area ranges in thickness from over 150 ft on the westernmost flight lines to near zero near flight line 200801. It is likely that these separate material types (Quaternary and Tertiary) act as one aquifer unit or are in close hydraulic communication. It is also possible that some siltstone layers common in the *To* could create local varying conditions in the vertical gradient between the two systems.

6) The full sequence of Cretaceous strata beneath eastern Nebraska was detected by the AEM system. Most units displayed unique resistivities that allowed for identification of the individual formations where CSD and NOGCC test hole information could be included. One exception to the individual unit characterization in the Cretaceous sequence was the similarity in resistive signatures between the Carlile and Greenhorn-Graneros Formations.

7) Several intervals of the Paleozoic system underlying the Cretaceous sequence were detected in the AEM survey. None of these units, consisting primarily of alternating limestone and shale, are utilized for groundwater over widespread areas in eastern Nebraska. These units were undifferentiated in the interpretation of the AEM survey results.

8) The approximately twenty mile reconnaissance grid spacing provided insight and information on a regional scale, allowing for greater understanding of where future detailed work could be directed. Denser grid spacing is required for smaller, specific water supply projects. The flight line spacing necessary in eastern Nebraska for characterization of the bedrock strata is less stringent than the recommended spacing for delineating the Quaternary and Tertiary systems.

The hydrostratigraphic framework resulting from the AEM reconnaissance survey provides a database of information on the structure of the groundwater resources available beneath the northern half of the ENWRA area. The body and appendices of the report contain the information used in the AEM interpretation and development of the hydrogeologic framework.

Recommendations for future work include:

1) Additional AEM surveys can now be conducted in areas where the reconnaissance survey located potentially extensive zones of principal aquifer materials, and in some locations, sand-rich, principal aquifer deposits within the Quaternary system.

2) The connectivity between groundwater and surface water features along the streams and rivers within the project area is not well understood at all locations, particularly in areas where high densities of irrigation wells exist. The addition of a near-surface, high resolution AEM streambed mapping program of the riparian area is recommended. This data would provide finer detail of the lithology of these critical areas, and more precisely characterize the extent and shape of the aquifers and aquitards that affect hydrologic connection to streams.

3) For locations where the topic of investigation involves localized aquifer features, tighter grid spacing is recommended, on the order of 600 to 1500 ft of separation between flight lines.

4) A CSD test hole program is recommended that includes penetration through the Dakota Formation, ideally in areas where the most extensive resistors (>20 ohm-meters) were detected in the AEM survey. The AEM also reveals where resistive Dakota Formation is overlain by resistive, unconsolidated principal aquifer deposits. Identification of these areas from the AEM data can provide suitable areas for investigating the degree of connection between the unconsolidated and bedrock aquifer sources in the region.

5) The AEM survey identified areas along the flight lines where a greater probability of groundwater recharge likely occurs. A high resolution AEM survey of these areas would quantify the geographic extent of these areas, the recharge potential, and the hydrologic connection to the subsurface.

6) It is recommended to utilize aquifer characterization techniques in conjunction with the AEM survey flight lines to improve the understanding of the variability in hydraulic conductivity, storage, and yield in both the Quaternary system and the resistive intervals of the Dakota Formation.

Table of Contents

1 Introduction 1
1.1 Purpose of Project 1
1.2 Previous Work 2
1.3 Description of Project Area 3
2 Project Area Hydrogeology 5
2.1 Geologic Setting 5
2.1.1 Surficial Geology 5
2.1.2 Tertiary Geology 8
2.1.3 Cretaceous Geology 8
2.1.4 Jurassic and Triassic Geology 8
2.1.5 Paleozoic System 8
2.2 Hydrogeologic Characteristics of the Quaternary System 10
2.2.1 Aquifer Characteristics 14
2.2.2 Connectivity to Surface Water 15
2.2.3 Connectivity to other Aquifers 16
2.3 Bedrock Aquifer Conditions 16
2.3.1 Extent/Structure of Aquifer 16
2.3.2 Aquifer Characteristics 17
2.3.3 Connectivity to Surface Water 18
2.3.4 Connectivity to other Aquifers 18
2.4 Water Quality 18
2.4.1 Quaternary Aquifer Water Quality 20
2.4.2 Bedrock Aquifer Water Quality 22
2.5 Water Use 23
3 Additional Background Information 26
3.1 Borehole Data 26
3.2 Historic Geologic Cross Sections 29
4 Geophysical Methodology, Acquisition and Processing 33
4.1 Geophysical Methodology 33
4.2 Utility Mapping 34

4.3 AEM Survey Instrumentation 35
4.4 Data Acquisition 38
4.5 Data Processing 39
4.5.1 Primary Field Compensation 39
4.5.2 Automatic Processing 40
4.5.3 Manual Processing and Laterally-Constrained Inversions 40
4.5.4 Power Line Noise Intensity (PLNI) 42
4.5.5 Magnetic Field Data 44
4.6 Spatially-Constrained Inversion 46
4.6.1 Determination of the DOI 51
5 Results and Interpretation 53
5.1 AEM Results and Interpretation 54
5.1.1 Interpretive Process 54
5.1.2 Resistivity-Lithology Relationship 57
5.2 Hydrogeologic Framework Interpretation 69
5.2.1 Quaternary/Tertiary System 70
5.2.2 Cretaceous Strata and Bedrock Aquifer System 75
5.3 Hydrogeologic Framework Interpretation by Individual NRD 88
5.3.1 Lewis and Clark NRD 88
5.3.2 Lower Elkhorn NRD 94
5.3.3 Papio-Missouri River NRD 102
5.3.4 Comparison of AEM Results with Previous Studies 109
5.4 Summary and Recommendations 114
5.4.1 Key AEM Survey Findings 114
5.4.2 Applicability and Recommendations Regarding Future Groundwater Investigations 117
6 Description of Data Delivered 121
7 References 127
Appendix 1: AEM Profiles and Interpretation A1-1
Appendix 2: Comparison of CSD Holes with AEM Profiles A2-1
Appendix 3: Depth of Investigation A3-1
Appendix 4: Data Deliverables A4-1
Appendix 5: Water Quality Diagrams A5-1

List of Figures

Figure 1-1: Map of the ENWRA project area, with the northern extent of the survey area (Phase I) and flight lines highlighted in green and yellow, respectively. The southern half of the project area (Phase II) is outlined in orange. 2

Figure 1-2: Map of northern ENWRA project area, including the largest cities and major roads within the study area. 4

Figure 1-3: Elevation and topographic expression of the northern ENWRA project area..... 4

Figure 2-1: Bedrock geology of the northern ENWRA project area, based on Burchett (1986)..... 5

Figure 2-2: Geologic time scale with lithostratigraphic sequence underlying Nebraska as defined by UNL-CSD (modified from Korus and Joeckel, 2011; Burchett, 1986; Condra and Reed, 1959). 6

Figure 2-3: Generalized till thickness map of Quaternary deposits in the northern ENWRA project area (CSD, 2014). 7

Figure 2-4: Map displaying the major streams and rivers within the northern ENWRA project area. 10

Figure 2-5: Mapped alluvial valley areas hosting alluvial aquifers in the northern ENWRA project area, modified from the Nebraska Groundwater Atlas (Korus et al.,2013b). 12

Figure 2-6: Mapped paleovalleys in the northern ENWRA project area, modified from the Nebraska Groundwater Atlas (Korus et al., 2013b). 12

Figure 2-7: Groundwater surface elevations in the northern ENWRA project area (CSD, 1995). 15

Figure 2-8: Thickness contours of the *Kd*/Maha aquifer in eastern Nebraska (Ellis 1984). The green indicates where the *Kd* is the uppermost subcropping bedrock (Burchett, 1986). Note that the contours and extent of *Kd* subcrop are from different map sources, thus some presence of *Kd* as indicated by the Nebraska bedrock geology map (Burchett, 1986) extends east of the 0 ft thickness contour from Ellis (1984). 17

Figure 2-9: Concentrations of TDS, calcium, chloride, and sodium (x-axis) in water samples verses depth (y-axis) Data are from the USGS NWIS. 19

Figure 2-10: Public supply wells within the northern ENWRA project area. 24

Figure 2-11: Registered wells within the northern ENWRA project area with depth to the static water level indicated by color code. 24

Figure 2-12: Progression of irrigation well development from the pre-1960s (upper left) to 2015 (lower right). Blue dots indicate existing wells and yellow dots indicate new wells constructed during the indicated decade (NDNR). 25

Figure 3-1: Locations of CSD tests holes in the northern ENWRA project area. 26

Figure 3-2: Locations of boreholes containing lithologic information in the northern ENWRA project area. 27

Figure 3-3: Locations of boreholes containing stratigraphic information in the northern ENWRA project area. 27

Figure 3-4: Locations of boreholes containing geophysical logs in the northern ENWRA project area. 28

Figure 3-5: Locations of geologic cross sections within the northern ENWRA project area. 29

Figure 3-6: Original cross section from CSD OFR 109 (left) and the digitized cross section (right). 31

Figure 3-7: 3D view of geo-referenced geologic cross sections used to aid AEM interpretation. 32

Figure 4-1: Schematic of an AEM survey 33

Figure 4-2: A) Example of a dB/dt sounding curve. B) Corresponding inverted model values. C) Corresponding resistivity earth model. 34

Figure 4-3: Map of the expected utilities in the northern ENWRA project area. 35

Figure 4-4: SkyTEM 508 frame, including instrumentation locations and X and Y axes. 36

Figure 4-5: Photos of the SkyTEM508 system on the ground (above) and in suspension beneath the helicopter (below). 37

Figure 4-6: Flights lines as collected by date for the northern ENWRA project area. 38

Figure 4-7: Example locations of EM coupling with pipelines or power lines. 41

Figure 4-8: A) AEM data affected by coupling, shown in Figure 4-7, in Aarhus Workbench editor. The top group of lines is the Low Moment and the bottom is the High Moment. B) AEM data with area affected by coupling removed. 41

Figure 4-9: A) Inversion results where AEM data affected by coupling with pipelines and power lines were not removed. B) Inversion results where AEM data affected by coupling were removed. 42

Figure 4-10: Power Line Noise Intensity (PLNI) map of the northern ENWRA project area. 43

Figure 4-11: Locations of inverted data (red lines) along the AEM flight lines in the northern ENWRA project area. Black line segments indicate decoupled (removed) data. 43

Figure 4-12: Magnetic Total Field data corrected for diurnal drift, with IGRF removed. 44

Figure 4-13: Regional magnetic Total Field data within the northern ENWRA project area boundary. Derived from Bankey et al. (2002). 45

Figure 4-14: 3D magnetic field analytical signal calculated from the diurnal and IGRF corrected magnetic Total Field data. 45

Figure 4-15: An example of an AEM profile illustrating the increase in model layer thickness with depth. 47

Figure 4-16: Borehole resistivity logs compared with inverted AEM models. A: Well 3-A-52, 1,700 ft from the AEM line. B: Well 3-A-53, 2,512 ft from AEM line. C: Well 4-A-52, 527 ft from AEM line. The green line shows the original borehole logs while the blue is the same log resampled to match the layering used within the inversions. The purple line is the inverted model result without a-priori information while the red shows the result when the logs were used. 48

Figure 4-17: Borehole resistivity logs compared with inverted AEM models. A: Well 8-A-53, 1,768 ft from AEM line. B: Well 15-A-55, 3,132 ft from AEM line. The green line shows the original borehole logs while the blue is that log resampled to match the layering used within the inversions. The purple line is the inverted model result without a-priori information while the red shows the result when the logs were used. 48

Figure 4-18: Borehole resistivity logs compared with inverted AEM models. A: Well 8-LE-03, 1,540 ft from AEM line. A: Well 13-LE-99, 2,349 ft from AEM line. The green line shows the original borehole logs while the blue is that log resampled to match the layering used within the inversions. The purple line is the inverted model result without a-priori information while the red shows the result when the logs were used. 49

Figure 4-19: Cross-plot of inverted resistivities compared with the resampled borehole resistivity for the 13 boreholes within the closer spaced flight lines. 50

Figure 4-20: Difference between data point residuals produced by SCIs with and without using the borehole conductivity data as a-priori information. Red indicates an improvement in the residuals by greater than 0.1. 50

Figure 4-21: Data residuals distribution produced by the SCIs in the 10-mile reconnaissance lines both using the resistivity logs as a-priori and without them. 51

Figure 4-22: Sample of AEM resistivity inversion model with the 0.1 DOI marked as grey boxes at the bottom of the image. 52

Figure 5-1: AEM flight lines with line numbers in the northern ENWRA project area. 53

Figure 5-2: Color codes for aquifer materials, stratigraphy, and lithology used in the interpretive profiles and 3D figures in this section and in the report appendices. 54

Figure 5-3: Box and whisker plots for the resistivity ranges for the nine most common unconsolidated materials within the Quaternary system. 58

Figure 5-4: Histogram plot displaying the distribution of resistivities by major aquifer material color categories (blue- non-aquifer material, tan- marginal aquifer, yellow-principal aquifer, brown- sand-rich, coarse intervals of the principal aquifer). 59

Figure 5-5: Pie charts of the distribution of material within each resistivity range for the aquifer materials used in the interpretation of the AEM data- 0-12 ohm-m (left) and 12-20 ohm-m (right). 60

Figure 5-6: Pie charts of the distribution of material within each resistivity range for the aquifer materials used in the interpretation of the AEM data- 20-50 ohm-m (left), and 50 ohm-m and above (right). 60

Figure 5-7: Pie chart of the overall lithology indicated in the 58 e-logs used to characterize the relationship of lithology and resistivity across the ENWRA project area. 61

Figure 5-8: Pie charts showing overall percentage of lithologies in selected CSD test holes in the northern ENWRA project area. 62

Figure 5-9: Histogram of the distribution of the fractional difference in the thickness of the principal aquifer materials using 20 and 21 ohm-m resistivity thresholds. 64

Figure 5-10: Example cross section illustrating the small difference between use of a 20 ohm-m threshold or a 21 ohm-m threshold to define the principal aquifer. The solid black line enclosing the yellow (principal aquifer material) represents the 20 ohm-m threshold and the dotted black line enclosing the principal aquifer material represents the 21 ohm-m threshold. 64

Figure 5-11: Box and whiskers plot of the resistivity distribution of the Cretaceous and Paleozoic bedrock units discussed in the interpretation of the AEM data. 66

Figure 5-12: Deep oil and gas borehole resistivity logs (green lines) compared with inverted AEM models (purple lines). A: Well 2616719000, 5,186 ft from the AEM line, B: Well 2616721003, 12,838ft from AEM line. 66

Figure 5-13: Box and whisker plot for the major lithologic texture categories within the *Kd* from CSD e-logs located across the entire ENWRA project area. 67

Figure 5-14: Resistivity count distribution by major grain size category for CSD test holes screened in the Kd. Plot A (top) represents all coarse unconsolidated and consolidated deposits; plot B (middle) represents all unconsolidated and consolidated fines, and plot C (bottom) represents a composite of both coarse and fine materials, color coded by the ranges of 0-20, 20-40, and 40 ohm-m and above used in the interpretive figures of the Kd beneath the ENWRA project area. 68

Figure 5-15: A northeastward view of the 3D hydrostratigraphic framework for the northern ENWRA project area, including geologic materials ranging from Quaternary deposits to Paleozoic bedrock. See Figure 5-2 for the color codes of the materials and geologist strata displayed. Vertical exaggeration is 50x. Refer to Figure 5-2 for a color legend of hydrostratigraphy/lithology. 73

Figure 5-16: A southwestward view of the 3D hydrostratigraphic framework for the northern ENWRA project area, displaying the limited distribution of principal aquifer materials in the eastern subregion of the project area in the LENRD and LCNRD. See Figure 5-2 for the color codes of the materials and geologist strata displayed. Vertical exaggeration is 60x. Refer to Figure 5-2 for a color legend of hydrostratigraphy/lithology. 74

Figure 5-17: Northwestward view of the northern ENWRA project area displaying the locations of historic and contemporary CSD geologic cross sections. The color scale is shown in Figure 5-2. 80

Figure 5-18: Eastward view of the northern ENWRA project area displaying the locations of historic and contemporary CSD geologic cross sections. The color scale is shown in Figure 5-2. 81

Figure 5-19: Comparison of TEM model, borehole log, lithology, and stratigraphy at CSD test hole 5-GT-80. 82

Figure 5-20: Combined display of AEM data (second panel), hydrostratigraphic interpretation (third panel), and CSD cross section (bottom panel) for flight line 100501 near Wayne, NE. The location of the AEM flight line and CSD cross section is displayed in the top panel. 84

Figure 5-21: Zoomed in view along the eastern extent of AEM flight line 100501, demonstrating the thin intervals of material indicated in the test hole logs that correspond to only the averaged resistivity data across intervals of greater thickness. This is particularly evident in 31-A-51 and 9-A-64. 85

Figure 5-22: Combined display of AEM data (second panel), hydrostratigraphic interpretation (third panel), and CSD cross section (bottom pane) for flight line 101601 near Oakland, NE. The location of the AEM flight line and CSD cross section is displayed in the top panel. 86

Figure 5-23: Combined display of AEM data (second panel), hydrostratigraphic interpretation (third panel), and CSD cross section (bottom pane) for flight line 200101, the westernmost north-south flight line in the reconnaissance survey area. The location of the AEM flight line and CSD cross section is displayed on the right side of the panel. 87

Figure 5-24: Flight lines within the LCNRD acquired in Phase 1 of the ENWRA AEM survey. 88

Figure 5-25: 3D hydrogeologic framework from the reconnaissance AEM survey only within the LCNRD. The district boundary is displayed in red, with flight lines labeled in white and major drainages displayed as blue lines. The stratigraphy color codes are in Figure 5-2. 89

Figure 5-26: Interpreted profile for west-east flight line 100201 that extends from west to east within the midsection of the LCNRD. The To is delineated by the orange line and the CSD 1995 regional water table surface is indicated by dashed blue line. West is on the left, east to the right. The stratigraphy color codes are in Figure 5-2 91

Figure 5-27: Interpreted profile for south-north flight line 200101 that extends through the south-central portion of the LCNRD. The To is delineated by the orange line and the CSD 1995 regional water table

surface is indicated by dashed blue line. South is on the left, north to the right. The LCNRD is present to the right of the 15416740 ft Northing. The stratigraphy color codes are in Figure 5-2. 91

Figure 5-28: Interpreted profile for south-north flight line 200801 that extends through the south-central portion of the LCNRD. The *To* is delineated by the orange line and the CSD 1995 regional water table surface is indicated by dashed blue line. South is on the left, north to the right. The LCNRD is present to the right of 15435070 ft Northing. The stratigraphy color codes are in Figure 5-2. 92

Figure 5-29: Interpreted profile for south-north flight line 201301 that extends through the south-central portion of the LCNRD. The *To* is delineated by the orange line and the CSD 1995 regional water table surface is indicated by dashed blue line. South is on the left, north to the right. The LENRD-LCNRD boundary begins at 15452340 ft Northing. The stratigraphy color codes are in Figure 5-2. 92

Figure 5-30: Flight lines within the LENRD acquired in the first phase of the ENWRA AEM survey..... 94

Figure 5-31: 3D hydrogeologic framework from the reconnaissance AEM survey only within the LENRD. The district boundary is displayed in red, with flight lines labeled in white and major drainages displayed in blue. The stratigraphy color codes are in Figure 5-2. 95

Figure 5-32: Interpreted profile for west-east flight line 101301 that extends through the south-central portion of the LENRD. The To is delineated by the orange line and the CSD 1995 regional water table surface is indicated by dashed blue line. West is on the left, east to the right. The stratigraphy color codes are in Figure 5-2. 97

Figure 5-33: Interpreted profile for west-east flight line 100501 that extends through the north-central portion of the LENRD. The To is delineated by the orange line and the CSD 1995 regional water table surface is indicated by dashed blue line. West is on the left, east to the right. The LENRD-PMRNRD boundary is at 2260790 ft Easting. The stratigraphy color codes are in Figure 5-2. 97

Figure 5-34: Interpreted profile for south-north flight line 200401 that extends through the western extent of the LENRD. The To is delineated by the orange line and the CSD 1995 regional water table surface is indicated by dashed blue line. North is on the right, south to the left. The LENRD-PMRNRD boundary is at 15449600 ft Northing. The stratigraphy color codes are in Figure 5-2. 98

Figure 5-35: Interpreted profile for south-north flight line 201801 that extends through the eastern extent of the LENRD. The CSD 1995 regional water table surface is indicated by dashed blue line. North is on the right, south to the left. The LENRD-LCNRD boundary is at 15390670 ft Northing. The stratigraphy color codes are in Figure 5-2. 98

Figure 5-36: Area between the Elkhorn River and Maple Creek drainages with extensive sand-rich, principal aquifer material in the southeast corner of the LENRD. Vertical exaggeration is 60x. The stratigraphy color codes are in Figure 5-2. 100

Figure 5-37: Flight lines within the PMRNRD acquired in Phase 1 of the ENWRA AEM survey. 102

Figure 5-38: 3D hydrogeologic framework views of the PMRNRD from the reconnaissance AEM survey. The district boundary is displayed in red, with flight lines labeled in white and major drainages displayed in blue. See Figure 5-2 for the aquifer and bedrock material resistivity thresholds and stratigraphic codes. 103

Figure 5-39: Interpreted profile for south-north flight line 202001 (left) that extends along the western side of the southern half of the PMRNRD. The CSD 1995 regional water table surface is indicated by dashed blue line. North is on the right, south to the left. The flight line intersects the LENRD in the following ranges: 15151000 - 15177635 ft Northing, 15198810 - 15235710 ft Northing. The stratigraphy color codes are listed in Figure 5-2. 105

Figure 5-40: Interpreted profile for flight line 101701.1 (right) that extends west-east through the south-central section of the PMRNRD northwest of the Omaha metropolitan area. The CSD 1995 regional water table surface is indicated by dashed blue line. East is on the right, west to the left. The PMRNRD starts at 2339350 ft Easting. The stratigraphy color codes are listed in Figure 5-2. 106

Figure 5-41: Interpreted profile for south-north flight line 201901.2 (left) that extends through the northern one-quarter of the PMRNRD. The CSD 1995 regional water table surface is indicated by dashed blue line. North is on the right, south to the left. The PMRNRD starts at 15313125 ft Northing. The stratigraphy color codes are listed in Figure 5-2. 106

Figure 5-42: 3D framework of the southern PMRNRD flight lines (right) displaying the extent of the principal aquifer material and resistive intervals in the *Kd*. Vertical exaggeration is 30x. See Figure 5-2 for the resistivity threshold and stratigraphy legend. 108

Figure 5-43: Resistivity profile of flight line 300402 (above) in the southern PMRNRD indicating the Humboldt Fault in the Paleozoic strata. The map to the left shows the location of the fault-flight line intersection. 108

Figure 5-44: Locations of prior study airborne geophysical survey studies in the northern ENWRA project area. 109

Figure 5-45: Clarkson flight lines shown with the ENWRA flight line in the area. Inverted models are compared at the marked locations. 110

Figure 5-46: Comparison of inverted models between the Clarkson and ENWRA 2014 surveys. The models shown in panel A are 133 ft apart, panel B 53 ft, panel C 91 ft, and panel D 137 ft. The X-axes resistivities are linear. 111

Figure 5-47: Display of aquifer material near Clarkson, NE with a 700 ft grid line spacing (white lines). The yellow lines demonstrate how some portion of the aquifer would have been missed if the AEM flight line spacing were set at 0.5 or 1.0 miles. 112

List of Tables

Table 2-1: Aquifers in Quaternary to Cretaceous stratigraphic units in eastern Nebraska. 14

Table 2-2: Statistical results of water-quality analyses from groundwater samples collected in or near the project area, from all wells. Units in milligrams per liter unless stated otherwise. Data are from the US Geological Survey NWIS database; (NA- not analyzed; N- number of samples). 19

Table 2-3: Statistical results of water quality analyses from groundwater samples collected in or near the project area, from stream-valley/alluvial wells. Units are in milligrams per liter unless stated otherwise. Data are from the US Geological Survey NWIS database (NA- not analyzed; N- number of samples). 21

Table 2-4: Statistical results of water quality analyses from groundwater samples collected in or near the project area from wells in glacially-derived deposits. Units are in milligrams per liter unless stated otherwise. Data are from the US Geological Survey NWIS database; (NA- not analyzed; N- number of samples). 21

Table 2-5: Statistical results of water quality analyses from groundwater samples collected in or near the project area from *Kd* wells. Units are in milligrams per liter unless stated otherwise. Data are from the US Geological Survey NWIS database; NA, not analyzed; N, number of samples. 22

Table 3-1: Geologic cross sections from OFR-109 incorporated in the hydrostratigraphic interpretation (Divine et al., 2010; Korus et al., 2012). 30

Table 4-1: Positions of instruments on the SkyTEM508 frame, using the center of the frame as the origin in feet. 37

Table 4-2: Positions of corners of the SkyTEM508 transmitter coil, using the center of the frame as the origin in feet. 37

Table 4-3: Locations of magnetic field base station instruments. 37

Table 4-4: Airports and state parks used for landing and refueling by date of acquisition. 39

Table 4-5: Production log displaying the number of production flights conducted each day and total line miles and kilometers surveyed. A limited number of flight lines did overlap. 39

Table 4-6: Thickness and depth to bottom for each layer in the SCI inverted AEM models. The thickness of the model layers increase with depth as the resolution of the AEM technique decreases. 46

Table 4-7: List of wells with borehole resistivity logs used as a-priori information for the SCI. 49

Table 6-1: Channel name, description, and units for 20141126_345_Nebraska_ENWRA1_XRI.xyz with EM, mag, DGPS, Inclinometer, altitude, and associated data. 122

Table 6-2: Channel name, description, and units for ENWRA2014_SCIresults.xyz with EM inversion results..... 123

Table 6-3: Files containing borehole information..... 124

Table 6-4: Channel name, description, and units for collar files. 124

Table 6-5: Channel name description and units for borehole data. 125

Table 6-6: Channel name description and units for the interpretation results file. 126

List of Abbreviations

1D	One-dimensional
2D	Two-dimensional
3D	Three-dimensional
A* m^2	Ampere meter squared
AEM	Airborne Electromagnetic
Bgl	Below Ground Level
dB/dt	Change in amplitude of magnetic field with time
CSD	Conservation and Survey Division, Nebraska Geological Survey
DOI	Depth of Investigation
DGPS	Differential global positioning system
em, EM	Electromagnetic
ENWRA	Eastern Nebraska Water Resources Assessment
FDHEM	Frequency-Domain Helicopter Electromagnetic
Ft	Feet
Ft/d	Feet per day
Ft^2/d	Feet squared per day
Ft^3/s	Cubic feet per second
GIS	Geographic Information System
gpd/ft	Gallons per day per foot
GX	Geosoft executable
HEM	Helicopter Electromagnetic
IGRF	International Geomagnetic Reference Field
in/yr	Inches per year
Kc	Carlile Formation
KcKgg	Carlile & Greenhorn-Graneros Formations
Kd	Dakota Formation
Km	Kilometers
LBBNRD	Lower Big Blue Natural Resources District
LCI	Laterally-Constrained Inversion
LPNNRD	Lower Platte North Natural Resources District
LPSRD	Lower Platte South Natural Resources District
MAG	Magnetic (data); Magnetometer (instrument)
MCG	Minimum curvature gridding
mg/L	Milligrams per liter
mi	Miles

mi^2	Square miles
Ma	Megaannus (million years)
µS/cm	Microsiemens per centimeter
NAD83	North American Datum of 1983
NDNR	Nebraska Department of Natural Resources
NNRD	Nemaha Natural Resources District
NRD	Natural Resources District
NOGCC	Nebraska Oil and Gas Conservation Commission
NWIS	National Water Information System
OM	Oasis montaj
PFC	Primary Field Compensation
PLNI	Power Line Noise Intensity
PMRNRD	Papio-Missouri River Natural Resources District
Rx	Receiver
SCI	Spatially-Constrained Inversion
STD	Standard Deviation
TDS	Total Dissolved Solids
TEM	Transient Electromagnetic
TDEM	Time-Domain Electromagnetic
TRSZ	Thurman-Redfield Structural Zone
Tx	Transmitter
UBBNRD	Upper Big Blue Natural Resources District
USGS	United States Geological Survey
UTM	Universal Transverse Mercator
V/m^2	Volts per meter squared
XRI	Exploration Resources International

1 Introduction

1.1 Purpose of Project

Sound management of groundwater and surface water in eastern Nebraska has become increasingly important in recent years. There are expanding pressures placed on the resource by the ever growing demands for agricultural production, population growth and urbanization, potential contamination from natural and anthropogenic sources, industrial needs, and the persistent threat of drought. The combination of these stresses on water resources has increased the need for detailed hydrogeologic frameworks of the subsurface so that the resource can be better understood.

This report describes the findings of the first phase of an airborne electromagnetic (AEM) survey conducted in October 2014 across several natural resources districts (NRDs) that are part of the Eastern Nebraska Water Resources Assessment (ENWRA) in northeastern Nebraska. The first phase covered, approximately, the northern half of the ENWRA area (Figure 1-1), and hereafter will be referred in this report as the "northern ENWRA project area." The AEM survey data were collected along reconnaissance (recon) lines spaced approximately 20 miles apart across an area from the Antelope-Madison County eastward to near the Missouri River, and from near the Missouri River in Cedar County to the Platte River in Dodge and Colfax Counties. The AEM survey in the first phase of flights included parts of four NRDs participating in ENWRA: the Lewis and Clark (LCNRD), Lower Elkhorn (LENRD), Papio-Missouri River (PMRNRD), and the Lower Platte North (LPNRD). For organizational purposes, this report (Volume I) formally discusses the findings of the AEM survey for the LCNRD, LENRD, and the PMRNRD, although some inclusion of the Lower Platte North (LPNNRD) occurs due to the southern extent of the phase I flight lines. A small portion of the flight lines in the PMRNRD were collected in the Spring 2015 survey and are included in Volume I. Volume II of this report includes the assessments of the LPNNRD, as well as the Lower Platte South and Nemaha NRDs.

In addition to the AEM data acquired during this investigation, data and findings from previous studies, along with geologic descriptions and geophysical logs from University of Nebraska-Lincoln Conservation and Survey Division (CSD) and Nebraska Oil and Gas Conservation Commission test holes (NOGCC) were utilized to develop the hydrogeologic framework of the region.

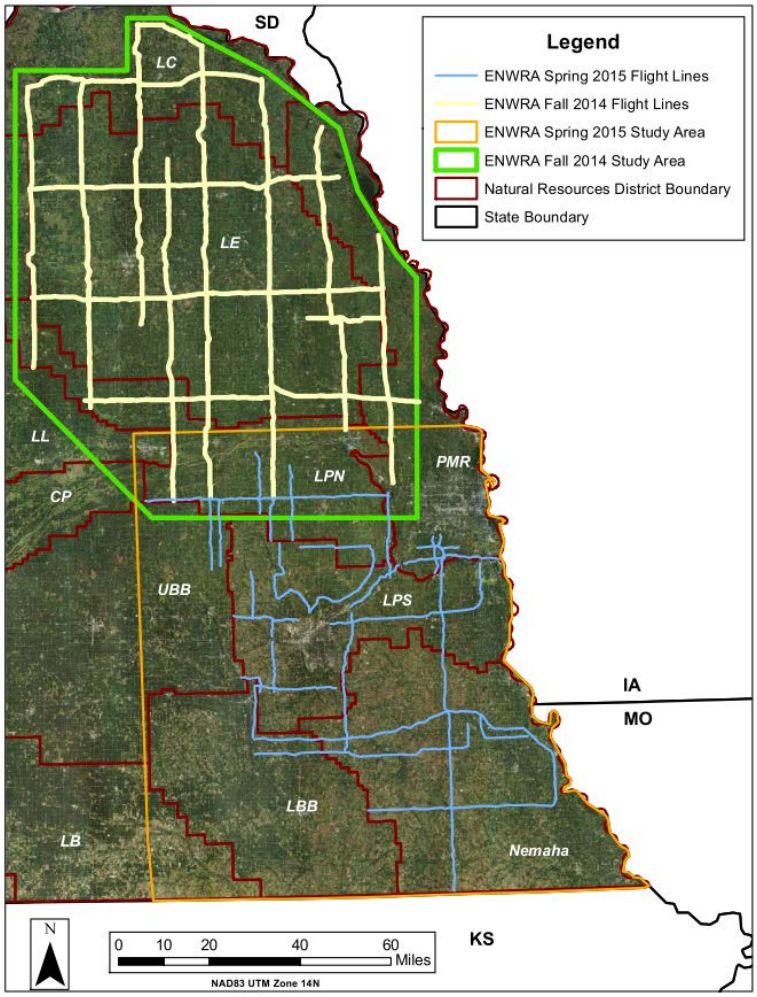


Figure 1-1: Map of the ENWRA project area, with the northern extent of the survey area (Phase I) and flight lines highlighted in green and yellow, respectively. The southern half of the project area (Phase II) is outlined in orange.

1.2 Previous Work

The use of AEM technology to map and evaluate groundwater resources has gained momentum over the last 20 years in the United States and abroad. The state of Nebraska has been on the forefront of implementing AEM for water resources management over the last decade with projects across the state in a variety of geologic settings. In recent years, ENWRA has coordinated efforts between area Natural Resources Districts (NRDs), CSD, the U.S. Geological Survey (USGS), and Exploration Resources International Geophysics, LLC (XRI) in support of several projects designed to characterize glacial outwash and buried paleovalley aquifers across the eastern part of the state.

In March 2007, AEM methods were implemented to characterize the hydrogeologic conditions in the Platte River valley near Ashland, NE, as well as in areas underlain by glacial till near Firth and Oakland, NE (Abraham et al., 2011, Korus et al., 2013a). In the following years, individual reports utilizing the AEM data collected in 2007 were released by the USGS and CSD. In 2009, a multi-faceted investigation

incorporating the 2007 AEM data and 2009 ground-based geophysical techniques was conducted by the USGS to characterize the hydrogeologic setting near Oakland, NE. In 2009, the LPSNRD funded development of a three-dimensional (3D) hydrostratigraphic framework of the subsurface near Swedeburg, NE based on an AEM survey. Also in 2009, the LPSNRD funded a similar investigation of the hydrostratigraphy near Sprague, NE (Smith et al., 2009; Divine and Korus, 2012).

In 2013, the LENRD contracted with XRI to conduct an AEM survey near the towns of Clarkson and Howells, NE to characterize the extent of the Quaternary aquifer in the area following the 2012 drought (Abraham et al., 2013). Also in 2013, XRI completed an AEM survey covering over 800 line-miles in Butler and Saunders counties northwest of the city of Lincoln, NE for the LPSNRD (Carney et al., 2014). This survey revealed extensive buried paleovalley aquifers beneath thick sequences of till. Additionally, intervals of Cretaceous bedrock units were imaged in the survey. In the fall of 2014, XRI conducted an AEM survey of nearly 1,500 line-miles across a subsection of the LENRD at a three mile flight line spacing to assess the general hydrogeologic character of the subsurface and upper bedrock in the northwest portion of the district and to investigate the appropriate length (i.e.- large spacing for greater areal coverage) of flight line spacing for conducting airborne investigations in eastern Nebraska's glaciated terrain. The survey revealed the subsurface character to depths beyond 1,200 ft in this investigation (Exploration Resources International, 2015). Thus, AEM surveys of the glacial terrain of eastern Nebraska have followed a progressive, long-term plan spanning nearly eight years. This body of work shows continuing advancements in the science and application of AEM to support groundwater management.

1.3 Description of Project Area

The area investigated by the reconnaissance surveys (project area) spans approximately 7,760 square miles (mi^2) in northeast Nebraska (Figure 1-2). The elevation of the area, presented in Figure 1-3, ranges from 835 ft to 2,235 ft above sea level**.** It is underlain by parts of five of Nebraska's eight topographic regions—Dissected Plains, Plains, Rolling Hills, Sand Hills, and Valleys (Elder et al., 1951). This area stretches from the rolling, loess-mantled, glacially-derived landscape (Gosselin et al., 1996) on the east to the Holocene, sand-covered, non-glaciated areas on the west.

Principal cities within the project area, based on 2010 census data, include (largest to smallest) Fremont (26,397), Norfolk (24,210), Columbus (22,111), Wayne (5,660), Madison (2,438), Pierce (1,767), Stanton (1,577), and Wisner (1,170) (U.S. Census Bureau, 2013).

Land use/land cover within the project area is primarily agricultural, including irrigated and non-irrigated corn and soybeans. Secondary land use is rangeland, pastureland, and grasslands with some alfalfa crops, urban areas, riparian forest and woodlands (School of Natural Resources University of Nebraska-Lincoln, 2005). Center-pivot irrigation is the primary groundwater irrigation method within the project area, using approximately 15,051 registered irrigation wells (NDR Registered Well Database).

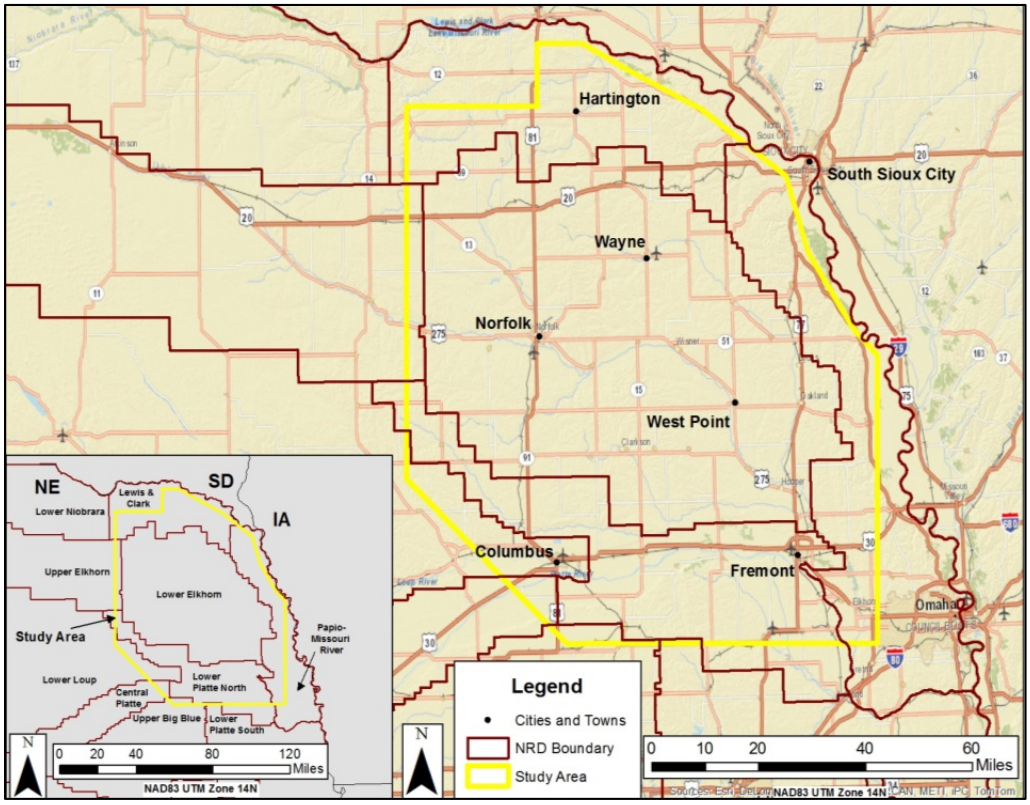


Figure 1-2: Map of northern ENWRA project area, including the largest cities and major roads within the study area.

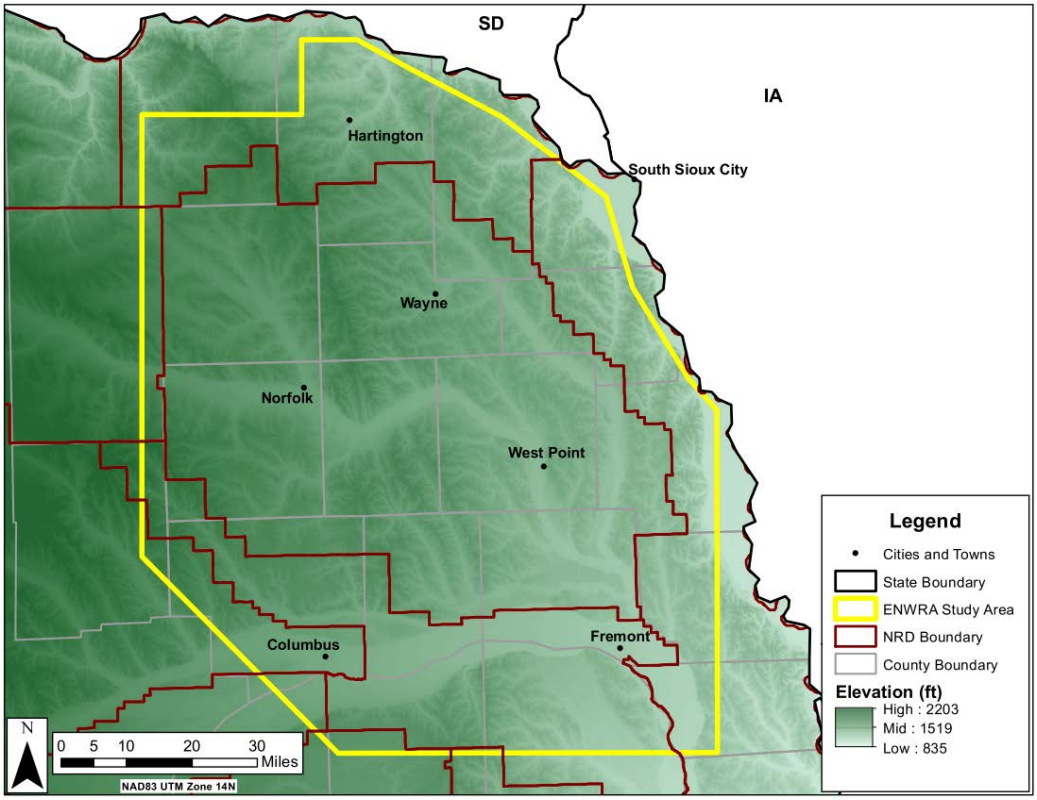


Figure 1-3: Elevation and topographic expression of the northern ENWRA project area.

2 Project Area Hydrogeology

2.1 Geologic Setting

Bedrock geology (Figure 2-1) in the project area is comprised of Tertiary, Cretaceous, and Paleozoic deposits. Paleozoic bedrock consists of undifferentiated Pennsylvanian (*IP*) and Mississippian (*M*) strata. Cretaceous bedrock units include the Pierre Shale (*Kp*), Niobrara Formation (*Kn*), Carlile Shale (*Kc*), Greenhorn Limestone and Graneros Shale (*Kgg*), and the Dakota Formation (*Kd*). The Tertiary bedrock present consists of the Ogallala Group (*To)*, which also serves as a principal aquifer in the western part of the project area. The Tertiary deposits are present only in the western third of the project area. The Cretaceous and Paleozoic deposits underlie the entire area. The southeast portion of the area (east of and south of West Point, NE) is underlain by *Kd*, which locally can yield potable water.

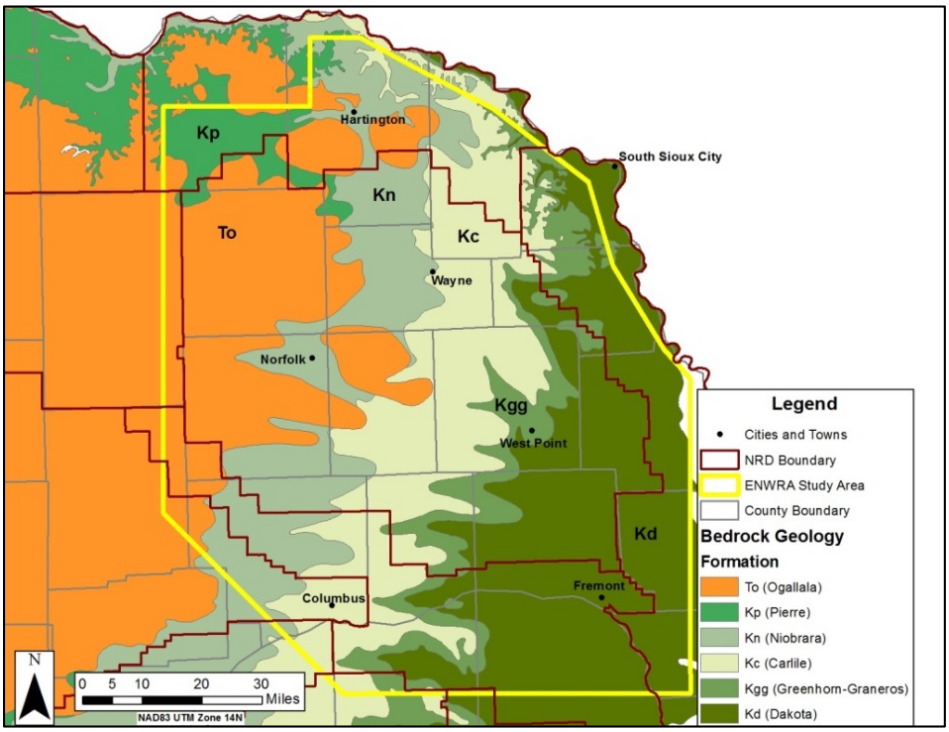


Figure 2-1: Bedrock geology of the northern ENWRA project area, based on Burchett (1986).

2.1.1 Surficial Geology

The complex Pleistocene and Holocene (Quaternary) geology in northeastern Nebraska consists of myriad sequences of clay, silt, till, sand, and gravel overlying bedrock units, which are capped by loess deposits at many locations. Figure 2-2 displays the geologic time scale with the CSD's lithostratigraphic sequence that underlies the state (Korus and Joeckel, 2011). The surficial geology of the project area is typical of western mid-continental glaciated areas of North America where buried Quaternary sand and gravel glacial outwash deposits or paleovalleys, comprised of unconsolidated Plio-Pleistocene sand and gravel units, underlie extensive areas of glacial till. In much of northeastern Nebraska, glacial till typically

underlies loess units (e.g., Peoria, Gillman Canyon Formation, and Loveland Loess deposits). Present day surface water systems have incised the loess and till to create wide stream valleys in some locations.

Age (Ma)	Era	Period		Epoch	Lithostratigraphy	Lithology	Max Thickness (ft)	Lith/ Strat Color Code
0.01	Cenozoic	Quaternary		Holocene	DeForest Fm, other units	dune sand, alluvium	NA	
				Pleistocene	Peoria Loess	loess (silt)	35	
					Gilman Canyon Fm.	loess (silt)	5	
					Loveland Loess	loess (silt)	25	
					Kennard Fm.	loess (silt)	25	
					Pre-Illinoian glacial deposits	till, outwash, fines	>400	
2.6		Tertiary (*T*)	Neogene	Pliocene	Broadwater Fm, corr. units	sand and gravel	70	
5.3				Miocene	Ogallala Group (*To*)	sand, sandstone, silt, siltstone, gravel, caliche	650	
23			Paleogene	Oligocene	*Only unnamed units in NE Nebraska identified in early Eocene*	sandstone & conglomerate	NA	
33.9				Eocene				
55.8				Paleocene				
65.5	Mesozoic	Cretaceous (*K*)		Late Cretaceous	*Upper Late Cretaceous units absent*			
					Pierre Shale (*Kp*)	shale, shaly chalk, siltstone, sandstone	1,970	
					Niobrara Fm (*Kn*)	shaly chalk, limestone	570	
					Carlile Shale (*Kc*)	shale, minor sandstone	300	
					Greenhorn Limestone & Graneros Shale (*Kgg*)	limestone, shale	60	
99.6				Early Cretaceous	Dakota Group (*Kd*)	sandstone, conglomerate, siltstone, mudstone, shale	600	
251					*Lower Early Cretaceous units absent*			
	Paleozoic	Permian (*P*)			Chase Group	limestone, evaporites, shale	300	
299					Council Grove Group		300	
		Carboniferous	Pennsylvanian (*[P]*)		Admire Group	limestone, shale, mudstone, sandstone	150	
					Wabaunsee Group		300	
					Shawnee Group		200	
					Douglas Group		100	
					Lansing Group		75	
					Kansas City Group		200	
					Pleasanton Group		40	
					Marmaton Group		125	
318					Cherokee Group		300	
			Mississippian (*M*)		Osage-Meramec, Kinderhook Groups	limestone, shale, dolomite, siltstone, chert	500	
359		Devonian			*Strata only subcrops in Nebraska, generally below investigative depth of AEM system*		560	
416		Silurian					450	
444		Ordovician					>600	
488		Cambrian			Elk Creek Carbonatite	intrusion complex	NA	
542	Precambrian							

Figure 2-2: Geologic time scale with lithostratigraphic sequence underlying Nebraska as defined by UNL-CSD (modified from Korus and Joeckel, 2011; Burchett, 1986; Condra and Reed, 1959).

CSD test holes and drillers logs obtained from NDNR indicate glacial till units are prevalent across the project area and make up the majority of the surficial geologic deposits. These units, which can often exceed 200 ft in thickness, serve as upper confining layers to buried paleovalley aquifers. Figure 2-3 displays a generalized map of till thickness across eastern Nebraska (University of Nebraska-Lincoln School of Natural Resources, 2014). These deposits can impede or reduce recharge to groundwater systems because of the low permeability of the clay within the till. Comprised of localized sand and gravel, the till is consistent with glaciated areas experiencing lateral, push, and terminal moraines.

Plio-Pleistocene and Holocene sand and gravel units, deposited as glacial outwash or by fluvial systems sit unconformably on Cretaceous bedrock in many locations beneath the project area. Thicknesses of the sand and gravel deposits vary by location but generally do not exceed 300 ft (Gosselin et al., 1996). The paleovalley units appear to be preglacial, synglacial, or interglacial in origin and are not well understood (Gates et al., 2014). The paleovalley units underlying thick till sequences in eastern Nebraska can be greater than 6 miles wide, 62 miles long (Gates et al., 2014) and can be up to 200 ft thick (Fredrick et al., 2006). Locally, CSD test holes indicate that the sand and gravel units are, typically, not well sorted, and are interlayered with silts and clays. Some of the paleovalleys are “deeply covered” by Loveland loess, or Peorian loess. Certain paleovalleys in eastern Nebraska extend eastward (Divine et al., 2009) and some trend southeastward (Condra and Reed, 1959). Easterly to southeasterly trends for paleovalley aquifers in eastern Nebraska appear to be the most common orientations for these subsurface features.

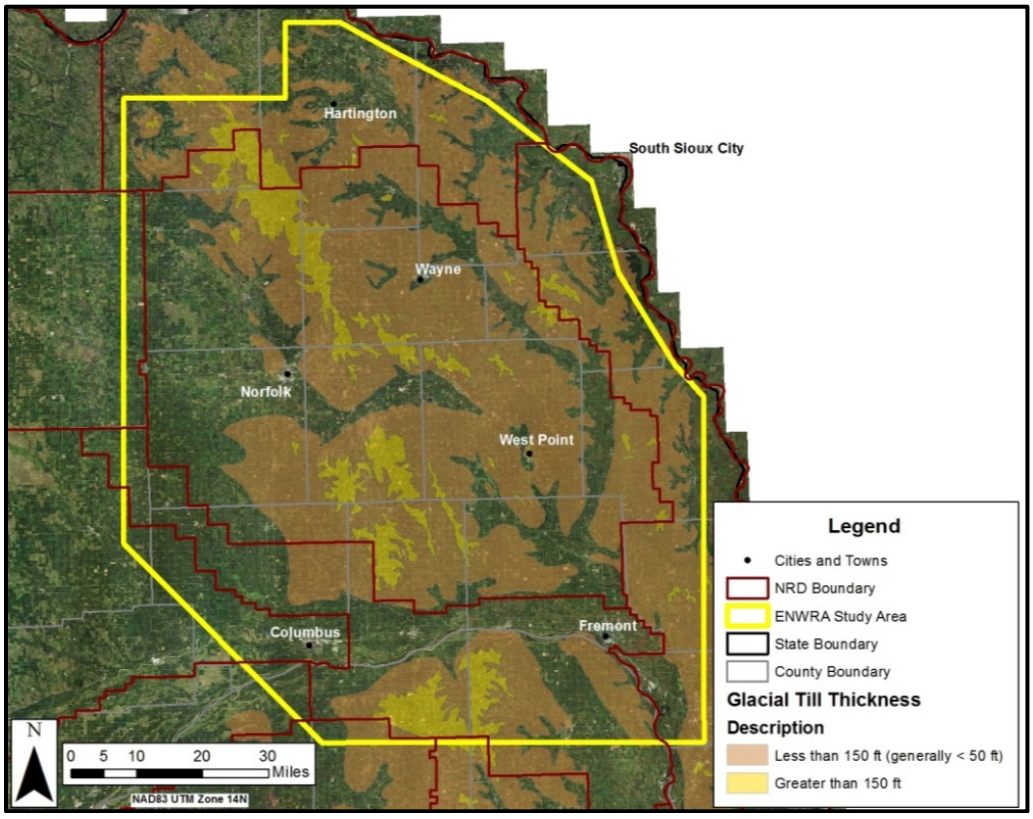


Figure 2-3: Generalized till thickness map of Quaternary deposits in the northern ENWRA project area (CSD, 2014).

2.1.2 Tertiary Geology

The *To* is the only widespread Tertiary geologic unit in the project area and is predominantly composed of fluvial material which comprised of unconsolidated to consolidated irregularly distributed beds of silt, clay, sand, and gravel (Souders, 2000). The *To* is the primary geologic strata of the regionally extensive High Plains aquifer. Some members of the *To* contain partially-cemented, friable sands or sandstone (Condra and Reed, 1959). The *To* thins and pinches out to the east and rests unconformably above underlying Cretaceous strata (Divine, 2012). The *To* is found primarily in the western half of the project area. Where present, the *To* acts as a primary aquifer and, generally, is saturated and yields sufficient quantities of groundwater for irrigation purposes. Areas of the *To* with the greatest abundance of groundwater occur where the Platte River or its ancestral drainages developed (Diffendal, 1995).

2.1.3 Cretaceous Geology

Both Upper and Lower Cretaceous units are present in the project area. The Upper Cretaceous bedrock formations are the *Kp, Kn*, *Kc* (CSD TH 24-A-51), *Kgg* (CSD TH 26-A-51 and TH 25-B-63), which lie unconformably over the *Kd*. Together these formations are comprised of interbedded to sandy shale, indurated to shaly chalk, thin layers of bentonite, limestone, and massive sandstone (Condra and Reed, 1959; Gutentag et al., 1984). These formations thin and pinch out eastward (Divine, 2012), but where present, act as a lower confining unit to saturated Quaternary deposits. None of the Upper Cretaceous formations yield considerable amounts of potable groundwater within the project boundaries. However, in some areas of eastern Nebraska, where fractured, the *Kn* is known to yield water for irrigation purposes (Gutentag et al., 1984; Miller and Appel, 1997).

Underlying the Upper Cretaceous formations is the regionally extensive *Kd*. This formation is comprised primarily of massive to interbedded sandstone with ironstone and some argillaceous to slightly sandy shale (Condra and Reed, 1959). The sandstone in the *Kd* typically has low permeability and storage compared to the unconsolidated units overlying it. A hydraulic connection can exist in locations where the *Kd* is in contact with overlying saturated Quaternary deposits (Gutentag et al., 1984).

2.1.4 Jurassic and Triassic Geology

Strata considered to correlate with Jurassic and Triassic deposits have been identified in cuttings in western Nebraska. However, these units are not known to exist in eastern Nebraska (Condra and Reed, 1959).

2.1.5 Paleozoic System

Historic cross sections and lithologic logs from deep oil and gas wells allow for the identification of Paleozoic units in limited locations of the project area. Although strata is identified in the following subsections by geologic period, all Paleozoic units are undifferentiated in the interpretive analysis for this report.

2.1.5.1 Permian Geology

Permian deposits, composed primarily of massive to bedded limestone, fossiliferous limestone, shale, evaporites, sandstone, and siltstone are present beneath southern and eastern Nebraska. Some of the carbonates can be dolomitic and interbedded with shale. Although some of these units crop out in southeast Nebraska, they are missing in the stratigraphic sequence immediately beneath the project area. This information on the strata's absence in the project area is based on stratigraphic selections described in Nebraska Oil and Gas Conservation Commission (NOGCC) test holes.

2.1.5.2 Carboniferous Geology

Carboniferous deposits, Upper (Pennsylvanian) and Lower (Mississippian) subsystems underlie all of Nebraska except for a few square miles in the northeast part of the state (Condra and Reed, 1959). Undifferentiated deposits of the Carboniferous System include the Wabaunsee, Shawnee, Douglas, Pedee, Lansing, Kansas City, Bronson, Marmaton, Cherokee, Osage-Meramec, and Kinderhook Groups. Korus (2012) reports *IP* deposits that extend beneath parts of the project area are the undifferentiated Kansas City and Lansing Groups, and the undifferentiated Marmaton and Pleasanton Groups. Similar to the Permian deposits, these Carboniferous groups are comprised of massive to bedded and fossiliferous limestone that can be dolomitic with interbedded shale, evaporites, sandstone, and siltstone. Shale deposits can be substantial sequences that are comprised of argillaceous, arenaceous, fissile, and/or limy type shale (Condra and Reed, 1959). The Kansas City and Lansing Groups are primarily inter-bedded limestone and shale (Hanson et al., 2012). In addition, the Kansas City, Lansing, Marmaton, and Pleasanton Groups are part of the Western Interior Plains confining system overlying the upper aquifer unit of the Western Interior Plains aquifer system—part of which a member is the Kinderhook Group (Jorgensen et al., 1993; Signor et al., 1996).

2.1.5.3 Devonian Geology

Devonian deposits unconformably underlie Carboniferous through the southeastern one-third of Nebraska. The Devonian deposits are largely a sequence of limestones, dolomites, and shales that thin westward and northwestward and are absent over the Cambridge Arch (Condra and Reed, 1959). It is unknown to what extent Devonian rocks exist in the project area.

2.1.5.4 Silurian Geology

Silurian deposits underlie the east to southeast quarter of Nebraska and are thickest in the southeast corner of the state and thin northward. While most Silurian rocks in Nebraska have been dolomitized, they act as an important groundwater reservoir in the Omaha, NE area (Condra and Reed, 1959).

2.1.5.5 Ordovician Geology

Ordovician deposits underlie parts of eastern Nebraska including the principle units of the Richmond and Trenton Groups. These deposits generally are oolitic and hematitic shales overlying dolomites. Similar to the Silurian deposits, they produce some groundwater in deep wells in the Omaha area. While the presence of groundwater from Ordovician deposits increases to the west, these water resources are highly mineralized (Condra and Reed, 1959).

2.2 Hydrogeologic Characteristics of the Quaternary System

Major streams and rivers within the project area are shown in Figure 2-4. Across much of the project area, stream-dissected glacial till have created a dendritic pattern of perennial and seasonal streams. The largest surface-water system in the project area is the Elkhorn River (U.S. Geological Survey, 2015) which flows easterly to southeastward from the Sand Hills west of the project area to its confluence with the Platte River west of Omaha, NE. Mean annual discharge in 2013 at Norfolk, NE (USGS station number 06799000) was 287.3 cubic feet per second (ft^3/s) and 517.9 ft^3/s at West Point, NE. Tributaries to the Elkhorn River include the North Fork of the Elkhorn River near Pierce, NE (USGS station number 06799100; 2013, 34.3 ft^3/s), Logan Creek (USGS station number 06799445; 2013, at Wakefield, NE 84.8 ft^3/s; USGS station number 06799500; 2012, near Uehling, NE, 243 ft^3/s) (U.S. Geological Survey, 2015), and Maple Creek near Nickerson, NE (USGS station number 06800000, 34.3 ft^3/s), as well as many smaller streams. The North Fork of the Elkhorn River and Logan Creek drain southward and discharge into the Elkhorn River.

A limited number of surface-water impoundments are present in the project area, with the largest feature located at the Willow Creek State Recreation Area (700 acre flood control reservoir) southwest of Pierce, NE, and many other smaller lakes, sandpits, and reservoirs. Numerous sandpits and small lakes are located adjacent, or in close proximity, to the Elkhorn River or other major streams.

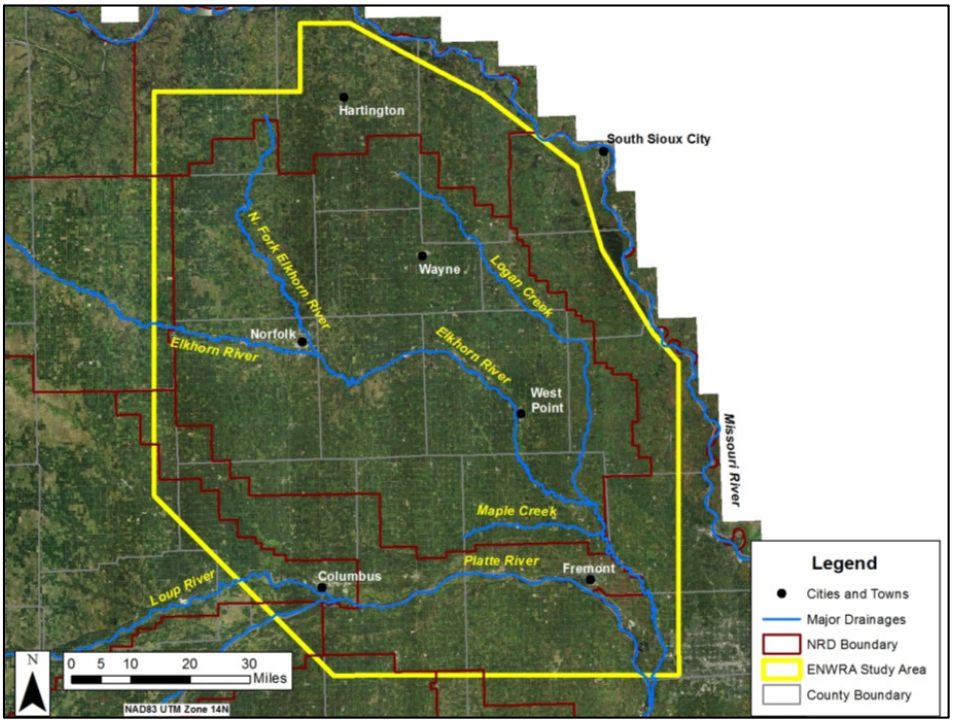


Figure 2-4: Map displaying the major streams and rivers within the northern ENWRA project area.

Regional groundwater-flow direction within the project area is primarily northeast to southwest (Bentall, 1971; Flowerday et al., 1998) and locally can be hydraulically connected to shallower aquifers or surface water systems (Stanton et al., 2007). Groundwater levels are located at shallower depths in

the alluvial valleys and at greater depths beneath glaciated areas, and typically reach maximum depths from extensive groundwater pumpage during the crop growing months. Groundwater levels typically return to shallower, pre-stress levels in the March to June timeframe. Annual depths of drawdown and recharge of aquifers depend on the type of aquifer (e.g., confined or unconfined), proximity of the aquifer to the land surface, and the magnitude of stress exhibited on the system during the pumping season, combined with the amount of recharge available to the aquifer. Groundwater under confined systems, such as in aquifers beneath glacial till, typically exhibits more drawdown than groundwater in unconfined systems that are present in alluvial settings.

Potentiometric gradients show groundwater movement from upland areas toward stream valleys. Hilly topography and complex heterogeneity within the glacial-drift terrain can create local flow systems (Gates et al., 2014). Contrasts of hydraulic conductivity within the principal aquifers of eastern Nebraska, including the Maha aquifer, can commonly cause significant vertical groundwater flow gradients (Summerside et al., 2001).

Two principal Quaternary hydrogeologic units are present within the project area. The first are saturated alluvial deposits that make up the stream-valley (valley fill) aquifers (Figure 2-5). The second are glacial-drift aquifers which are alluvial and paleo-alluvial or paleo-glacial deposits of Plio-Pleistocene age that underlie till and loess deposits in the uplands and/or that make up the paleovalley deposits (Figure 2-6). Saturated Quaternary deposits in northeast Nebraska are a complex mixture of unconsolidated, saturated sand and gravel deposits. These saturated deposits can be confined to unconfined, deep to shallow, and/or regional and local, and, in places, interbedded with glacial till (Bentall, 1971; Miller and Appel, 1997; Flowerday et al., 1998; Stanton et al., 2007). Stream-valley and glacial-drift systems locally can be hydraulically connected with other, similar systems and/or bedrock aquifers. In addition, aquifers in the project area are typically associated with modern or abandoned stream valleys or with elongated paleovalleys (Gates et al., 2014; Szilagyi et al., 2005). Alluvium near the glacial-till border, deposited from Platte River tributaries are Pliocene to Holocene in age (Diffendal, 1995). Table 2-1 contains summary information for each known aquifer (Quaternary through Cretaceous) within the area. Included in this table is the geologic system hosting the aquifer, aquifer thickness, a general discussion regarding the aquifer framework, groundwater flow system characteristics, and aquifer parameters.

The stream-valley aquifers yield groundwater at rates that support the widespread use of wells for irrigation and other industrial needs, specifically near the Elkhorn River, the North Fork of the Elkhorn, and the Logan and Maple Creeks. Most of the water in stream-valley or alluvial aquifers is under unconfined or water-table conditions with local confined conditions where overlying fine-grained sediments cap the aquifers. Stream-valley aquifers consist mostly of Holocene sand and gravel. The stream-valley sand and gravel deposits in many locations have been reworked from older glacial-drift deposits and are difficult to distinguish from glacial outwash (Miller and Appel, 1997). Locally, stream-valley aquifers can be hydraulically connected to underlying semi-consolidated or bedrock aquifers, such as the *To* or *Kd*. In much of the project area, stream-valley aquifers are associated with the High Plains Aquifer whose primary unit is the *To*.

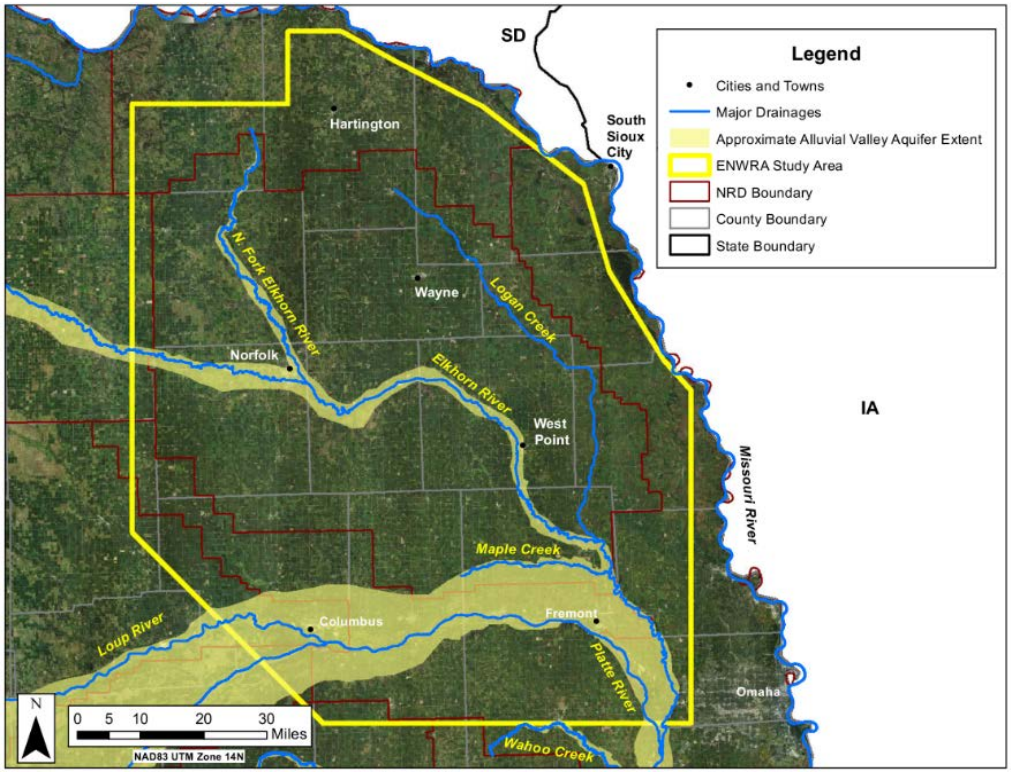


Figure 2-5: Mapped alluvial valley areas hosting alluvial aquifers in the northern ENWRA project area, modified from the Nebraska Groundwater Atlas (Korus et al.,2013b).

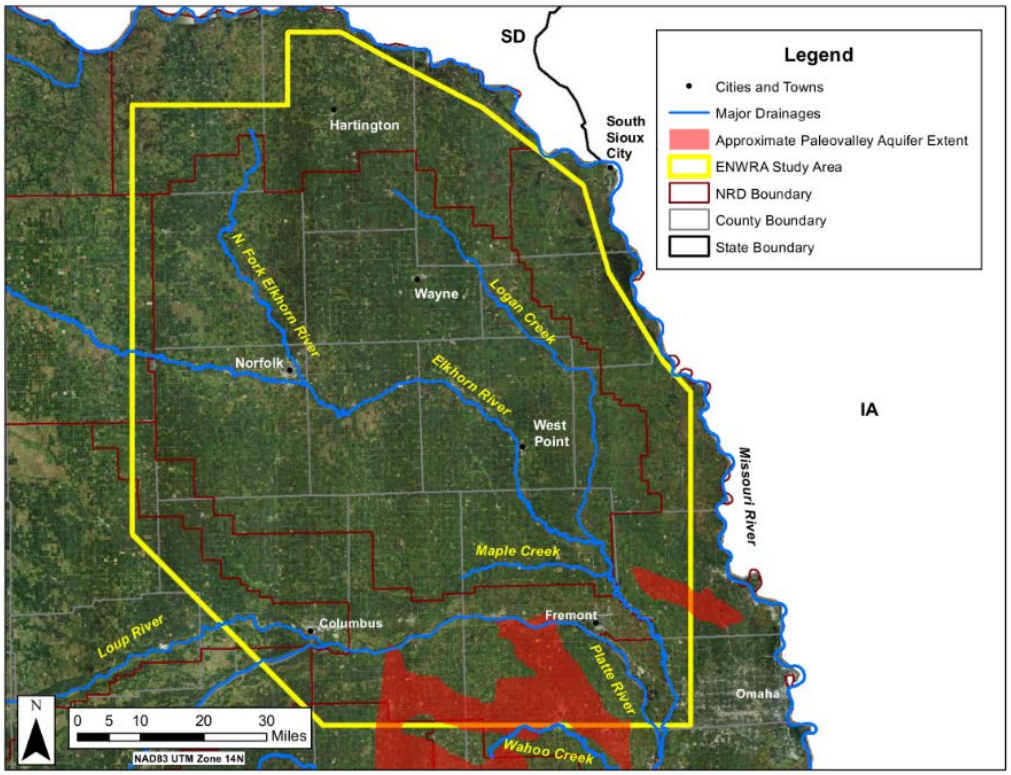


Figure 2-6: Mapped paleovalleys in the northern ENWRA project area, modified from the Nebraska Groundwater Atlas (Korus et al., 2013b).

Availability of groundwater in glacial-drift aquifers is highly variable. The potentiometric head in glacial-drift aquifers is often a composite surface. The aquifers are comprised of unconfined and confined systems due to the complex interbedding of deposits with varying permeability and large numbers of locally confining units (Miller and Appel, 1997). Consequently, groundwater in glacial-drift aquifers could be under confined conditions in one area and unconfined conditions in others. Results of a composite aquifer test conducted in a glacial-drift aquifer west of Oakland, NE indicated a transmissivity for a paleovalley aquifer of about 67,000 gpd/ft (9,000 ft^2/d) and a hydraulic conductivity of about 72 ft/d (U.S. Geological Survey, personal comm., 2009).

Recharge to stream-valley aquifers is largely from local precipitation, although additional sources of recharge can occur from downward percolation of irrigation waters or inflow from underlying permeable aquifers. Estimated regional mean annual recharge rates for stream valleys within the project area range from about 3.7 to 5.5 inches per year (in/yr) with local annual recharge rates up to 6.4 in/yr. In the uplands beyond the stream valleys, regional estimated annual recharge rates generally range from 2.4 to 5.5 in/yr (Szilagyi et al., 2005). An analysis of statewide data determined that the total recharge for the Nebraska glaciated region averaged about 2.2 in/yr (56 mm/year) (Szilagyi and Jozsa, 2013; Gates et al., 2014) and was similar to rates determined using other methods (Nolan et al., 2007; Gates et al., 2014).

Table 2-1: Aquifers in Quaternary to Cretaceous stratigraphic units in eastern Nebraska.

System	Series	Hydrologic unit	Maximum thickness (ft)
Quaternary	Holocene, Pleistocene	Aquifer in undifferentiated alluvial deposits	Generally less than 100 ft
Undifferentiated sand and gravel units in stream-valley systems. Stream-aquifer systems can be intermixed with older glacial sand and gravel making the deposits difficult to distinguish from older glacial outwash. Hydraulic head is typically unconfined. Recharge is principally from local precipitation and is rapid if the source area is primarily sand and gravel. Wells are capable of yielding up to several thousand gpm.			
Quaternary	Holocene, Pleistocene	Aquifer in undifferentiated glacial-drift deposits	Up to 300 ft
Undifferentiated sand and gravel units in glacial-drift aquifers. Hydraulic head is generally under confined conditions, with isolated unconfined conditions elsewhere. Thickness of glacial-drift aquifers vary greatly. Comprised largely of sand and gravel from ancestral river channels or glacial outwash that became capped by till or loess. Some paleovalleys are several miles wide and tens of miles long. Recharge mostly from precipitation infiltration or inflow from adjacent hydraulically connected aquifers. Well yields are highly variable; some capable of up to several thousand gallons per minute but vary greatly by location. Isolated aquifers are capable of sustaining potable quality water for domestic or stock purposes only.			
Cretaceous	Upper	Confining units of the Pierre, Niobrara, Carlile, or Greenhorn–Graneros Formations	Variable
Where present, largely serve as regional confining units. Niobrara Formation may produce water where secondary fracturing occurs.			
Cretaceous	Lower	Aquifer in sandstone of the *Kd*	Total thickness variable. Up to 600 ft in the project area
Locally, the *Kd* serves as an aquifer or as a confining unit. The aquifer is generally located in loosely-cemented, medium- to fine-grained sandstone. Hydraulic head typically confined with local unconfined conditions encountered. Groundwater more potable in eastern part of the state, where the *Kd* underlies saturated Quaternary deposits, hydrologic connection can occur. Westerly, the *Kd* becomes more mineralized and is found deeper beneath the surface. Where *Kd* units lie in close proximity to the land surface, recharge is primarily from local precipitation, otherwise largely from inflow from adjacent hydrologically-connected aquifers. Sandstones are capable of producing potable water to irrigation and municipal wells with yields can be as much as 1,000 gallons per minutes locally.			

2.2.1 Aquifer Characteristics

The overall elevation of the water table within the project area is shown in Figure 2-7. The surface displayed in this figure is the 1995 CSD regional water table surface. Although local flow systems are present throughout the region, the general trend in the direction of groundwater movement is from northwest to southeast, with elevations ranging from over 1,800 ft asl in the west/northwestern area of the project area to around 1,100 ft asl near the project area's eastern boundary.

Overall specific yield in the project area ranges from 0.05 to 0.20, with 0.15 to 0.20 in alluvium and unconfined systems in and adjacent to the Elkhorn and the North Fork of the Elkhorn River and 0.05 to 0.10 in confined areas underlying the upland till. Specific yield is 0.20 beneath large areas west and northwest of Wayne, NE. Conditions in the *To* generally range from 0.10 to 0.20 (Olafsen-Lackey, 2005a; Olafsen-Lackey and Summerside, 2005). Little information exists on the storativity in the Quaternary aquifer material of the project area. In 2009, ENWRA and the USGS conducted a pumping test in a paleovalley setting in the southern ENWRA area near Hickman, NE. This test revealed storativity values in the $5x10^{-4}$ - $6x10^{-4}$ range.

Lower and upper transmissivity values range from 20,000 gpd/ft (2,700 ft^2/d) to 150,000 gpd/ft (20,000 ft^2/d). Transmissivity values are predominantly on the order of 50,000 gpd/ft in alluvium and unconfined systems with local areas of 20,000 or 100,000 gpd/ft. One area along the Elkhorn River west of Norfolk, NE shows a transmissivity of 150,000 gpd/ft. Confined systems are predominantly 20,000 gpd/ft with local areas of 50,000 gpd/ft found northwest of Wayne (Olafsen-Lackey, 2005b; Olafsen-Lackey and Summerside, 2005). An aquifer test in the Oakland area indicated transmissivity values in the glacial-drift pale valley aquifer at approximately 67,000 gpd/ft. This value is of the same magnitude as the 50,000 gpd/ft reported previously for this area (Olafsen-Lackey and Summerside, 2005).

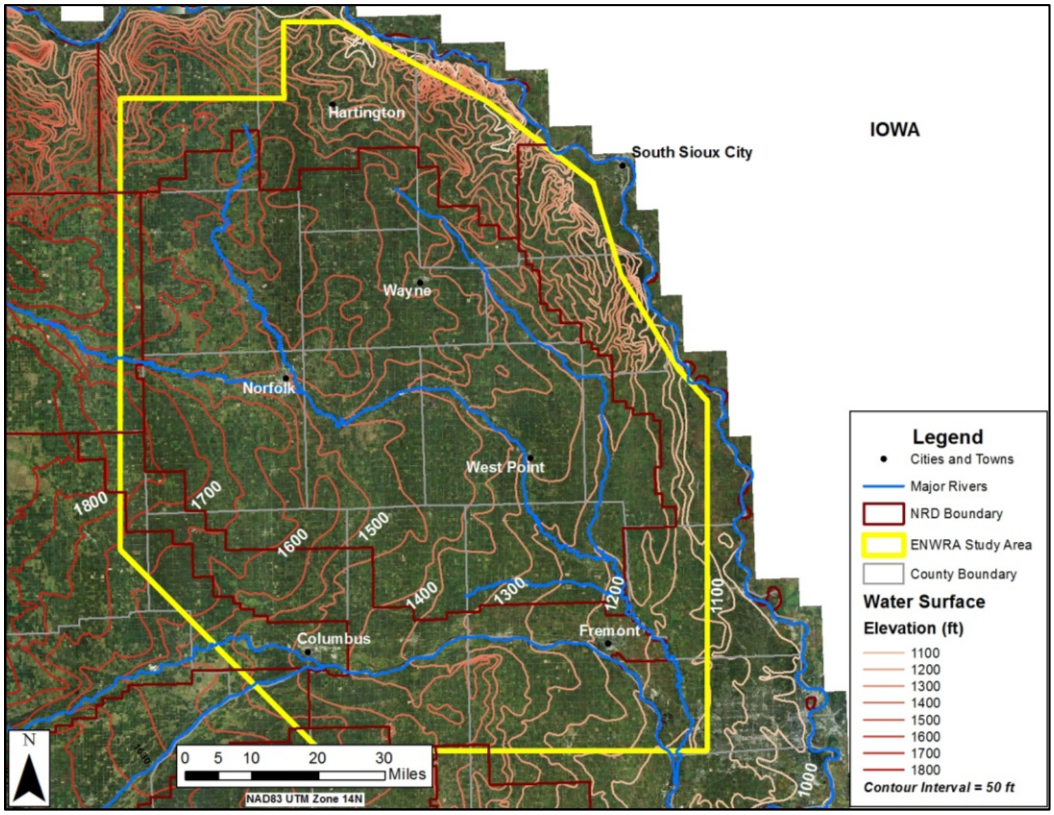


Figure 2-7: Groundwater surface elevations in the northern ENWRA project area (CSD, 1995).

Lower and upper ranges of horizontal hydraulic conductivity in Madison and Pierce Counties were reported between 30 to 50 ft/d (Stanton et al., 2010). Horizontal hydraulic conductivity from a paleovalley aquifer test in the Oakland area show values in the glacial-drift aquifer of 100 to 120 ft/d with a composite value of 72 ft/d. Overall, most horizontal conductivity values within the project area likely range from 10 ft/d in wells open to the *To* to 100 ft/d in wells screened in alluvium and glacial-drift sand and gravel.

2.2.2 Connectivity to Surface Water

Groundwater flow connectivity to surface water features is poorly characterized in the glaciated areas of eastern Nebraska. However, Peterson and Strauch (2007) report streamflow measurements at 531 sites conducted in November 2006 in the Elkhorn and Loup River basins and selected streams in the Niobrara and Platte River basins in north-central Nebraska. Most of these sites were located throughout the

Elkhorn and Loup River basins, while 49 were located in the project area. Results at these 49 sites showed streamflow increasing in a downstream direction, indicating surface-water baseflow increasing downstream in these areas. Streamflow measurements were not collected in the highly glaciated areas of the project area.

Springs are common along several tributaries of the Elkhorn River. Logan Creek and Maple Creek basins experience spring flow and locally have drains installed to keep groundwater levels from flooding farmland. Many of the springs flow primarily during early- to mid-growing season in smaller tributaries; whereas they flow perennially in the major tributaries (Fredrick et al., 2006).

Goeke (2010) reports estimates of 50 to 90 percent of baseflow in the Elkhorn is made up of groundwater. This is thought to be due to less overland runoff in comparison to areas such as the Republican River basin, and much more groundwater contribution from coarse-textured, sandy soils. Overland flow in the project area is more prominent during periods of frequent precipitation and depending on antecedent conditions, can become groundwater recharge or continue as overland flow (Fredrick et al., 2006).

2.2.3 Connectivity to other Aquifers

Locally, Plio-Pleistocene deposits are hydraulically connected to shallower aquifers and streams (Gosselin et al., 1996). Where connected, the deeper aquifers can discharge into the shallow aquifers or into surface streams and play an important role in water chemistry. The amount of communication between the two systems (stream-valley and glacial-drift) is unknown and not well understood. Communication, either horizontally or vertically, likely occurs temporally and/or aerially between stream-valley aquifers and glacial-drift aquifers. It is thought that temporal communication changes with increased pumping during irrigation season (June to September). During this time, groundwater gradients change and communication between the two systems can be enhanced. Aerial communication also occurs as it is very possible that a glacial-drift aquifer (such as a paleovalley aquifer) could be in communication with an aquifer or stream at one location and not another.

2.3 Bedrock Aquifer Conditions

2.3.1 Extent/Structure of Aquifer

Two regionally extensive bedrock aquifers exist in the project area. The western half is underlain in areas by the High Plains aquifer, which is comprised primarily of the *To* (Figure 2-1). This unit extends eastward into the project area from the main body of the aquifer that extends from South Dakota to Texas. According to the CSD statewide geologic bedrock map, a smaller, isolated portion of the *To* covering approximately 150 square miles is present east of Norfolk, NE and underlies the city of Stanton. The High Plains aquifer in this area typically ranges from 25 ft to near 100 ft in thickness, but can approach 300 ft in some locations (Gutentag et al., 1984).

The second regional bedrock aquifer system is the Maha aquifer, composed of permeable sandstone within the *Kd* (Miller and Appel, 1997; Gosselin et al., 2001). The *Kd*/Maha aquifer is considered a

secondary aquifer source in eastern Nebraska (Divine et al., 2009). Ellis (1984) presented a structural map of the "Dakota aquifer system" (Maha) in eastern Nebraska which indicates the unit thinning eastward with a relatively steep gradient immediately beneath the project area (Figure 2-8). From west to east, the unit thins from approximately 600 ft to about 100 ft. Regionally, the system thickens northwestward to over 900 ft in north-central Nebraska.

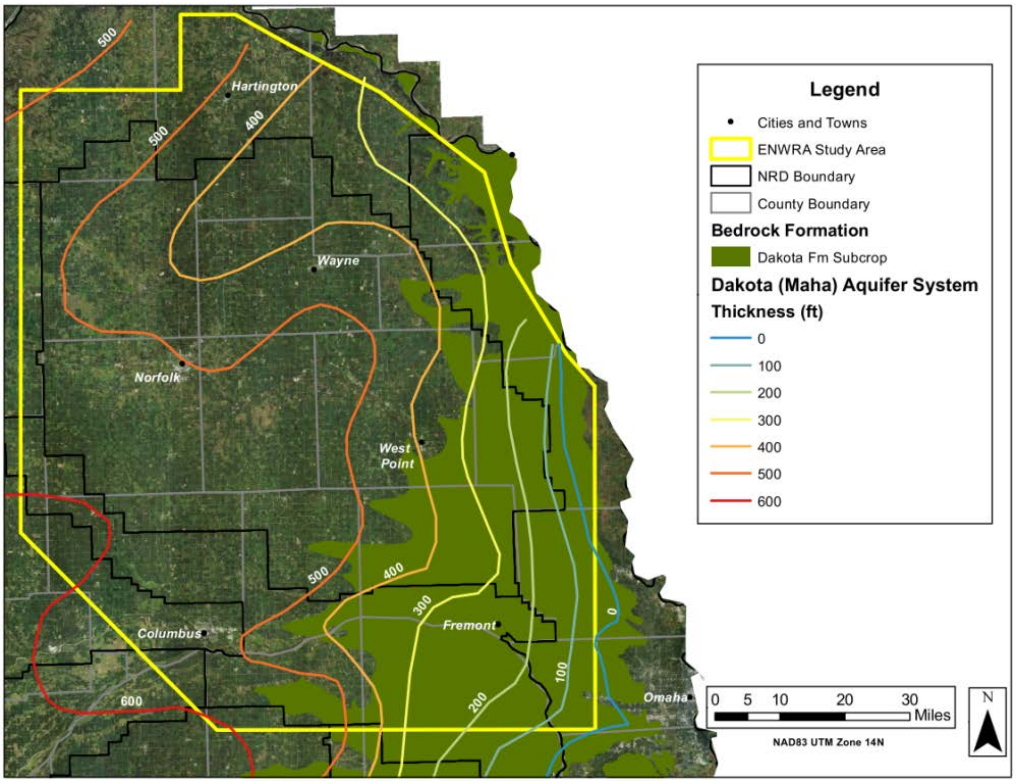


Figure 2-8: Thickness contours of the *Kd*/Maha aquifer in eastern Nebraska (Ellis 1984). The green indicates where the *Kd* is the uppermost subcropping bedrock (Burchett, 1986). Note that the contours and extent of *Kd* subcrop are from different map sources, thus some presence of *Kd* as indicated by the Nebraska bedrock geology map (Burchett, 1986) extends east of the 0 ft thickness contour from Ellis (1984).

2.3.2 Aquifer Characteristics

Available aquifer parameter data are based primarily on regional aquifer evaluations. Transmissivity within the *Kd*/Maha aquifer beneath the project area ranges from around 7,500 to 75,000 gpd/ft (1,000 to 10,000 ft^2/d). In the south-central portion of the project area, transmissivities exceed 75,000 gpd/ft (10,000 ft^2/d) beneath Colfax and northern Butler Counties (Helgesen et al., 1993).

Limited information exists on the porosity of the *Kd*/Maha aquifer. Helgesen et al. (1993) present a regional porosity map within this aquifer based on borehole geophysical logs and laboratory-derived values from literature originating in the oil and gas industry. The nearest contour to the project area, which sits north-south across central Nebraska indicates a porosity value of 0.3. Specific yield estimates for sandstones in the Dakota aquifer in Kansas and Colorado range from 0.1 to 0.2. No storage coefficient values for the confined portion of the system have been identified. However, a specific storage value of 9.5×10^{-7} per ft of aquifer was reported (Helgesen et al., 1993). Multiplying this by 400

ft, the average thickness of the Maha aquifer beneath of the project area, results in a storage coefficient of 3.8×10^{-4}.

2.3.3 Connectivity to Surface Water

Recharge to the *Kd/*Maha aquifer beneath the project area is limited to locations where the bedrock is close to the surface. This occurs most often along deeply-incised surface drainages. In other regions of the *Kd/*Maha aquifer, recharge occurs via infiltration of precipitation along exposed outcrops or shallow subcrops (Helgesen et al., 1993).

Connection to surface water features is limited to where outcrops of the *Kd* are in direct contact with streams at the surface or where permeable bedrock and or fractures are separated from the surface streams by highly permeable streambed sediments.

2.3.4 Connectivity to other Aquifers

Communication with overlying buried glacial outwash aquifers likely occurs, but specific quantification of these fluxes is not known. Gosselin et. al (2001) identified geochemical groundwater signatures that indicated a source from overlying glacial outwash. The degree of communication between the Quaternary and Cretaceous groundwater flow systems is not well understood and likely varies considerably due to local, ambient vertical gradients or through influence of pumping that occurs from both aquifers. Upward vertical communication of groundwater from underlying bedrock units is also possible. The highly saline sources in the *Kd*/Maha aquifer southeast of the project area in Lancaster County have been attributed to sources from the underlying Paleozoic units (Helgesen et al., 1993).

2.4 Water Quality

A total of 740 historic water quality samples were analyzed from the USGS National Water Information System (NWIS) to determine water chemistry characteristics of the project area, — 423 water samples from 184 stream-valley or alluvial wells, 192 water samples from 62 glacial-fill wells, 32 water samples from 31 High Plains aquifer wells, and 93 water samples from 29 wells tapping Cretaceous strata (most likely *Kd*). The water-quality samples from the High Plains aquifer wells likely were collected from wells screened in or open to the *To*. The High Plains aquifer also includes Quaternary deposits.

Median specific electrical conductance for all groundwater samples was 718 µS/cm (Table 2-2). Median calcium, sodium, chloride, and total dissolved solids (TDS) were 99.5, 25.9, 3.6, 39.0, and 448 mg/L, respectively (Figure 2-9 [sulfate not shown], Table 2-2). The maximum specific conductance value was 4,710 µS/cm and the maximum calcium, sodium, chloride, sulfate, and TDS concentrations were 527, 281, 110, 1,390, and 2,470 mg/L, respectively. The maximum value for both specific conductance and TDS was from a sample in a shallow glacial well open to loess or till deposits. Specific conductance values averaged 2,550 µS/cm from 5 water samples. So the 4,710 µS/cm reading would appear as or approach an outlier value.

Water quality data plots are included in Appendix 5 and all water quality data is provided in the data deliverables.

Table 2-2: Statistical results of water-quality analyses from groundwater samples collected in or near the project area, from all wells. Units in milligrams per liter unless stated otherwise. Data are from the US Geological Survey NWIS database; (NA- not analyzed; N- number of samples).

	Minimum	1st Quartile	Median	Mean	3rd Quartile	Maximum	NA's	N
Water temperature (°C)	8.3	11.5	12.5	12.9	13.9	143	18	723
Specific conductance (µS/cm at 25 °C)	96	597	718	764.1	889.8	4710	2	739
pH (standard units)	5.9	7	7.2	7.309	7.6	8.5	83	658
Dissolved oxygen	0.1	0.2	0.7	2.438	4.1	17.2	384	357
Bicarbonate, as CaCO3	37	390	440	465	494	1,240	628	287
Calcium	10.1	82	99.5	103.9	120	527	0	741
Magnesium	1.9	16	21.9	23.63	29	90.5	0	741
Sodium	4.34	17	25.9	30.73	36	281	0	741
Sodium adsorption ratio	0.13	0.4	0.6	0.6956	0.8	3.52	0	741
Potassium	1.41	4.1	6.345	7.136	9	29	18	723
Chloride	1	27	93.5	102.6	162.8	267	2	739
Sulfate	0.18	16	39	77.88	89	1390	1	740
Fluoride	1	19	23	28.7	35	93	213	528
Silicate	8.2	27.75	33	32.5	39	66.8	200	541
TDS	85	355	448	483.2	571	2460	23	718

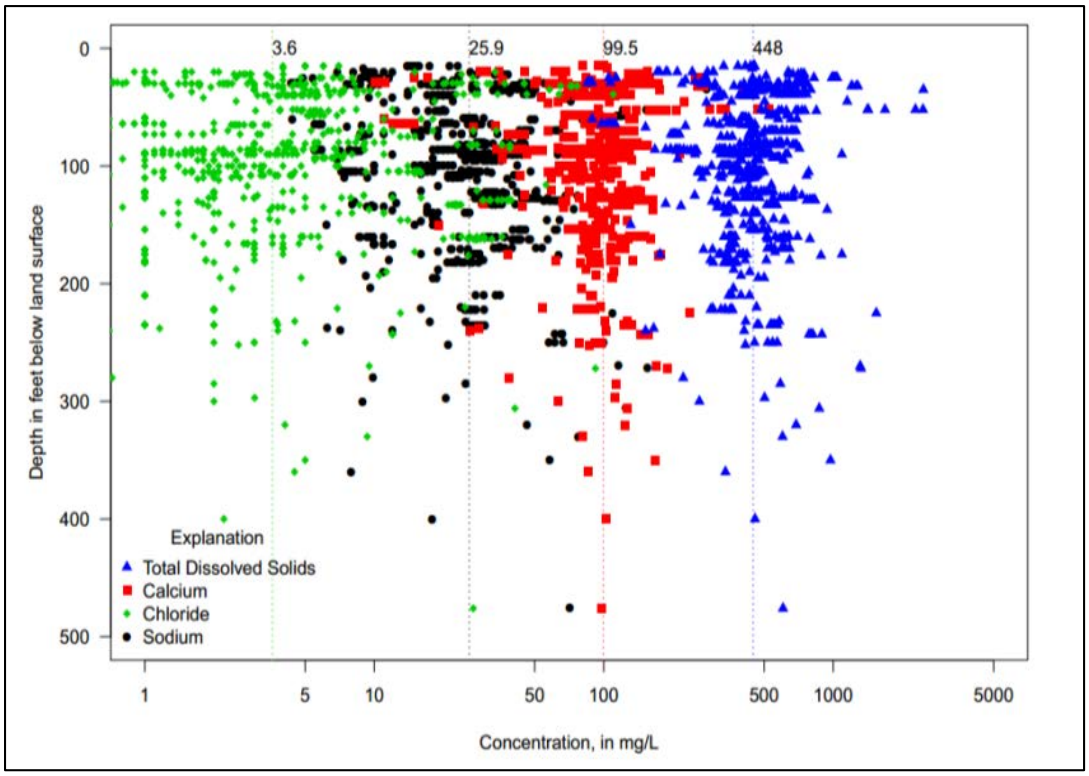


Figure 2-9: Concentrations of TDS, calcium, chloride, and sodium (x-axis) in water samples verses depth (y-axis) Data are from the USGS NWIS.

Most groundwater in the area appears fresh. In some locations, larger specific conductivity, sulfate, and TDS concentrations were observed. The quality of the groundwater in the project area should pose no interference for interpretation of AEM data.

2.4.1 Quaternary Aquifer Water Quality

Groundwater quality in both stream-valley and glacial-fill (Quaternary surficial aquifers) depends largely on overlying deposits. In areas where low yield deposits (i.e., till and loess) overlie aquifers, groundwater quality largely is less impacted than those where sand and gravel deposits are near land surface. In stream-valley systems, groundwater is in close proximity to the land surface and therefore subject to water quality changes due to land use/land cover.

Median specific conductance values from water-quality samples collected from stream-valley and glacial wells were 663 µS/cm (Table 2-3) and 779 µS/cm (Table 2-4), respectively. These values are lower than water samples from the *Kd* wells where median specific conductance was 845 µS/cm (Table 2-5). For stream-valley wells the median calcium, sodium, chloride, sulfate, and TDS concentrations were 91.0, 20.2, 3.20, 40.0, and 413 mg/L, respectively (Table 2-3). The maximum specific conductance value was 1,930 µS/cm and the maximum calcium, sodium, chloride, sulfate, and TDS concentrations were 237, 116, 56.0, 875, and 1,540 mg/L, respectively (Table 2-3). For glacial-fill wells the median calcium, sodium, chloride, sulfate, and TDS concentrations were 104, 33.4, 3.37, 29.0, and 468 mg/L, respectively (Table 2-4). The maximum specific conductance value was 4,710 µS/cm and the maximum calcium, sodium, chloride, sulfate, and TDS concentrations were 527, 281, 110, 1,390, and 2,470 mg/L, respectively (Table 2-4).

Generally, median concentrations of ions and TDS in groundwater were slightly higher in water samples from glacial-fill wells than from stream-valley wells. Sulfate was the only exception where the stream-valley systems contained higher sulfate concentrations than glacially-derived systems. This is thought to be due to the larger dissolved oxygen concentrations observed in the glacial systems than the stream-valley aquifers (2.50 to 0.65 mg/L). Small dissolved oxygen concentrations would help promote oxidation-reduction reactions (redox), which can increase SO_4 concentrations. Dissolved oxygen, however, was not collected in most stream-valley groundwater samples.

Table 2-3: Statistical results of water quality analyses from groundwater samples collected in or near the project area, from stream-valley/alluvial wells. Units are in milligrams per liter unless stated otherwise. Data are from the US Geological Survey NWIS database (NA- not analyzed; N- number of samples).

	Minimum	1st Quartile	Median	Mean	3rd Quartile	Maximum	NA's	N
Water temperature (°C)	8.3	11.7	12.9	12.9	14	22.2	10	413
Specific conductance (µS/cm at 25 °C)	96	513	663	682	857	1,930	2	421
pH (standard units)	5.9	7.1	7.3	7.44	7.8	8.5	17	406
Dissolved oxygen	0.1	0.2	0.65	1.77	1.82	9	343	80
Bicarbonate, as CaCO3	37	44	413	330	437	699	402	21
Calcium	10.1	68	91	93.7	120	237	0	423
Magnesium	1.9	14	20	21.8	28	89	0	423
Sodium	4.34	11	20.2	23.4	29	116	0	423
Sodium adsorption ratio	0.2	0.32	0.5	0.55	0.68	1.8	0	423
Potassium	1.53	4.1	6.1	6.42	8.1	17	9	414
Chloride	0.54	1.7	3.2	6.43	5.94	56	2	421
Sulfate	0.8	15	40	67.4	84.8	875	1	422
Fluoride	0.1	0.3	0.3	0.35	0.4	0.9	50	373
Silicate	12	29.8	33	33.8	39	53	46	377
TDS	85	320	413	434	537	1,540	13	410

Table 2-4: Statistical results of water quality analyses from groundwater samples collected in or near the project area from wells in glacially-derived deposits. Units are in milligrams per liter unless stated otherwise. Data are from the US Geological Survey NWIS database; (NA- not analyzed; N- number of samples).

	Minimum	1st Quartile	Median	Mean	3rd Quartile	Maximum	NA's	N
Water temperature (°C)	9.1	11.6	12.3	12.5	13.2	20.8	7	185
Specific conductance (µS/cm at 25 °C)	418	687	779	910	915	4,710	0	192
pH (standard units)	6.5	6.9	7	7.08	7.2	8.2	48	144
Dissolved oxygen	0.1	0.4	2.5	3.51	6.4	17.2	24	168
Bicarbonate, as CaCO3	192	429	477	545	514	1,240	123	69
Calcium	63	94	104	122	117	527	0	192
Magnesium	11	19.2	24.4	27.7	29.9	90.5	0	192
Sodium	8.73	25	33.4	42.8	47	281	0	192
Sodium adsorption ratio	0.13	0.59	0.73	0.94	1.04	3.52	0	192
Potassium	1.41	3.81	5.44	7.67	8.98	29	0	192
Chloride	<1.00	1.58	3.37	7.76	5.99	110	0	192
Sulfate	<0.18	15.8	29	78.5	58.2	1,390	0	192
Fluoride	0.17	0.3	0.4	0.49	0.6	1.22	104	88
Silicate	14.9	30.8	33.6	32.5	37.6	50.4	104	88
TDS	261	408	468	576	618	2,470	1	191

2.4.2 Bedrock Aquifer Water Quality

Water quality within the bedrock aquifers varies considerably by location and depth. Quality in the *Kd* in eastern Nebraska varies from (1) a Ca(±Mg)HCO_3-type water associated with local precipitation and where the *Kd*/Maha aquifer is unconfined, (2) a $CaSO_4$ and Ca-Na SO_4-type water associated with meltwater from Pleistocene glaciers and where the confining unit is thick, or (3) mixed waters of either $CaSO_4$ and Ca-Na SO_4-type water or NaCl-type water, which represent a possible interaction of the first two types of water or recharge waters have been displaced by NaCl at depth (Gosselin et al., 2001). In the project area, water quality in the *Kd* likely is a $CaSO_4$ and Ca-Na SO_4-type water.

Groundwater can be potable in areas where the *Kd* is unconfined or subject to recharge from local precipitation. TDS concentrations at these locations can be 500 mg/L or less (Ellis, 1984). Elsewhere, groundwater in the *Kd* can be highly mineralized (Stanton et al., 2007).

Table 2-5: Statistical results of water quality analyses from groundwater samples collected in or near the project area from *Kd* wells. Units are in milligrams per liter unless stated otherwise. Data are from the US Geological Survey NWIS database; NA, not analyzed; N, number of samples.

	Minimum	1st Quartile	Median	Mean	3rd Quartile	Maximum	NA's	N
Water temperature (°C)	10.8	11	11.5	13.4	13	143	1	92
Specific conductance (µS/cm at 25 °C)	582	755	845	880	938	2,050	0	93
pH (standard units)	6.7	7	7.1	7.1	7.2	7.7	18	75
Dissolved oxygen	0.1	0.1	0.3	0.48	0.6	2.4	11	82
Bicarbonate, as CaCO3	367	372	384	385	392	410	87	6
Calcium	70.1	104	119	118	129	215	0	93
Magnesium	14.2	21.5	23.7	25.3	29.7	47	0	93
Sodium	16	27.4	32.7	43.3	43.7	186	0	93
Sodium adsorption ratio	0.4	0.63	0.73	0.94	0.99	3	0	93
Potassium	<3.21	6.73	9.9	9.74	11.4	28	9	84
Chloride	<1.00	2	14	17.3	25.6	106	0	93
Sulfate	<2.00	68.9	90	127.3	157	755	0	93
Fluoride	0.71	0.87	0.92	1.1	1.1	2.8	59	34
Silicate	8.2	12.7	14	13.9	14.8	21.9	50	43
TDS	292	460	534	559	602	1,490	9	84

The median specific conductance value from water quality samples collected from *Kd* wells was 845 µS/cm (Table 2-5). As mentioned, this median value is higher than median specific conductance water samples from the stream-valley and glacial wells (Table 2-3 and Table 2-4). For *Kd* wells, the median calcium, sodium, chloride, sulfate, and TDS concentrations were 119, 32.7, 14.0, 19.0, and 534 mg/L, respectively (Table 2-5). These values are also larger than water samples collected from stream-valley and glacial wells. The single glacial well has large specific conductance and TDS values.

Maximum calcium, sodium, chloride, sulfate, and TDS concentrations from *Kd* wells were 215, 186, 106, 755, and 1,490 mg/L, respectively (Table 2-5). Maximum calcium, chloride, and TDS concentrations were

smaller than samples from glacial wells, a condition which is likely due to samples collected from the glacial wells discussed above.

2.5 Water Use

The public supply wells within the ENWRA area are displayed in Figure 2-10. The greatest concentrations of public wells are near the more populated area of northeast Madison County. Registered wells other than public supply wells are found throughout the ENWRA, with irrigation wells being the most numerous. The densest concentrations of irrigation wells are in the western third of the ENWRA as well as in smaller areas near the center and southeastern parts of the project area. Domestic wells are scattered throughout the ENWRA, with the greatest concentration surrounding the Norfolk, NE area.

Figure 2-11 displays the depth to groundwater in the registered wells. Relatively shallow groundwater (less than 50 ft below the subsurface) is present along the surface drainages that slope east/southeastward across the district, most notably along the Elkhorn and North Fork of the Elkhorn River valleys. Trending north/south through the middle of the project area is a zone of wells where groundwater is typically 150 ft deep or greater. In the western third of the area, depth to groundwater is slightly more variable, with the static levels typically between 50 and 150 ft. This variation could be due to wells tapping different aquifers, as the *To* is present in this area. Similar patterns in depth to groundwater are also apparent in the north-central portion of the project area.

Figure 2-12 demonstrates the increase in the number of registered irrigation wells across the northern ENWRA project area from the mid-20th century through 2014 (DNR registered well database, accessed May, 2015). Before the 1960s, irrigation wells were mainly prevalent along the valleys of the major river drainages where shallow groundwater levels typically persist. Over time, as technological advancements of pumps and center-pivot systems allowed for more widespread implementation of irrigation above deeper aquifers and more variable terrain, the number of wells across the northern ENWRA area increased rapidly. The 1970s witnessed the largest increase in the use irrigation wells, with the growth occurring primarily in the western one-fourth of the area, primarily within the LENRD. The increase in irrigation in these areas corresponds to where the High Plains aquifer (*To*) is present. Over the next two decades, the areas already developed continued to fill in with additional wells with isolated areas across the LENRD gaining more irrigation wells. Since 2000, a rapid increase in the number of irrigation wells within the northern LENRD and the LCNRD occurred, likely as a response to the 2001-02 drought that occurred across the High Plains. The irrigation well distribution maps inferentially demonstrate that in parts of the LENRD and the PMRNRD, aquifer resources are not suitable to support widespread groundwater irrigation. Even the maps within the most recent two decades show large areas of these two NRDs with only sparse distributions of irrigation wells in comparison to the surrounding areas. Supporting evidence of the subsurface conditions causing this lack of irrigation wells will be demonstrated in the AEM findings in following sections of this report.

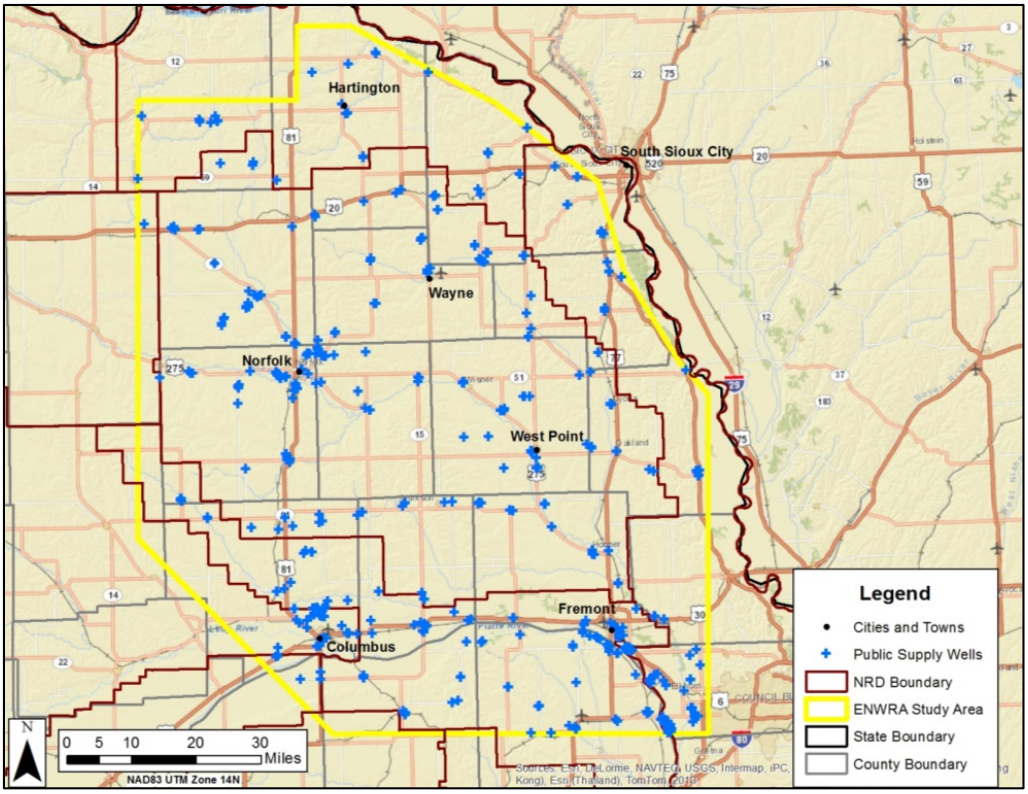


Figure 2-10: Public supply wells within the northern ENWRA project area.

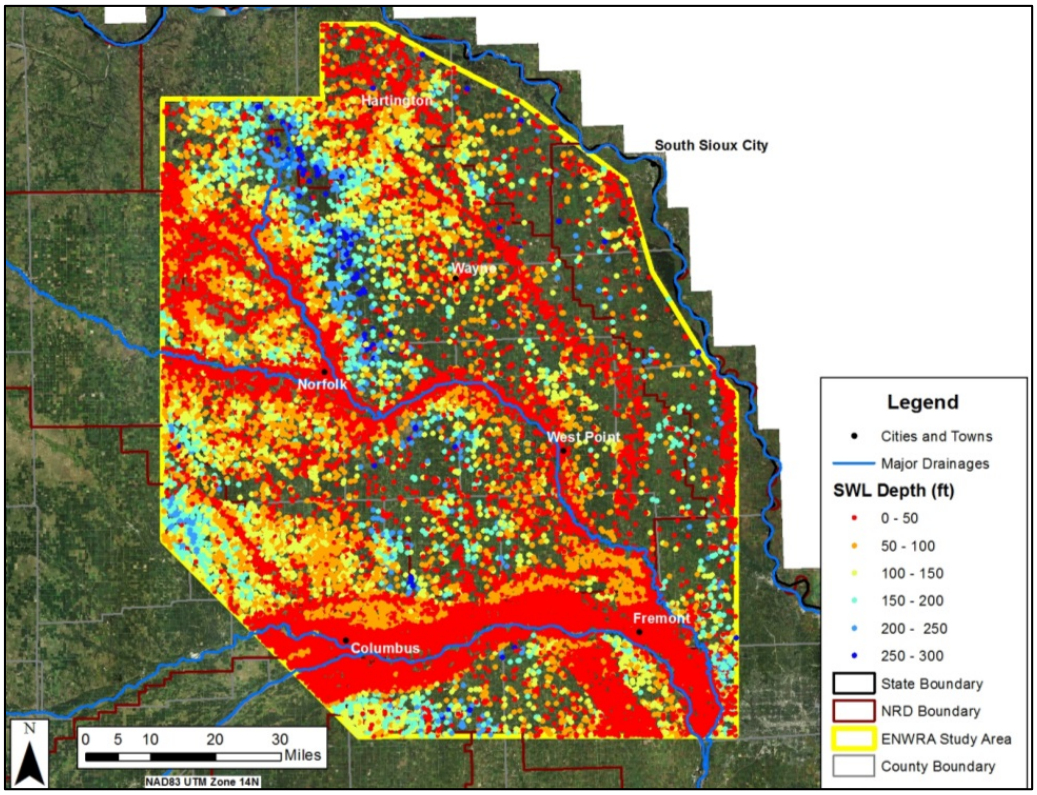


Figure 2-11: Registered wells within the northern ENWRA project area with depth to the static water level indicated by color code.

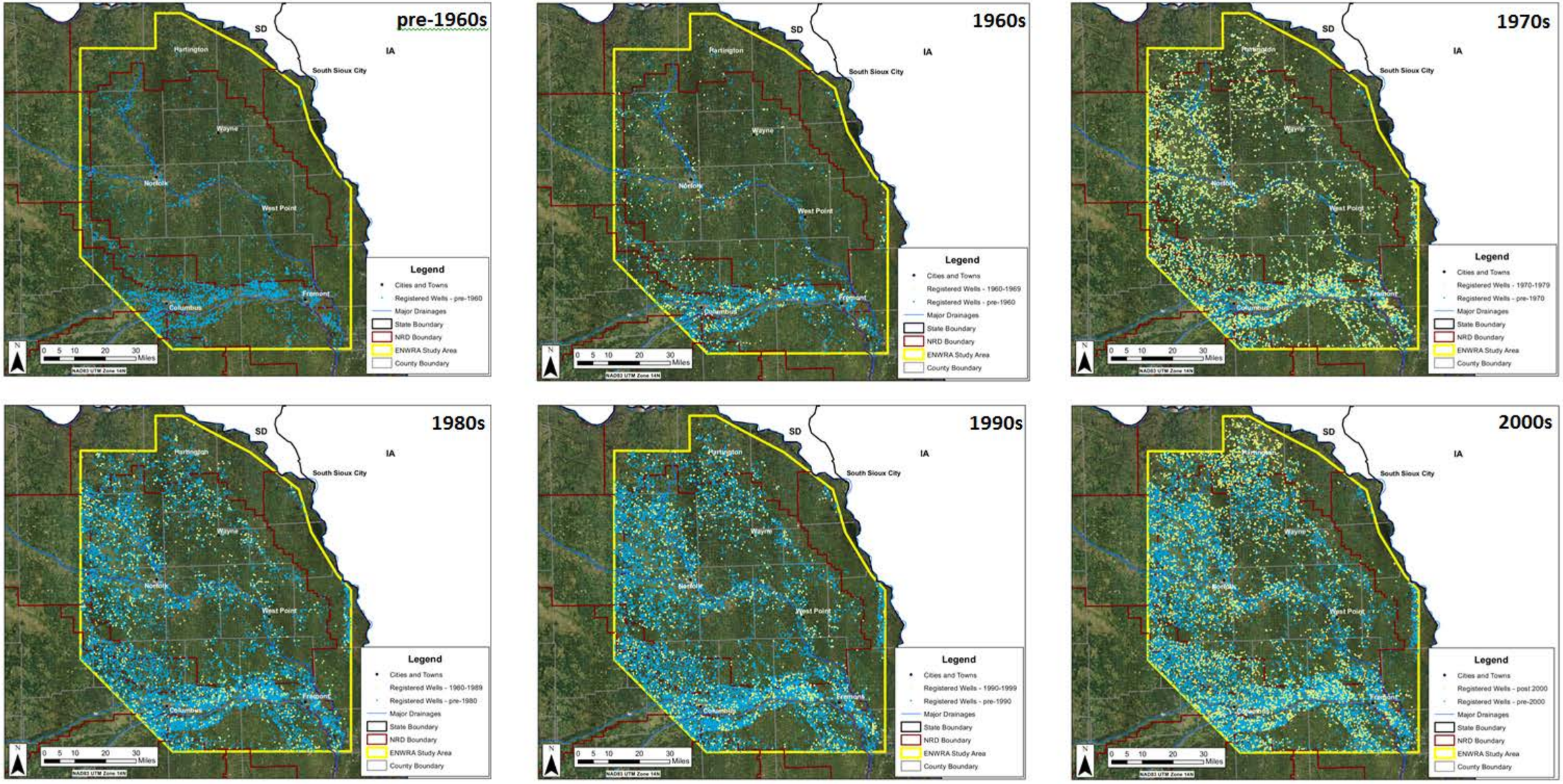


Figure 2-12: Progression of irrigation well development from the pre-1960s (upper left) to 2015 (lower right). Blue dots indicate existing wells and yellow dots indicate new wells constructed during the indicated decade (NDNR).

3 Additional Background Information

Various sources of background information were used to interpret the AEM data, which is discussed in Section 5.

3.1 Borehole Data

Borehole data for this project consisted of a combination of lithologic, stratigraphic, and downhole geophysical logs. Appendix 4 contains all borehole data utilized. The majority of borehole data were acquired from the Nebraska Statewide Test Hole Database (CSD, 2014), which contains information from boreholes drilled between 1930 and 2003 by the CSD and other cooperating agencies. CSD test holes drilled subsequent to 2003 were provided as a dataset directly from ENWRA and are shown in Figure 3-1. Additional borehole data were also acquired from the Nebraska Oil and Gas Conservation Commission (NOGCC) (Nebraska Oil and Gas Conservation Commision, 2008).

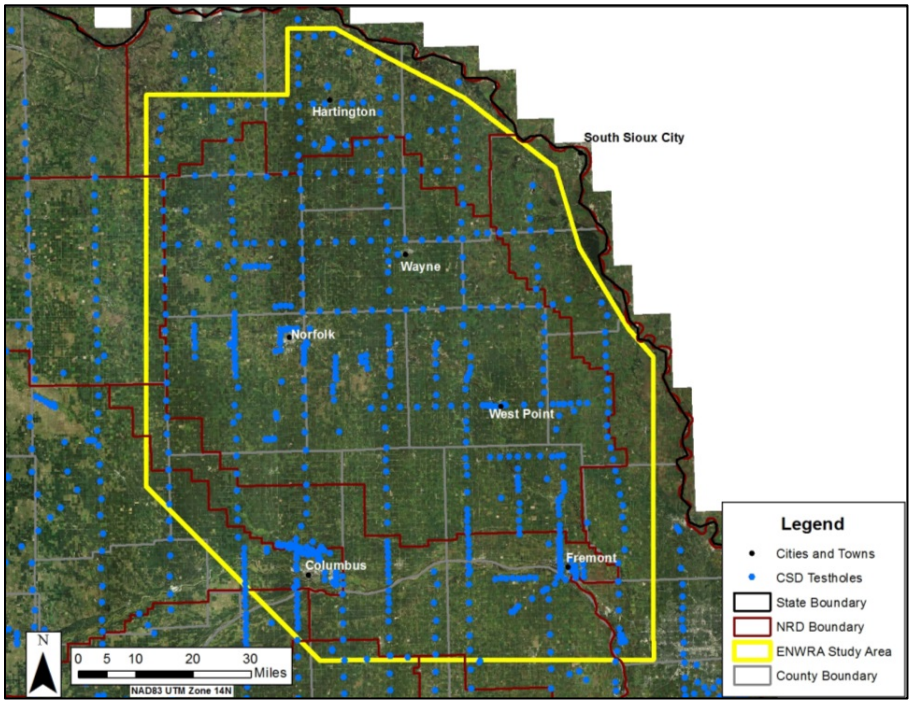


Figure 3-1: Locations of CSD tests holes in the northern ENWRA project area.

The CSD test holes are more numerous and generally much shallower than the oil and gas boreholes, typically less than 500 ft in depth and most do not extend far into bedrock material. Oil and gas boreholes can extend to depths greater than the AEM earth-resistivity models (discussed in Section 5). However, they typically lack the level of near-surface detail provided by the CSD boreholes.

The lithologic and stratigraphic borehole data from both the CSD and oil and gas boreholes were examined in detail. In some instances, specific interval descriptions were generalized to present both datasets with concise lithology and stratigraphy logs. A total of 695 lithology logs and 476 stratigraphy logs were obtained from CSD boreholes; 7 lithology logs and 7 stratigraphy logs were obtained from oil and gas boreholes. The locations of the boreholes containing lithology and stratigraphy data used are depicted in Figure 3-2 and Figure 3-3.



Figure 3-2: Locations of boreholes containing lithologic information in the northern ENWRA project area.

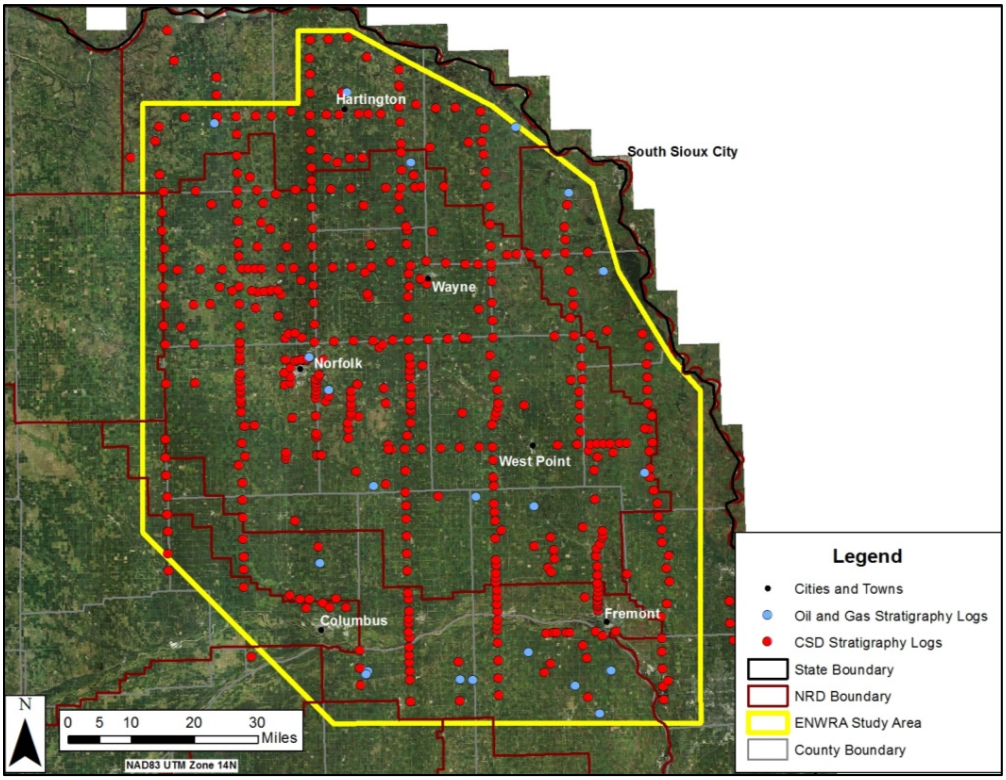


Figure 3-3: Locations of boreholes containing stratigraphic information in the northern ENWRA project area.

Geophysical logs from both CSD boreholes and oil and gas boreholes contained resistivity logs collected from a variety of downhole resistivity and/or induction tools. A total of 104 resistivity logs were obtained from CSD boreholes, with 80 of these logs from boreholes drilled prior to 1998 and 24 from wells drilled after 1998. The geophysical logs from boreholes drilled prior to 1998 usually contain both self-potential data and single-point resistivity data. The geophysical logs from boreholes drilled after 1998 contain a combination of natural gamma, self-potential, single-point resistivity, 16-inch normal resistivity, 64-inch normal resistivity, lateral resistivity, specific conductance of borehole fluid, and borehole fluid temperature data. Geophysical logs were also obtained from two oil and gas wells. These data were acquired as an image of the original paper log which was then converted into digital format. Oil and gas borehole geophysical logs contain a combination of self-potential, short normal resistivity, lateral resistivity, spherically-focused resistivity and deep- and medium-induction log data. A variety of factors can lead to geophysical borehole data that does not accurately measure subsurface physical properties, such as drilling fluid infiltration and improper or infrequent borehole tool calibration.

Each resistivity log was compared to the initial AEM data for correlation, both in magnitude of the reported resistivity values and structural interval delineation. A total of 34 resistivity logs were considered to be high quality data and located in close proximity to the AEM flight lines. These logs were used as constraints in the final AEM data inversion (Section 4.6). The locations of the boreholes containing geophysical logs used in this project are displayed in Figure 3-4.

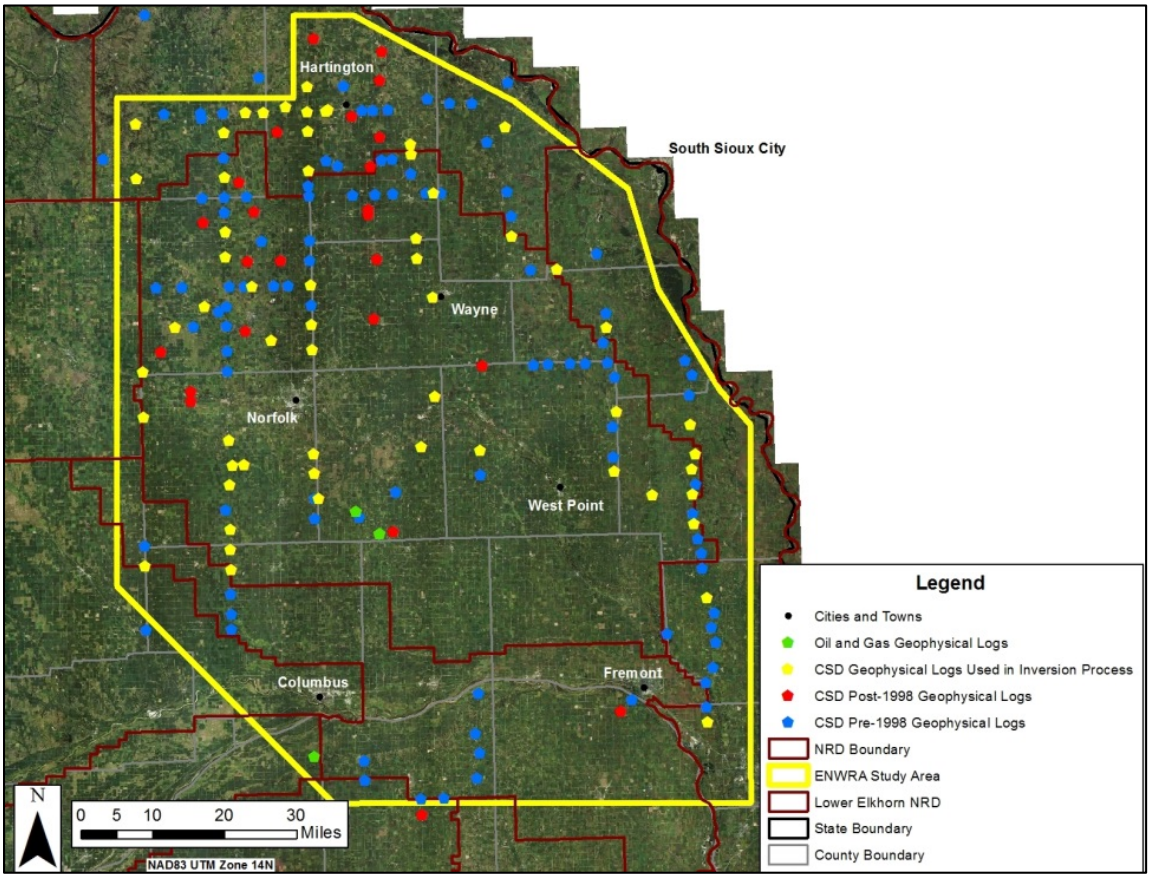


Figure 3-4: Locations of boreholes containing geophysical logs in the northern ENWRA project area.

3.2 Historic Geologic Cross Sections

Several published and previously unpublished geologic cross sections were digitized and geo-referenced (Divine et al., 2010; Korus et al., 2012). The quality of the sections ranged from rough pencil drafts to publishable documents. Figure 3-5 shows their locations and

Table 3-1 lists the cross section names.

Corel Draw was used to digitize each cross section. An example of a cross-section digitization is shown in Figure 3-6. Care was taken to properly place identified CSD borings as these were used to geo-reference each image. Each digitized image was broken up into smaller panels, where each panel began and ended at a known borehole. pbEncom Discover Profile Analyst (PA; pbEncom, 2015) was used to apply positional data to each panel. Figure 3-7 shows the cross-sections in a 3D view in PA. These digitized profiles were used in the interpretation of the AEM results discussed in Section 5.

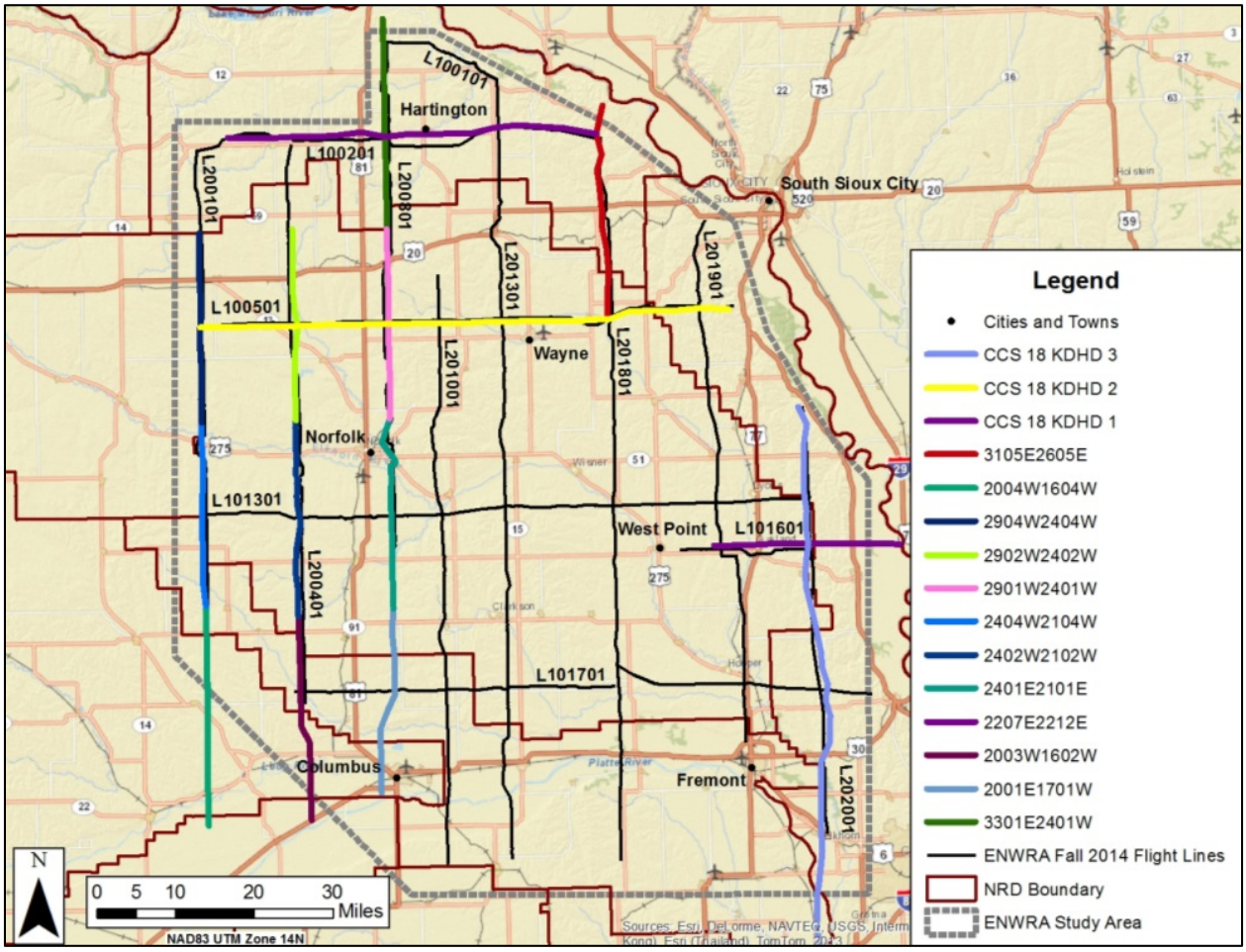


Figure 3-5: Locations of geologic cross sections within the northern ENWRA project area.

Table 3-1: Geologic cross sections from OFR-109 incorporated in the hydrostratigraphic interpretation (Divine et al., 2010; Korus et al., 2012).

Image Name	Associated Line Name
Burt_gen.jpg	2207E2212E
Burt_Saunders.jpg	2208E1208E
Cedar_Madison.jpg	3301E2401W
Dixon_NS.jpg	3105E2605E
Madison_sections.jpg	2401W2101W (top profile)
Madison_sections.jpg	2402W2102W (middle profile)
Madison_sections.jpg	2404W2104W (bottom profile)
Pierece_3NS_EW.jpg	2705W2601W (D-D')
Pierece_3NS_EW.jpg	2901W2401W (C-C')
Pierece_3NS_EW.jpg	2902W2402W (B-B')
Pierece_3NS_EW.jpg	2904W2404W (A-A')
Pierece_Thurston.jpg	2705W2708E
Platte.jpg	2001W1701W (top profile)
Platte.jpg	2003W1602W (middle profile)
Platte.jpg	2004W1604W (bottom profile)

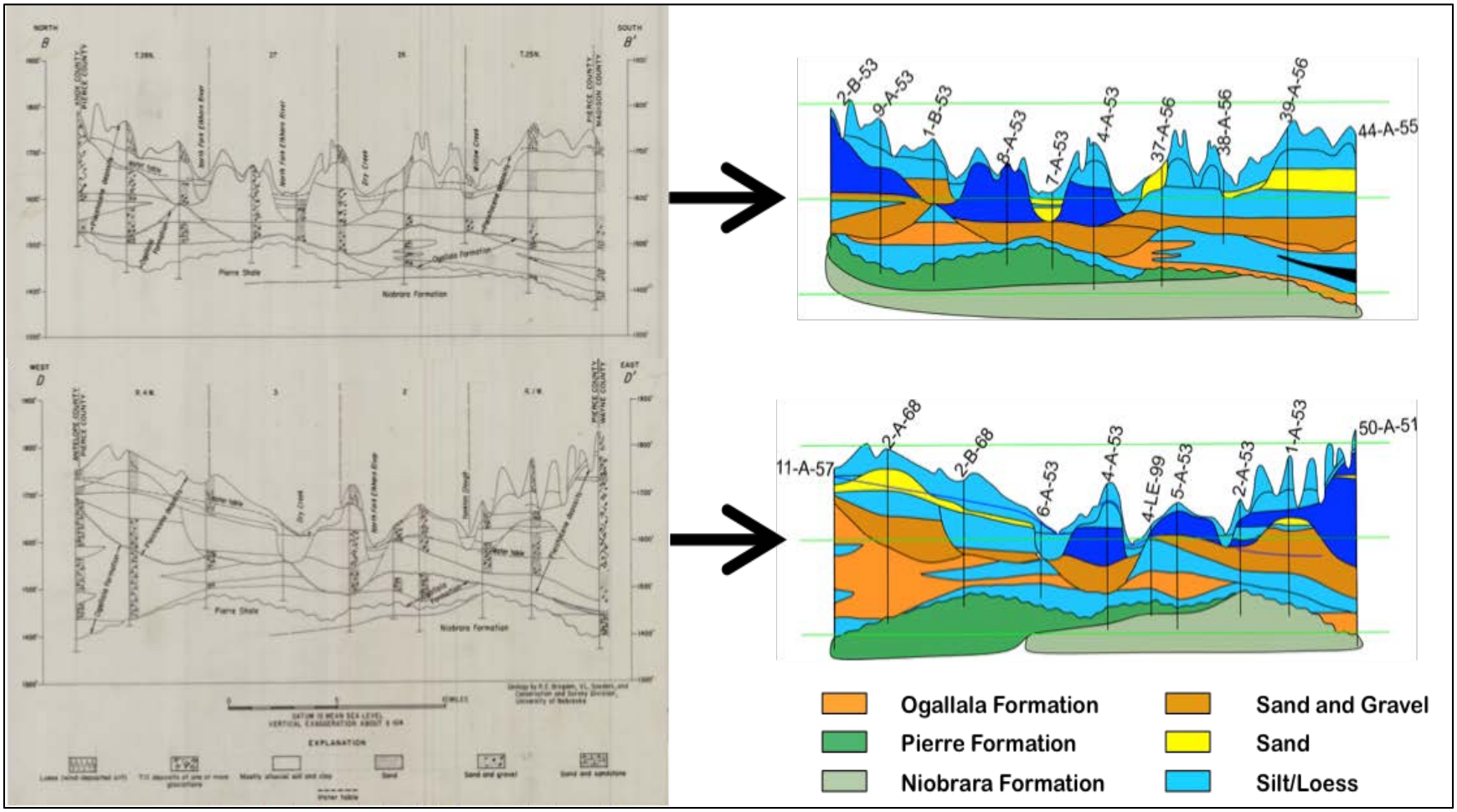


Figure 3-6: Original cross section from CSD OFR 109 (left) and the digitized cross section (right).

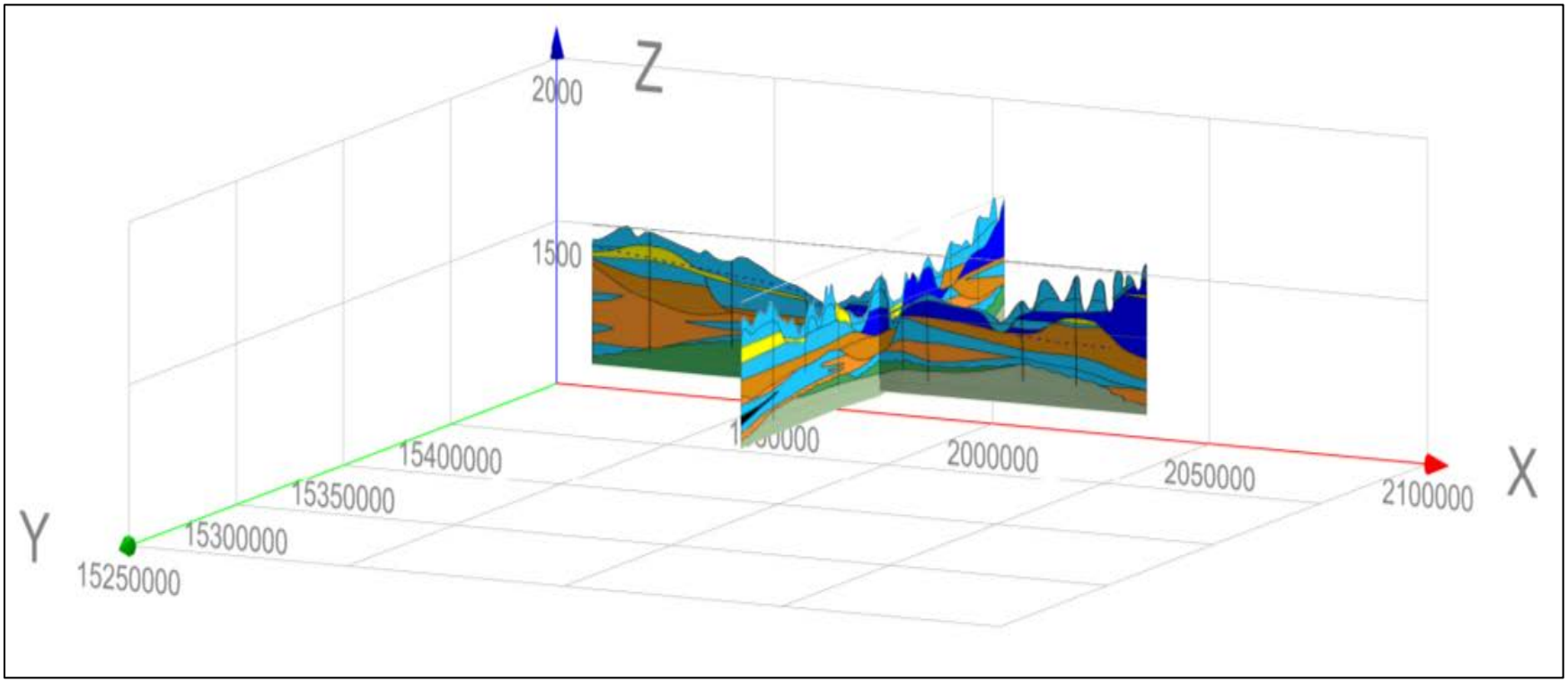


Figure 3-7: 3D view of geo-referenced geologic cross sections used to aid AEM interpretation.

4 Geophysical Methodology, Acquisition and Processing

4.1 Geophysical Methodology

AEM (Airborne Transient Electromagnetic (TEM)) investigations provide characterization of electrical properties of earth materials from the land surface downward using electromagnetic induction. Figure 4-1 gives a conceptual illustration of the airborne TEM method.

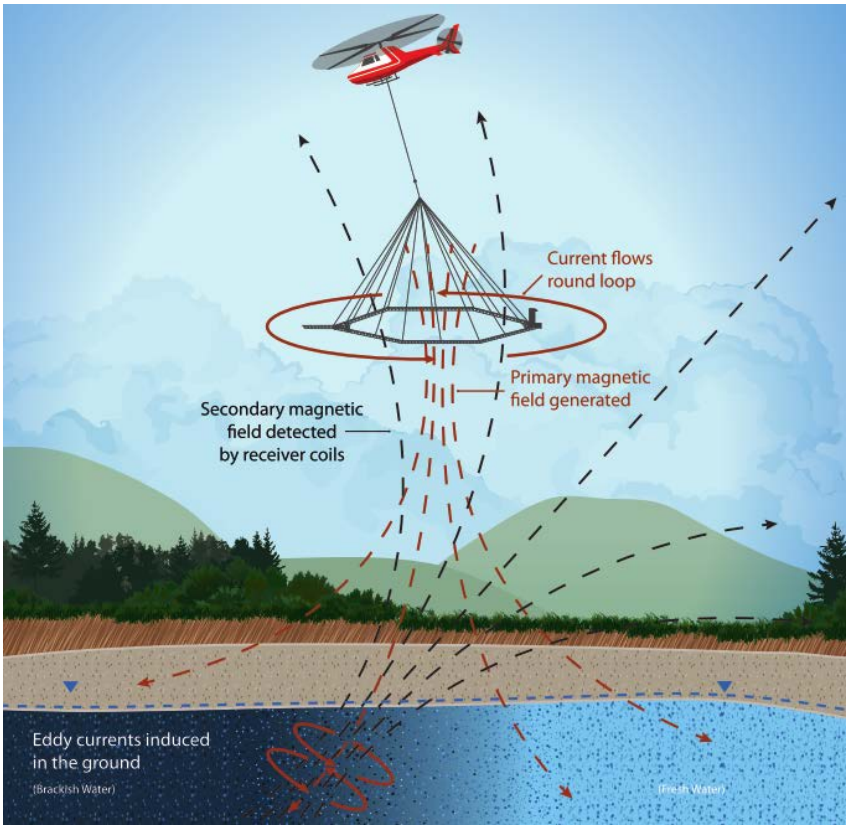
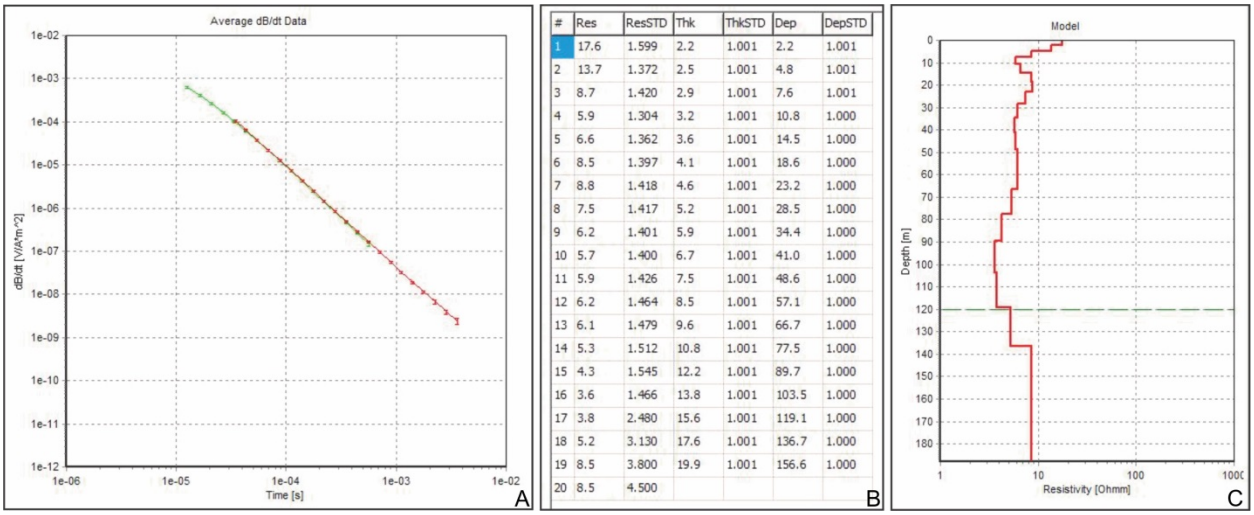


Figure 4-1: Schematic of an AEM survey

To collect TEM data, an electrical current is sent througha large loop of wire consisting of multiple turns which generates an electromagnetic (em) field. This is called the transmitter (Tx) coil. After the em field produced by the Tx coil is stable, it is switched off as abruptly as possible. The em field dissipates and decays with time, traveling deeper and spreading wider into the subsurface. The rate of dissipation is dependent on the electrical properties of the subsurface (controlled by the material composition of the geology including the amount of mineralogical clay, the water content, the presence of dissolved solids, the metallic mineralization, and the percentage of void space). At the moment of turnoff, a secondary em field, which also begins to decay, is generated within the subsurface. The decaying secondary em field generates a current in a receiver (Rx) coil, per Amperes Law. This current is measured at several different moments in time (time gates). From this current, the time rate of decay of the magnetic field, B, is determined (dB/dt). When compiled in time, these measurements become a “sounding” at that location. Each AEM measurement produces an em sounding at one point on the surface.

The sounding curves are numerically inverted to produce a model of subsurface resistivity as a function of depth. Inversion relates the measured geophysical data to probable physical earth properties. Figure 4-2 shows an example of a dual-moment TEM dB/dt sounding curve and the corresponding inverted electrical resistivity model.



#	Res	ResSTD	Thk	ThkSTD	Dep	DepSTD
1	17.6	1.599	2.2	1.001	2.2	1.001
2	13.7	1.372	2.5	1.001	4.8	1.001
3	8.7	1.420	2.9	1.001	7.6	1.001
4	5.9	1.304	3.2	1.001	10.8	1.000
5	6.6	1.362	3.6	1.001	14.5	1.000
6	8.5	1.397	4.1	1.001	18.6	1.000
7	8.8	1.418	4.6	1.001	23.2	1.000
8	7.5	1.417	5.2	1.001	28.5	1.000
9	6.2	1.401	5.9	1.001	34.4	1.000
10	5.7	1.400	6.7	1.001	41.0	1.000
11	5.9	1.426	7.5	1.001	48.6	1.000
12	6.2	1.464	8.5	1.001	57.1	1.000
13	6.1	1.479	9.6	1.001	66.7	1.000
14	5.3	1.512	10.8	1.001	77.5	1.000
15	4.3	1.545	12.2	1.001	89.7	1.000
16	3.6	1.466	13.8	1.001	103.5	1.000
17	3.8	2.480	15.6	1.001	119.1	1.000
18	5.2	3.130	17.6	1.001	136.7	1.000
19	8.5	3.800	19.9	1.001	156.6	1.000
20	8.5	4.500				

Figure 4-2: A) Example of a dB/dt sounding curve. B) Corresponding inverted model values. C) Corresponding resistivity earth model.

4.2 Utility Mapping

The primary source of noise in geophysical electromagnetic surveys are other electromagnetic devices that are part of typical municipal utility infrastructure. These include, for example, power lines, railroads, pipelines, and water pumps. Prior to AEM data acquisition, during the survey design of the ENWRA area, three types of utilities (pipelines, railroads, and power lines) were located. Various public power districts in eastern Nebraska provided power line locations, in either a Google Earth ".kmz" or ".cad" format that were then converted to a Geographic Information Systems (GIS) Arc shapefile format. Public power entities that provided power line location data included: Auburn Board of Public Works, Burt County Power District, Butler County Power District, Cedar-Knox Power District, City of Freemont, Cornhusker Public Power District, Cuming County Power District, Elkhorn Rural Public Power District, Lincoln Electric Systems, Loup Power District, Nebraska Public Power District, Nemaha-Marshall Electric Cooperative, Norris Public Power District, North Central Public Power District, Northeast Nebraska Public Power District, Omaha Public Power District, Polk County Rural Public Power District, Seward County Public Power District, and the Stanton County Public Power District.

A GIS Arc shapefile of railroads in Nebraska was downloaded from the United States Department of Agriculture's Natural Resource Conservation Service (United States Department of Agriculture, 2014) and a shapefile of the pipelines in Nebraska was purchased from Platts (Platts, 2014). Maps, shown in Figure 4-3, of the three utilities were exported in GeoTIFF and .kmz formats and were used during data processing and interpretation.

The locations of the flight lines were modified from a regularly spaced design grid to one with flight lines optimized in order to avoid electromagnetic coupling with the previously mentioned utilities.

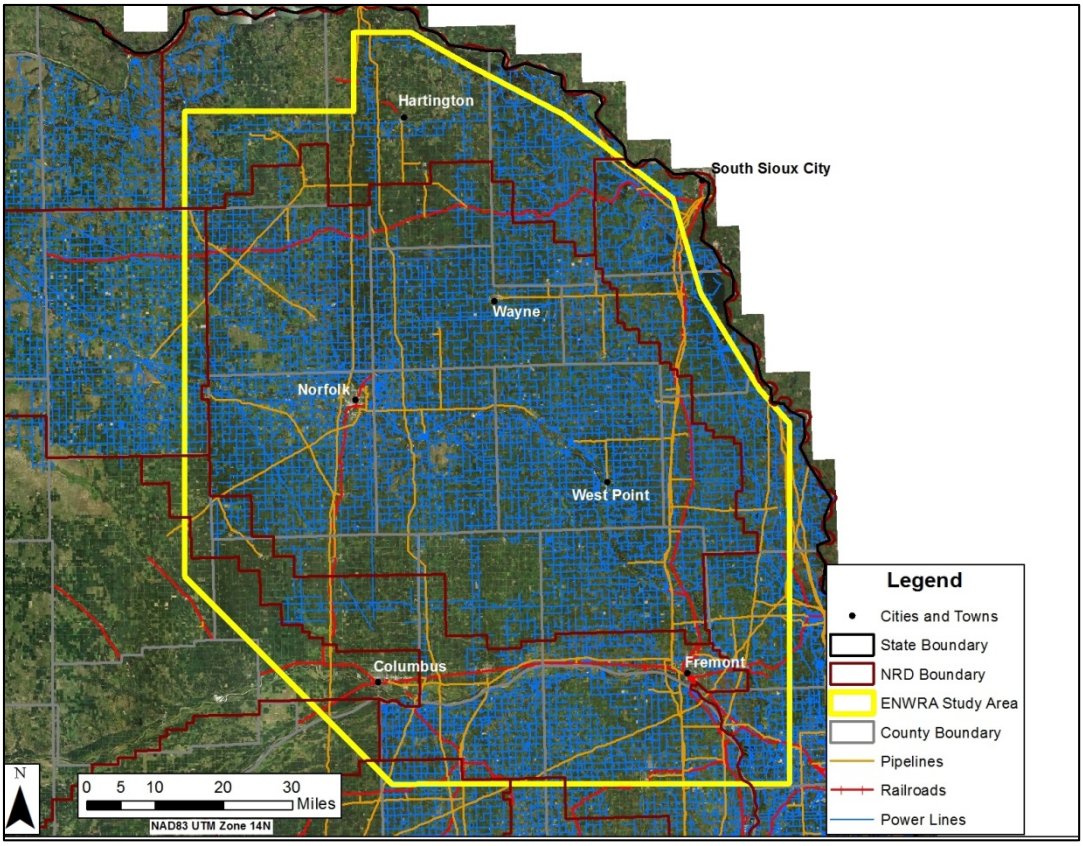


Figure 4-3: Map of the expected utilities in the northern ENWRA project area.

4.3 AEM Survey Instrumentation

AEM data were acquired using the SkyTEM 508 (508) airborne electromagnetic system (SkyTem Airborne Surveys Worldwide, 2015). The 508 is a rigid frame, dual-magnetic moment (Low and High) transient airborne electromagnetic (TEM) system. The area of the 508 Tx coil is 5,769.5 ft2 (536 m2) and the coil contains eight (8) turns of wire. A peak current of 8.6 amps is passed through one turn of wire in the Tx for Low Moment measurements and a peak current of 127 amps is passed through the eight turns of wire for High Moment measurements. This results in peak Tx Low and High magnetic moments of ~4,600 Ampere-meter-squared ($A*m^2$) and ~540,000 $A*m^2$, respectively.

The SkyTEM 508 system utilizes an offset Rx positioned slightly behind the Tx resulting in a 'null' position which is a location where the intensity of the primary field from the system transmitter is minimized. This is desirable because you want to minimize the amplitude of the primary field at the Rx to maximize the sensitivity of the Rx to the secondary fields. The SkyTEM 508 multi-turn Rx coil has an effective area of 1,130 ft^2 (105 m^2). In addition to the Tx and Rx that constitute the TEM instrument, the SkyTEM 508 is also equipped with a Total Field magnetometer and data acquisition systems for both of these instruments. The SkyTEM 508 also includes two each of laser altimeters, inclinometers/tilt meters, and differential global positioning system (DGPS) receivers. Positional data from the frame mounted DGPS receivers are recorded by the AEM data acquisition system. The magnetometer includes a third DGPS receiver whose positional data is recorded by the magnetometer data acquisition system. Figure 4-4 gives a simple illustration of the SkyTEM 508 frame and instrument locations. The image is viewed along

the +z axis looking at the horizontal x-y plane. The axes for the image are labeled with distance in meters. The magnetometer is located on a boom off the front of the frame (right side of image). The Tx coil is located around the octagonal frame and the Rx Coil is located at the back of the frame (left side of image).

The coordinate system used by the 508 defines the +x direction as the direction of flight, the +y direction is defined 90° to the right and the +z direction is downward. The center of the transmitter loop, mounted to the octagonal SkyTEM frame is used as the origin in reference to instrumentation positions. Table 4-1 lists the positions of the instruments (in feet) and Table 4-2 lists the corners of the transmitter loop (marked with red circles in Figure 4-4).

The DGPS and magnetometer mounted on the frame of the SkyTEM508 require the use of base stations, which are located on the ground and are positioned in an area with low cultural noise. Data from the magnetometer and DGPS base stations were downloaded each day after the end of the day's AEM flights. The DGPS and magnetometer base stations were placed at the Universal Transverse Mercator (UTM) coordinate system locations listed in Table 4-3. The horizontal geodetic reference used is North American Datum of 1983 (NAD83 in feet). All elevations are from USGS's National Elevation Dataset, referenced to the North American Vertical Datum of 1988; with feet as the unit of measurement.

For this ENWRA survey, the 508 was flown at an average speed of 50.0 mi/hr (80.5 kilometers/hr) at an average flight height of 141.4 ft (43.1 m) above land surface, using the sling-load cargo system of an AS350 FX2 helicopter. Figure 4-5 displays pictures of the 508 on the ground and in operation.

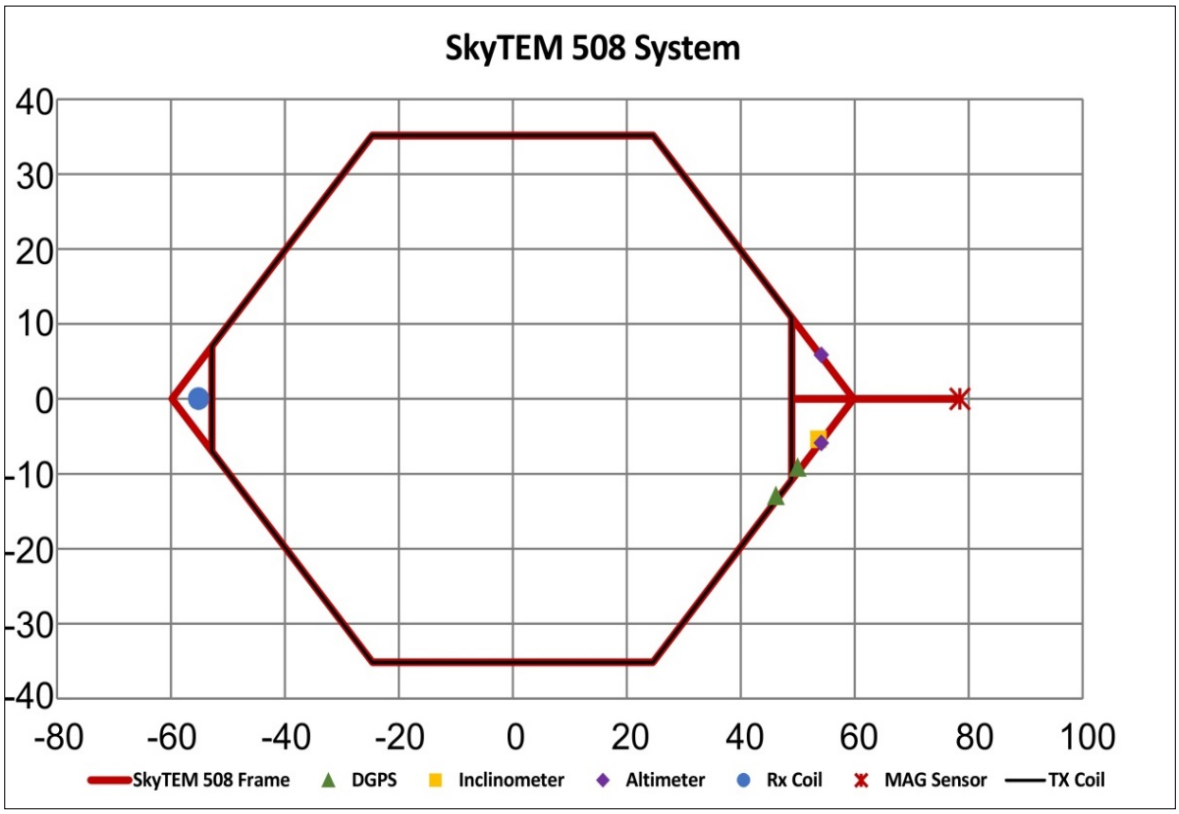


Figure 4-4: SkyTEM 508 frame, including instrumentation locations and X and Y axes.



Figure 4-5: Photos of the SkyTEM508 system on the ground (above) and in suspension beneath the helicopter (below).

Table 4-1: Positions of instruments on the SkyTEM508 frame, using the center of the frame as the origin in feet.

	DGPS 1	DGPS 2	Inclinometer 1	Inclinometer 2	Altimeter 1	Altimeter 2	MAG Sensor	Rx Coil
X	50.00	46.16	53.64	53.64	54.13	54.13	79.79	-55.12
Y	9.15	12.96	5.38	5.38	5.87	-5.87	0.00	0.00
Z	-0.52	-0.52	-0.39	-0.39	-0.39	-0.39	-1.51	-6.56

Table 4-2: Positions of corners of the SkyTEM508 transmitter coil, using the center of the frame as the origin in feet.

Tx Corners	1	2	3	4	5	6	7	8
X	24.64	48.95	48.95	24.64	-24.64	-52.82	-52.82	-24.64
Y	35.17	10.86	-10.86	-35.17	-35.17	-6.99	6.99	35.17

Table 4-3: Locations of magnetic field base station instruments.

Instrument	Easting (ft)	Northing (ft)	UTM Zone
Magnetometer Base Station 1	2067151	15254064	14 N
Magnetometer Base Station 2	2065339	15255616	14 N
DGPS Base Station	2065311	15255605	14 N

4.4 Data Acquisition

All SkyTEM systems are calibrated to a ground test site in Lyngby, Denmark prior to being used for production work (HydroGeophysics Group Aarhus University, 2010; HydroGeophysics Group Aarhus University, 2011; Foged et al., 2013). The calibration process involves acquiring data with the system hovering at different altitudes from 16.4 to 164 ft (5 to 50 m) over the Lyngby site. Acquired data are processed and a scale factor (time and amplitude) is applied so that the inversion process produces the model that approximates the known geology at Lyngby.

For the ENWRA survey, upon installation of the navigational instruments in the helicopter and assembly of the SkyTEM508 system, several test flights were flown in Nebraska to ensure that the equipment was operating within technical specifications. Initial survey set-up procedures included measurement of the transmitter waveforms, verification that the receiver was properly located in a null position, and verification that all positioning instruments were functioning properly. High altitude tests, used to verify system performance, were flown once at the beginning of the survey and repeated throughout the survey. In the field, visual quality control of the operational parameters for the EM and magnetic field sensors including current levels, positioning sensor dropouts, acquisition speed, and system orientation were conducted with proprietary SkyTEM software following each flight.

Airborne data were collected over the survey grids across the project area from 11 – 19 October 2014 and approximately 889.9 line-miles (1432 line-kilometers) were acquired (Figure 4-6). Various airports and state parks were used as landing and refueling locations. These locations are listed in Table 4-4. Table 4-5 lists the locations, dates, and total line miles and corresponding line-kilometers flown for each block investigated in this project.

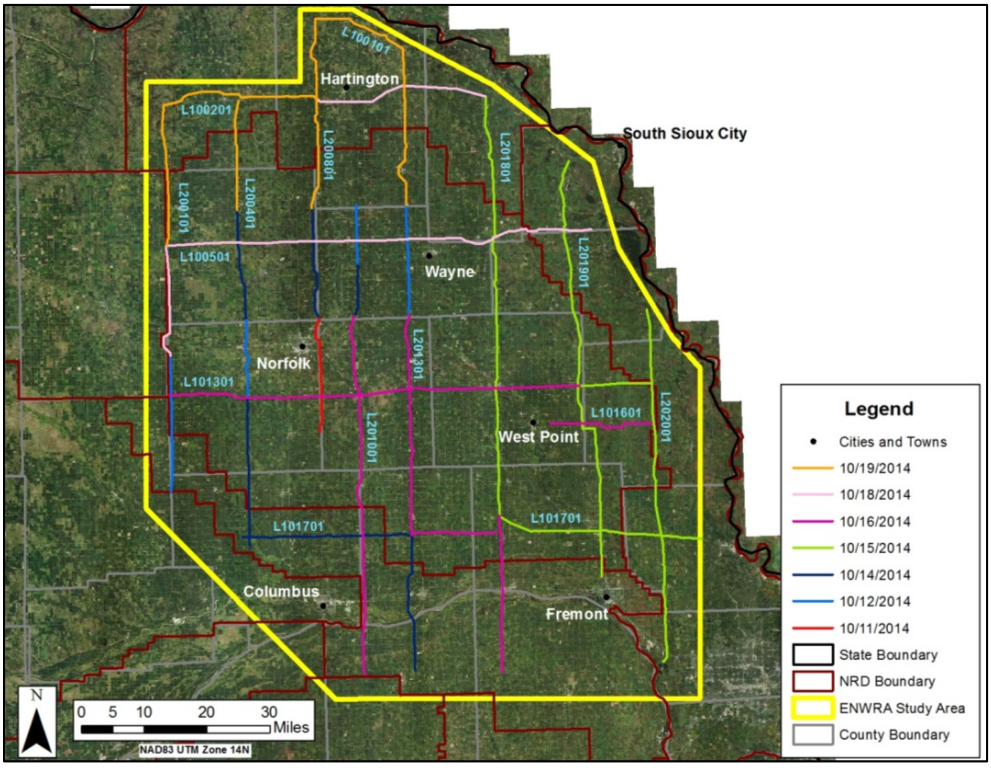


Figure 4-6: Flights lines as collected by date for the northern ENWRA project area.

Table 4-4: Airports and state parks used for landing and refueling by date of acquisition.

Date	Flight Number	Area Working
10/11/2014	1	Norfolk, NE
10/11/2014	2	Norfolk, NE
10/11/2014	3	Norfolk, NE
10/12/2014	1	Norfolk, NE
10/12/2014	2	Norfolk, NE and Wayne, NE
10/12/2014	3	Wayne, NE
10/13/2014	1	Wayne, NE
10/13/2014	2	Wayne, NE
10/14/2014	1	Wayne, Ne and Pierce, NE (Willow Creek State Park/Rec Area)
10/14/2014	2	Pierce, NE (Willow Creek State Park/Rec Area) and Norfolk, NE
10/14/2014	3	Norfolk, NE and Fremont, NE
10/15/2014	1	Fremont, NE and South Sioux City, NE (Powder Creek State Park/Rec Area)
10/15/2014	2	South Sioux City, NE (Powder Creek State Park/Rec Area) and Fremont, NE
10/15/2014	3	Fremont, NE and Tekamah, NE
10/16/2014	1	Tekamah, NE and Norfolk, NE
10/16/2014	2	Norfolk, NE and David City, NE
10/16/2014	3	Norfolk, NE and David City, NE
10/18/2014	2	Norfolk, NE and Martin Field, NE
10/18/2014	2	Martin Field, NE and Hartington, NE
10/19/2014	1	Hartington, NE
10/19/2014	1	Hartington, NE

Table 4-5: Production log displaying the number of production flights conducted each day and total line miles and kilometers surveyed. A limited number of flight lines did overlap.

Date	Production Flights	Line-mi	Line-km
10/11/2014	1	19.6	31.6
10/12/2014	2	65.0	104.6
10/14/2014	3	85.3	137.2
10/15/2014	3	239.2	385.0
10/16/2014	3	191.1	307.6
10/18/2014	1	122.6	197.4
10/19/2014	2	139.6	224.6
	Total:	**889.9**	**1432.1**

4.5 Data Processing

4.5.1 Primary Field Compensation

A standard SkyTEM data acquisition procedure is that the acquired raw data are sent to SkyTEM in Denmark for Primary Field Compensation (PFC) prior to continued data processing by XRI (Schamper et al., 2014). The primary field of the transmitter affects the recorded early time gates, which in the case of the Low Moment, are helpful in resolving the near surface resistivity structure of the ground. The Low Moment uses a saw tooth waveform which is calculated and then used in the PFC correction to correct the early time gates.

4.5.2 Automatic Processing

The AEM data collected by the 508 were processed using Aarhus Workbench version 4.2.7.2 (HydroGeophysics Group Aarhus University, 2011).

Automatic processing algorithms provided within the Workbench program are initially applied to the AEM data. GPS locations were filtered using a stepwise, second-order polynomial filter of 9 seconds with a beat time of 0.5 seconds, based on flight acquisition parameters. The AEM data are corrected for tilt deviations from level and so filters were also applied to both of the tilt meter readings with a median filter of 3 seconds and an average filter of 2 seconds. The altitude data were corrected using a series of two polynomial filters. The lengths of both eighth-order polynomial filters were set to 30 seconds with shift lengths of 6 seconds. The lower and upper thresholds were 1 and 100 meters, respectively.

Trapezoidal spatial averaging filters were next applied to the AEM data. The times used to define the trapezoidal filters for the Low Moment were $1.0x10^{-5}$ sec, $1.0x10^{-4}$ sec, and $1.0x10^{-3}$ sec with widths of 5, 8 and 10 seconds. The times used to define the trapezoid for the High Moment were $1.0x10^{-4}$ sec, $1.0x10^{-3}$ sec, and $1.0x10^{-2}$ sec with widths of 8, 10, and 20 seconds. The trapezoid sounding distance was set to 2.5 seconds and the left/right setting, which requires the trapezoid to be complete on both sides, was turned on. The spike factor and minimum number of gates were both set to 25 percent for both soundings. Lastly, the locations of the averaged soundings were synchronized between the two moments.

4.5.3 Manual Processing and Laterally-Constrained Inversions

After the implementation of the automatic filtering, the AEM data were manually examined using a sliding two minute time window. The data were examined for possible electromagnetic coupling with surface and buried utilities and metal, as well as for late time-gate noise. Data affected by these were removed. An example of locating areas of EM coupling with pipelines or power lines, and recognizing and removing coupled AEM data in Aarhus Workbench is shown in Figure 4-7 and Figure 4-8, respectively. Examples of two inversions, one without EM coupling and the other with EM coupling, are shown in Figure 4-9.

The AEM data were then inverted using a Laterally-Constrained Inversion (LCI) algorithm (HydroGeophysics Group Aarhus University, 2011). The profile and depth slices were examined, and any remaining electromagnetic couplings were masked out of the data set.

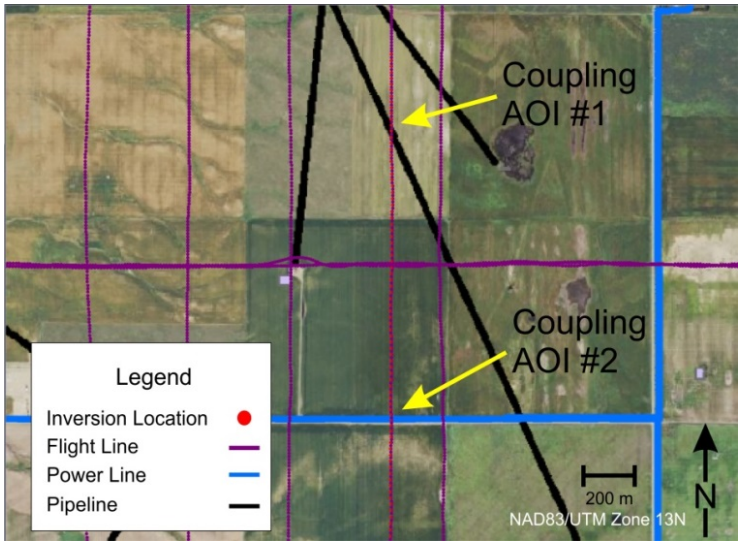


Figure 4-7: Example locations of EM coupling with pipelines or power lines.

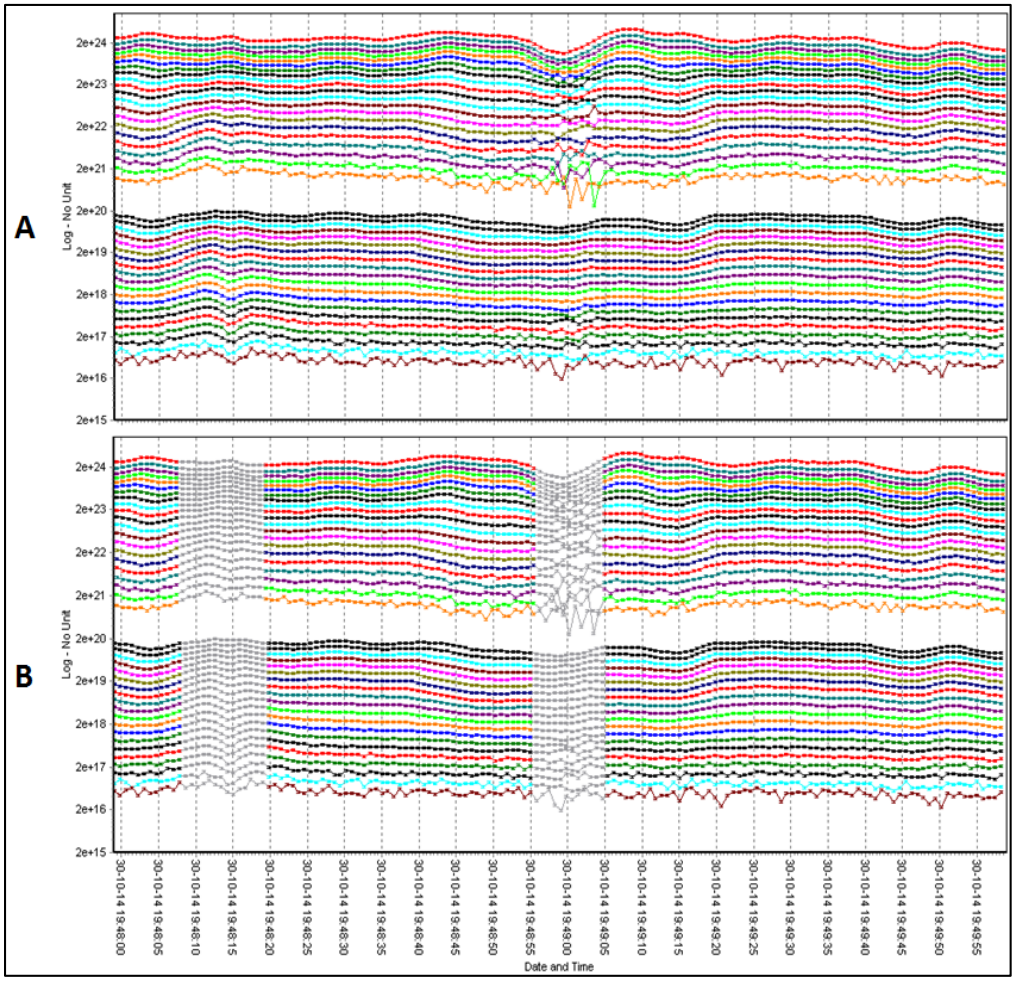


Figure 4-8: A) AEM data affected by coupling, shown in Figure 4-7, in Aarhus Workbench editor. The top group of lines is the Low Moment and the bottom is the High Moment. B) AEM data with area affected by coupling removed.

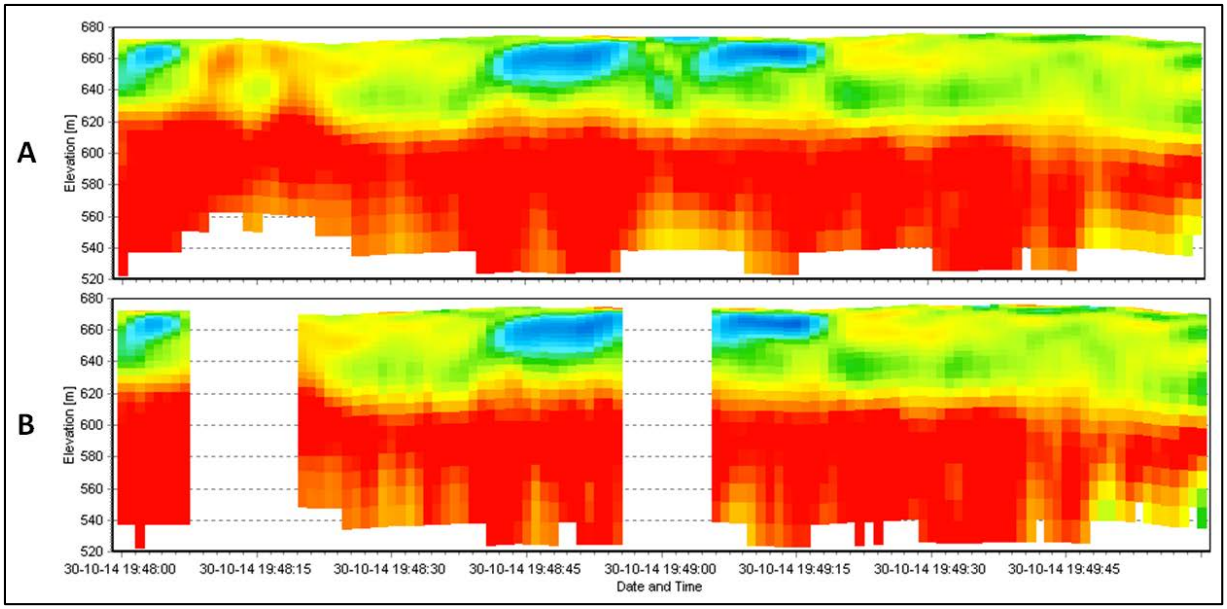


Figure 4-9: A) Inversion results where AEM data affected by coupling with pipelines and power lines were not removed. B) Inversion results where AEM data affected by coupling were removed.

4.5.4 Power Line Noise Intensity (PLNI)

The PLNI channel assists in identifying possible sources of noise from power lines. The PLNI is produced by performing a spectral frequency content analysis on the raw received Z-component SkyTEM data. For every Low Moment data block, a Fourier Transform (FT) is performed on the latest usable time gate data. The FT is evaluated at the local power line transmission frequency (60 Hz) yielding the amplitude spectral density of the local power line noise. The PLNI data for the ENWRA survey area are presented in Figure 4-10. Pipelines, unless they are cathodically-protected, are not mapped by the PLNI. Figure 4-11 shows the flight lines where data was removed following decoupling of data due to infrastructure and late time-gate noise.

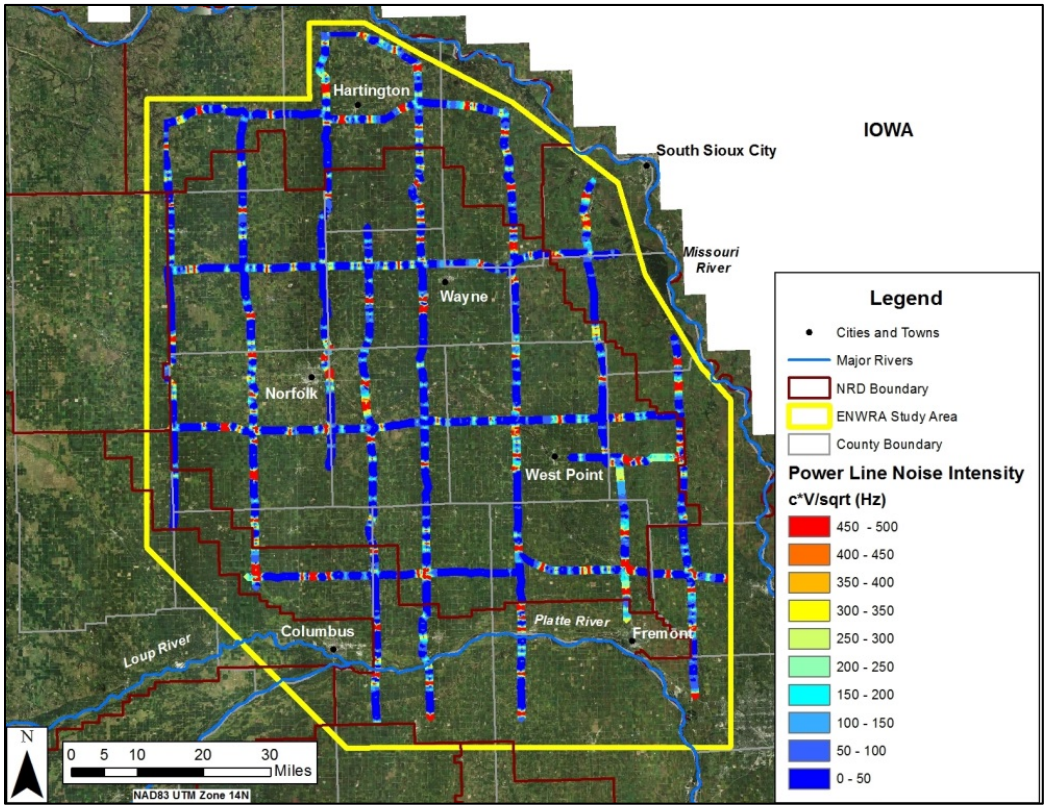


Figure 4-10: Power Line Noise Intensity (PLNI) map of the northern ENWRA project area.

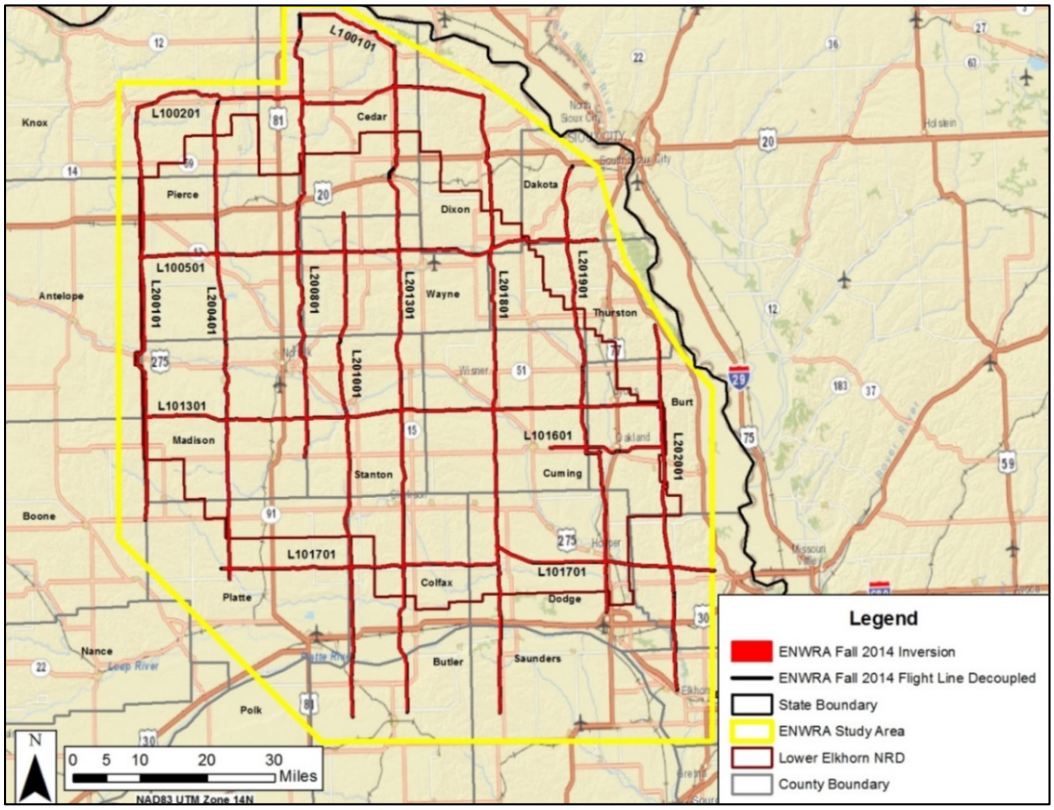


Figure 4-11: Locations of inverted data (red lines) along the AEM flight lines in the northern ENWRA project area. Black line segments indicate decoupled (removed) data.

4.5.5 Magnetic Field Data

As discussed above, the SkyTEM 508 includes a Total Field magnetometer. The magnetic field data can yield information about infrastructure as well as geology. Figure 4-12 shows the magnetic Total Field data after correcting for diurnal drift and removing the International Geomagnetic Reference Field (IGRF). This data compares well with the regional magnetic data shown in Figure 4-13 (Bankey et al., 2002) with the exception of the high anomaly surrounding the city of Wayne, NE. The line spacing of the regional data is 5 miles which could explain the difference in amplitude magnitude in this area.

The 3D magnetic field analytic signal is presented in Figure 4-14. The analytic signal indicates areas of sharp changes in the magnetic field such as those caused by metallic infrastructure. This data is used in decoupling efforts.

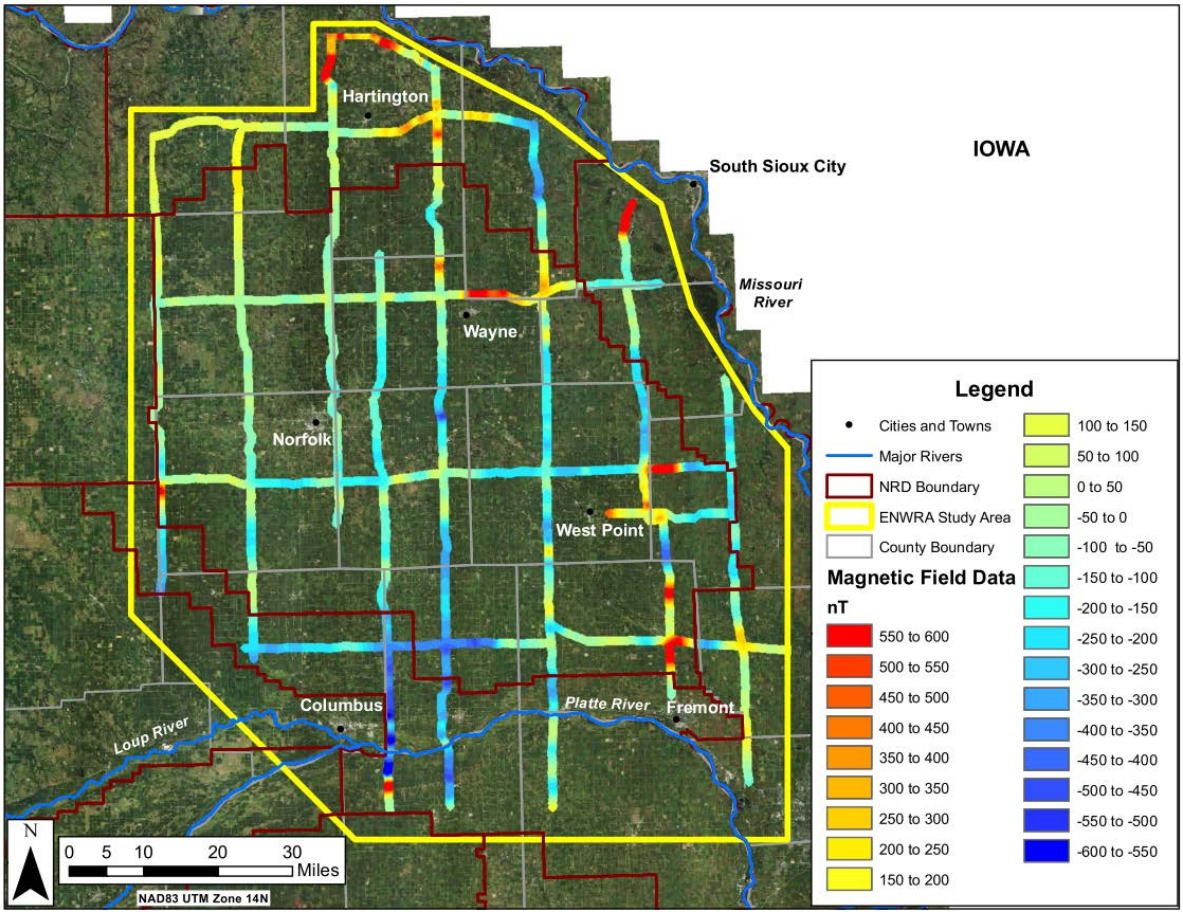


Figure 4-12: Magnetic Total Field data corrected for diurnal drift, with IGRF removed.

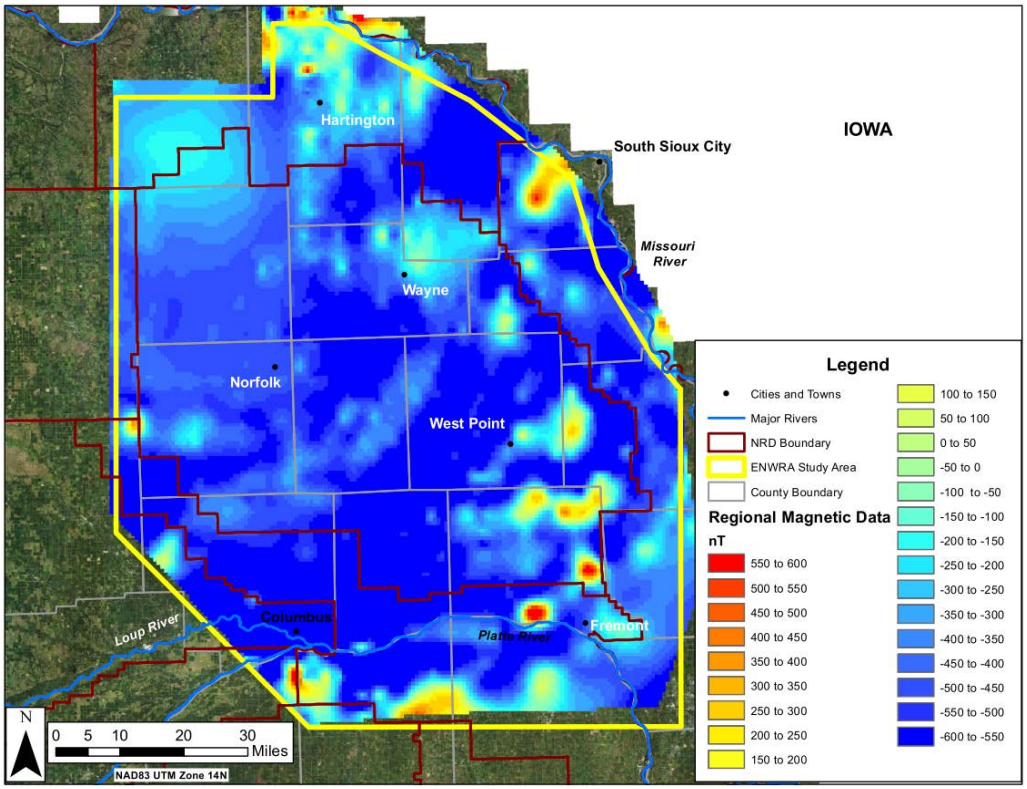


Figure 4-13: Regional magnetic Total Field data within the northern ENWRA project area boundary. Derived from Bankey et al. (2002).

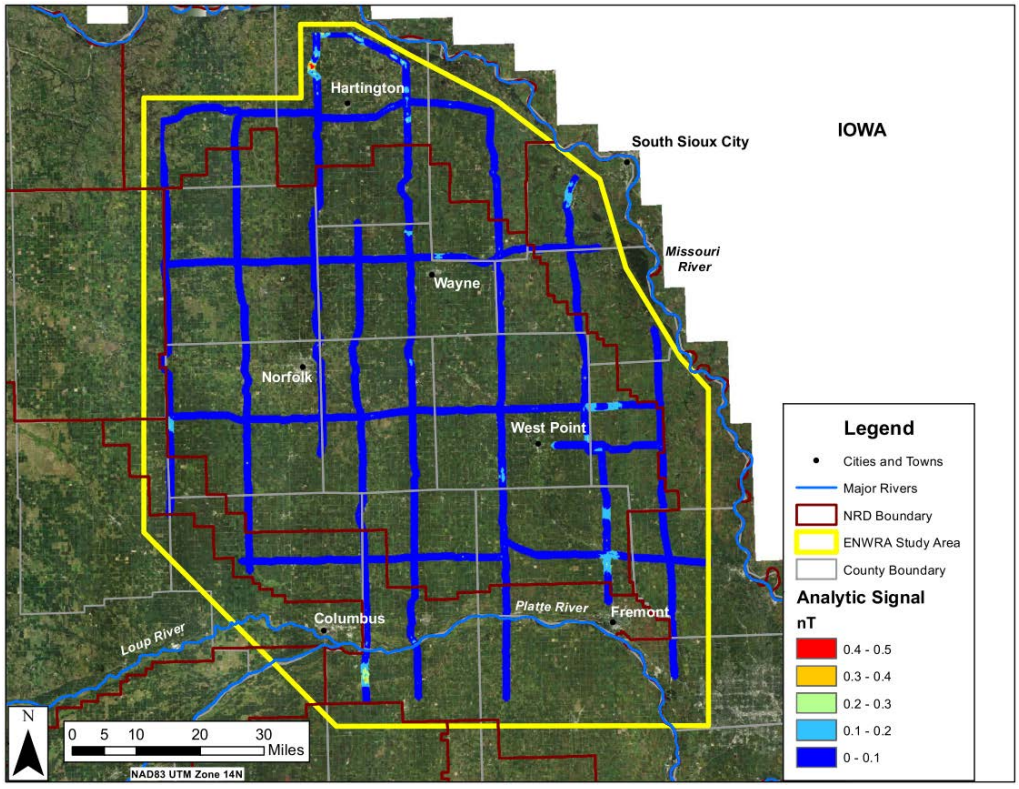


Figure 4-14: 3D magnetic field analytical signal calculated from the diurnal and IGRF corrected magnetic Total Field data.

4.6 Spatially-Constrained Inversion

Following the initial decoupling and LCI analysis, Spatially-Constrained Inversions (SCI) were performed. SCI inversions use EM data along, and across, flight lines within user-specified distance criteria (Viezzoli et al., 2008).

A smooth model inversion of 30 layers, each with a starting resistivity of 10 ohm-m, was used (equivalent to a 10 ohm-m half space). The thickness of the first layer of the model was 16.4 ft (5 m) with the thickness of each consecutive layer increasing by a factor of 1.1. The bottom of the 29th layer was set to 1,640.4 ft (500 m), and it had a thickness of 133.5 ft (40.7 m). The thickness of the layers increases with depth (Table 4-6 and Figure 4-15) as the resolution of the technique decreases. The reference distance was set to 328 ft (100 m) with a power law of 0.5. The constraint levels, ResVerSTD and ResLatStD, were set to 2 and 1.3, respectively, for all layers.

In addition to the recovered resistivity models the SCI also produces data residual values (single sounding error residuals), total residual values (total model residual error values), and Depth of Investigation (DOI) estimates. The data residual compares the measured data with the response of the inverted model. The total residual is a weighted average of the data residual and the model residual (Christensen et al., 2009; SkyTEM Airborne Surveys Worldwide, 2012). The DOI estimates the depth to which the AEM data are sensitive to changes in the resistivity distribution at depth (Christiansen and Auken, 2012).

Table 4-6: Thickness and depth to bottom for each layer in the SCI inverted AEM models. The thickness of the model layers increase with depth as the resolution of the AEM technique decreases.

Layer	Depth to Bottom (ft)	Thickness (ft)	Layer	Depth to Bottom (ft)	Thickness (ft)
1	16	16	16	488	51
2	34	18	17	543	54
3	53	19	18	601	59
4	74	21	19	665	63
5	96	22	20	733	68
6	120	24	21	806	73
7	145	26	22	885	79
8	173	28	23	971	85
9	203	30	24	1062	92
10	235	32	25	1161	99
11	270	35	26	1268	107
12	307	37	27	1383	115
13	347	40	28	1507	124
14	391	43	29	1641	133
15	438	47			

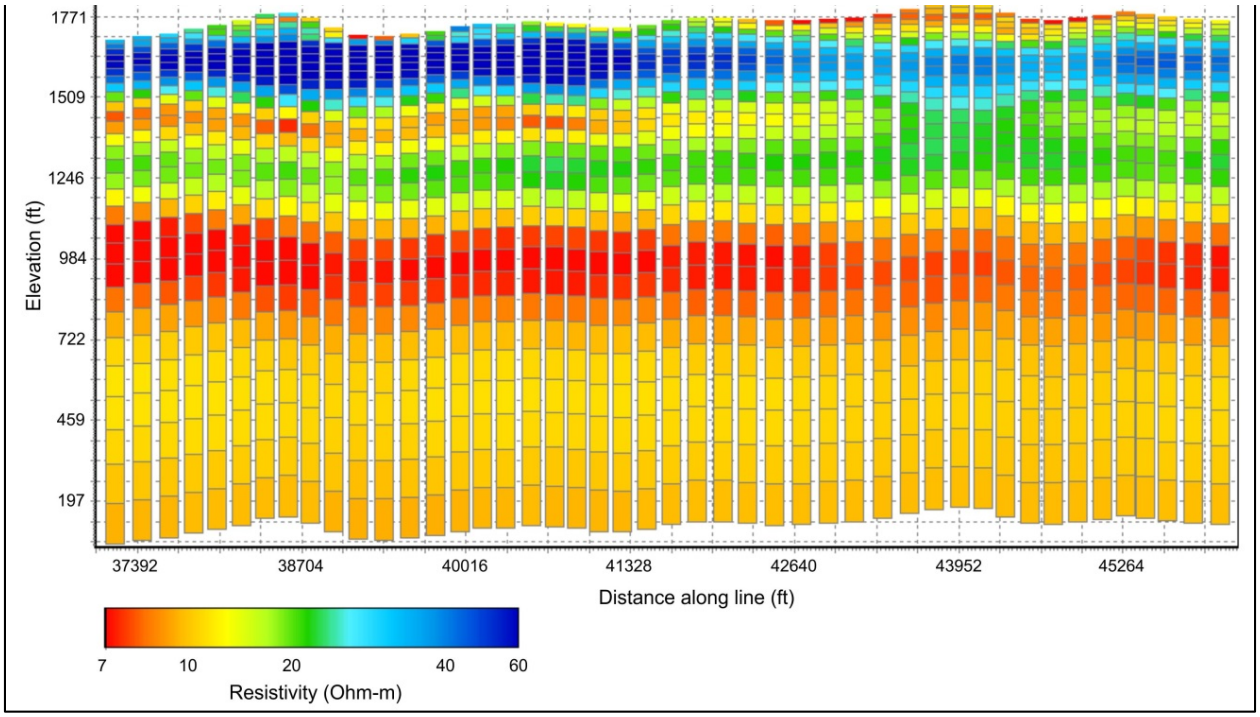


Figure 4-15: An example of an AEM profile illustrating the increase in model layer thickness with depth.

Lastly, 41 of the borehole conductivity logs, listed in Table 4-7, were used to constrain the inversion with a lateral standard deviation (STD) constraint of 2.0 and a reference distance of 3,280 ft (1,000 m) (HydroGeophysics Group Aarhus University, 2011). A variety of a-priori STD values and reference distances were tested including STDs of 1.5 and 2, and reference distances of 3,280 ft (1,000 m) and 9,840 ft (3,000 m). Workbench resamples the geophysical logs to match the layer widths and depths set for the SCI results. Figure 4-16 and Figure 4-17 compare the borehole logs with the starting model and the inverted model results for select boreholes. The green line shows the original borehole logs while the blue is that log resampled to match the layering used within the inversions. The purple line is the inverted model result without a-priori information while the red shows the result when the logs were used. In some instances the borehole logs did not greatly affect the inversion result, as shown in Figure 4-18. For these models there is possible error within these logs, or the resistivity structure of the ground varies significantly between the borehole locations and the AEM model location. Figure 4-19 shows a cross plot of the inverted resistivities compared with the resampled borehole resistivity for the 13 boreholes that were located very close to the flight lines.

The data residuals for the inversion using the resistivity logs were compared to those that didn't include the borehole logs. A STD value of 2.0 with a reference distance of 3,280 ft (1,000 m) produced the best results with improved data residuals (shown in Figure 4-20). Their distribution became tighter and lower (Figure 4-21). A small bulge did appear in the distribution around 0.7. It was determined that including the resistivity logs in the inversion still produced better results than those without the borehole logs.

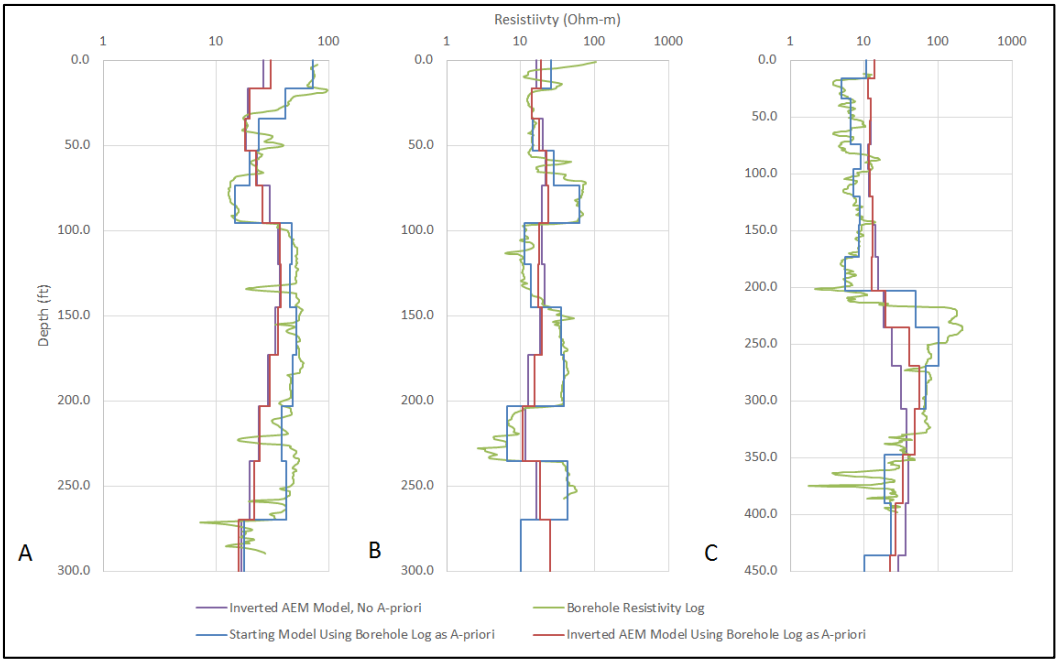


Figure 4-16: Borehole resistivity logs compared with inverted AEM models. A: Well 3-A-52, 1,700 ft from the AEM line. B: Well 3-A-53, 2,512 ft from AEM line. C: Well 4-A-52, 527 ft from AEM line. The green line shows the original borehole logs while the blue is the same log resampled to match the layering used within the inversions. The purple line is the inverted model result without a-priori information while the red shows the result when the logs were used.

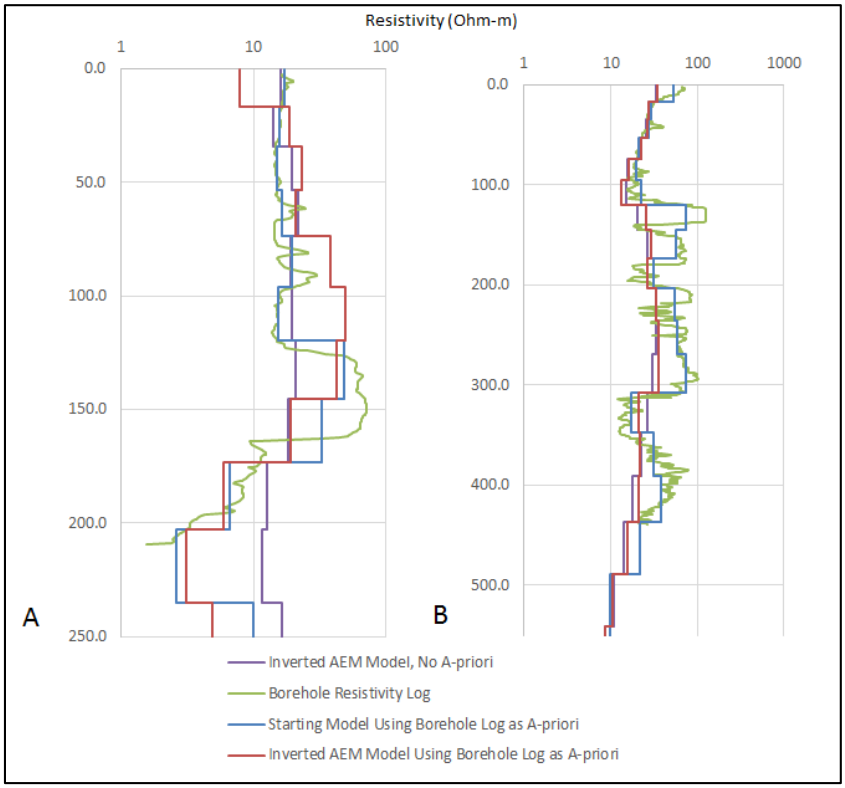


Figure 4-17: Borehole resistivity logs compared with inverted AEM models. A: Well 8-A-53, 1,768 ft from AEM line. B: Well 15-A-55, 3,132 ft from AEM line. The green line shows the original borehole logs while the blue is that log resampled to match the layering used within the inversions. The purple line is the inverted model result without a-priori information while the red shows the result when the logs were used.

Table 4-7: List of wells with borehole resistivity logs used as a-priori information for the SCI.

Well	Easting (ft)	Northing (ft)	Well	Easting (ft)	Northing (ft)
2-A-52	2206272	15232708	15-A-53	2046740	15480822
3-A-52	2082386	15306556	15-A-55	2021091	15239880
3-A-53	2038184	15353127	16-A-55	2024109	15221711
3-A-57	1952653	15472049	17-A-55	2021626	15207095
4-A-52	2082038	15324771	18-A-52	2159547	15373766
4-B-63	2373039	15124308	18-B-63	2304736	15217075
4-B-64	2162661	15235333	19-A-55	2022160	15174314
6-A-57	1953201	15431978	20-A-55	2022397	15159743
6-A-63	2361917	15218772	21-A-55	2022636	15145173
6-GT-80	2332504	15199651	21-A-62	2373117	15033154
7-A-63	2364302	15229785	21-B-64	2224727	15470114
8-A-53	2018883	15374665	22-B-63	2306209	15260868
8-LE-03	2087189	15197325	26-A-52	2229477	15390033
11-A-55	2083843	15230058	27-B-63	2299011	15322645
11-A-64	2262597	15365384	29-A-52	2155121	15450209
11-B-53	2078682	15499638	33-A-52	2154957	15457496
12-A-53	2017922	15432952	34-A-55	1959789	15147877
13-A-53	2017380	15465740	41-A-52	2079033	15481423
13-B-63	2360903	15251560	41-A-55	1958300	15257157
13-LE-99	2084122	15215488	43-A-55	1957850	15289942
14-A-53	2033286	15480586	15-A-53	2046740	15480822

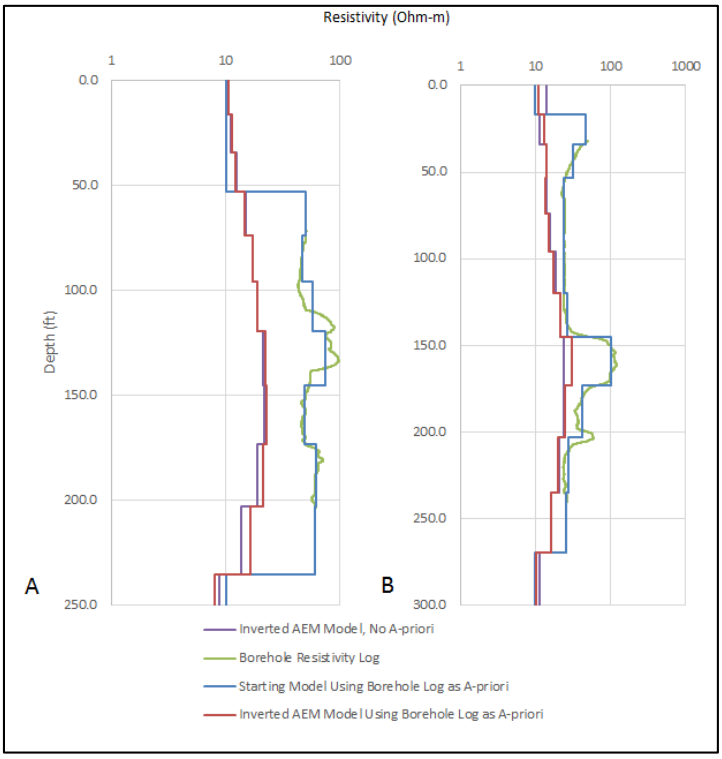


Figure 4-18: Borehole resistivity logs compared with inverted AEM models. A: Well 8-LE-03, 1,540 ft from AEM line. A: Well 13-LE-99, 2,349 ft from AEM line. The green line shows the original borehole logs while the blue is that log resampled to match the layering used within the inversions. The purple line is the inverted model result without a-priori information while the red shows the result when the logs were used.

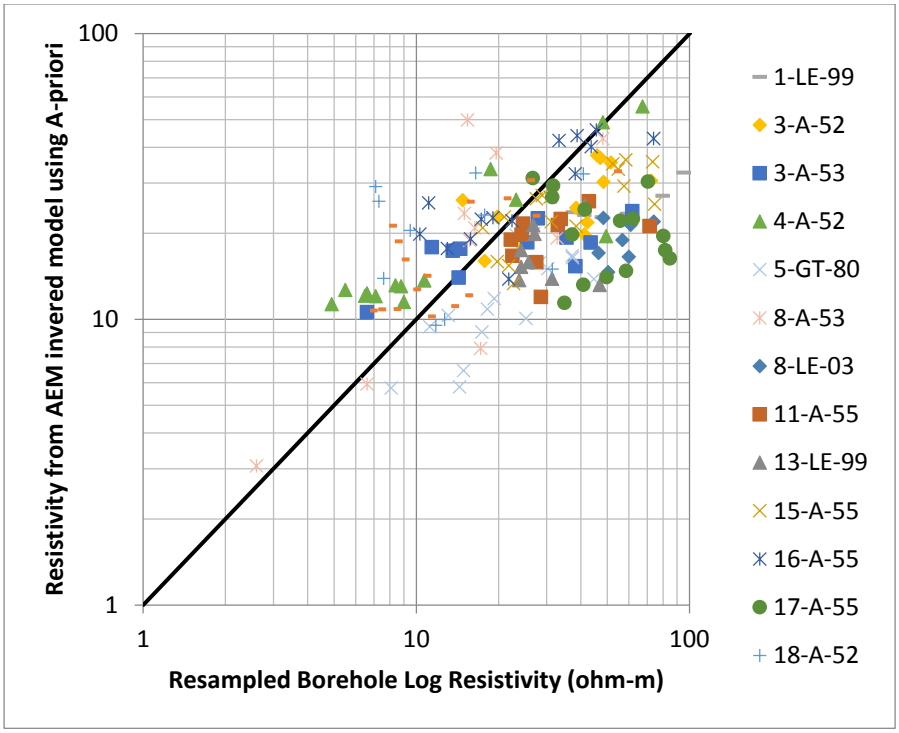


Figure 4-19: Cross-plot of inverted resistivities compared with the resampled borehole resistivity for the 13 boreholes within the closer spaced flight lines.

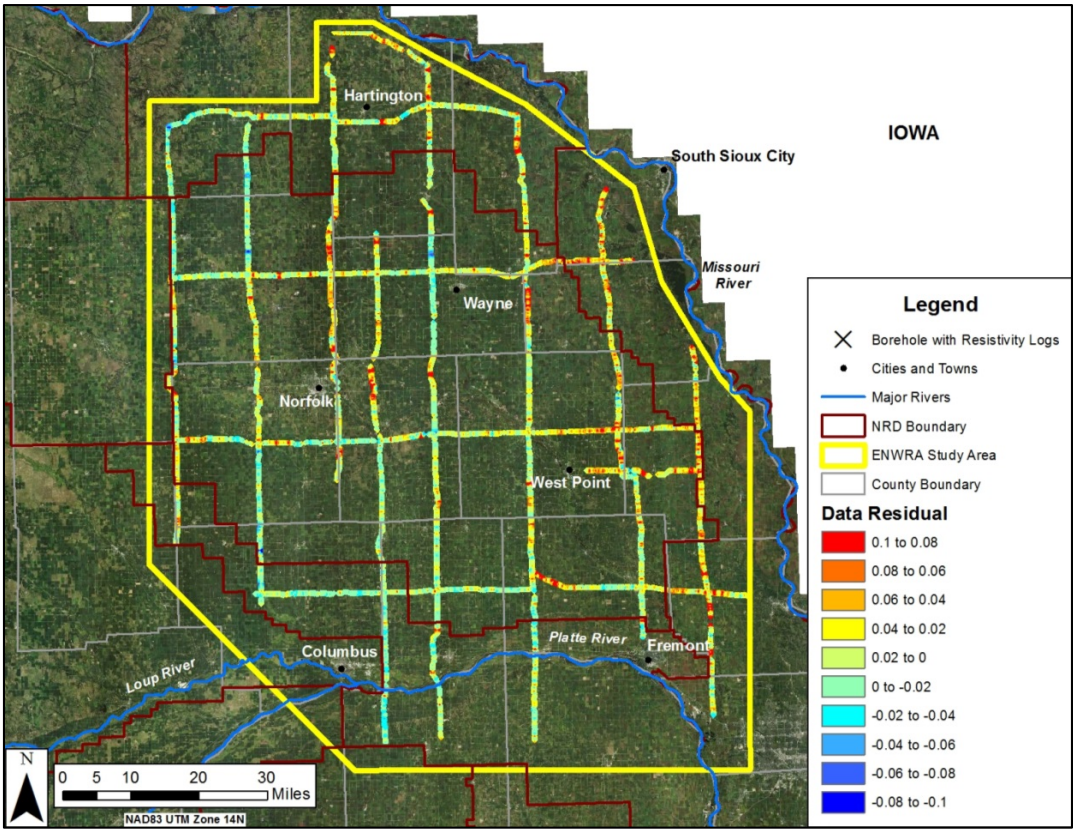


Figure 4-20: Difference between data point residuals produced by SCIs with and without using the borehole conductivity data as a-priori information. Red indicates an improvement in the residuals by greater than 0.1.

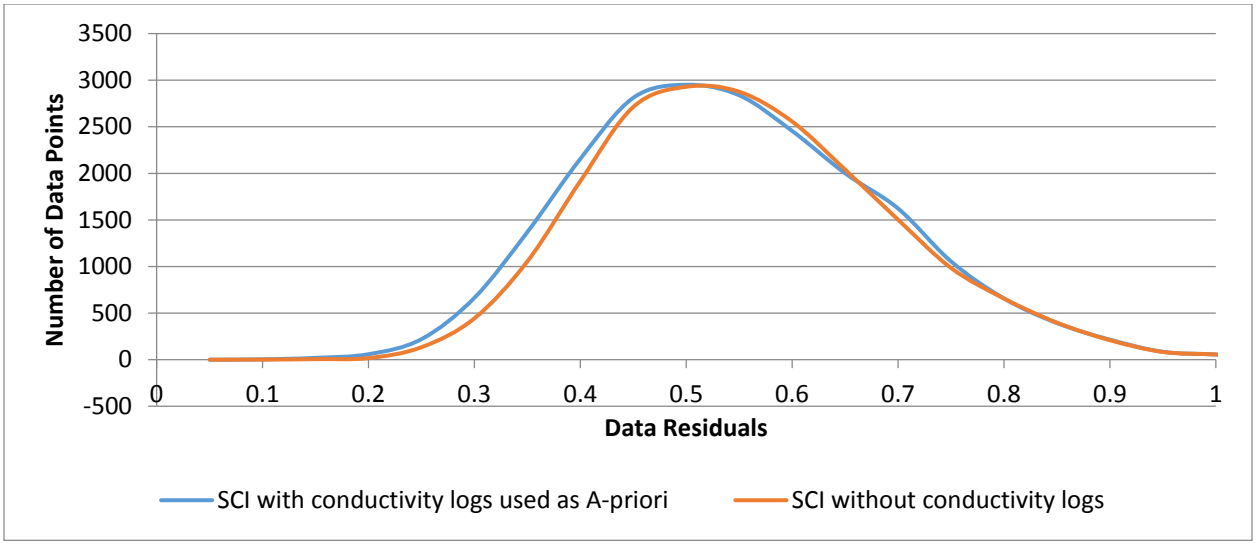


Figure 4-21: Data residuals distribution produced by the SCIs in the 10-mile reconnaissance lines both using the resistivity logs as a-priori and without them.

4.6.1 Determination of the DOI

The Depth of Investigation (DOI) plays a critical role in data interpretation. The DOI is a numerical estimation of the depth below which the resolution of a model, resulting from a numerical inversion, diminishes. This depth develops primarily due to the limitations of the TDEM method including: the equipment and methodology used for data acquisition, the noise in the data, and the resistivity structure (the geology) being investigated (Christiansen and Auken, 2012).

In addition to inverting the AEM data, Aarhus Workbench also calculates depths of investigation (DOI) for each inverted sounding, both a DOI Upper and a DOI Lower. 'Upper' refers to a shallower DOI estimate while 'Lower' refers to a deeper one. The derivation of these depths is presented in Christiansen and Auken (2012) and discussed in more detail in Appendix 3.

The Aarhus Workbench uses inverted model sensitivities (the Jacobian) determined during the last inversion step, along with an estimate of data uncertainty to calculate the DOI's. The Jacobian matrix is the sensitivity of the data to perturbations at the current location in model-space. As such, the Jacobian is also a representation of the sensitivity of changes in the model to the observed data.

The last step in this process is calculation of the cumulative sensitivities, by summing up the individual thickness-normalized sensitivities, starting with the bottom layer. That is, for a 30-layer model (which is usually used in all the XRI Workbench inversions) the cumulative sensitivity for the 30th layer is the thickness-normalized sensitivity for the 30th layer. Then the cumulative sensitivity for the 29th layer is the sum of the cumulative sensitivity for the 30th and the thickness-normalized sensitivity for the 29th layer. The cumulative sensitivity for the 28th layer would be the sum of the cumulative sensitivity for the 29th layer and the thickness-normalized sensitivity for the 28th layer.

However, there is a difference between *resolution* of a property and *detection* of a property. Resolution means that the properties of interest are accurately recovered through inversion. Detection indicates that while the true value of a property may not be accurately resolved, there is still some sensitivity, in

the data, to changes in that property. The DOI is generally the line of demarcation between resolution and detection.

Christiansen and Auken (2012) define the global threshold value as that cumulative sensitivity which indicates "*the miminum amount of sensitivity needed for indicative information*". They further state that "*setting the threshold value is very much a question of fine-tuning based on experience, intuition, and comparing different models with different methods. The threshold value suggested here is purely empiric…. Setting a higher threshold value will decrease the DOI, and a lower value will increase the DOI.*"

The upper and lower DOIs typically exported by the Aarhus Workbench are for cumulative sensitivities 1.2 (upper DOI) and 0.6 (lower DOI). However, additional cumulative sensitivity values can also be developed and exported including 0.4, 0.2, and 0.1. Variations in the character of the DOI's are functions of the resistivity of the sounding for which the DOI is calculated. The DOI contours for the cumulative sensitivity thresholds will be much deeper under resistive zones and shallower under conductive zones. An example of a DOI produced using a 0.1 cumulative sensitivity is shown on the profiles in Figure 4-22 and in Appendix 3.

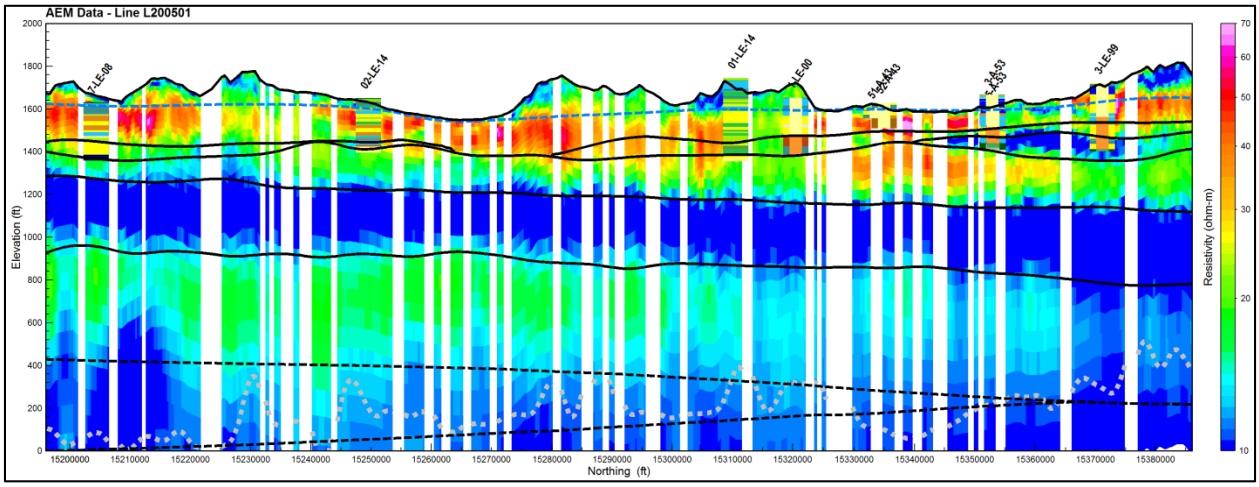


Figure 4-22: Sample of AEM resistivity inversion model with the 0.1 DOI marked as grey boxes at the bottom of the image.

5 Results and Interpretation

A total of 889.9 line miles (1432.1 line km) of AEM data were collected in Phase 1. Of that total, 151.5 lines miles (243 line km), 17 percent, were removed due to electromagnetic coupling with infrastructure leaving a total of 738.4 line miles (1188.3 line km) for inversion and interpretation. Had the flights line paths not been optimized prior to data collection, the expected data retention would have been 32 percent instead of 83 percent (using an approximate 656 ft (200 m) radius of interference). Locations of where data was removed are provided in the previous section in Figure 4-11. Figure 5-1 shows the locations of where data was collected along with the flight line numbers in the southern ENWRA project area.

Figure 5-2 includes the color codes for the aquifer materials as well as the stratigraphy and lithology labels used in figures in this section as well as in the appendices of this report.

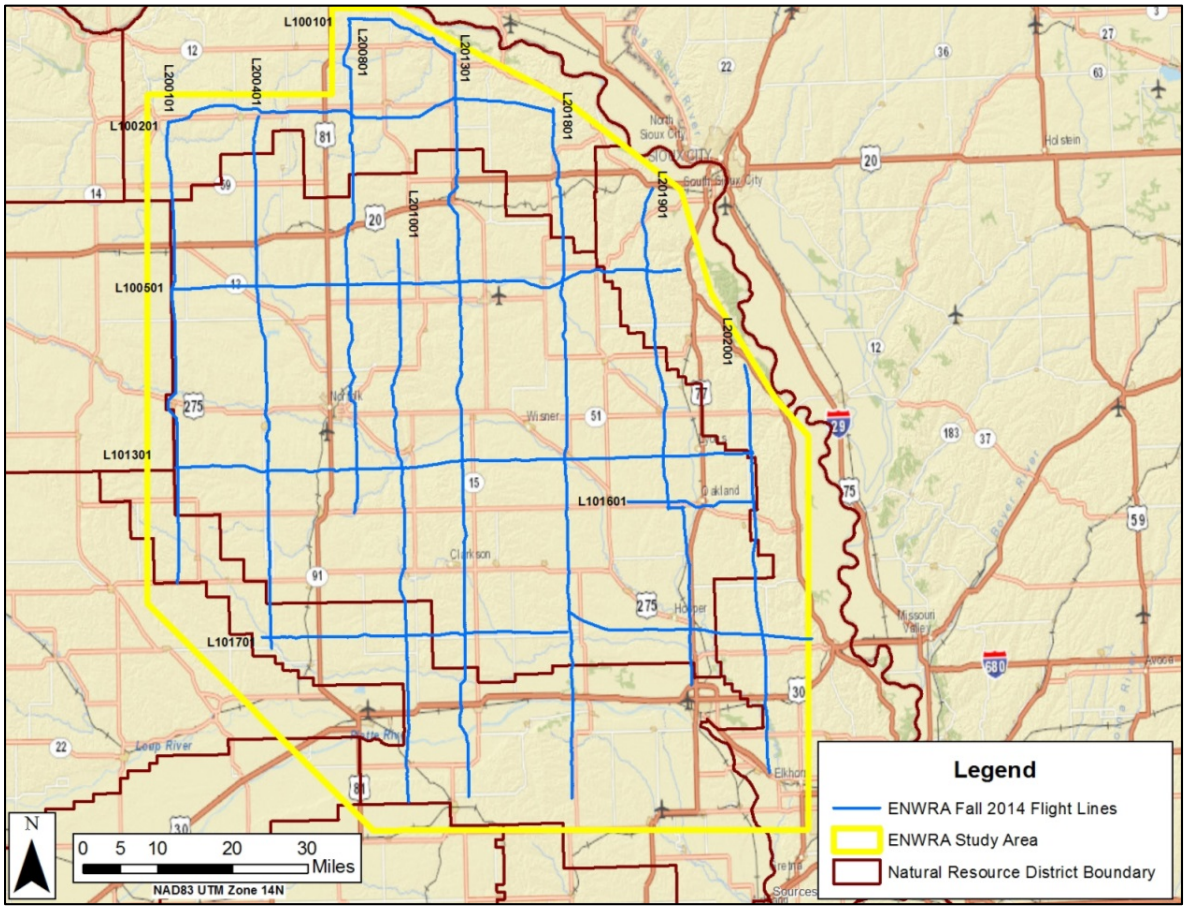


Figure 5-1: AEM flight lines with line numbers in the northern ENWRA project area.

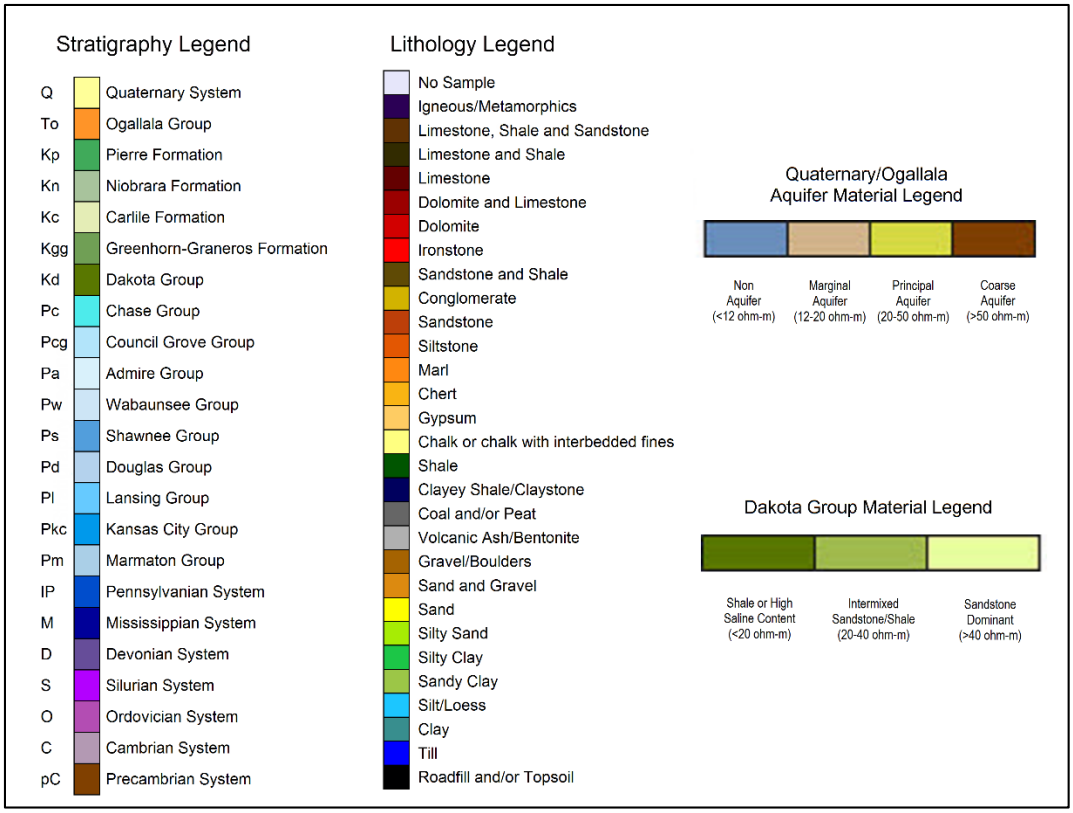


Figure 5-2: Color codes for aquifer materials, stratigraphy, and lithology used in the interpretive profiles and 3D figures in this section and in the report appendices.

5.1 AEM Results and Interpretation

5.1.1 Interpretive Process

After final processing of the AEM data, characterization of the subsurface was performed in cross-section format using pbEncom PA. In this step, contacts between the bedrock (Paleozoic and Cretaceous), Tertiary, and Quaternary deposits were selected for every flight line in the project area. The interpreted geological units included the *To, Kp, Kn, Kc, Kgg, and Kd*. Undifferentiated *IP* and *M* were also detected in this survey and are described briefly in this section (Korus and Joeckel 2011). The Greenhorn Limestone and Graneros Shale (*Kgg*) were not geophysically distinct from the *Kc* at all locations. Since these units generally function as aquicludes over the project area, they were grouped as one in the representation of the AEM data and the hydrostratigraphic framework of the project area. The selection process benefited from the use of CSD and NOGCC borehole logs, which provided lithologic, stratigraphic, and geophysical information. The historical CSD cross-sections (Divine et al., 2010; Korus et al., 2012) were projected in pbEncom PA to aid in interpreting the AEM data. The interpretations were simultaneously checked against the CSD's Nebraska bedrock geology map (Burchett 1986) and other geological maps in the northern portion of the project area (Burchett and Carson 1966a, b, c, d). After the cross-section interpretations of the geological contacts were completed, the results were compared in 3D with the NOGCC boreholes, CSD boreholes, CSD historic bedrock surfaces, and CSD cross-sections (Divine et al., 2010; Korus et al., 2012).

Areas of offsets between intersecting AEM flight lines were minimized by reinterpreting the information based on visualization of the AEM data in a 3D display. During the interpretation process, a limited number of CSD stratigraphic assignments were determined to be in disagreement with the AEM results. These discrepancies can be categorized as follows: 1) incorrect stratigraphic selections of *Kd* versus *Kp*; 2) AEM-enhanced stratigraphic selections that provided additional data to indicate *Kp* and not Quaternary deposits; 3) incorrect categorization of Tertiary (Oligocene) White River Group that were confirmed as *Kp* from the AEM; and 4) picks that indicated *To* but were interpreted as Quaternary from the AEM. It was also determined that the NOGCC stratigraphic assignments contained inaccurate indications of the bedrock depth. These stratigraphic data were omitted. The NOGCC stratigraphic selections in the boreholes within the Cretaceous and Paleozoic units were utilized in the interpretation.

In addition to the geologic profiles, historic bedrock geology maps were used to assist in the interpretation of the AEM inversion results (Divine et al., 2010; Korus et al., 2012). The contours from these data sources were georeferenced and digitized using GIS software. The resulting digitized contour lines were then gridded to create either surfaces of the bedrock unit tops and bases or thickness maps.

Regional surface grids of geologic formations were produced during this process. To create these grids, the elevations of the interpreted top of the formation as well as data from CSD and NOGCC holes were compiled into an Oasis montaj (OM) database. The interpreted elevation data were then gridded for each formation independently using the OM minimum curvature gridding (MCG) algorithm with a 1,500-ft cell size, a blanking distance of 50,000 ft, and the cells to extend beyond set to 50. All other parameters were either left as the default or blank. The large blanking distance was required to fill in between the broadly spaced recon lines, where 15 miles or more separated adjacent flight lines. CSD and NOGCC holes were used to provide additional formation elevation data throughout the project area. The 1,500-ft cell size preserved most of the spatial resolution obtained from the AEM data but minimized artifacts from the MCG routine. While the MCG routine performs reasonably well with honoring the data, in areas where the spatial density of data points is low, the MCG routine may trend towards an overall average data value. This may cause artifacts in the final grid through grid values that are not supported by data in the general vicinity. A smaller cell size resulted in these gridding artifacts on the boundary of the project area and where only recoaissance lines were available (i.e. no CSD or NOGCC holes available). A 9-point convolution filter was applied to each grid using a pre-defined Hanning filter under GRIDFILT GX within OM. This type of filter is common in image processing and was used to reduce high-frequency noise in the grid.

The parameters utilized in this process resulted in grids that were continuous across the project area, but also extended outside the project area or beyond the areal extent of the interpreted feature in the AEM data. Once generated, each individual grid was masked to remove gridded data that was either outside the project area or in areas where that geologic surface was not identified. The mask was generated from the AEM interpretation, CSD and NOGCC test holes, and the project area bedrock geology map. In areas where no AEM data or drill holes were available, the contours for each geologic unit were followed as depicted on the CSD bedrock geology map (Burchett, 1986).

Once masked, the grids were sampled to the location of the AEM data within OM and visually inspected for consistency. In areas of sparse data, grid surfaces did not meet or overlap (e.g. the gridded bedrock surface exceeded the DEM elevation by a small interval (< 5 ft) in a minor number of instances). In areas of incongruity, data were manually adjusted to ensure geologic surfaces met appropriately or did not overlap. This manual editing was conducted only on the geologic surface data that coincided with the location of the AEM data and used to generate the cross section plots presented in this report. The digital regional grids provided with this report will show discontinuities throughout the project area where different geologic surfaces meet or pinch out. In most cases, this is typically less than 30 feet, but some areas exist where the elevation offset of successive geologic units is 75 ft or more.

Following construction of the bedrock surface, the consolidated and unconsolidated deposits were isolated within the AEM data. A voxel resistivity grid was made of the AEM data using a 1,000 ft^2 horizontal cell with the thickness related to the model cell thickness (Section 4.6). The voxel was then sliced at the bedrock surface. This surface was the top of the *To, Kp, Kn, KcKgg*, or the *Kd,* depending on location in the project area. Note that the *Kc* and *Kgg* are combined as one hydrostratigraphic unit (further discussion on this merging of units is provided later in this section). The voxel values were then sampled on the AEM flight path cross-sections to indicate the location of the resistive intervals that are interpreted as unconsolidated Quaternary aquifer materials. The aquifer and non-aquifer materials in the Quaternary system were separated by four major resistivity thresholds selected in pbEncom PA. These ranges include 1-12 ohm-m, representing non-aquifer materials ("aquitard"- primarily glacial till, loess), 12-20 ohm-m, representing marginal aquifer deposits with potential for interlayered silt and clay, 20-50 ohm-m, indicating the Quaternary system's principal aquifer, and the interval of 50 ohm-m or greater, indicating the coarsest, sand-rich intervals within the principal aquifer (further discussion is provided in the following section regarding the selection of these threshold ranges). These surfaces were then gridded to provide formation or geologic material top and bottom along the flight line. The *To* resistive material was coupled with the overlying Quaternary resistive material, as it was assumed that the aquifers in these units commonly act as one, or are in close hydrologic communication where this overlap occurs in the project area. *T*he *Kd* resistors were also sampled from a sliced voxel model at a resistivity range of 20 ohm-m or greater.

To assist in the determination of the saturated materials, the 1995 CSD statewide water table was mapped into the cross-sections.

It should be noted that care must be exerted not to use the voxel information beyond the flight lines, as the voxels are not constrained and thus will not provide information due to the large interpolation distances between flight lines. In some areas on the interpretation profiles, there are slight differences at the land surface and the underlying geologic interpretation. This is an artifact of displaying a 3D model along a line profile feature.

5.1.2 Resistivity-Lithology Relationship

5.1.2.1 Quaternary System

A critical aspect of a geophysical survey, for whatever purpose, is assessing the nature of the material detected by the geophysical method applied in the investigation. In regards to the ENWRA reconnaissance line survey, assessment of the sediment character in both the Quaternary system and the consolidated bedrock strata was conducted to determine the overall composition of the major categories used to define the aquifer and aquitards. A numerically robust assessment of the resistivity thresholds used to characterize non-aquifer, marginal and principal aquifer, including sand-rich intervals in the principal aquifer was calculated. This allows for the characterization of the ranges of resistivities present in the major geologic units described in this report. It should be noted that this analysis encompasses all Quaternary and bedrock data from both subregions of the ENWRA project area as defined in this report. Separate analyses we conducted for both areas, and results confirmed that virtually no differences were evident between the two areas, thus justifying the application of the resistivity thresholds described in this section for the entire ENWRA area.

Data for this analysis was utilized from locations across the ENWRA reconnaissance line area. The relationship between resistivity and lithology type was assessed by performing an association function that linked nine lithologic descriptor codes for Quaternary sediments used in the CSD test hole lithologic characterization with the resistivity values across that particular depth interval as indicated in the 58 high-graded resistivity logs applied in the AEM data inversion (33 from the northern area, 25 from the southern area). With this approach, several thousand points became available for each lithologic description in the test holes used in this analysis. From this list of associated resistivity levels and pre-categorized lithologies, statistical analyses were performed to aide in defining the various thresholds used to determine the aquifer material type in the project area subsurface. The following sections contain descriptions of each analysis performed.

Figure 5-3 displays a box and whiskers plot of the resistivity range for each of the nine unconsolidated materials in the Quaternary system. These plots indicate the spread of the range of resistivities for each of the materials, including the 75^{th} and 25^{th} quartiles, median values, and the IRQ*1.5 (whiskers) (Tukey, 1977). Included in the background of the plot are the divisions in resistivity between the aquitard and the three aquifer designations in the AEM interpretations. Glacial till (blue) has an interquartile range of resistivities from approximately 17 to 45 ohm-m, with a median value of 25 ohm-m and maximum and minimum values of around 90 and 11 ohm-m, respectively. This plot indicates that for glacial till, there is a wide spread of resistivity. This should not be unexpected, as glacial till can be composed of a wide variety of unsorted sediment sizes, including gravel and sand intermixed with fines.

Silt/loess has a similar resistivity distribution as glacial till, but with a higher median near 29 ohm-m, and a lower minimum value near 2 ohm-m. This wide range could be a result of silt and loess being combined in one category, where silts from different horizons that are intermixed with other fines such as fine sand or clay could create the wide range in values for this material.

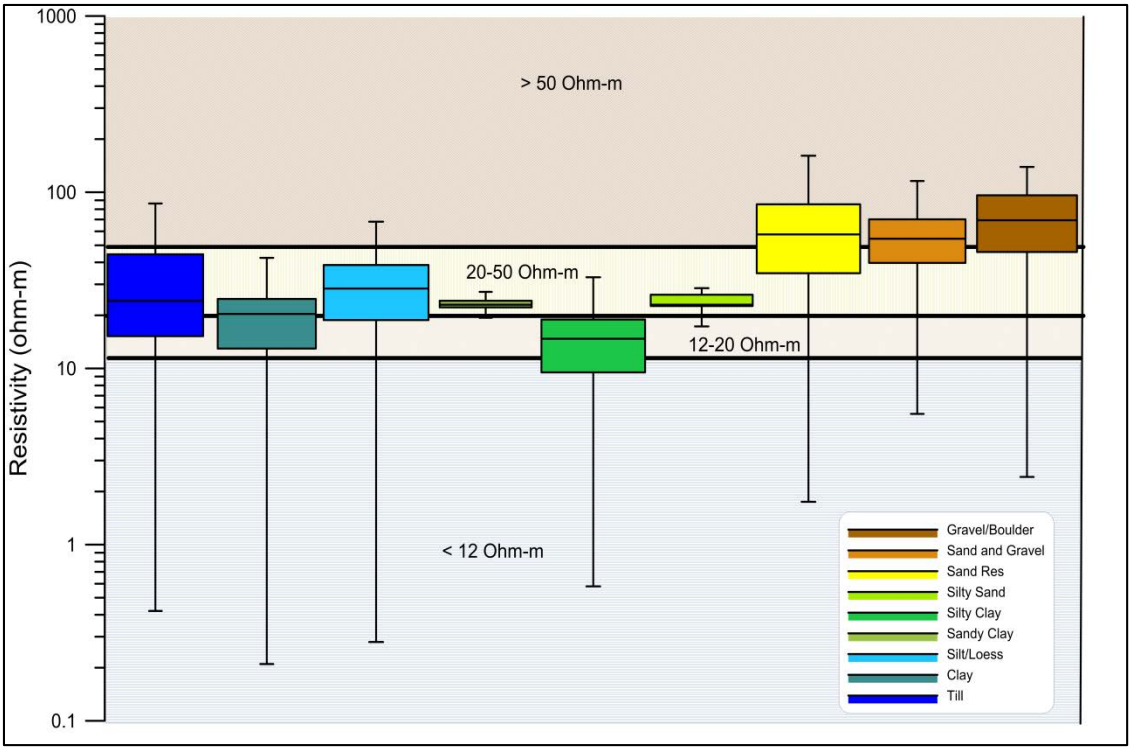


Figure 5-3: Box and whisker plots for the resistivity ranges for the nine most common unconsolidated materials within the Quaternary system.

For the lithologic category clay, the median value is close to glacial till, but with a lower maximum value (approximately 40 ohm-m) and lower minimum value (3 ohm-m). These differences should be expected, as glacial till is typically composed of more resistive materials in comparison to clay materials alone.

Silty clay has the lowest median value of the 9 categories displayed in Figure 5-3 (approximately 14 ohm-m). Silty sand and sandy clay each have very similar characteristics in this plot, which should be expected as these lithologic categories are similar.

The distribution of sand, sand and gravel, and gravel and boulder categories are considerably higher than the median and interquartile ranges of the fine materials displayed on the Figure 5-3. The median resistivity of the three coarse sediment ranges is 55 ohm-m or higher, and the lowest 25th quartile (sand) is 35 ohm-m, indicating that 75 percent of the resistivity values for each of these three coarse categories is 35 ohm-m or higher. Sand also has the maximum (117 ohm-m) and the minimum (7 ohm-m) values of the three coarse sediment categories.

Figure 5-4 displays a histogram of the unconsolidated material distribution by frequency count of materials associated with resistivities from the 33 borehole geophysical logs assessed from across the project area. The color-defined bins of the histogram show the thresholds for resistivity used to define the major aquifer material type in the interpretation of the AEM data. Non-aquifer material (blue), shows a distribution on the log-scale x-axis from 1 to 12 ohm-m. This material range corresponds primarily to intervals of resistivity associated with silty clay, clay, silt/loess, and till. The tan area, between 12 and 20 ohm-m, is defined by a mix of fine to coarse sediments, with abundant silty clay still

present. The principal aquifer (yellow) is defined by materials ranging from 20 to 50 ohm-m. This interval has a considerable peak of material with a resistivity approximately in the 22-27 ohm-m range and a secondary peak in the 45 to 50 ohm-m range. The fourth category on the histogram represents materials 50 ohm-m and greater, which corresponds to the coarse, sand-rich intervals of the principal aquifer. This interval is considerably lower in the frequency count than the primary aquifer, but by highlighting this interval, discreet sections of the aquifer are revealed showing possible depositional trends in the Quaternary deposits as well as identifying areas where the potential for high-yield wells is the greatest.

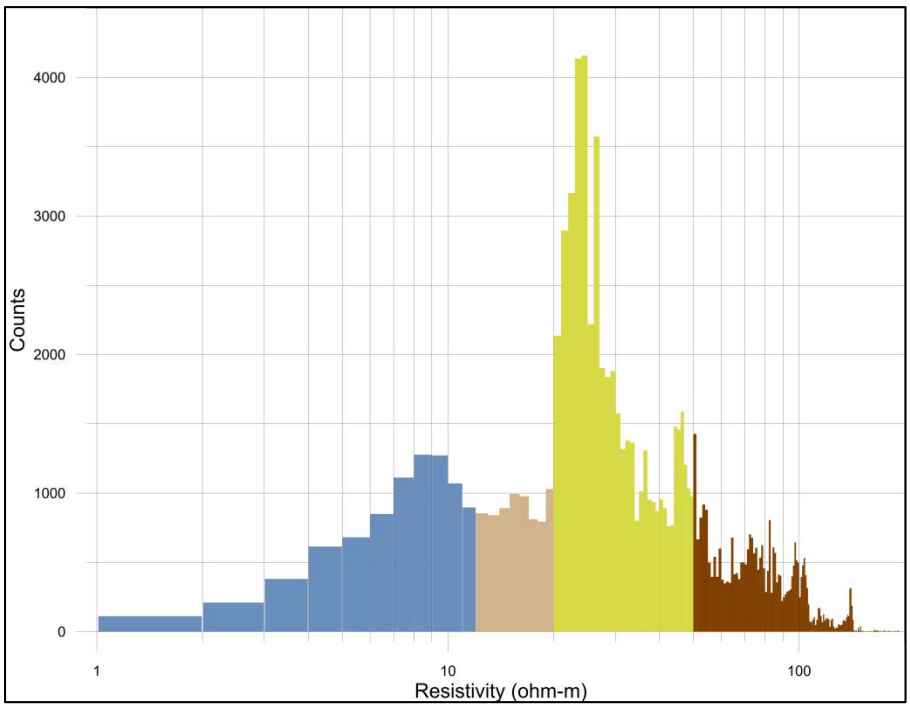


Figure 5-4: Histogram plot displaying the distribution of resistivities by major aquifer material color categories (blue- non-aquifer material, tan- marginal aquifer, yellow-principal aquifer, brown- sand-rich, coarse intervals of the principal aquifer).

Figure 5-5 and Figure 5-6 display pie charts that indicate the distribution of sediment type within each aquifer material range (0-12, 12-20, 20-50, >50 ohm-m). As would be expected, fine materials (silt/loess, clay, till) are the predominant material types for the non-aquifer material (0-12 ohm-m). For marginal aquifer material (12-20 ohm-m), slightly over 14 percent of the material in this range has a component of sand, with silt/loess, till, and clay comprising over 75 percent of this range. For principal aquifer material, over 37 percent of the material consists of coarse materials, and for the coarse portion of the principal aquifer at 50 ohm-m or greater, over 85 percent of the lithology consists of coarse material.

Figure 5-7 displays the overall distribution of sediment type as indicated in the 58 e-logs used to assess the lithology-resistivity relationship across in the project area. Over 48% of the lithologies indicated by the e-logs were categorized as sand, sand and gravel, or gravel and boulders. Silt/loess was the second highest category at 27.2 percent. This should be expected, considering the presence of silt within the

many of the major depositional features in the project area (loess, till, outwash, alluvium). Glacial till is the second most abundant non-coarse material at over 13 percent. The remaining categories containing some component of clay is just over 10 percent of the overall distribution.

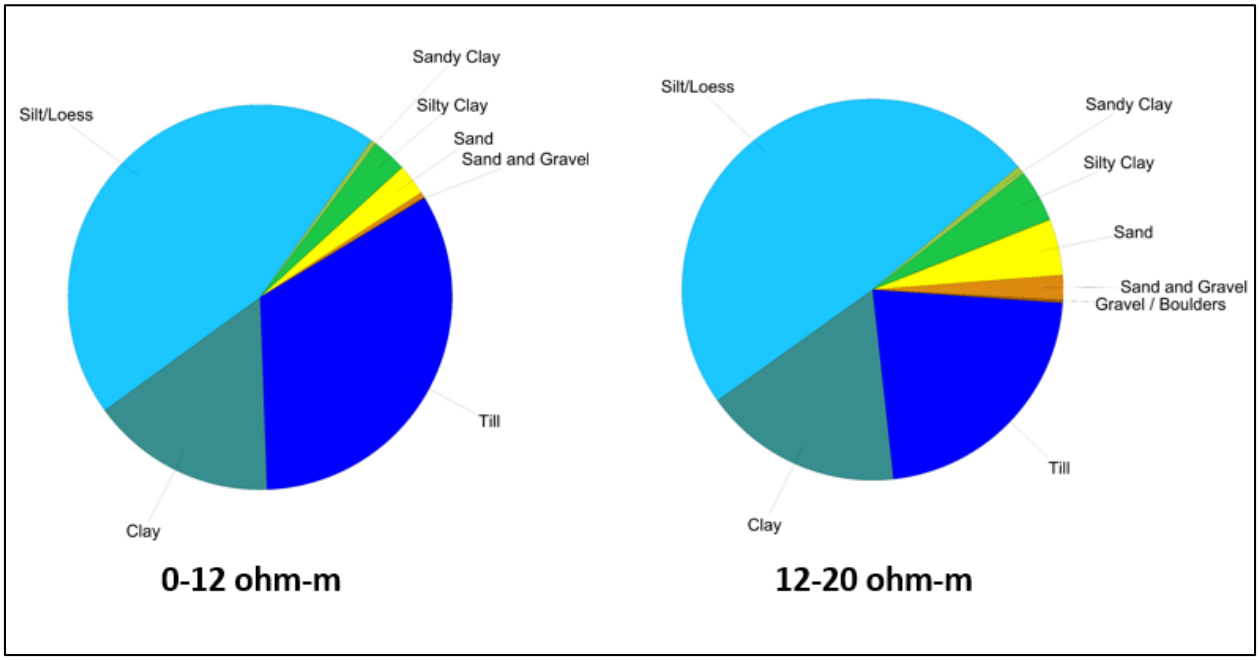


Figure 5-5: Pie charts of the distribution of material within each resistivity range for the aquifer materials used in the interpretation of the AEM data- 0-12 ohm-m (left) and 12-20 ohm-m (right).

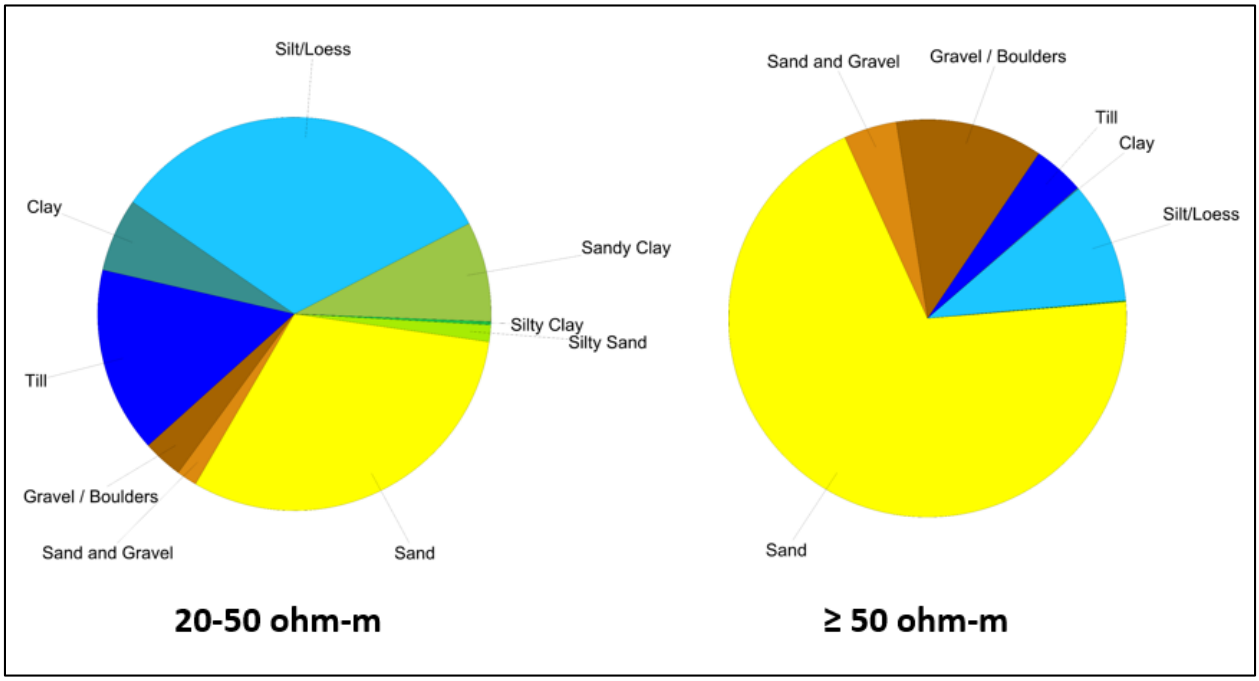


Figure 5-6: Pie charts of the distribution of material within each resistivity range for the aquifer materials used in the interpretation of the AEM data- 20-50 ohm-m (left), and 50 ohm-m and above (right).

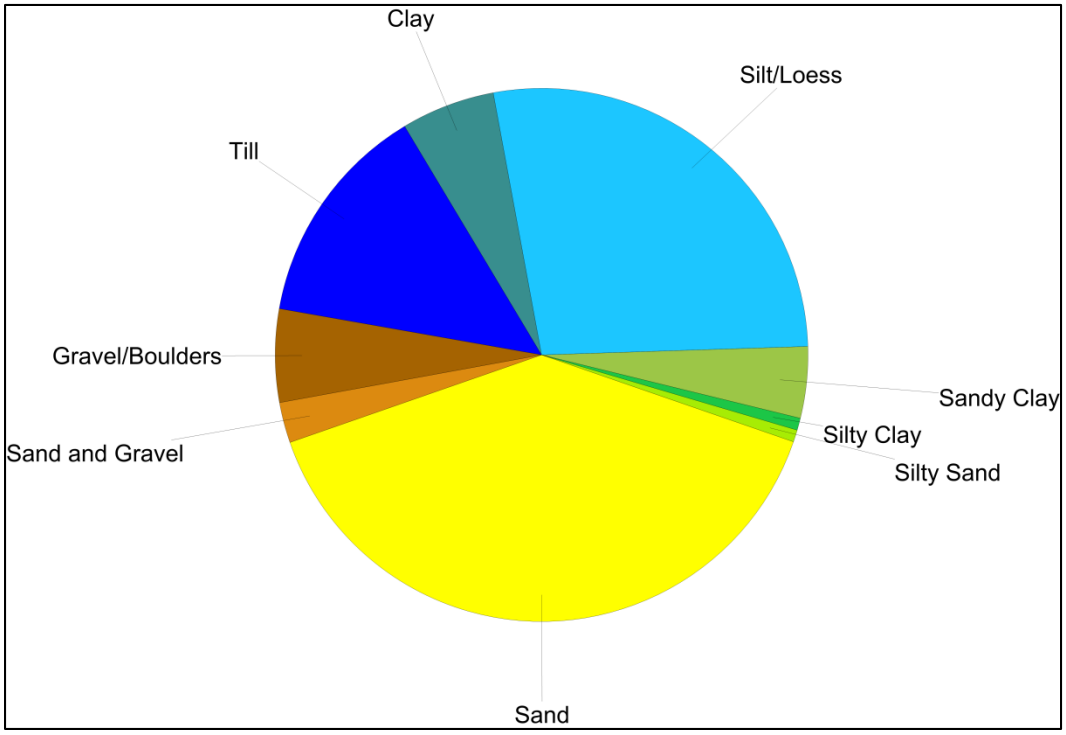


Figure 5-7: Pie chart of the overall lithology indicated in the 58 e-logs used to characterize the relationship of lithology and resistivity across the ENWRA project area.

Figure 5-8 displays 4 pie charts showing overall percentage of lithologies in selected CSD test holes located within the project area. These charts are displayed with the CSD glacial till thickness map set in semi-transparent shading to demonstrate the relationship of the percentage of each major material with the extent and thickness of the till within the project area. At CSD test holes 8-A-53 and 4-A-52, the glacial till component in the holes are the largest of the four locations analyzed, with nearly two-thirds of 8-A-53 consisting of glacial till. Test hole 4-A-52 has a larger sand component, which is likely a result of this hole being located above the 40 ohm-m or greater, sand-rich zone of the principal aquifer north of Norfolk. Each of these locations is situated where the CSD map indicates till to be present.

At test hole 16-A-55, which sits at the western edge of the extent of glaciated region of eastern Nebraska, till is absent, with sand and sand and gravel comprising nearly half of the lithologic content in the hole. The remaining half is predominately silt/loess with minor amounts of clay and silty clay. This hole is located in an area along flight line 200101 where sand-rich, principal aquifer materials are present (Appendix 1). Finally, test hole 5-GT-80, located just west of the city of Wayne and in the area defined as primarily marginal aquifer or non-aquifer material, the pie chart reveals the predominant material in the hole was silt/loess (two-thirds), with the remaining one-third characterized as sand. This hole is located within an area demarcated with an absence of glacial till. In AEM profile 201401, the distribution of material in this hole is predominately silt/loess, with only minor intervals of sand, which matches closely with the pie-chart distribution. The hole sits on the edge of a body of marginal aquifer that contains small intervals of principal aquifer material. This hole thus demonstrates that silt-sized particles can still be considered part of the marginal aquifer in the AEM interpretation if sand intervals are also present.

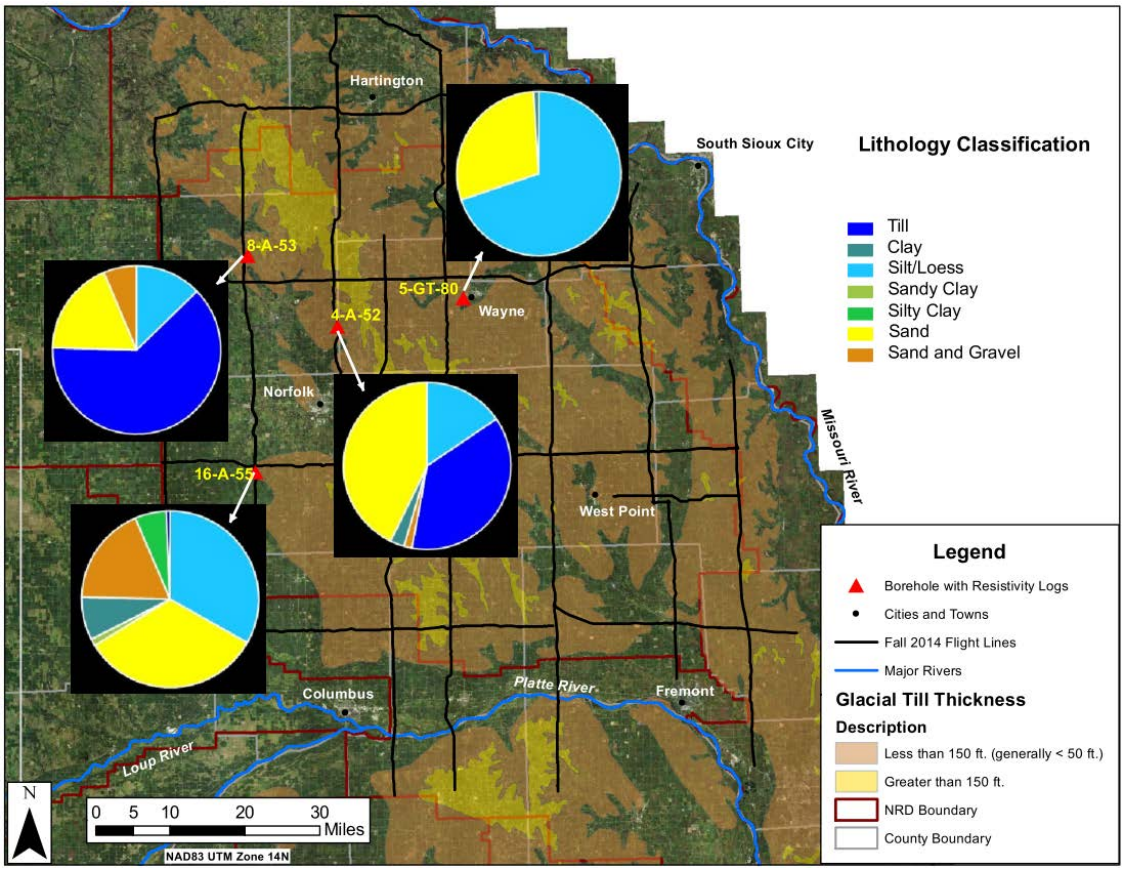


Figure 5-8: Pie charts showing overall percentage of lithologies in selected CSD test holes in the northern ENWRA project area.

The section of the project area north of Norfolk and the Elkhorn River and west of flight line 200801 is underlain by the most prolific aquifer material in the project area. This area appears to have a combination of depositional environments providing potential for optimal groundwater development, including the presence of the *To* and an abundance of glacial outwash deposits that are sourced from the glacial margin to the east. Recent deposition of alluvium from eastward meandering drainages, including former channels of the North Fork of the Elkhorn and Elkhorn Rivers also contribute to the overall aquifer resources in the west subregion.

Basis for Resistivity Thresholds in Quaternary System

Based on the discussion above in Section 5.1.2, the Quaternary and Tertiary material were separated into four characteristic aquifer materials including non-aquifer (aquitard), marginal, principal, and coarse aquifer material. These breaks were determined based on the distribution of the resistivities (Figure 5-4) and the lithology (Figure 5-5 and Figure 5-6). However, the question can arise as to the sensitivity of the selection of the thresholds, specifically the lower threshold for the principal aquifer material (20 ohm-m). In order to assess this sensitivity, a test was conducted by analyzing the data set with thresholds of 20 and 21 ohm-m. The change in the percent thickness of the principle aquifer material was then calculated over the complete data set. It is important to note that the thickness was evaluated as being greater than or equal to both 20 and 21 ohm-m. For each of the thresholds (20 and 21 ohm-m), the

materials were calculated based on the methodology outlined in Section 5.0. The thicknesses of the principal aquifer material were then compared using the following:

$$T_{Diff} = \frac{abs(T_{20} - T_{21})}{T_{20}}$$

where T_{Diff} is the fractional difference in thickness, T_{20} is thickness of the principle aquifer material with resistivities greater than or equal to 20 ohm-m, and T_{21} is the thickness of the principal aquifer material with resistivities greater than or equal to 21 ohm-m.

This calculation was carried out for all data points within the 2014 flight area (Figure 5-1). The statistics of this change in thickness analysis indicate that the median fractional difference is at 0.04, or 4%, and a first quartile of 0.01 (1%), and a third quartile of 0.10 (10%). This indicates that 75% of the data indicates a thickness change of the principal aquifer materials of less than 10% when comparing thicknesses derived from both 20 ohm-m and 21 ohm-m thresholds. Thus Figure 5-9 displays a histogram of the distribution of the variation in interpreted thickness of the principal aquifer material using 20 and 21 ohm-m thresholds.

This analysis indicates that the sensitivity of picking 20 or 21 ohm-m is relatively insignificant for the overall interpretation of the thickness of the principal aquifer materials. Figure 5-10 demonstrates the impact on the interpreted cross sections with an example cross section showing both 20 and 21 ohm-m thresholds.

Figure 5-10 shows that the area encompassed by the 20 ohm-m threshold (solid black line) is slightly greater than the 21 ohm-m aquifer extent (dotted black line), which results in a thicker estimation of the principal aquifer material. This result is not unexpected as the lower resistivity value should encompass a larger range of resistivities of greater than or equal to 20 ohm-m. However, it can also be observed that the change in the interpretation is generally insignificant (see zoomed-in view in Figure 5-10), as the change in overall extent, when viewing the principal aquifer materials on a regional basis, is negligible when considering overall volume of the aquifer. It should be noted that in some areas where principal aquifer material is present at the land surface (indicated by blue arrow in Figure 5-10), but separate from the underlying main body of principal aquifer material, these intervals were included in the interpretation even if these features were separated by marginal aquifer material.

This approach was warranted since this interpretation is a discussion on the major aquifer features in the subsurface of the LENRD. Surficial resistive materials are considered critical in assessing areas of aquifer recharge and, thus, are included in the principal aquifer zone even where separation from the main principal aquifer materials can occur.

In summary, the results of this sensitivity analysis indicate that for 75% of the data, a thickness change of less than 10% occurred between a threshold change of 20 to 21 ohm-m. Overall, the interpreted principal aquifer materials show a stable solution that is not sensitive to a 1 ohm-m change in the principal aquifer material threshold.

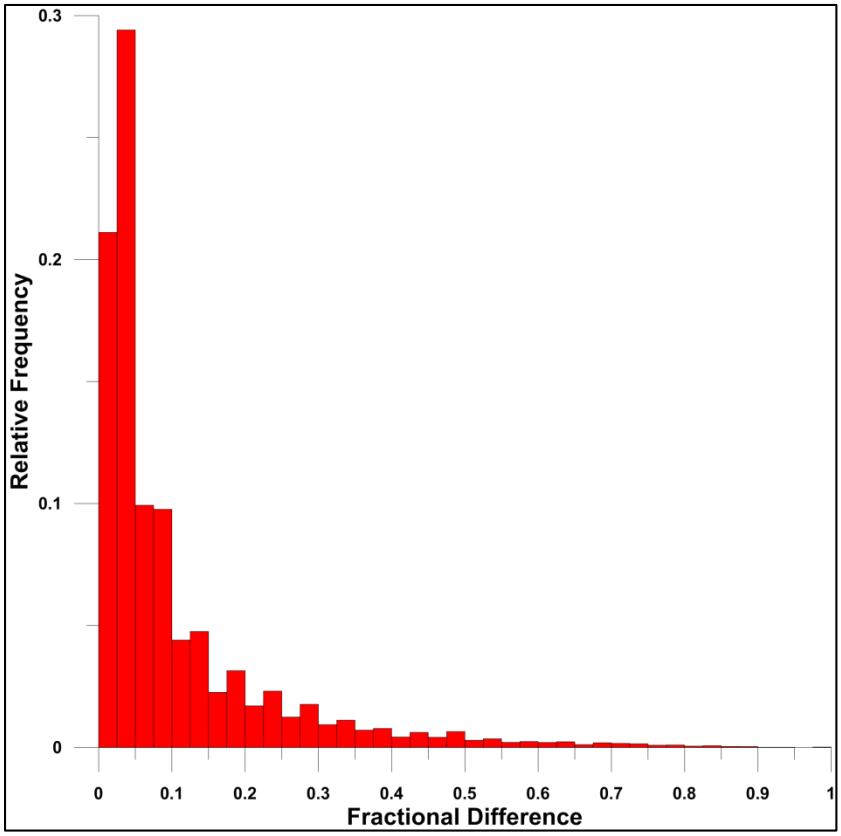


Figure 5-9: Histogram of the distribution of the fractional difference in the thickness of the principal aquifer materials using 20 and 21 ohm-m resistivity thresholds.

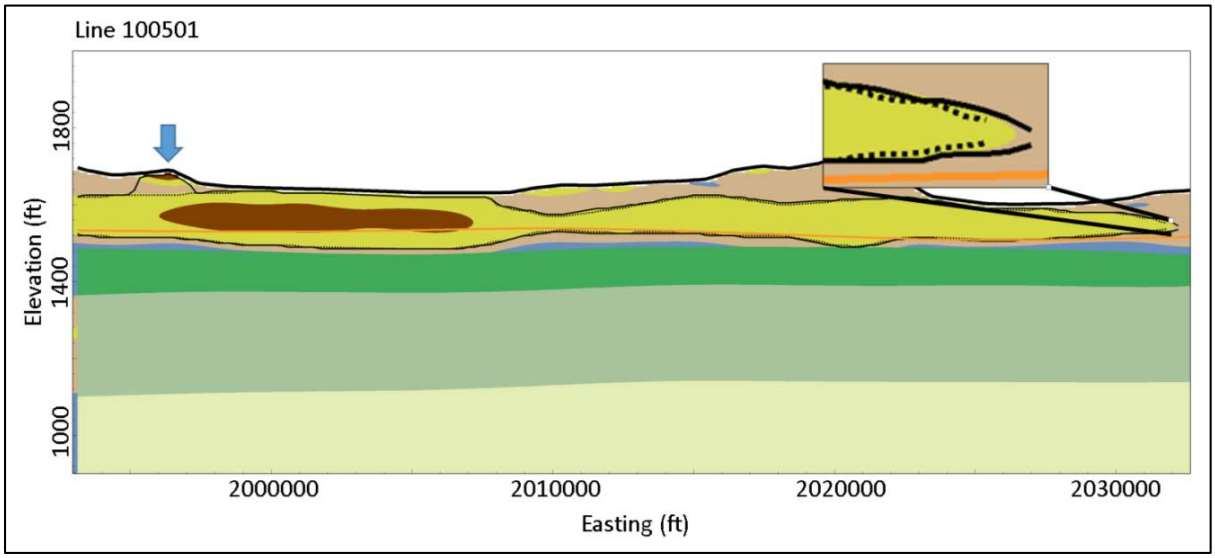


Figure 5-10: Example cross section illustrating the small difference between use of a 20 ohm-m threshold or a 21 ohm-m threshold to define the principal aquifer. The solid black line enclosing the yellow (principal aquifer material) represents the 20 ohm-m threshold and the dotted black line enclosing the principal aquifer material represents the 21 ohm-m threshold.

5.1.2.2 Bedrock Resistivity Thresholds

Figure 5-11 displays a box and whiskers plot of the resistivity distribution for the bedrock strata described in the interpretation section, including the *To* (which is present only beneath the northern half of the ENWRA project area). Analysis of the bedrock data was conducted on e-logs from CSD test holes that penetrated into the bedrock. The analysis also included oil and gas wells with data on Paleozoic strata. The median resistivity values for each unit in Figure 5-11 are 40 ohm-m or less. *Kp* has the lowest median (9 ohm-m) and lowest overall value of resistivity, as would be expected for a unit predominately composed of shale. *Kn* and *Kd* have similar distributions and maximum/minimum ranges, with one exception being the *Kd* having a lower median resistivity (approximately 20 ohm-m). The similarities in these two units on this plot exemplify how the *Kn*, which is predominately a shale and chalk, can contain resistive material, and the *Kd*, predominately a sandstone, can contain shale and other more conductive material. The *KcKgg*, and the undifferentiated Paleozoic strata also have similar resistivity characteristics, with median values around 16 ohm-m. The undifferentiated Paleozoic units show the widest range in detected resistivities, which should not be unexpected as this sequence contains resistive limestone and conductive shale units. The *To* has the narrowest distribution band of the formations displayed on Figure 5-11, with maximum and minimum resistivities of 45 and 12 ohm-m, respectively. The median value in the *To* is 30 ohm-m, a value that would be expected of interlayered sandstone, siltstone, sand, gravel, and silt. This narrow distribution for the *To* could be a result of the distal location of these sediments from their source area in the Rocky Mountains of Colorado and Wyoming.

Review of the NOGCC database provided three holes with electrical logs within three miles of a flight line across the entire ENWRA project area. Figure 5-12 displays the electrical resistivity logs compared with the closest AEM sounding for two NOGCC well locations in the northern ENWRA project area (wells 2616718000API and 2616721003API, 5,186 ft and 12,828 ft, respectfully, from the flight lines). This relatively close proximity allowed comparison of the AEM inversion model to the resistivity logs. It is important to note that the resistivity logs started within the Cretaceous strata. The comparisons show a general match to the AEM resistivities at depths in excess of 1,000 ft. It is also important to note that the averaging effect of the AEM models smooth out the thin resistive units around 600 ft in 261671900 and 500 ft in 2616721003. The logs compared to the AEM clearly indicate the inflection in the resistivity logs at 400 ft. This further provides assurance that the AEM is mapping the resistivity structure of the bedrock within the ENWRA survey area.

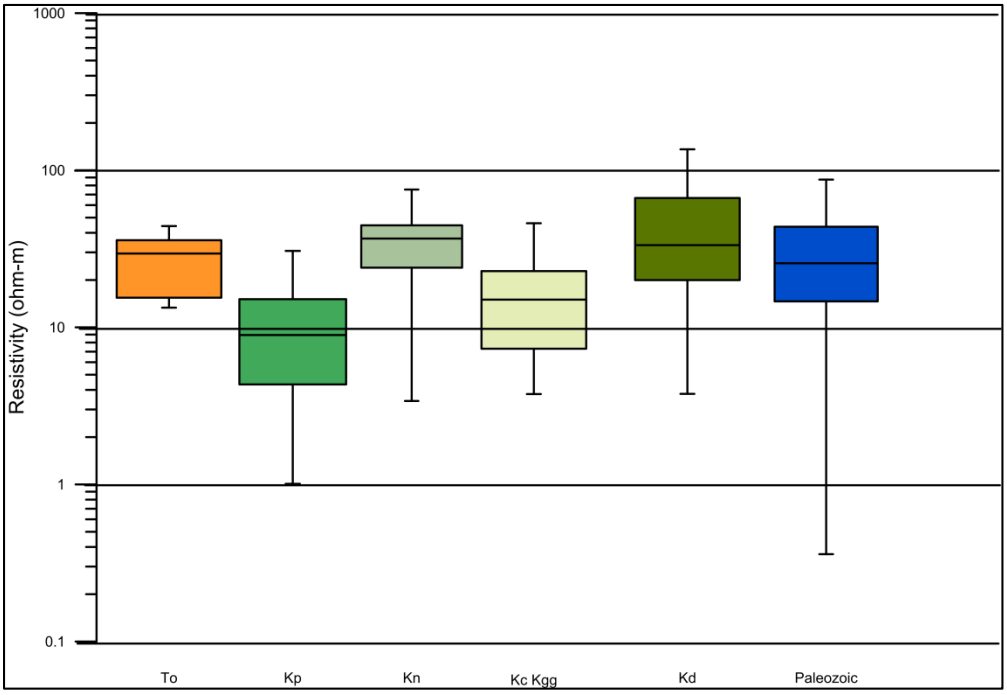


Figure 5-11: Box and whiskers plot of the resistivity distribution of the Cretaceous and Paleozoic bedrock units discussed in the interpretation of the AEM data.

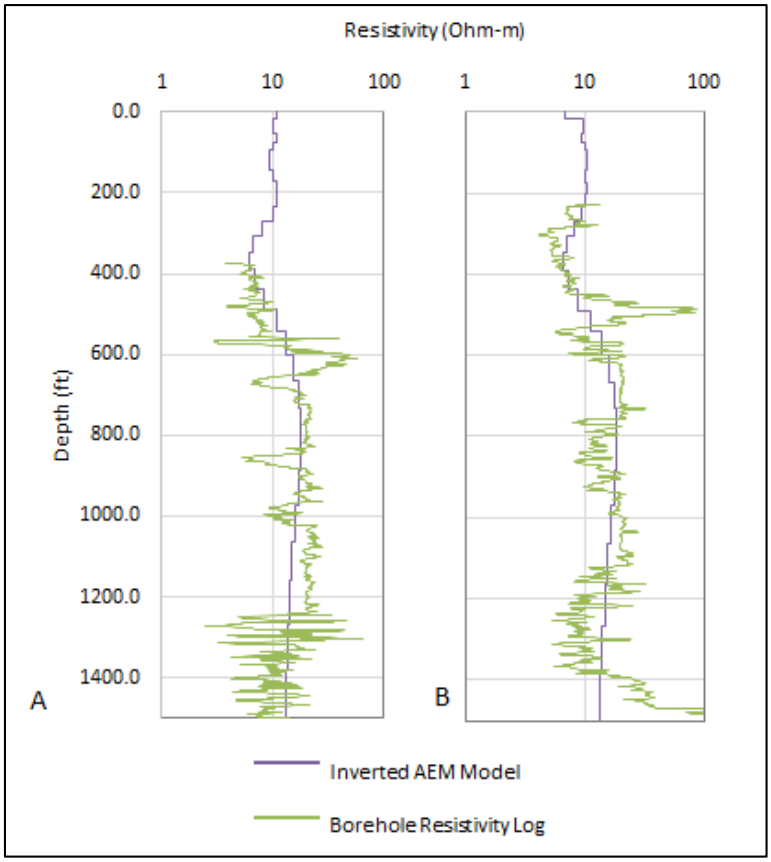


Figure 5-12: Deep oil and gas borehole resistivity logs (green lines) compared with inverted AEM models (purple lines). A: Well 2616719000, 5,186 ft from the AEM line, B: Well 2616721003, 12,838ft from AEM line.

Kd Resistivity Threshold

As a secondary aquifer resource in eastern Nebraska, the *Kd* holds potential as a new or additional groundwater source for users across parts of the ENWRA area. The AEM survey's DOI penetrated below the *Kd* in most locations, allowing for a full electromagnetic view of the formation, which can reveal changes in resistivity, and thus lithologic content and/or changes in water quality. To characterize the variability in the *Kd*'s resistivity, the relationship of lithology and resistivity was evaluated using the same method applied in associating unconsolidated lithologies to resistivity as described previously in this section. Resistivities were associated with each lithologic description in the CSD test holes that penetrated through the *Kd* in this process and are within the CSD's stratigraphic identification of the *Kd*. It should be noted that even what is presumably considered a consolidated formation, intervals of unconsolidated lithologies are noted in the CSD test hole descriptions.

Figure 5-13 shows a breakdown of textural size and nature of consolidation (unconsolidated (clay/silt) and consolidated fines (shale), unconsolidated (sand and gravel) and consolidated coarse (sandstone). The distribution for the coarse categories is similar, with the 25th quartile for each greater than 50 ohm-m, and median values over 70 ohm-m. Distributions for the fine textured materials are similar, with the median values range from 25 to 30 ohm-m. In these plots, however, shale has a wider range of values detected in comparison to unconsolidated fines. Thus, in the analysis of the lithology-resistivity relationship for the *Kd*, unconsolidated and consolidated fines were grouped together, as well as coarse-textured unconsolidated and consolidated materials. The objective of this analysis was to determine if any natural breaks in the resistivity distribution were evident to base selection of categorical ranges for showing the variation in resistivity within the *Kd*.

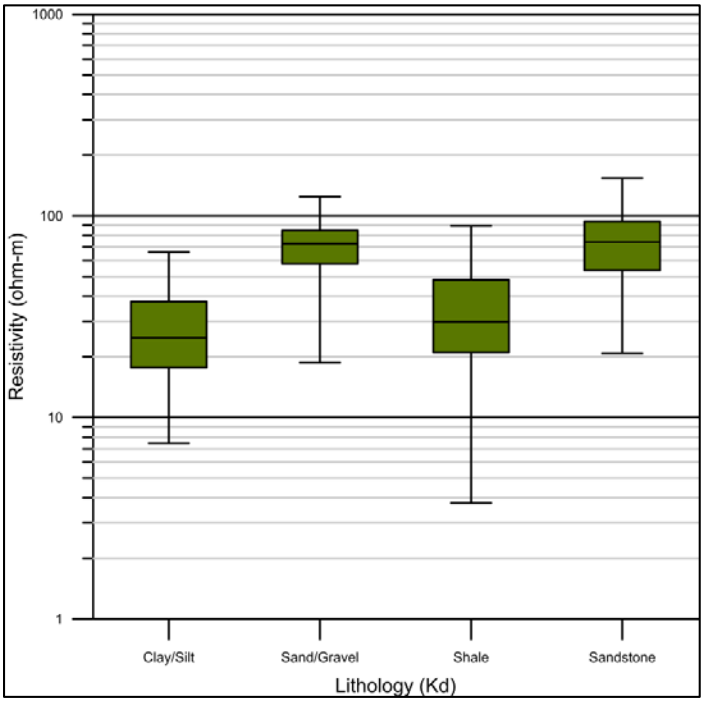


Figure 5-13: Box and whisker plot for the major lithologic texture categories within the *Kd* from CSD e-logs located across the entire ENWRA project area.

Figure 5-14 shows the count distribution of resistivity for coarse materials (top plot), fine materials (middle plot), and a composite of both major material distributions (bottom plt). From this distribution, it is evident that the bulk of fine textured materials are generally below 40 ohm-m, and that the bulk of the coarse textured distribution is above 30 ohm-m, with overlap of the two groups in the 20 to 40 ohm-m range. The plot for fine textured materials indicates bimodal distribution. The distribution below 10 ohm-m is likely due to brackish/saline water in the *Kd*, and the distribution greater than 10 ohm-m is most likely related to lithologic character.

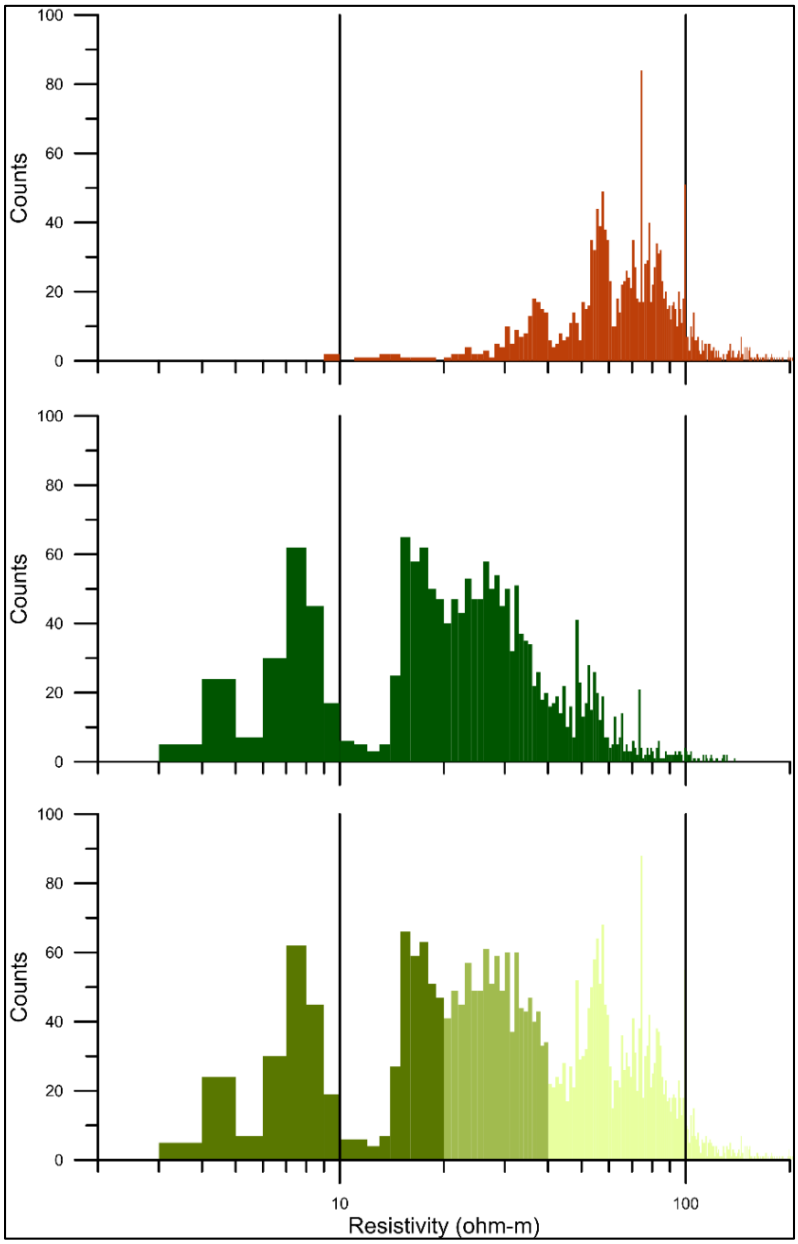


Figure 5-14: Resistivity count distribution by major grain size category for CSD test holes screened in the Kd. Plot A (top) represents all coarse unconsolidated and consolidated deposits; plot B (middle) represents all unconsolidated and consolidated fines, and plot C (bottom) represents a composite of both coarse and fine materials, color coded by the ranges of 0-20, 20-40, and 40 ohm-m and above used in the interpretive figures of the Kd beneath the ENWRA project area.

From these distributions, three general categories were selected from this distribution- 0-20 ohm-m, representing zones of the *Kd* predominately consisting of fines or high TDS pore water; 20-40 ohm-m, representing intervals of interbedded fine and coarse materials, and zones at or greater than 40 ohm-m, which are intervals of the *Kd* where coarse textured deposits comprise the bulk of the material at that interval. These ranges are not categorized as "aquifer materials" as in the Quaternary system descriptions, since little is known about the aquifer potential in the *Kd* based on resistivity alone. However, generalized inference can be made in that the higher the resistivities encountered, the greater the probability the interval will produce beneficial flow to a well. To determine if any relationship exists between the resistivities revealed by the AEM data and production wells, XRI reviewed all DNR registered well records within 0.5 miles of the southern ENWRA area flight lines for production rates of wells screened in the *Kd*. Overall, no discernible pattern was evident, as nearly all wells along these lines near the CSD test holes penetrated only into the upper 10 to 20 ft of sandstone and were used for domestic purposes, with registered rates normally ranging from 10 to 20 gpm. It is uncertain as to whether the *Kd* is capable of producing higher capacities to wells in these areas, as the wells currently existing at these locations typically do not require high pumping rates.

In conclusion, the evaluation of the relationship of lithology vs. resistivity in the *Kd* intervals resulted in 3 major intervals of resistivity, with the zones of 40 ohm-m or greater possibly indicating the areas of higher likelihood of groundwater development from the *Kd* sequence beneath the project area.

5.2 Hydrogeologic Framework Interpretation

The AEM reveals considerable variability in the Quaternary and Tertiary deposits across the northern ENWRA project area. "Quaternary system" is a term used in the interpretative section of this report to describe all unconsolidated materials overlying the *To* and Cretaceous bedrock, thus including aquifer and non-aquifer material alike. Figure 5-15 displays in 3D the overall distribution of materials (as described in the previous section) across the northern ENWRA project area, along with major drainages and NRD boundaries. The subsurface distribution of materials can be generally characterized into two somewhat distinct areas with smaller localized depositional features distributed at various locations within the survey. The area between flight lines 200801 and 201001 is an approximate line of demarcation, with most of the principal aquifer materials, including sand-rich intervals found west of this area. The principal aquifer beneath this area is composed of glacial outwash materials, younger fluvial deposits, both overlying *To*, the combination of which, creates principal aquifer deposits exceeding 200 ft in thickness at some locations.

East of flight lines 200801 and 201001, the aquifer is predominately marginal (with the exception of an area in the northeastern extent of the LENRD immediately east of flight line 200801 and north of flight line 100501), with more isolated pockets of principal aquifer interlayered with non-aquifer materials and capped by extensive deposits of till and loess in throughout the remainder of the LENRD, the eastern half of the LCNRD, and the PMRNRD. Interspersed within the region east of flight lines 200801 and 201001, particularly beneath and east of flight line 201801 are isolated and buried outwash deposits classified as principal and sand-rich aquifer material, as well as fluvial deposits underlying ancestral and present-day drainage areas. Additional bodies of principal and sand-rich aquifer intervals, primarily east

of flight line 200801, are also present along the northern edges of several flight lines near the Missouri River valley. The southern portion of the northern ENWRA project area includes extensive areas of principal aquifer material, primarily underlying and adjacent to the Platte River valley. South of the Omaha metropolitan area, principal aquifer material ranging typically from 50-100 ft thick is present above the bedrock strata, and is overlain typically by interlayered marginal and aquitard material. The Platte River valley in the far southern extent of the PMRNRD is comprised of approximately 80-125 ft of sand-rich principal aquifer material beneath most of the valley's profile in the AEM data. More detailed discussion on the distribution of aquifer and non-aquifer materials is included in following sections that discuss findings within the individual NRDs in the northern ENWRA project area.

To assist in the characterization of the aquifer underlying the project area, the 1995 Nebraska regional water table surface (CSD) was converted to a grid dataset and incorporated into the hydrostratigraphic interpretive profiles of the project area (blue dashed line in the profile figures). Overall, the regional water level surface conforms closely with the subsurface character revealed in the AEM profiles. In the drainage valleys, the surface matches closely with the land surface elevation, which would be expected where shallow groundwater conditions typically persist. Beneath the upland areas, the regional water level surface is typically found within the till deposits, indicating confined or semi-confined aquifer conditions, which are typical in the principal Quaternary aquifer in eastern Nebraska where thick till and loess sequences are present.

5.2.1 Quaternary/Tertiary System

5.2.1.1 Extent of Principal Aquifer

The aquifer materials in the northern ENWRA project area, including Quaternary and Tertiary deposits (where present), are identified with the colors tan (marginal aquifer), yellow (principal aquifer), and brown (coarsest, sand-rich intervals of the principal aquifer). These colors correspond to the resistivity ranges described at the beginning of Section 5.1. As discussed in the prior section and displayed in Figure 5-15, considerable variability exists in the aquifer resources that underlie the northern ENWRA project area. Flight lines 200801 and 201001 are labeled on Figure 5-15 to indicate the general area demarcating the transition of predominately principal aquifer with lesser areas of marginal aquifer/aquitard zones to primarily marginal to aquifer materials with more isolated zones of principal aquifer material. The principal aquifer material (yellow and brown) is found primarily in the west subregion, with less extensive and more isolated bodies of principal aquifer materials scattered throughout the remainder of the area surveyed in this project. The most extensive bodies of principal aquifer material are found primarily in the LENRD, with smaller, more localized intervals present in the LCNRD and PMRNRD (the Lower Platte North NRD is discussed in Volume II of this project report). Further discussion of these features is included in section 5.3.2. Beneath the northwestern one-third of the surveyed area, numerous intervals of sand-rich principal aquifer (>50 ohm-m) are present, notably at and north of west-east flight line 101301 and west of the North Fork of the Elkhorn River. The principal aquifer extends eastward from this area, reaching north-south flight line 200801, but generally with less sand-rich material. Much of this area includes Quaternary materials directly overlying *To*. The thickness of these resistive bodies (> 50 ohm-m) within the principal aquifer materials exceeds 150 ft in

some areas, particularly along the western edge of project area where thick *To* is overlain by Quaternary fluvial deposits (flight line 200101), beneath the Elkhorn River valley west of the city of Norfolk, and in an isolated body of resistive material east of flight line 200801 and north of flight line 100501. Other extensive bodies exceeding 100 ft in thickness are present beneath the western half of the surveyed area, mainly along flight lines 200101 and 200401, and in the far southern extent of the PMRNRD beneath flight lines 401001 and 300402. An AEM survey conducted by XRI in the fall of 2014 within the LENRD (Exploration Resources International, 2015) with a three-mile grid spacing reveals these resistive features in further detail, including the extent of these bodies and the proximity of nearby surface water features. Other isolated bodies of principal aquifer material, which included small sand-rich features are present in the far northwestern extent of the survey area, primarily along flight line 100201 in the LCNRD and within the northwestern half of the LPNNRD.

Much of the region east of flight lines 200801 and 201001 is underlain by mostly marginal aquifer and non-aquifer materials, with only isolated bodies of principal aquifer materials present (Figure 5-16). Most of these principal aquifer intervals appear to be isolated bodies of outwash interlayered within marginal aquifer and aquitard materials observed in flight lines 201301, 201801, 201901, and 202001. These features can range in thickness from 20 ft to over 150 ft, with the thickest intervals located in the eastern LENRD and the western PMRNRD. The remaining principal aquifer material feature in the eastern half of the eastern ENRWA project area is associated with the fluvial depositional features in the Elkhorn River-Maple Creek confluence area. This feature will be discussed in greater detail in section 5.3.2.3.

The principal aquifer, including several sand-rich zones, is present at shallow depths below the ground surface in the far western sections of the northern ENWRA project area, particularly along flight line 200101. The hydrostratigraphic framework revealed in the 2014 LENRD AEM survey (Exploration Resources International, 2015) further exemplifies the nature of these deposits in the western LENRD. Most of these areas are overlain with minimally conductive, non-aquifer material; this is a condition which could be associated with potential for relatively higher recharge rates to the aquifer. However, this assessment is based on the existing shallow subsurface geologic conditions only, as recharge is also influenced by other key factors, including soil type, slope, vegetation, and land use practices.

On the far western edge of the project area (Figure 2-1), the Quaternary system is underlain by *To* and *Kp*. Beyond the subcrop of the *To*, the *Kn* forms the basal bedrock unit beneath the Quaternary deposits in roughly the northwestern half of the project area. In the eastern half of this project area, the *KcKgg,* and the *Kd* are the bedrock units underlying the Quaternary system.

The distinction between the distribution of principal and marginal aquifer material is also revealed by the density of irrigation wells to the east and west of flight line 200801. In an approximately 170 square-mile sample area west of the North Fork of the Elkhorn River and north of the Elkhorn River, the density of irrigation wells is 3.6 per square mile, with an average registered pumping rate (for wells with non-zero registered pumping rates) of 866 gallons per minute (gpm). In a similar sized area between flight line 200801 and the city of Wayne, irrigation well density is 0.6 per square mile, with an average registered pumping rate of 734 gallons per minute. This indicates that in the area underlain by primarily

marginal aquifer, particularly within the eastern half the LENRD, there is generally less than one irrigation well per square mile, whereas in the area northwest of Norfolk, there is nearly one irrigation well per 160 acres. For irrigation wells tapping what is considered marginal aquifer, average registered pumping rates are over 100 gpm less than irrigation wells screened in the principal aquifer to the west.

5.2.1.2 Extent of Marginal Aquifer

Material considered marginal aquifer (12-20 ohm-m) is present throughout the entire project area and is detected along every flight line in the AEM survey. The material is variable in extent and thickness, and is also present above the 1995 Nebraska regional water level surface in numerous locations. As indicated in the previous section and displayed in Figure 5-16, the only aquifer resource available in much of the project area is considered marginal, based on the geophysical classification defined in this study. The material is mostly continuous west of flight lines 200801 and 201001, where it is interlayered with principal aquifer material. However, east of these flight lines, marginal aquifer material is the predominant aquifer source beneath the upland till deposits to the northeast and southeast of Norfolk as indicated along flight lines 201001, 201301, and 201801. These flight lines indicate that although the marginal aquifer materials can approach 200 ft in thickness, they are discontinuous and separated by aquitard materials. Along the far eastern portion of the LENRD and the western areas of the PMRNRD, the marginal aquifer materials become more continuous, with thicknesses exceeding 200 ft at many locations. Beneath the far southern extent of the PMRNRD, marginal aquifer generally ranges from 50 to 100 ft in thickness and overlies principal aquifer material (flight line 300202). Marginal aquifer material is present near or at the land surface across much of the western half of the northern ENWRA project area, and in isolated areas in the eastern half, particularly in the northeast corner of the project area. Although there is a larger portion of fines in the marginal aquifer material (Section 5.1.2) that can impede vertical movement of pore water to the water table, these marginal aquifer areas near the surface indicate where areal recharge to the aquifer occurs under optimal conditions. Beneath the thick till and loess sequences east of flight lines 200801 and 201001, recharge to the marginal aquifer bodies is likely minimal and focused in areas of preferential vertical flow (i.e. fractured till, deeply incised drainages).

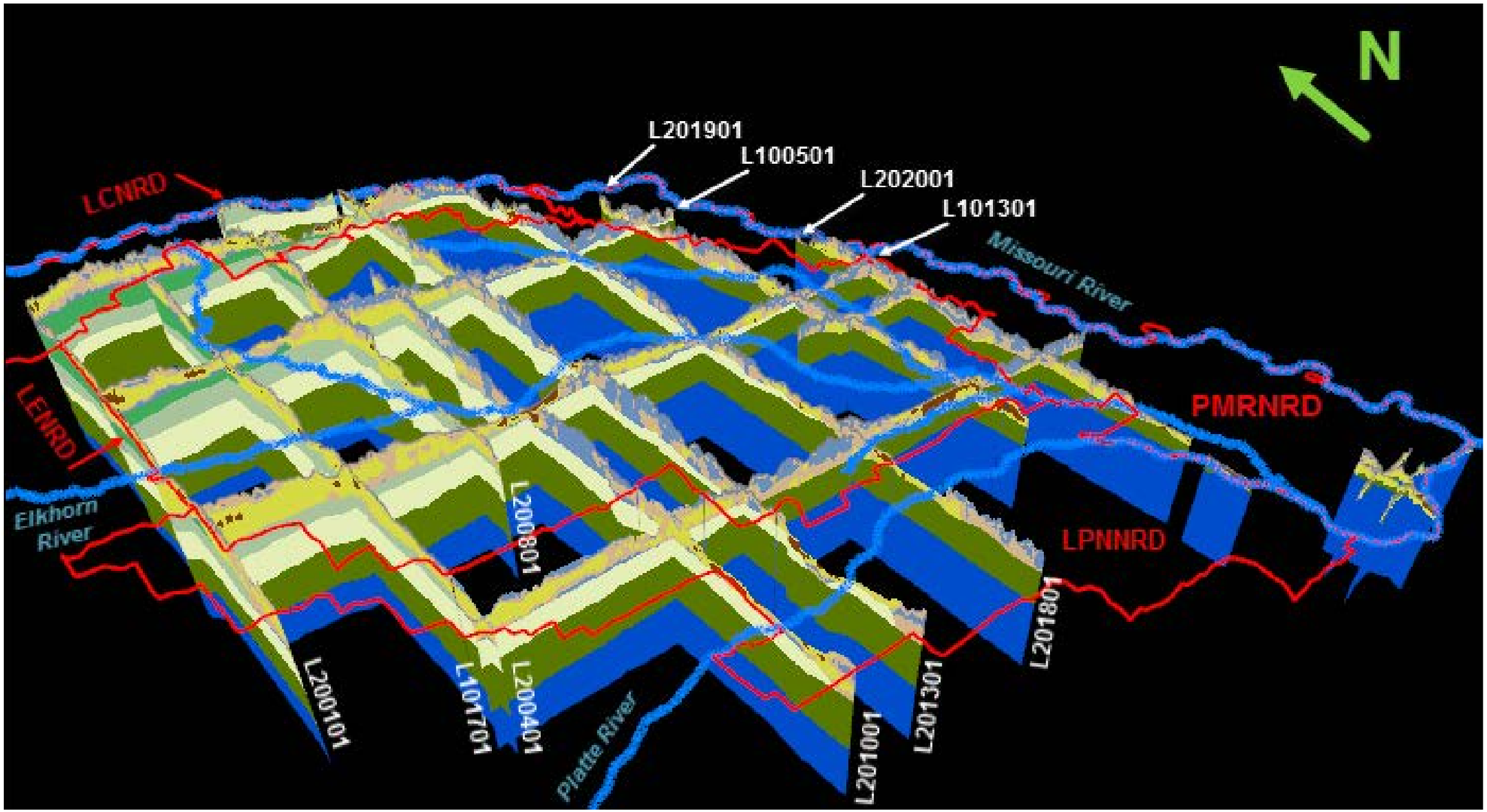


Figure 5-15: A northeastward view of the 3D hydrostratigraphic framework for the northern ENWRA project area, including geologic materials ranging from Quaternary deposits to Paleozoic bedrock. See Figure 5-2 for the color codes of the materials and geologist strata displayed. Vertical exaggeration is 50x. Refer to Figure 5-2 for a color legend of hydrostratigraphy/lithology.

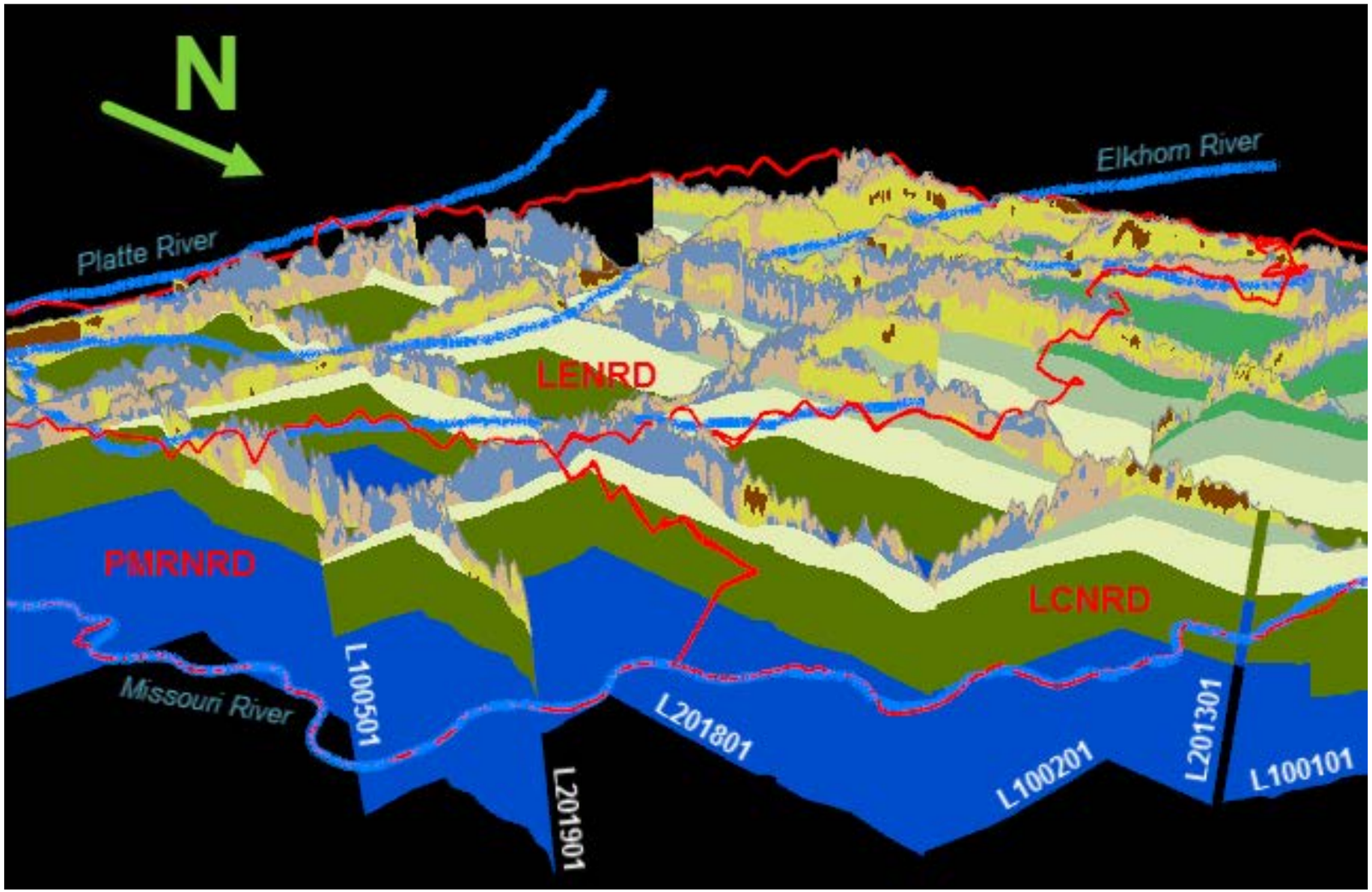


Figure 5-16: A southwestward view of the 3D hydrostratigraphic framework for the northern ENWRA project area, displaying the limited distribution of principal aquifer materials in the eastern subregion of the project area in the LENRD and LCNRD. See Figure 5-2 for the color codes of the materials and geologist strata displayed. Vertical exaggeration is 60x. Refer to Figure 5-2 for a color legend of hydrostratigraphy/lithology.

5.2.1.3 Non-Aquifer Materials

As described in section 2.1.1, loess, clay, and glacial till comprise the uppermost geologic materials at the land surface to depths exceeding two hundred feet in numerous locations and upwards of 400 ft in some isolated places. These deposits, along with other low-permeability materials (i.e.- mixtures of clay-rich sediments) are shown as light blue in the AEM interpretive profiles and 3D framework images in this section and Appendix 1. These intervals are considered "non-aquifer material" (aquitard). The AEM data reveals the combined thickness of these deposits in detail, with the intervals of greatest thickness present along a region trending northwest-southeast through the middle of the project area from the Missouri River to the Platte River. This area is associated with a moraine complex that extends from the Nebraska-South Dakota border to northern Kansas (Reed and Dreezen, 1965). The till deposits become discontinuous in the west half of the project area beyond the edge of the glaciated region of Nebraska. In this area, loess is the predominant surficial material that overlies older Plio-Pleistocene and Tertiary deposits. Figure 5-16 reveals the extent and thickness of aquitard material present in the eastern half of the northern ENWRA project area. In some areas, for example near the intersection of flight lines 100501 and 201801 (northeast of Wayne), the entire Quaternary system sequence is composed of material below 12 ohm-m in resistivity. The thickest intervals of aquitard material are found in the south-central portion of the LENRD, where upwards of 400 ft of non-aquifer material mantles the Cretaceous bedrock in parts of southeast Madison County, southwest Cumming County, and northeast Colfax County (10-15 miles southwest of West Point, NE). On the far eastern edge of the northern ENWRA project area, thick intervals of aquitard material persist, exceeding 200 ft in some locations. These aquitard materials overlie mostly marginal aquifer materials with isolated bodies of principal aquifer. In areas where basal aquitard sits atop of Cretaceous bedrock, the materials are likely remnant ground moraine till from the initial glaciation that entered Nebraska from the northeast during the early Pleistocene. This material was presumably reworked during subsequent retreat and advancements of the ice sheet during early Pleistocene time. In the far southern extent of the PMRNRD, aquitard materials are only present in isolated intervals and are typically less than 100 ft thick.

5.2.2 Cretaceous Strata and Bedrock Aquifer System

Underlying the Quaternary system and the *To* is a sequence of Cretaceous and Paleozoic bedrock strata approaching 200 ft thick in places. Although no major structural features are evident within the AEM project area, dip in the bedrock underlying the *To* and Quaternary deposits is revealed in the resistivity data. The most pronounced slope in the bedrock strata is observed in the AEM survey's west-east flight line profiles, where the Cretaceous and Paleozoic units dip westward towards the Central Nebraska Basin (Miller et al., 1964). This trend is particularly evident in flight lines 100201, 100501, and 101301, as well as many of the 3D interpretive figures in Appendix 1. The north-south flight line profiles also reveal northward dipping strata from near the southern border of the project area towards the Missouri River. Although less pronounced than the westward dip, examples of northward bedrock slope are apparent in AEM profiles 200401, 201001, and 200801. The strata appear to dip towards a trough on the south limb of the Siouxia Uplift/Transcontinental Arch located in southeastern South Dakota (Peterson, 1984).

5.2.2.1 Cretaceous Stratigraphic Sequence

Pierre Shale (Kp)

The uppermost Cretaceous unit present beneath the project area is the regionally ubiquitous *Kp*, which subcrops beneath the western half of the LCNRD and in the northwest corner of the LENRD. Maximum thickness of the *Kp* within the project area exceeds 400 ft in locations along flight lines 200101 and 200401 (Figure 5-15 and Appendix 1) in the southwest corner of the LCNRD and the northwest area of the LENRD. The thickness of the *Kp* decreases gradationally, to where the unit is less than 40 ft thick near its easternmost subcrop terminus along flight line 100501. The formation has a more abrupt southern terminus (flight line 200101), where the unit forms a wedge-shaped pinch-out from 200 ft to negligible thickness over a north-south distance of less than five miles just north of the Elkhorn River. Also indicated on flight line 200101 is an isolated, 100 ft thick remnant feature of *Kp* south of the Elkhorn River that straddles the LENRD-LPNNRD boundary. On the northern edge of the project area (flight line 100101), the formation is all but absent, with the exception of only a thin veneer, less than 40 ft thick, that caps a bedrock high in the north central portion of the LCNRD near the Missouri River valley.

Overall, the resistivity of the *Kp* is generally consistent in the 10-12 ohm-m or less range. The unit is not known to produce water in eastern Nebraska, and serves as a basal aquiclude beneath the High Plains aquifer (*To*).

Niobrara Formation (Kn)

Underlying the *Kp* are the chalk, limestone, and shale deposits of the *Kn*, which extends under the northwestern half of the project area. The unit is present as far east as flight line 201301. The gradational eastward pinch-out of the formation is clearly evident in flight lines 100201 and 100501. The *Kn* is the uppermost bedrock unit immediately below the Quaternary system, including principal aquifer materials, across much of the project area's west subregion. The thickness of the formation ranges from a maximum of 300-340 ft along flight lines 200101 and 200401 to less than 20 ft near its terminus in the east subregion of the project area. Flight line 100501 shows a pronounced change in thickness in the unit, where *Kn* that is draped by *To* thins from approximately 280-300 ft to less than 120 ft over a distance of less than five miles. It is not clear as to whether this feature resulted from erosional activity by the continental glaciers that blanketed the region during the Pleistocene. However, this area is overlain by a thick interval of principal and marginal aquifer as well as aquitard material, which is associated with glacial till and loess. The Quaternary system displayed in the western half of interpretive profile of 100501 has a "ramped" character near the change in *Kn* thickness, possibly indicating where the ice margin pushed against and over outcropping or shallow subcropping *Kn*. Sand-rich aquifer material, likely associated with coarse glacial outwash is present just west of this feature. These materials could have originated from near the ice margin if it had stagnated near this *Kn* erosional feature for extended periods of time.

The resistivity profile reveals lithologic variability in the formation, as resistivities range from around 12 ohm-m to nearly 40 ohm-m. The lower resistivities likely indicate shale and marl, the mid-range resistivities indicate chalk, and the highest resistivities are likely limestone. The *Kn* is not considered a widespread aquifer source in eastern Nebraska. However, beneath the major river valleys of the project

area, the uppermost interval of the *Kn* can contain fractures that transmit groundwater in hydraulic connection with overlying Quaternary aquifer materials. This condition is evident in resistivity profile along flight line 200801 (personal comm. with Sue Lackey, CSD, October 2013).

Carlile Shale & Greenhorn Limestone/Graneros Shale (Kc, Kgg)

Beneath the *Kn* stratigraphically is the *Kc*, which consists of interlayered shale, limestone, and sandstone. The maximum documented thickness of this unit is approximately 300 ft (Burchett, 1986). Similar to the overlying *Kn*, variability in resistivity is present throughout the *Kc*, as well as in the underlying *Kgg*. Although the *Kc* was identifiable in the resistivity data, the variability in resistivity within the *Kgg* made it difficult to discern clear contacts in the AEM data at all locations in the subsurface, thus, test hole data and 2D historic cross sections were relied on to guide the selection of the stratigraphic contacts of these units. Ultimately, these three units were grouped as one hydrostratigraphic unit in the interpretation of the AEM data (light green color associated with *Kc* in the color legend, denoted as *KcKgg* in subsequent references to these units). This combined hydrostratigraphic unit extends beneath most of the project area, terminating beneath the eastern and southern LENRD and in the central LPNNRD.

Across most of the project area's east subregion, the *KcKgg* serves as the basal bedrock unit beneath the Quaternary system. Along flight line 201901, isolated blocks of *KcKgg* ranging from approximately 75 to 125 ft in thickness are evident at several locations. A similar feature is present along flight line 201301 (Figure 5-15) beneath the Platte River valley. At this location, nearly 150 ft of *KcKgg* was completely excavated by erosional action from pre-Pleistocene drainages and later filled by unconsolidated aquifer and aquitard material. Also along 201301, variability in the erosional surface is evident north of the Platte River valley. Immediately south of the Elkhorn River, the thickness of the unit decreases from nearly 300 ft to approximately 100 ft within a distance of less than five miles. It is unclear as to whether this variation in bedrock topography existed pre-Pleistocene, or was the result of erosional activity by the continental ice sheet during the Ice Age. Collectively, the *KcKgg* units range in thickness from less than 50 ft near the eastern edge of the project area to over 400 ft beneath the west subregion of the project area. Hydrogeologically, the combined units of the *Kc* and *Kgg* act as an aquitard locally to the underlying *Kd*.

Dakota Formation (Kd)

The lowermost strata in the Cretaceous sequence is the *Kd*, which hosts the Maha aquifer in eastern Nebraska. The *Kd* is present beneath the entire project area, and is the uppermost bedrock unit in the extreme eastern extent of the LENRD and the PMRNRD. Flight lines 201901 and 100501 cross an area of the northern PMRNRD within a short distance of where the type-section of the *Kd* is located (Witzke and Ludvigson, 1994). The overall thickness of the *Kd* within the project area ranges from nearly 600 ft in the southwest corner of the LENRD (flight lines 200801 and 201001 (Appendix 1)) to a minimum thickness ranging from 100 to 150 ft beneath the PMRNRD. The *Kd* terminates east of the project area in western Iowa.

The *Kd* has a pronounced dip westward towards the Central Nebraska Basin along profiles 100201, 100501, and 100701, but has generally little slope in the eastern half of the project area (flight line

100601 and the eastern half of flight line 100701). In the northwest corner of the project area in the western LCNRD, the dip of the Cretaceous sequence results in a depth to the top of the *Kd* approaching 1,500 ft bgl (flight line 100201). This depth contrasts considerably with the depth to top of the *Kd* in the PMRNRD, where the formation is encountered at 100 to 150 ft bgl.

The *Kd* has variable resistivity, ranging from approximately less than 10 ohm-m to over 100 ohm-m (Figure 5-13). The resistive zones in the *Kd* are thicker and more extensive than those in the overlying units of the *Kc* and *Kgg* and provide potential targets for groundwater development. Extensive intervals beneath the eastern half of the project area is underlain by resistive material 20 ohm-m or greater (intermixed sandstone and shale), as indicated on all north-south flight lines east of 201301 and in flight line 101601, as well as south of the Omaha area in the far southern PMRNRD. Flight line 101701 indicates that much of the southern LENRD and the west central portions of the LPNNRD also have resistivities exceeding 20 ohm-m. Beneath several locations in the northern ENWRA project area (light yellow areas in the interpretive profiles) are isolated intervals of *Kd* with resistivities of 40 ohm-m or greater. Examples of these higher resistivity features within the *Kd* include locations beneath the PMRNRD and eastern LENRD, as indicated on the northern and southern sides of flight line 202001 and at locations along flight lines 100101, 201901, 101301, 101501, and 101601 (Appendix 1).

Resistive sections of the *Kd* greater than 20 ohm-m are absent in the far western extent of the project area. An area of less resistive material in the 10-15 ohm-m range is present along the western quarter of the project area that are in the deepest “down-dip” section of the *Kd* beneath the project area. With a lack of geologic test hole or geophysical borehole log control, it is not evident as to whether these more conductive intervals are porous sandstones containing brackish water, shale, or ironstone, all conditions that would cause a lower resistivities to be detected in the survey. This area of the *Kd* is known to have brackish water with TDS ranging from 1,000 to 5,000 milligrams per liter (Helgesen et al., 1993). With extended intervals of less resistive material, it is possible that the TDS levels are causing the change in the geophysical signature of the *Kd* in this area of the survey.

The bedrock surface topography that underlies the Quaternary materials varies across the project area, from generally flat to pronounced undulation where paleovalleys are filled with glacial outwash, till, or fluvial deposits from drainages existing prior to or during the glaciation of North America during the Pleistocene. Overall, the most pronounced areas of uneven topography in the Cretaceous bedrock occur typically where the *Kn* or *Kd* are the uppermost strata beneath the Quaternary and Tertiary units. As noted in the previous discussion on the *Kn*, the surface has considerable variability in the north-central area of the LENRD and the LCNRD. Beneath the eastern subregion of the project area, moderate variation in the *Kd* bedrock surface exists, with isolated deeper paleovalleys carved into the bedrock, as indicated near the middle of flight line 202001 and the southern half of flight line 201801. Variability in the bedrock surface topography also exists where the *KcKgg* is the uppermost surface, particularly along flight lines 201001, 201301, and 201801. Beneath the southern LENRD, the Cretaceous bedrock-Quaternary system contact becomes generally flat with only slight variation in the Cretaceous bedrock surface.

5.2.2.2 *Paleozoic Stratigraphic Sequence*

The depth of investigation for the AEM survey discussed in this report allowed for detection of the Paleozoic strata that underlies eastern Nebraska. As indicated in the geologic time scale and lithostratigraphic sequence (Figure 2-2), Paleozoic units from the Permian through Cambrian periods are present, primarily consisting of carbonates, evaporites, and clastic material indicative of cyclical transgressions and regressions of shallow seas inundating the region during the Paleozoic Era. Although test hole information was suitable for selection of individual Cretaceous units in the AEM data, sparse information at the depths of the Paleozoic units did not allow for the selection of individual formations. Thus, these units are identified only as the lumped, undifferentiated Paleozoic sequence.

The Cretaceous-Paleozoic contact is detected by the AEM survey across the northern ENWRA project area. The top of the Paleozoic sequence varies in depth from approximately 1,500 ft bgl on the western edge of the survey area to 400-500 ft bgl along the eastern flight lines in the LENRD and PMRNRD. Resistivities can vary considerably beneath the Cretaceous-Paleozoic contact, typically from less than 10 to over 50 ohm. This variability in resistivity indicates the varying sequences of more resistive limestone and conductive shale.

The Paleozoic beds detected in the AEM survey beneath the project area show similar westward structural trends as the overlying Cretaceous strata, with a pronounced dip along the west-east profiles. No discernable northward dip is evident in the Paleozoic units beneath the project area. These units are not widely used as an aquifer resource in eastern Nebraska, and further investigations would be required to assess the potential from groundwater development in the Paleozoic units underlying the project area, particularly in the deeper resistive features.

5.2.2.3 *Comparison with CSD Geologic Cross Sections and Test Holes*

Overall, the AEM profiles generally match the historic and contemporary cross sections (Divine et al., 2010; Korus et al., 2012) used in the AEM interpretive analysis. The multiple cross sections (Figure 5-17 and Figure 5-18) provided an additional background information dataset in the geologic interpretation process, which proved particularly useful in areas of the Cretaceous strata where units showed similar resistivities. The AEM profiles provide a resource for refinement of geologic cross sections previously created in eastern Nebraska, particularly in areas where formation contacts were estimated due to lack of test hole control.

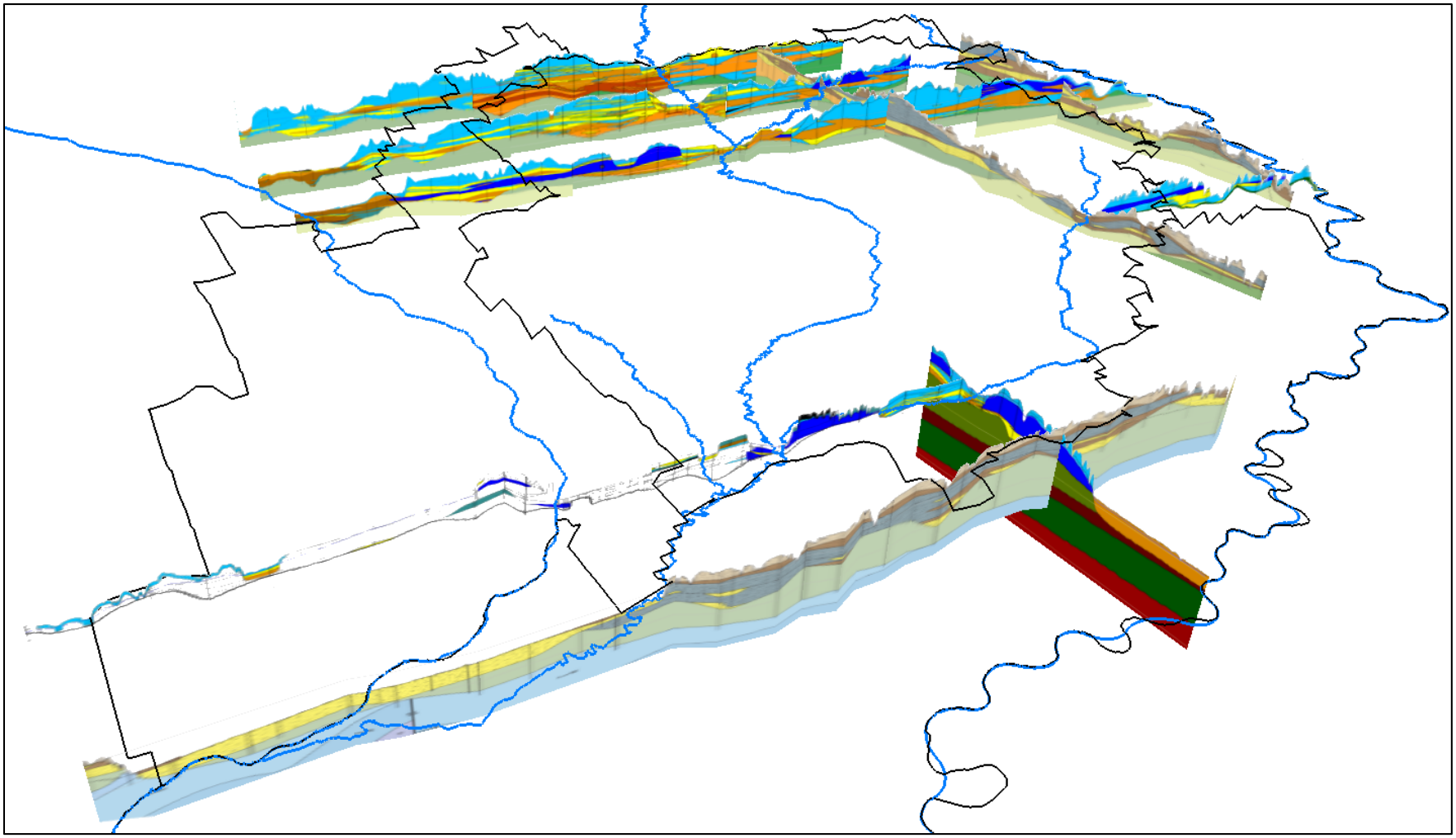


Figure 5-17: Northwestward view of the northern ENWRA project area displaying the locations of historic and contemporary CSD geologic cross sections. The color scale is shown in Figure 5-2.

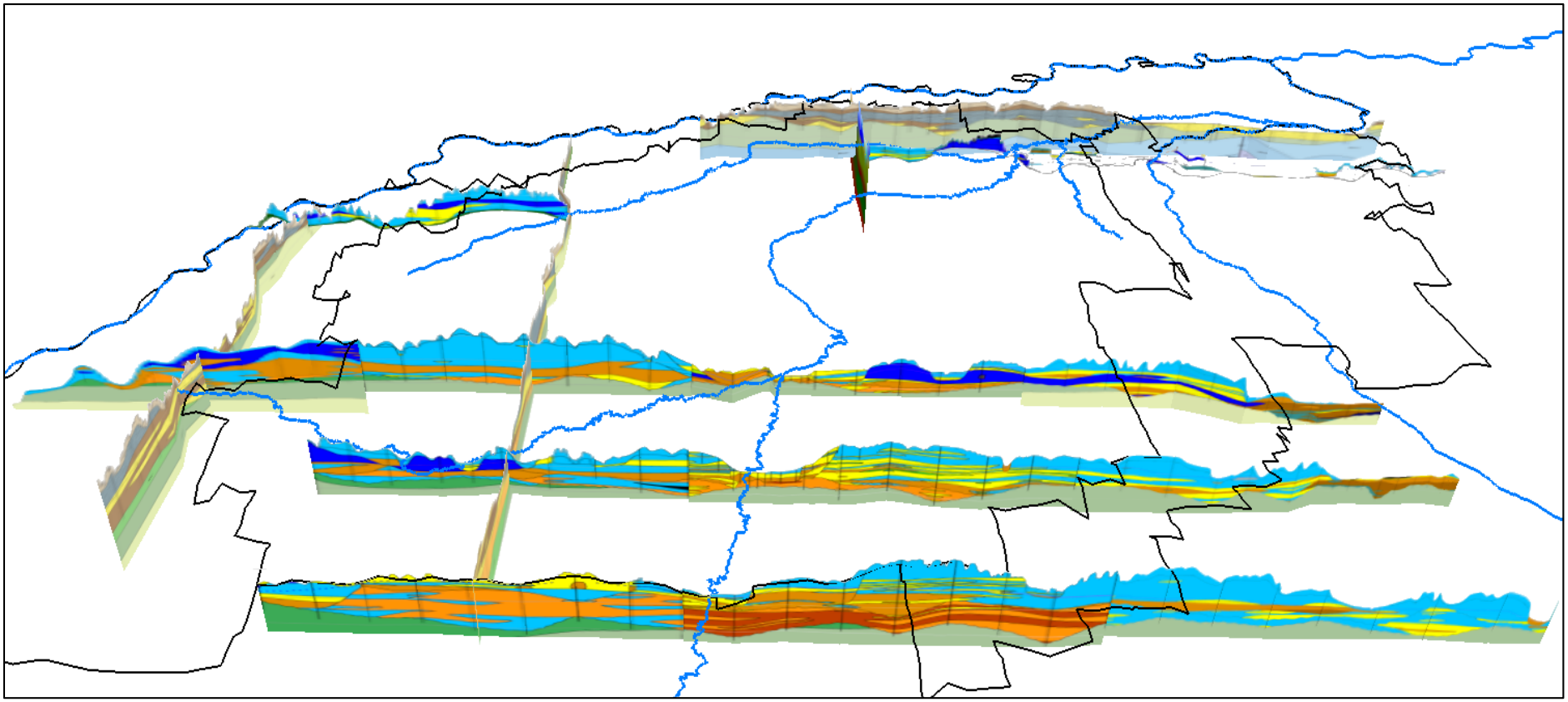


Figure 5-18: Eastward view of the northern ENWRA project area displaying the locations of historic and contemporary CSD geologic cross sections. The color scale is shown in Figure 5-2.

The AEM technique has an inherent averaging impact on the imaging of the subsurface, such that the inverted geophysical data cannot identify the fine lithologic details that can be gleaned from test hole logs such as thin laminae within thicker deposits or interbedded layers of a single formation. Section 4.6 (Spatially-Constrained Inversions) of this report indicates the thickness of the layers in the AEM inverted model. An example of this condition exists near the city of Wayne in the northeastern part of the LENRD. In this area, the Quaternary material is considered marginal aquifer to aquitard. When the AEM is compared to the CSD test hole and cross section information, it is clear that the details of the interbedded nature of fines and sands beneath this area cannot be identified from the AEM. Figure 5-19 shows the AEM model inversion fit to the data near CSD test hole 5-GT-80 (just west of Wayne). This plot exemplifies the nature of the aquifer throughout much of the eastern half of the project where isolated bodies of aquifer material, either marginal or principal, are interlayered with aquitard material. The lithology profile in this figure displays the limited vertical intervals of coarse materials available for designing screen intervals in wells where these geologic conditions persist.

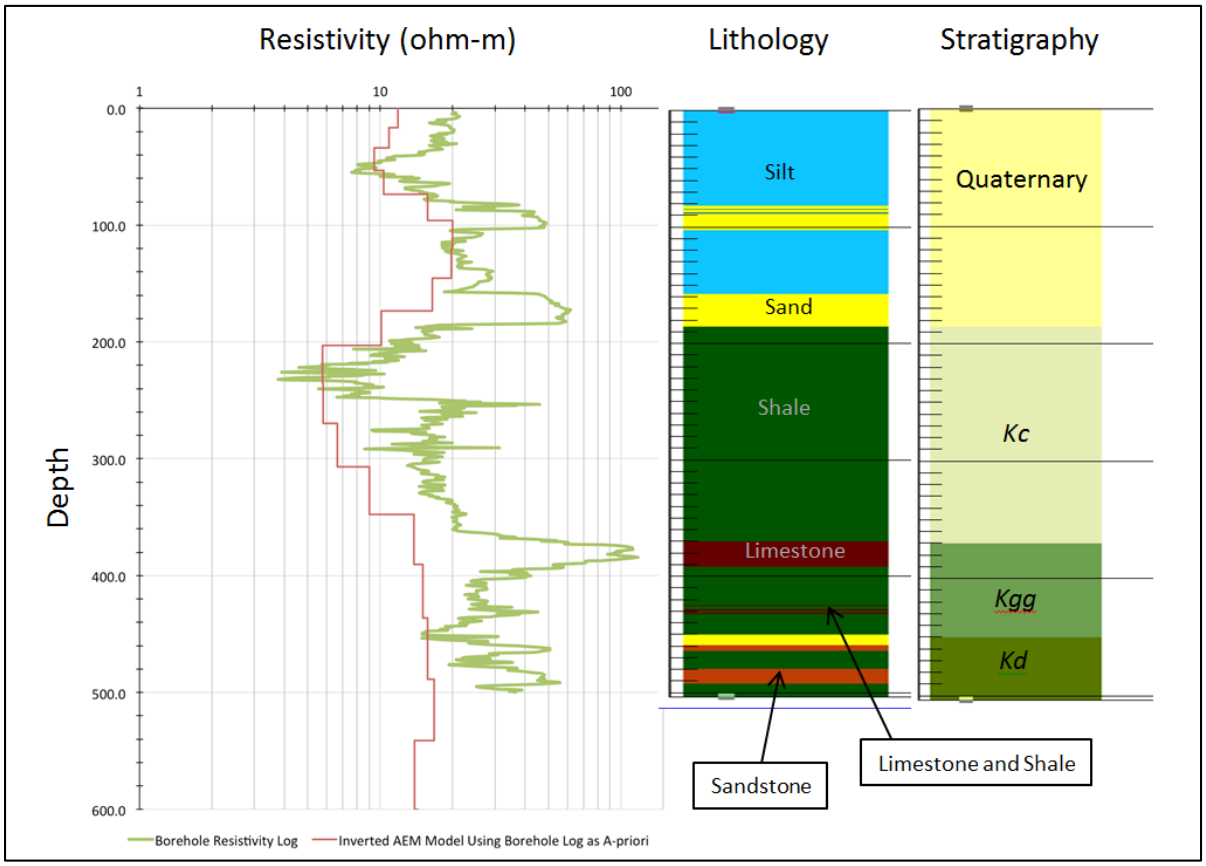


Figure 5-19: Comparison of TEM model, borehole log, lithology, and stratigraphy at CSD test hole 5-GT-80.

Registered wells in this area of the LENRD are capable of producing upwards of 200 gpm. Thus, the screened intervals in these wells include enough thin layers of sand interbedded with clay and silt that can yield suitable flow rates for productive wells (near CSD test holes 9-A-64, 10-A-64, 30-A-51 of flight line 100501 (Figure 5-20). Figure 5-21 includes a zoomed in view of flight line 100501 demonstrating this condition. The important consideration in this example is that the regional nature of the grids flown in

the project area does not have the additional supporting data of closely spaced flight lines to assist in resolving the finer nature of some of these thinner aquifer materials. Even with additional flight lines, it is still possible that the thin beds cannot be resolved. The AEM has the ability to provide an averaging view of the subsurface that provides a more scale appropriate view of the aquifer materials to inclusion into groundwater models. This is due to the reality that no model could be created with the capacity to include all the fine details of interlayered deposits and a bulk average aquifer property would need to be used.

Along flight line 100501 near wells 11-A-57, 2-A-68 and 2-B-68, the AEM CSD test holes, and cross sections are closely matched. The nature of the AEM taking a sounding approximately 250 ft apart allows for additional information to be applied to refining cross sections between test holes. The comparison between the Quaternary materials and the *To* shows similar contacts in the cross sections between AEM interpretation and CSD cross sections. Each of the three profiles displayed in comparative figures mutually support and lend strength to the final interpretation and hydrogeologic section. The CSD cross sections are particularly useful to provide information to fill in gaps in the AEM where data was missing (blank vertical lines) to produce the interpretative cross sections.

Line 100601 (Figure 5-22) was flown across the Oakland, NE area, which was included in a 2007 AEM survey (Abraham et al., 2011) during the first project year of ENWRA. The Oakland area was chosen in 2007 to be the test area for using AEM to image heavy glacial sediments at depth to map the underlying aquifer material. The system used was a frequency domain electromagnetic system with limited depth of penetration in these sediments due to large amounts of electrically conductive clay and silt. Near test holes 50-A-50, 2-EN-06, and TH-01-OAKLAND, a paleochannel exists that was not imaged in 2007. Using the time domain AEM system, this subsurface feature was imaged in the 2014 survey. The AEM matches the test holes and the CSD cross sections closely in this area. From this assessment, the paleochannel is considerably wider than previously thought, information of which can assist LENRD managers in better understanding the availability of groundwater in this area.

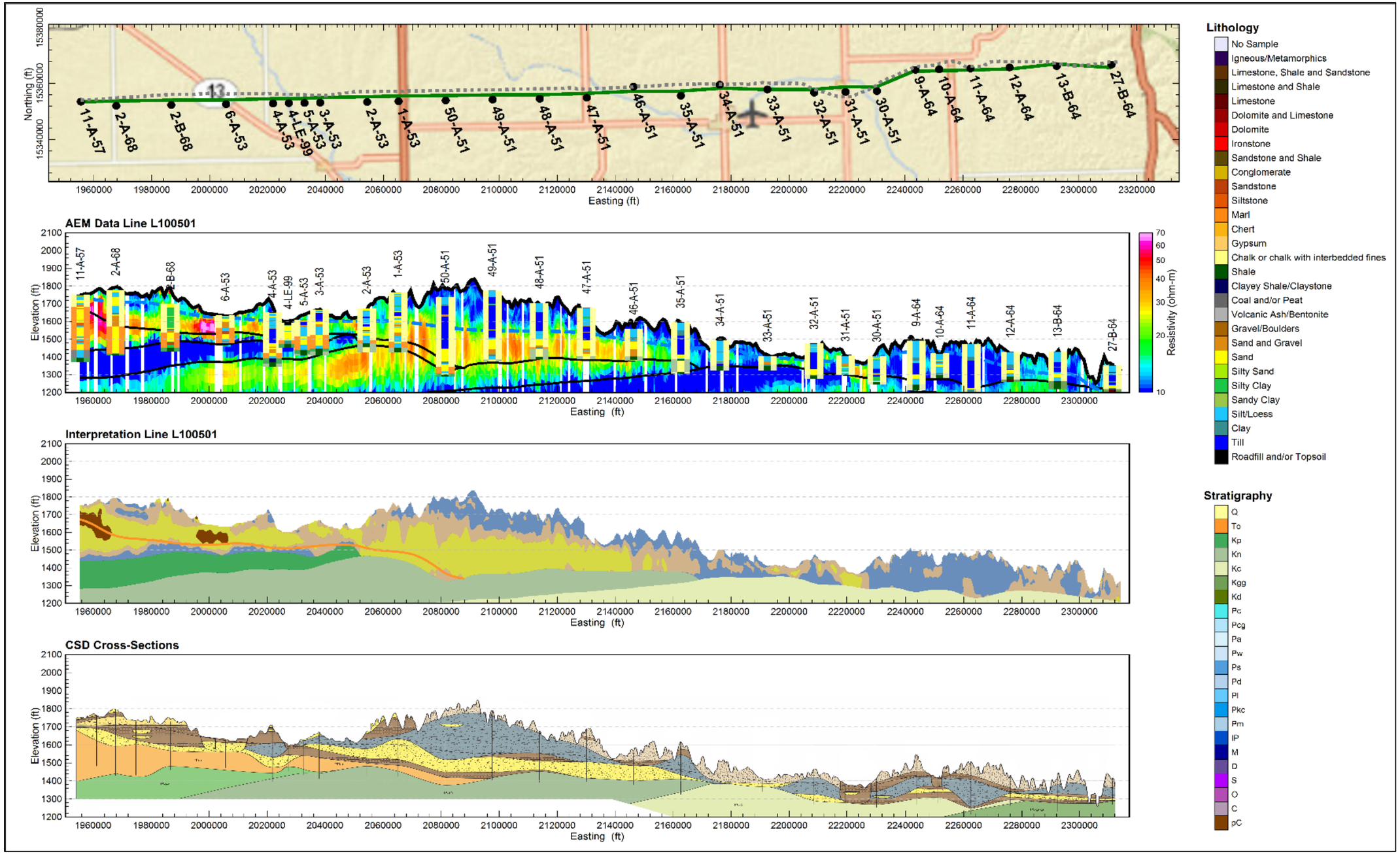


Figure 5-20: Combined display of AEM data (second panel), hydrostratigraphic interpretation (third panel), and CSD cross section (bottom panel) for flight line 100501 near Wayne, NE. The location of the AEM flight line and CSD cross section is displayed in the top panel.

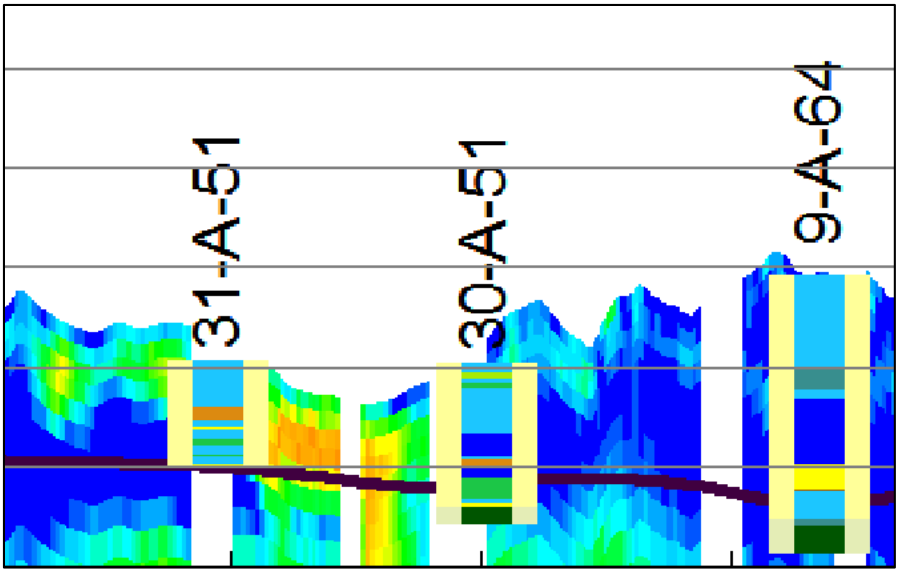


Figure 5-21: Zoomed in view along the eastern extent of AEM flight line 100501, demonstrating the thin intervals of material indicated in the test hole logs that correspond to only the averaged resistivity data across intervals of greater thickness. This is particularly evident in 31-A-51 and 9-A-64.

Figure 5-23 displays a comparison of AEM, hydrostratigraphic interpretation, and CSD cross section on the far western edge of the reconnaissance survey area in the LENRD that covers parts of five NRDs. This is an area underlain by extensive bodies of sand-rich, principal aquifer materials, primarily composed of *To* (resistive bodies beneath orange line), overlain by thinner resistive Quaternary deposits. Close agreement exists between the interpretive profile and the CSD cross section, including the extent of the principal aquifer features, the coarse deposits near the land surface, the thickness of non-aquifer materials on the south side of the profile, and the structure of the *Kp* and *Kn* beneath the *To*.

Note that the profiles displayed in Figure 5-20, Figure 5-22, and Figure 5-23 are included, along with the remainder of the AEM profile-interpretive section-CSD cross section figures, in Appendix 2.

In conclusion, the interpretations of the AEM data along the reconnaissance lines generally match well with CSD and NOGCC test holes and historic CSD cross sections. Deviations mostly occur the most where test holes are at greater distances from the flight lines. The AEM data allows geologists to now visualize the character of the materials between test holes, thus greatly minimizing the amount of speculative estimation of how geologic materials change in the subsurface where no data exists. The AEM does not, however, map very thin layers on the order of a few feet in thickness due to averaging effects in the inversion modeling process. This condition is not considered to greatly affect how the AEM data would import to groundwater models, where such minor features cannot be accounted for and where averaging of hydraulic parameters occur over thick sequences of aquifer materials.

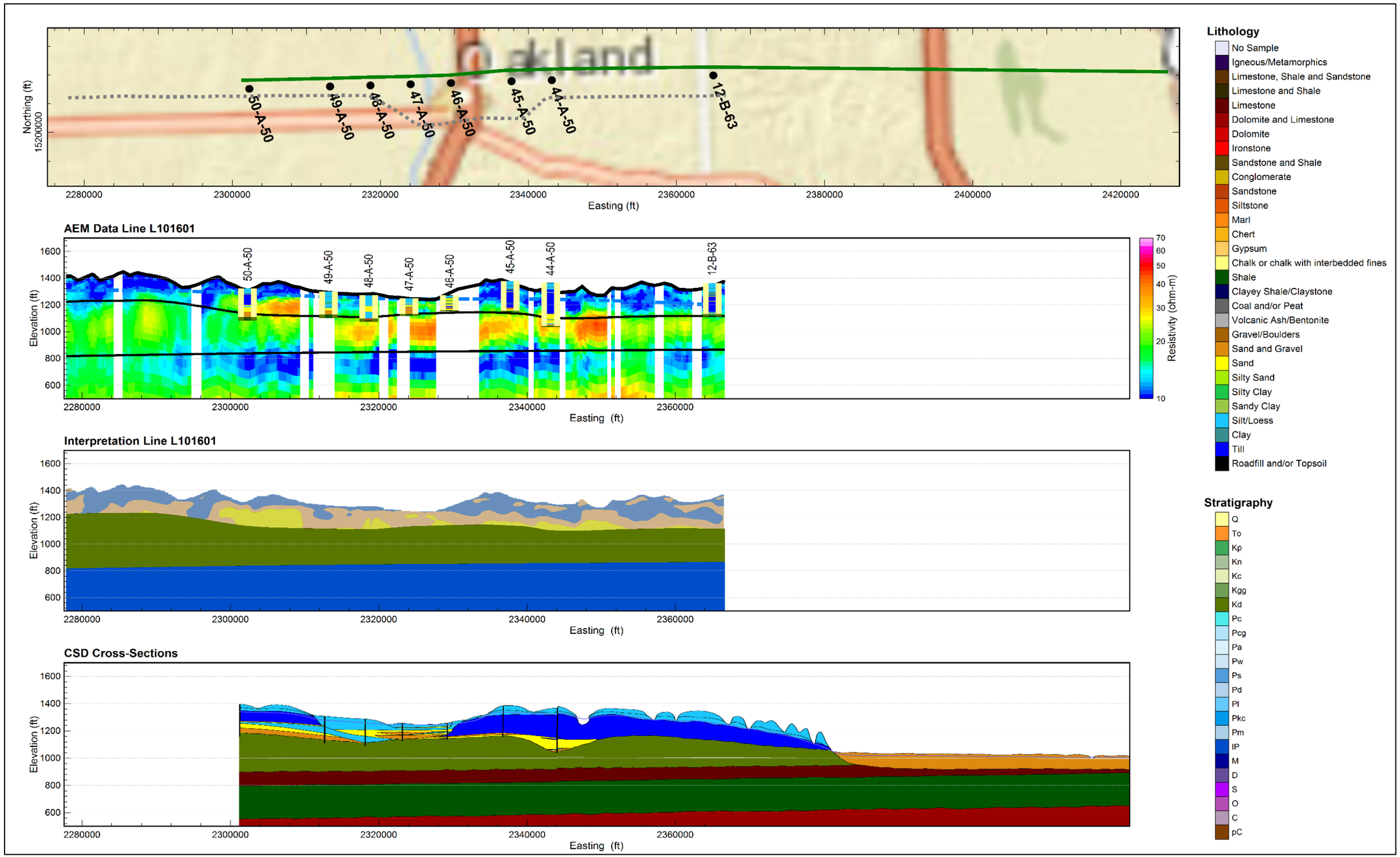


Figure 5-22: Combined display of AEM data (second panel), hydrostratigraphic interpretation (third panel), and CSD cross section (bottom pane) for flight line 101601 near Oakland, NE. The location of the AEM flight line and CSD cross section is displayed in the top panel.

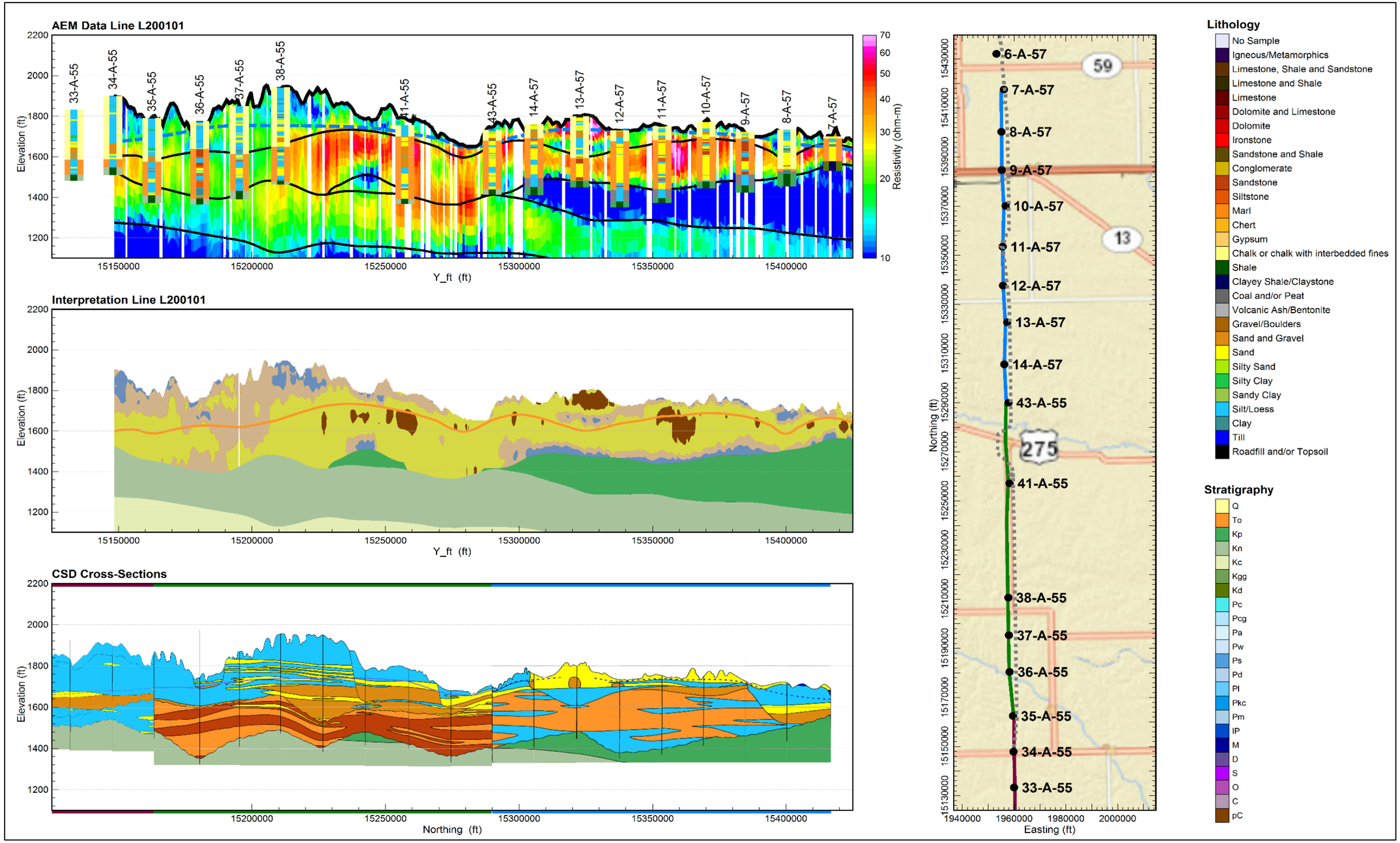


Figure 5-23: Combined display of AEM data (second panel), hydrostratigraphic interpretation (third panel), and CSD cross section (bottom pane) for flight line 200101, the westernmost north-south flight line in the reconnaissance survey area. The location of the AEM flight line and CSD cross section is displayed on the right side of the panel.

5.3 Hydrogeologic Framework Interpretation by Individual NRD

5.3.1 Lewis and Clark NRD

The LCNRD includes the northern extents of five north-south reconnaissance lines as well as two west-east flight lines that cross most of the district's mid-section (100201) and a portion of the district's far north-central (100101) area (Figure 5-24). The seven flight lines reveal the varying character of the Quaternary materials present beneath the NRD as well as the Cretaceous bedrock. Discussion of the individual aquifer systems is provided in the following subsections. While reviewing this section, the reader is encouraged to utilize the flight line KMZs in Google Earth to interactively view the flight lines discussed in this section. The 3D hydrologic framework of the LCNRD is shown in Figure 5-25.

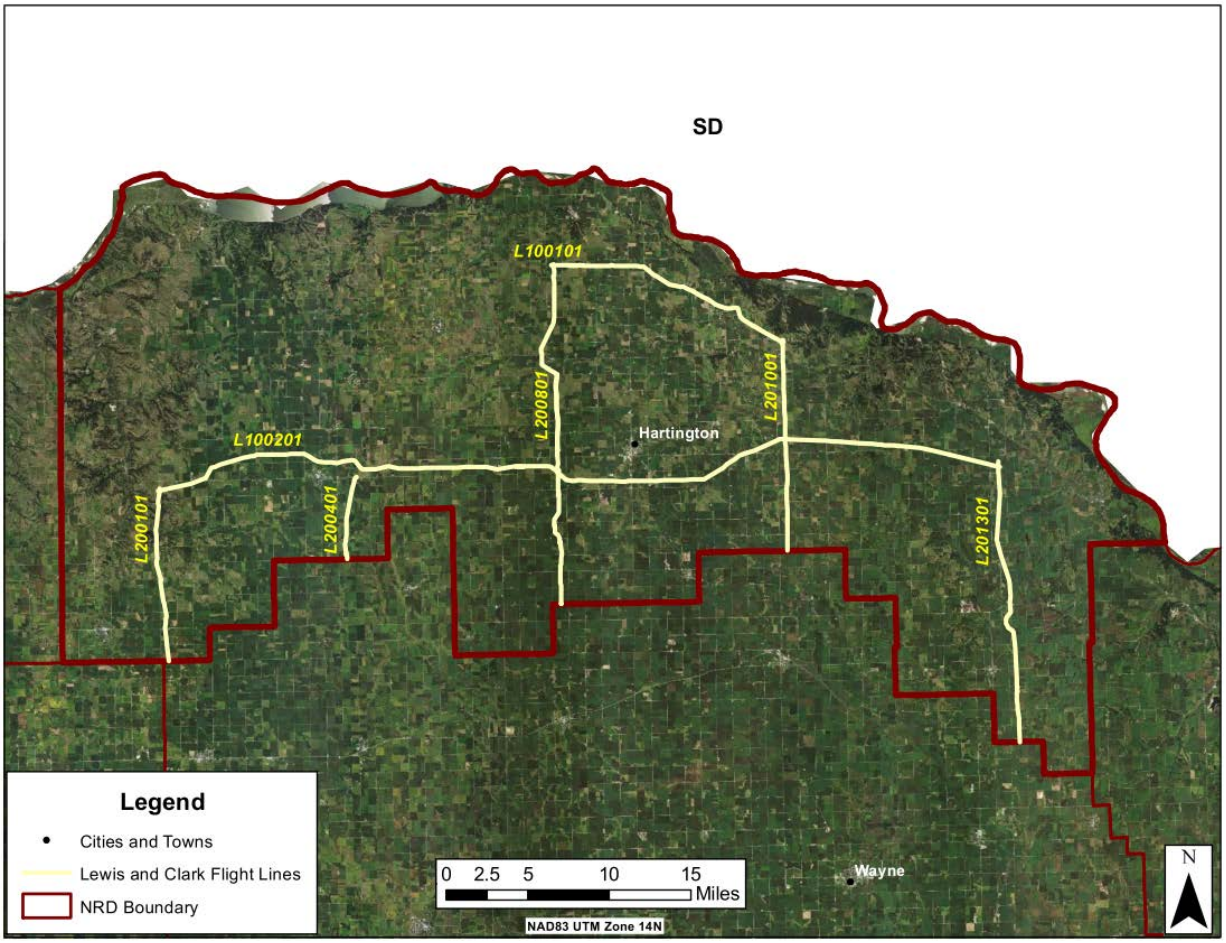


Figure 5-24: Flight lines within the LCNRD acquired in Phase 1 of the ENWRA AEM survey.

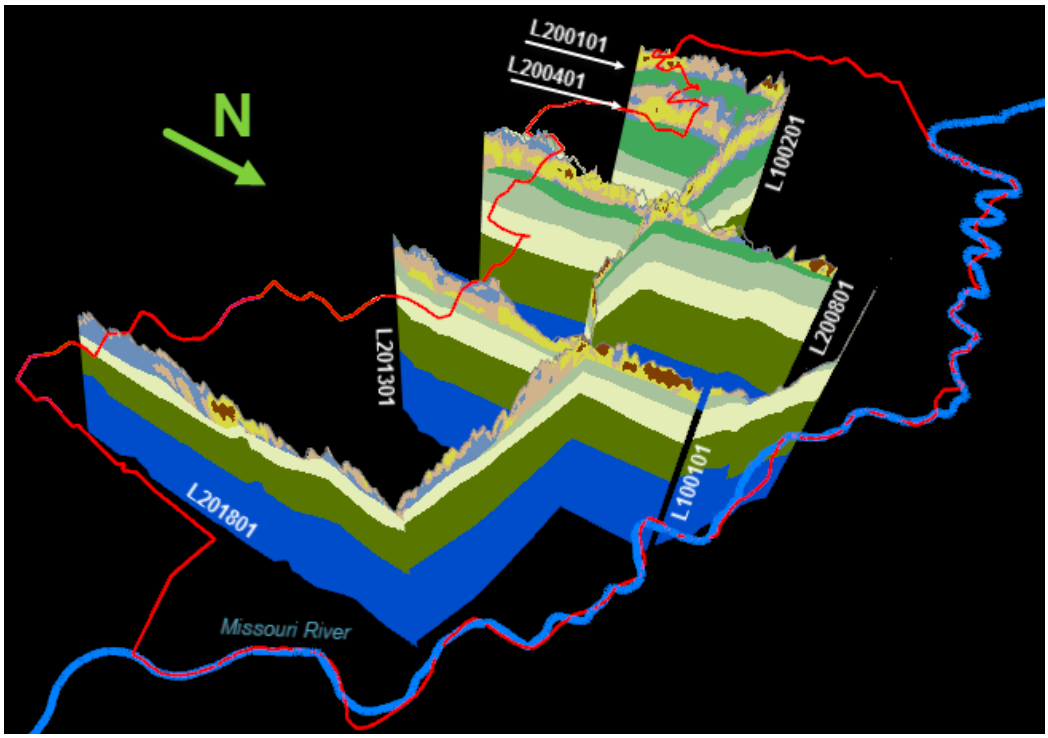


Figure 5-25: 3D hydrogeologic framework from the reconnaissance AEM survey only within the LCNRD. The district boundary is displayed in red, with flight lines labeled in white and major drainages displayed as blue lines. The stratigraphy color codes are in Figure 5-2.

5.3.1.1 Quaternary/Tertiary System beneath the LCNRD

The Quaternary system shows considerable variation in thickness and character across the LCNRD, from generally being devoid of aquifer material in the north-central section of the NRD (flight line 100101) to areas with principal aquifer deposits exceeding 300 ft, which in some areas contain isolated sand-rich intervals.

Flight line 100201 (Figure 5-26) reveals the general trend of interpreted materials across the LCNRD from west to east, which can be summarized as generally having marginal and principal aquifer material in the western half of the surveyed area within the district, and a general lack of extensive principal aquifer material in the eastern half of the surveyed area. This trend is further substantiated by the pattern of registered wells across the district (Figure 2-11), where a high density of wells occurs in the western half of the district, but with a sparser pattern of registered wells in the districts' eastern half. Figure 5-26 also reveals that some resistive materials, including sand-rich portions exceeding 50 ohm-m, are situated above the 1995 CSD regional water table surface. This pattern is best exemplified (Figure 5-26 between Easting values 2100000 and 2150000 where sand-rich principal aquifer material is present above the regional water table surface in the uplands between the Bow Creek and East Bow Creek drainages. This feature is also evident on the northern edges of flight lines 200101 (Figure 5-27) 200801 (Figure 5-28) and 201301 (Figure 5-29). Another area of shallow, unsaturated principal aquifer material is evident on the far western extent of flight line 100201, where approximately 200 ft of principal and sand-rich principal aquifer material are present at the land surface. Overall, within the surveyed portions of the LCNRD, the thickest intervals of principal aquifer material are not completely saturated based on

the depth of the CSD 1995 regional water table surface. Locations where near-surface, unsaturated zones of principal or marginal aquifer exist in the subsurface are best suited for managed aquifer recharge projects (MAR), as higher rates of recharge to the aquifer likely occur in these areas.

In other locations along flight line 100201, as well as parts of flight line 200401 (Appendix 1), unsaturated principal aquifer material is overlain by intervals of marginal aquifer and aquitard material, some of which exceed 150 ft in thickness. Flight line 200801 (Figure 5-28) displays the general subsurface conditions from south to north within the LCNRD, with extensive intervals of principal aquifer materials in the south that thin considerably northward that are overlain by materials of varying thickness and resistivity. East of flight line 200801, the trend in material type in the subsurface shifts considerably, where marginal aquifer and aquitard materials persist, with only isolated principal aquifer and sand-rich principal aquifer intervals.

Based on the elevation of the 1995 CSD water table surface, aquifer conditions range from unconfined to confined. Confined conditions are indicated where the water table surface is located within aquitard materials in flight line 200401 (Appendix 1). In many areas, including along flight line 100201, the CSD water table surface is situated within principal aquifer interval, but below overlying aquitard materials that are comprised of till and loess. These areas likely receive minimal recharge, and the materials act as unconfined aquifers where and when pumping occurs. However, it cannot be understated that the CSD water table surface is a regionally configured dataset, and recent, more locally defined conditions likely deviate from the general trends revealed by this surface.

Flight line 100101 (Appendix 1), extends for over 15 miles subparallel to the Missouri River valley. Along most of this profile, only a thin veneer (50 ft or less) of the Quaternary system, mostly non-aquifer material, is present overlying a bedrock valley carved into Cretaceous strata. Along the western one-fourth of this profile, a sequence of material with mixed resistivities approaching 80 ft thick sits atop a bedrock ridge. Additionally, material classified as principal aquifer mantles the bedrock on the far eastern extent of the profile, but is expected to be unsaturated as the 1995 CSD water table surface is present below this interval. The depression in the bedrock surface appears to influence present-day surface drainages, as the Bow Creek watershed drains northward from uplands in the LCNRD's midsection. Although no significant aquifer is present in this area as revealed by flight line 100101, the Quaternary materials can provide yields to irrigation and domestic wells where thin and/or perched seams of saturated materials are present. Review of DNR records indicate that even in the area of thin marginal aquifer material, over 200 wells of varying use and pumping capacity are present within close proximity of the flight line.

The *To* is also present beneath portions of the surveyed area of the LCNRD. The unit is present as far east as flight line 201301 in an isolated interval between eastings 2150000 and 2175000 on flight line 100201. The unit pinches out on the southern fringes of the NRD on flight lines 200101, 200401, and 200801. The thickness of the *To* as interpreted from the AEM data typically does not exceed 100 ft in the LCNRD (flight line 201301). Aquitard, marginal, and principal aquifer materials are present within the zones interpreted as *To*.

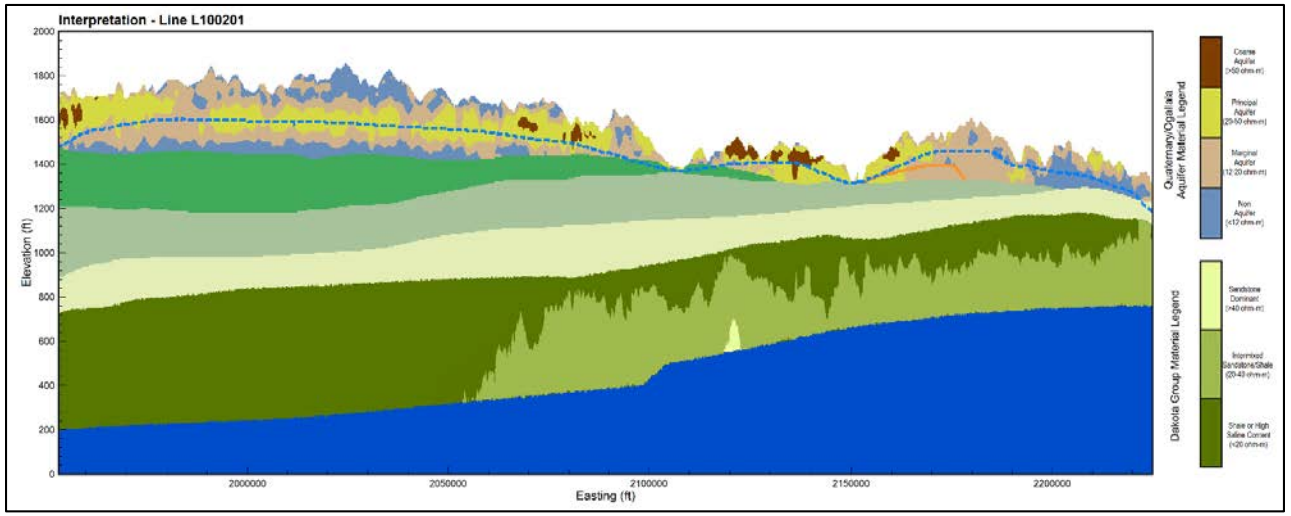


Figure 5-26: Interpreted profile for west-east flight line 100201 that extends from west to east within the midsection of the LCNRD. The To is delineated by the orange line and the CSD 1995 regional water table surface is indicated by dashed blue line. West is on the left, east to the right. The stratigraphy color codes are in Figure 5-2

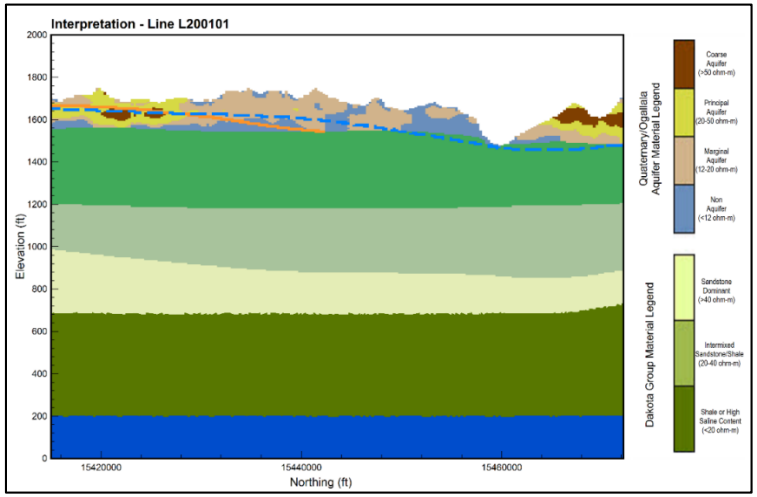


Figure 5-27: Interpreted profile for south-north flight line 200101 that extends through the south-central portion of the LCNRD. The To is delineated by the orange line and the CSD 1995 regional water table surface is indicated by dashed blue line. South is on the left, north to the right. The LCNRD is present to the right of the 15416740 ft Northing. The stratigraphy color codes are in Figure 5-2.

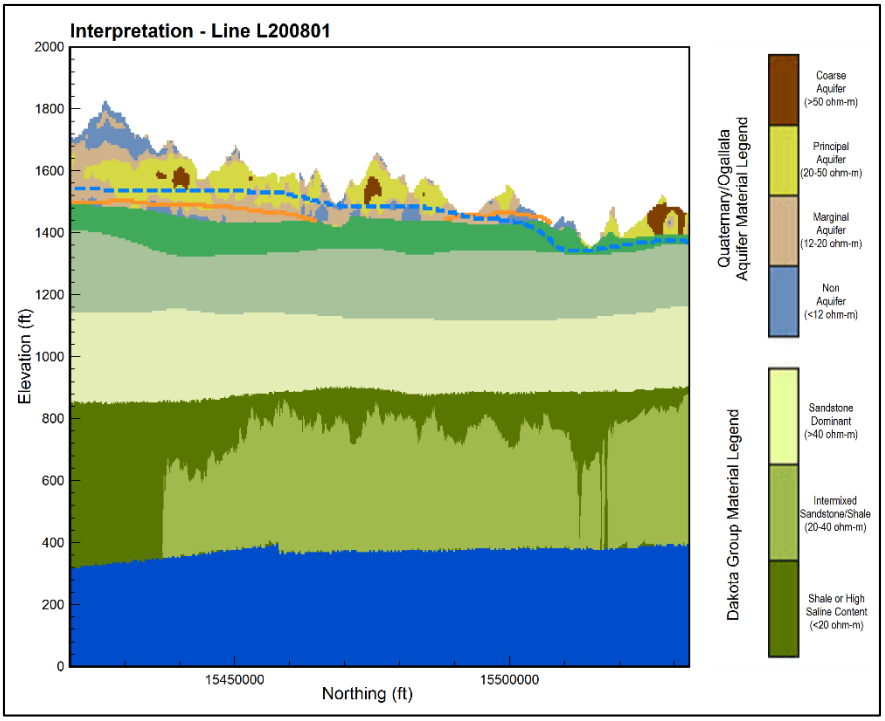


Figure 5-28: Interpreted profile for south-north flight line 200801 that extends through the south-central portion of the LCNRD. The *To* is delineated by the orange line and the CSD 1995 regional water table surface is indicated by dashed blue line. South is on the left, north to the right. The LCNRD is present to the right of 15435070 ft Northing. The stratigraphy color codes are in Figure 5-2.

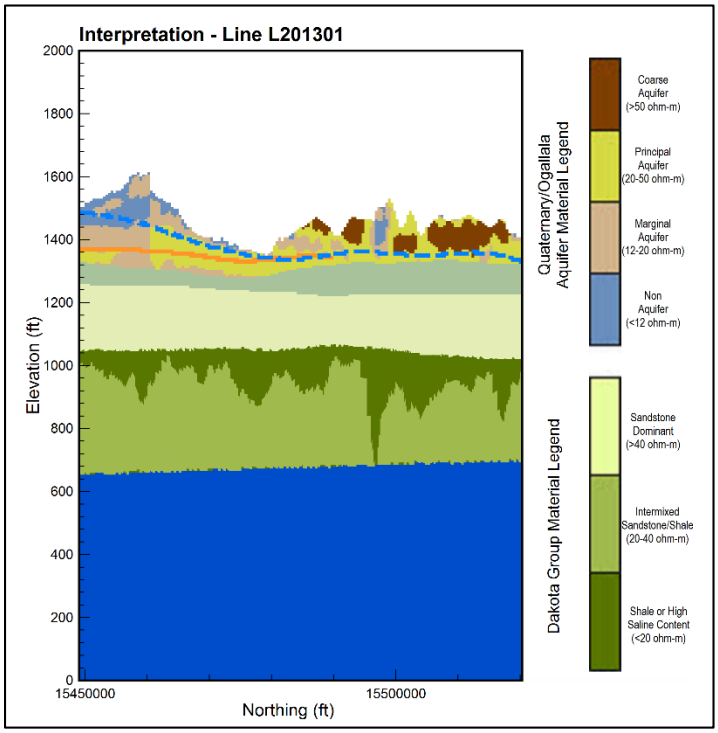


Figure 5-29: Interpreted profile for south-north flight line 201301 that extends through the south-central portion of the LCNRD. The *To* is delineated by the orange line and the CSD 1995 regional water table surface is indicated by dashed blue line. South is on the left, north to the right. The LENRD-LCNRD boundary begins at 15452340 ft Northing. The stratigraphy color codes are in Figure 5-2.

5.3.1.2 Cretaceous and Paleozoic Sequence beneath the LCNRD

The AEM data reveals the full extent of the Cretaceous strata beneath northeast Nebraska in the surveyed portion of the LCNRD, and includes undifferentiated Paleozoic units. Flight line 100201 (Figure 5-26) reveals the full Cretaceous sequence beneath northeast Nebraska and also exhibits the westward dip of the units westward towards the Central Nebraska Basin. The *Kp* terminates just east of Easting value 2125000. The *Kp* approaches 300 ft in thickness on the western edge of flight line 100201, and thins eastward towards its terminus. Near the southern border of the LCNRD along flight line 200101 (Figure 5-27), the thickness of the *Kp* approaches 400 ft. Flight line 100101 indicates a thin veneer of *Kp* on top of the bedrock ridge on the western half of the flight line. On the profile of flight line 100201, the *Kp* appears to be incised by the Bow Creek drainage (near Easting value 2100000) and likely outcrops on the edges of this watershed.

The *Kn* is situated below the *Kp* and is present across most of flight line 100201 before terminating near Easting value 2200000 on Figure 5-26. The *Kn* approaches a maximum thickness of approximately 300 ft on the western edge of flight line 100201, and is nearly 400 ft near the southern NRD border along flight line 200101. The *Kn* is not present beneath the eastern quarter of the LCNRD. Beneath the *Kn* is the combined *KcKgg*, which has a maximum thickness of approximately 200 ft near the middle of flight line 100201 (near Easting value 2075000). The *KcKgg* is present beneath the LCNRD as far east as flight line 201801, and along this flight line, it is the uppermost bedrock unit in contact with the overlying Quaternary system.

Beneath the *KcKgg* is the *Kd*, which hosts the Maha aquifer in eastern Nebraska. The *Kd* thickness ranges from 500 to 600 ft beneath most of the LCNRD. The westward dip of the Cretaceous sequence is most pronounced in the *Kd* as displayed in flight line 100201 (Figure 5-26). Displayed on the interpretive profiles are the variations in resistivity within the *Kd*. In the flight line 100201 profile, the 20-40 ohm-m zone terminates between Easting values 2025000 and 2050000. This area indicates where the water contained within the *Kd* possibly becomes brackish. The interpreted *Kd* interval throughout flight line 200101, including southward beyond the LCNRD are in the 10-12 ohm-m range, which could a result of brackish water present in the formation. No deep water samples are available to verify this condition, however. The 20-40 ohm-m range of *Kd* resistivities is common beneath the LCNRD from flight line from 200801 eastward to the edge of the survey area. Evaluation of the resistivity profiles can provide additional insight into where the best target intervals may exist in the 20 ohm-m or greater zones for development of *Kd*/Maha aquifer resources beneath the LCNRD. For example, resistive features greater than 20 ohm-m are present in flight lines 100101, 100201, 200801 (Figure 5-28), and 201301 (Figure 5-29). The resistive features in flight line 100101 at the base of the *Kd* exceed 40 ohm-m.

Underlying the thick sequence of *Kd* beneath the LCNRD are undifferentiated Paleozoic strata. Variable resistivity is evident within the Paleozoic strata across each of the profiles cross the district. The DOI of the AEM investigation is within the Paleozoic sequence. However, even above the DOI, the Paleozoic sequence is several hundred feet thick. The Paleozoic sequence beneath the LCNRD dips westward towards the Central Nebraska Basin. No individual units within the Paleozoic sequence are considered

aquifer resources beneath the district. Any exploration of these intervals could be guided by targeting resistive intervals within these sequences as revealed by the AEM survey, however.

5.3.2 Lower Elkhorn NRD

A majority of the first phase of the ENWRA AEM survey covered the LENRD. Eight north-south reconnaissance flight lines cross the district, and three west-east tie-lines cover the entirety of the district, with a shorter west-east flight line also included from the West Point, NE area to the eastern district boundary (Figure 5-30). The general trend in the distribution of materials in the Quaternary system essentially provides a conceptualization of how the entirety of the northern ENWRA project area is structured, as the same patterns are present in the LCNRD, as well as the similar nature of deposits in the far eastern LENRD and the PMRNRD. The LENRD is underlain by some of the most prolific deposits of principal and sand-rich principal aquifer material, as well as some of the thickest intervals of aquitard materials detected in the AEM survey.

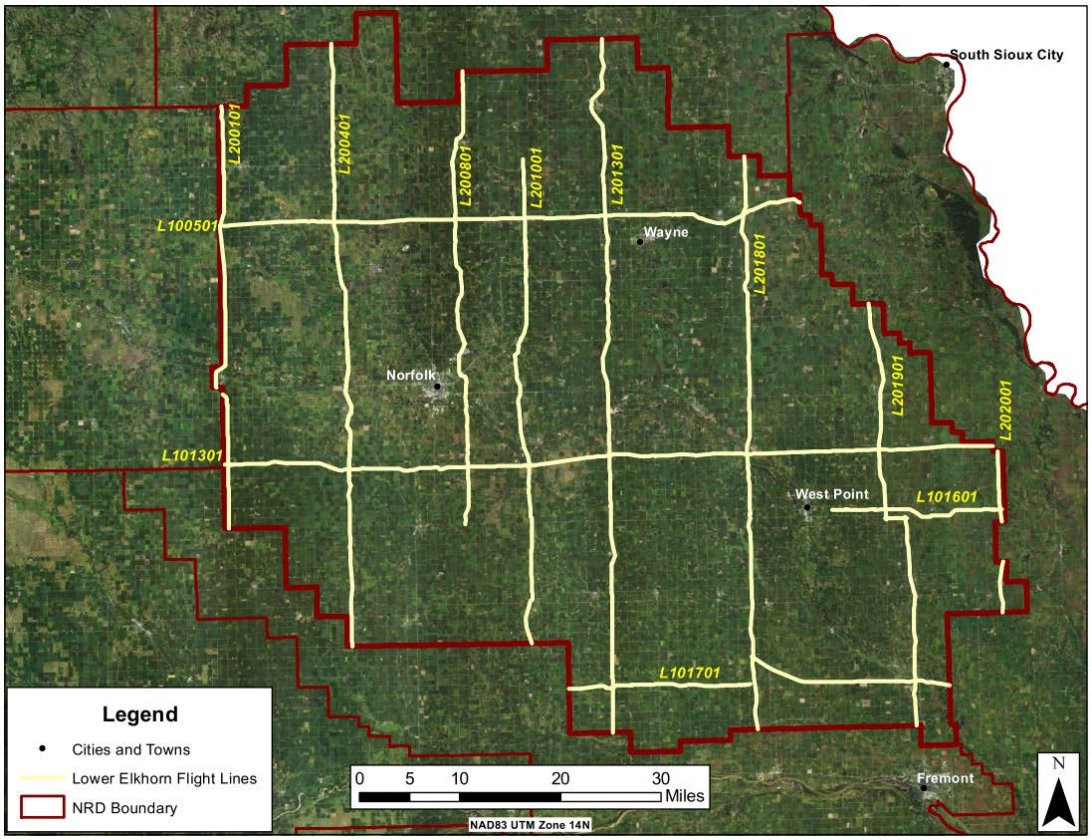


Figure 5-30: Flight lines within the LENRD acquired in the first phase of the ENWRA AEM survey.

In the Fall of 2014, XRI completed a smaller, more tightly-spaced AEM survey within the LENRD in concert with Phase I of the ENWRA reconnaissance survey (Exploration Resources International, 2015). This survey included an area across roughly the northwest half of the district with gridded flight lines spaced 3-5 miles apart. This survey revealed in greater detail individual intervals of sand-rich principal aquifer deposits found throughout the western half of the northern ENWRA survey area within the LENRD. Several of these features are located beneath surface drainages and are in hydraulic

communication with the Elkhorn River, North Fork of the Elkhorn River, and Maple Creek. The survey also reveals in closer detail the extent and thickness of the marginal aquifer and aquitard materials in the eastern half of the district. Figure 5-31 displays the 3D hydrologic framework of the LENRD.

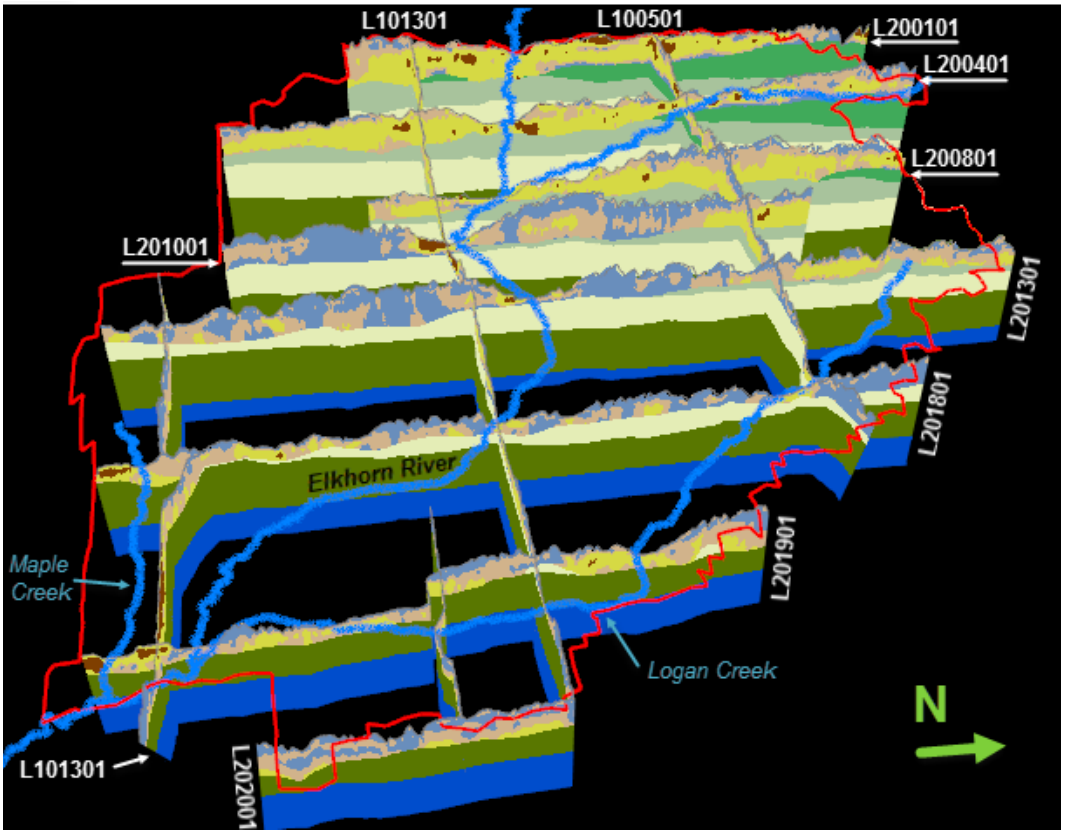


Figure 5-31: 3D hydrogeologic framework from the reconnaissance AEM survey only within the LENRD. The district boundary is displayed in red, with flight lines labeled in white and major drainages displayed in blue. The stratigraphy color codes are in Figure 5-2.

Within the LENRD, additional smaller scale AEM surveys have been conducted in the last decade (Oakland, 2007; Clarkson-Howells area, 2013). These surveys were flown with grid lines with much closer spacing for greater detail in local hydrogeologic framework development. Comparison of these surveys with the northern ENWRA project area survey are provided in section 5.3.2.3.

While reviewing this section, the reader is encouraged to utilize the flight line KMZs in Google Earth to interactively view the flight lines discussed in this section. The stratigraphy color codes in the figures are identified in Figure 5-2.

5.3.2.1 Quaternary/Tertiary System beneath the LENRD

Across the western one-third of the LENRD, numerous intervals of principal aquifer and sand-rich principal aquifer (>50 ohm-m) are present, notably at and north of west-east flight line 101301 and west of the North Fork of the Elkhorn River. These zones are also evident in Figure 5-32 through Figure 5-35 (yellow and brown colors). The principal aquifer extends eastward from this area, reaching north-south flight line 200801, but generally with less sand-rich material. Much of this area includes Quaternary

materials directly overlying *To*. The thickness of the most resistive bodies (> 50 ohm-m) within the principal aquifer materials exceeds 200 ft in some areas, particularly along the western edge of project area where thick *To* is overlain by Quaternary fluvial deposits (flight line 200101), beneath the Elkhorn River valley west of the city of Norfolk, and in an isolated body of resistive material east of flight line 200801 and north of flight line 100501. Other extensive bodies ranging from 100-150 ft thick are present beneath the western subregion, mainly along flight lines 200101 and 200401. Other isolated bodies of principal aquifer material, which included small sand-rich features are present in the west subregion, primarily along flight line 100201 in the LCNRD and within the northwestern half of the LPNNRD.

The principal aquifer, including several sand-rich zones, is present at shallow depths below the ground surface in the west area of the LENRD, particularly along flight line 200101. The hydrostratigraphic framework revealed in the 2014 LENRD AEM survey (Exploration Resources International, 2015) further exemplifies the nature of these deposits in the western LENRD. Most of these areas are overlain with minimally conductive, non-aquifer material; a condition which could indicate relatively higher recharge rates to the aquifer. This assessment is based on the existing shallow subsurface geologic conditions only, as recharge is also influenced by other key factors, including soil type, slope, vegetation, and land use practices.

As described in Section 5.2.1.2, marginal aquifer and aquitard material are present throughout the region of the LENRD east of flight lines 201001 and 200801. In some areas, the entire Quaternary system above the Cretaceous bedrock consists of aquitard material. Examples of such areas are indicated in Figure 5-33 and Figure 5-35. In many areas of the eastern half of the LENRD, marginal aquifer is the only Quaternary aquifer resource, and many of these areas have appreciable volumes of aquitard material present. Marginal aquifer material is still capable of producing well yields of several hundred gallons per minute, but the likelihood of encountering intervals of fines when drilling wells is much greater, thus necessitating wells with multiple screened intervals across the borehole to capture any coarse material that is present. In this region of the LENRD, the presence of aquitard material as revealed in the hydrostratigraphic framework from the survey is useful in indicating where exploration for new groundwater development should be avoided and characterization of where recharge to the aquifer is limited.

As discussed in section 5.2.1.1, the distribution of principal and marginal aquifer material in the LENRD is also revealed by the density of irrigation wells in roughly the western and eastern halves of the LENRD, where in the eastern half, irrigation well density is less than one per square mile, and in the western half of the district, there are nearly 4 irrigation wells per square mile.

Beneath the western one-third of the LENRD, the Quaternary system is underlain by *To* and *Kd* (Figure 2-2). Beyond the subcrop of the *To*, the *Kn* forms the basal bedrock unit beneath the Quaternary deposits beneath the midsection of the LENRD. In the eastern half of this project area, the *KcKgg,* and the *Kd* are the bedrock units underlying the Quaternary system.

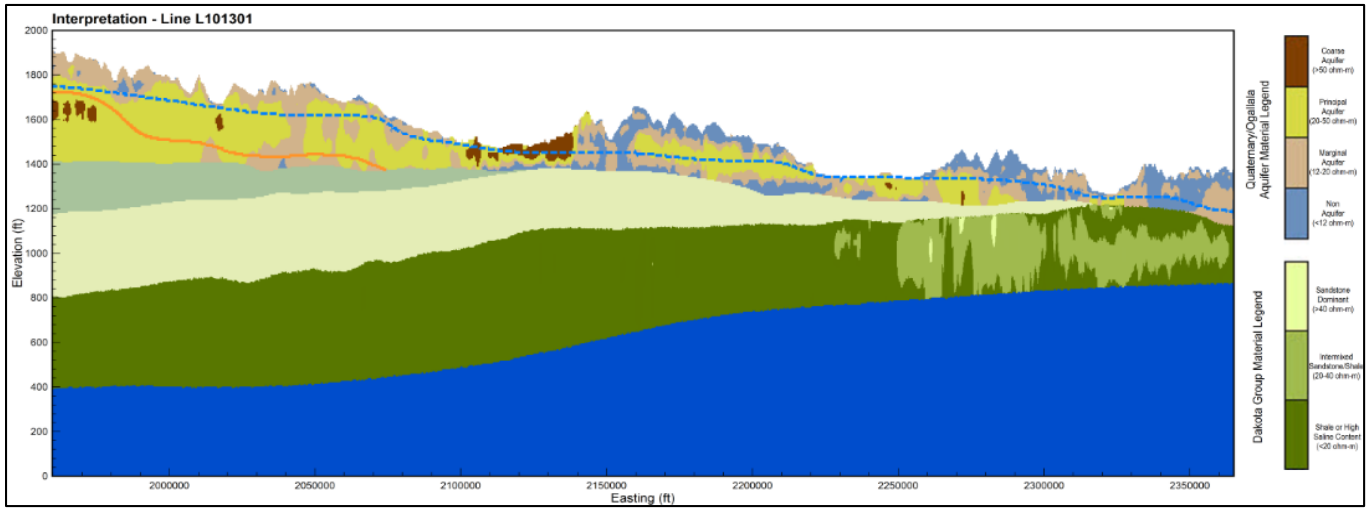


Figure 5-32: Interpreted profile for west-east flight line 101301 that extends through the south-central portion of the LENRD. The To is delineated by the orange line and the CSD 1995 regional water table surface is indicated by dashed blue line. West is on the left, east to the right. The stratigraphy color codes are in Figure 5-2.

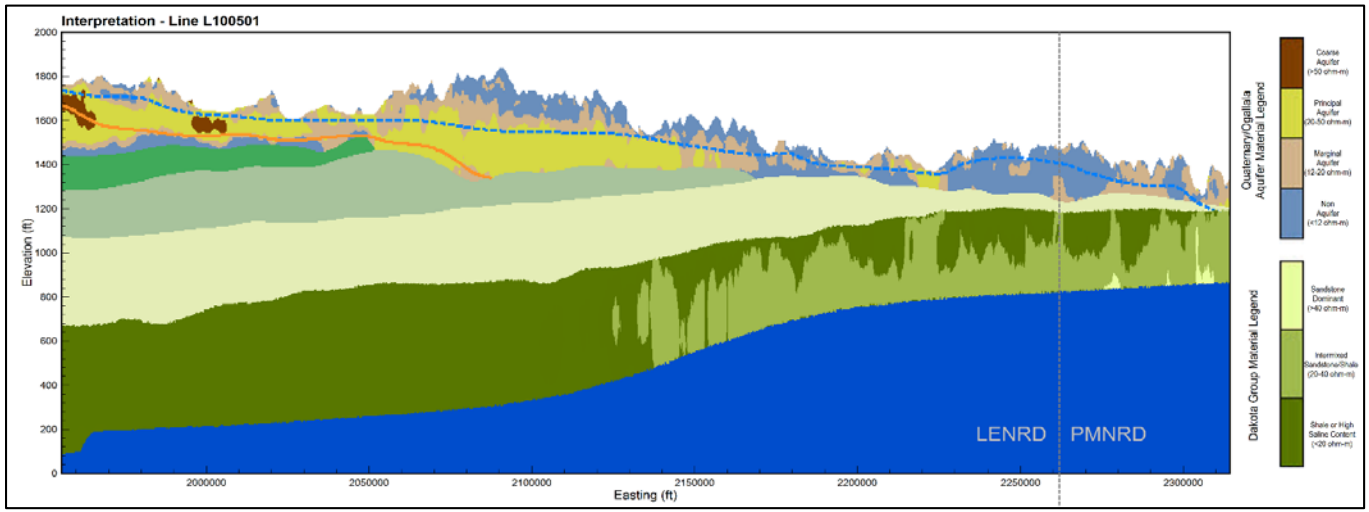


Figure 5-33: Interpreted profile for west-east flight line 100501 that extends through the north-central portion of the LENRD. The To is delineated by the orange line and the CSD 1995 regional water table surface is indicated by dashed blue line. West is on the left, east to the right. The LENRD-PMRNRD boundary is at 2260790 ft Easting. The stratigraphy color codes are in Figure 5-2.

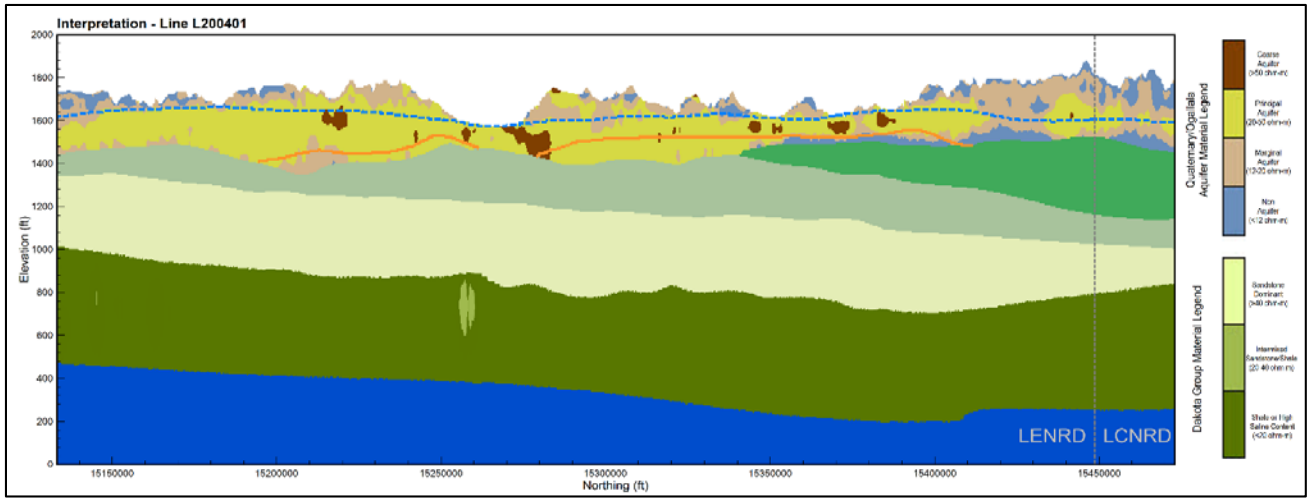


Figure 5-34: Interpreted profile for south-north flight line 200401 that extends through the western extent of the LENRD. The To is delineated by the orange line and the CSD 1995 regional water table surface is indicated by dashed blue line. North is on the right, south to the left. The LENRD-PMRNRD boundary is at 15449600 ft Northing. The stratigraphy color codes are in Figure 5-2.

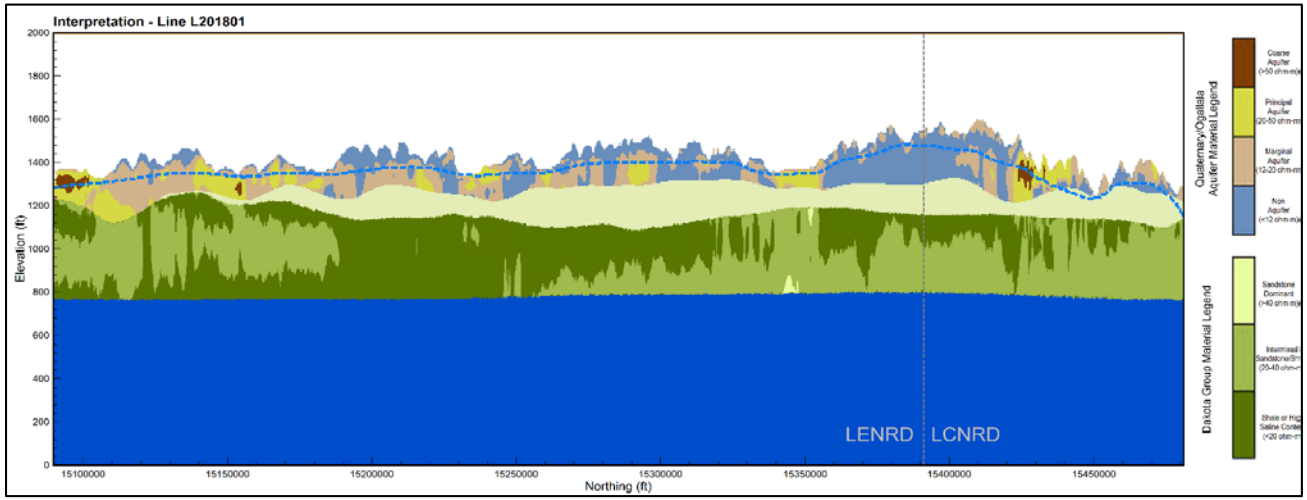


Figure 5-35: Interpreted profile for south-north flight line 201801 that extends through the eastern extent of the LENRD. The CSD 1995 regional water table surface is indicated by dashed blue line. North is on the right, south to the left. The LENRD-LCNRD boundary is at 15390670 ft Northing. The stratigraphy color codes are in Figure 5-2.

Although the *To*- the primary host strata of the High Plains aquifer- is known to contain consolidated and semi-consolidated intervals of sandstone and siltstone, it is included in the discussion of the principal aquifer where it exists beneath the project area. This approach to characterizing the hydrostratigraphy is based on the connection of these separate geologic units and the behavior of the coarse, unconsolidated Quaternary materials acting as one aquifer with the underlying *To*. The *To* exceeds 150 ft in thickness along the western edge of the LENRD (flight line 200101). The easternmost extent of the *To* is less than 20 miles east of this flight line, where the unit terminates near the north-south flight line 200901. This eastward thinning of the *To* (indicated as the area beneath the orange lines in the 2D profiles) is clearly indicated in the 2D profiles in Figure 5-32 and Figure 5-33.

It should be noted that the separate body of *To* identified in the bedrock geology map of the state (Burchett, 1986) was not revealed by the AEM data. This separate *To* feature is located partially in the same area underlain by an area of sand-rich, principal aquifer southeast of Norfolk. It is possible that these coarse Quaternary deposits were originally mapped as *To* during the creation of the statewide geologic map in the 1970s (Burchett, 1986). Examination of the CSD test holes in this area did not reveal any consolidated or semi-consolidated material in the subsurface at depths where the *To* would be expected. Along with this evidence from the CSD boreholes, there is no evidence of this *To* feature in the project area flight line block or the nearby recon lines.

Near the southeast corner of the LENRD (Figure 5-36), one of the largest sand-rich depositional features detected in the AEM survey is evident along the west-east flight line 101701.1 between the Elkhorn River and Maple Creek. Located approximately 12 miles northwest of Fremont, this feature extends over 10 miles in width and is over 200 ft thick at its deepest locations. This body of resistive material is in close proximity to the resistive materials on the southern edge of nearby north-south flight line 101901, but it is unclear as to how far north this feature extends beyond flight line 101701. If this body of principal aquifer extends two to five miles north of flight line 101701, it would directly underlie the Elkhorn River and thus likely have a strong hydraulic connection with the river in this area. A review of 147 irrigation well records from the NDNR Registered Well Database for wells between the Elkhorn River and Maple Creek indicates irrigation wells in this area average 894 gpm. Of these 147 wells, 69 were registered with rates of 1,000 gpm or greater. The productivity of irrigation wells between flight line 101701 and the Elkhorn River indicates that this feature likely extends at least as far north as the Elkhorn River.

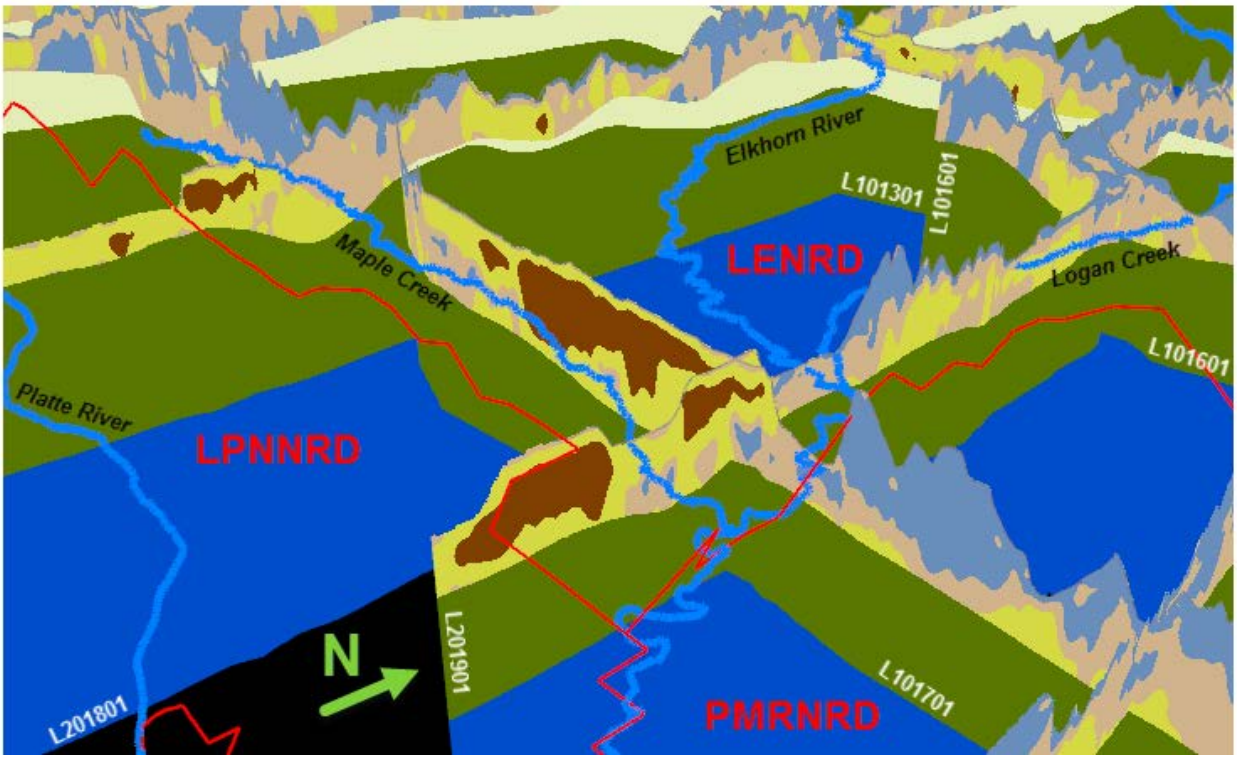


Figure 5-36: Area between the Elkhorn River and Maple Creek drainages with extensive sand-rich, principal aquifer material in the southeast corner of the LENRD. Vertical exaggeration is 60x. The stratigraphy color codes are in Figure 5-2.

5.3.2.2 Cretaceous and Paleozoic Sequence beneath the LENRD

The complete sequence of eastern Nebraska's Cretaceous strata is present beneath the LENRD. The units show pronounced westward dip along the west-east AEM profiles, and slight dip northward in the north-south profiles. The *Kp* is present beneath the northeast corner of the district, and is evident in flight lines 100501 and 200401 (Figure 5-28 and Figure 5-29). The unit is over 300 ft thick on the north side of flight line 200401. The unit thins eastward and southward and terminates with minimal thickness near the Northing value of 15337500 ft. Underlying the *Kp* is the *Kn*, which is present beneath two-thirds of the LENRD. The unit thins eastward, from 200-300 on the west to less than 50 ft near its terminus near Easting value 2175000 ft. The top of the *Kn* surface shows variable topography in the northern extent of the district, and is the uppermost bedrock immediately beneath the Quaternary system beyond the *Kp* subcrop. Underlying the *Kn* is the combined *KcKgg*, which is present beneath nearly the entire LENRD. The unit is approximately 400 ft thick beneath the western side of the district and thins eastward gradationally to its eastern terminus near the LENRD-PMRNRD boundary. The top of the *Kc* is generally flat to slightly undulating across most of the project area, with the exception of north-south flight line 201301, where in the southern one-third of the profile, erosion appears to have excavated some of the material, creating an erosional surface immediately beneath the Quaternary system.

The *Kd* extends beneath the entirety of the LENRD and is the only bedrock strata with potential for widespread development across the region. The unit is thickest and deepest on the west side of the district. In this area, the *Kd* is over 500 ft thick in places, with the top of the formation ranging from 1,000 to 1,200 ft bgl. Beneath the eastern half of the district, the *Kd* is considerably shallower, with

depth to the top of the formation ranging from 100 ft bgl beneath incised drainages and 200-300 ft beneath the loess mantled uplands between the major drainages. In the eastern part of the LENRD, the

Kd ranges in thickness from 300-400 ft. Figure 5-32 through Figure 5-35 indicate the variability in resistivity beneath the LENRD. The more resistive areas (20 ohm-m or greater) represent where permeable intervals could be present within the unit, and where targets for potential well testing and development in the *Kd* exist. These zones are most common beneath the eastern half of the district. It is possible that water is present within the pore spaces of the *Kd* in the western half of the district, but that higher TDS levels at greater depths within the formation are responsible for the lower resistivities. However, the presence of more resistive features beneath the eastern half of the district is opportune for future exploration, as *Kd* is found at considerably shallower depths in this area. Some groundwater users in the LENRD have discovered the utility of the *Kd* as an aquifer source, as numerous registered well logs from the NDNR Registered Well Database indicated well screens set in sandstone beneath the Quaternary system with varying rates of registered production. Thus, it is known that the *Kd* can produce beneficial rates of groundwater beneath the district. Use of the AEM data can further be utilized for sighting future target areas for testing and development of the formation for multiple uses of groundwater.

Also detected in the AEM survey are undifferentiated Paleozoic strata that underlie the *Kd*. The detected sequence above the DOI thickens westward across the LENRD, from around the 100-200 ft range along flight line 201801 to over 500 ft beneath flight line 200101. The west-east profiles across the LENRD indicate the Paleozoic beds to be dipping westward towards the Central Nebraska Basin at a similar angle to the overlying Cretaceous strata. The Paleozoic units are not a known aquifer resource beneath the LENRD. However, future exploration for groundwater resources within these intervals could be guided by targeting resistive intervals within these sequences as revealed by the AEM survey.

5.3.3 Papio-Missouri River NRD

The AEM survey over the PMRNRD included two extended north-south profiles, two shorter west-east profiles in the northern and central sections of the district, and a cluster of flight lines in the far southern extent of the district south of the Omaha metropolitan area (Figure 5-37). The profiles reveal the character of the Quaternary system along the eastern edge of the state as well as the underlying bedrock that reveals the structure of the *Kd* and Paleozoic systems. Flight line 202001 traces along the west central section of the PMRNRD, and in a few areas, straddles the border with the LENRD. However, it is assumed that the geology revealed by the AEM is similar in the PMRNRD at these locations. The 3D hydrogeological framework is shown in Figure 5-38.

While reviewing this section, the reader is encouraged to utilize the flight line KMZs in Google Earth to interactively view the flight lines discussed in this section.

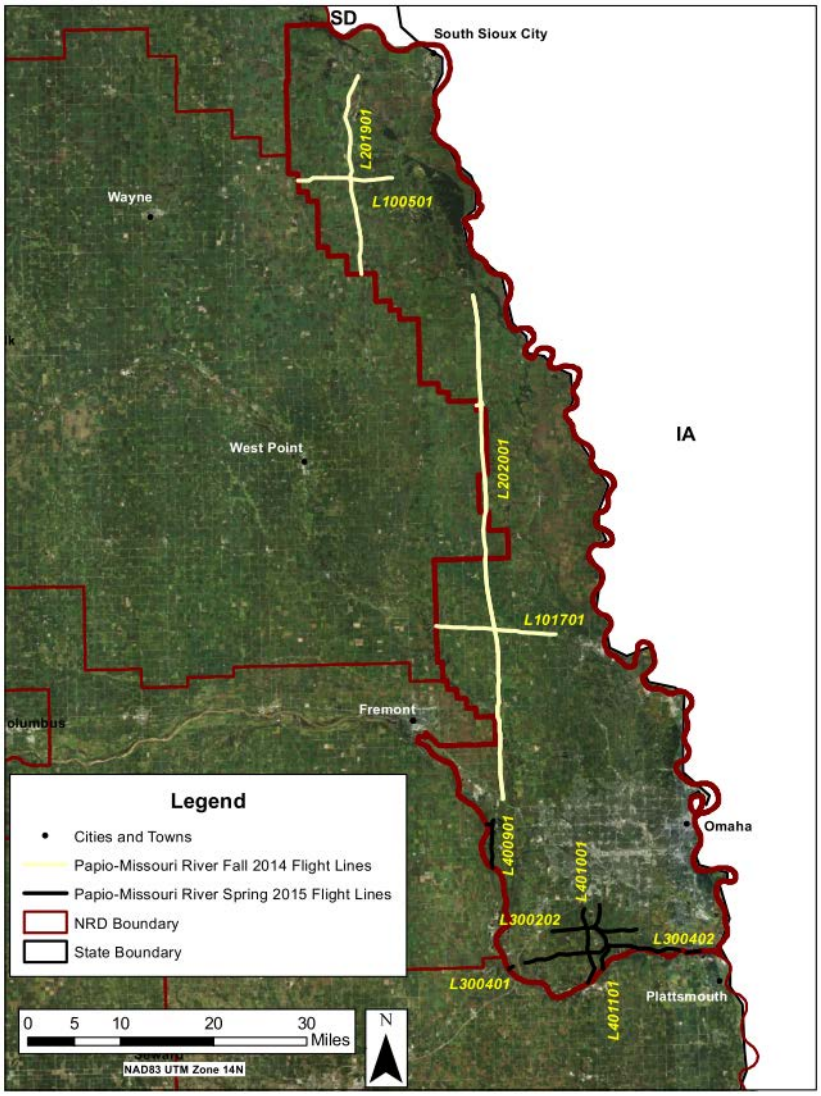


Figure 5-37: Flight lines within the PMRNRD acquired in Phase 1 of the ENWRA AEM survey.

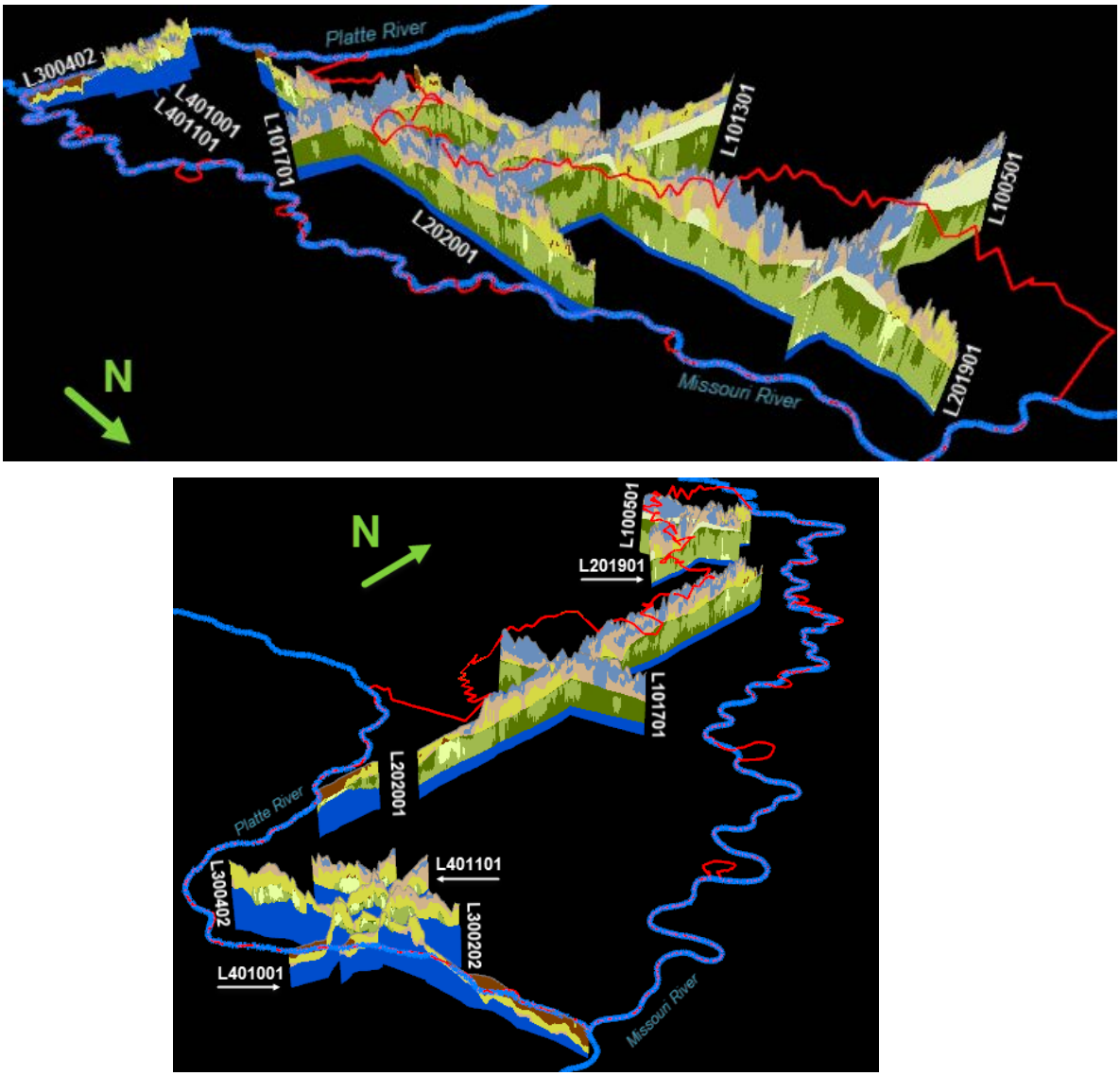


Figure 5-38: 3D hydrogeologic framework views of the PMRNRD from the reconnaissance AEM survey. The district boundary is displayed in red, with flight lines labeled in white and major drainages displayed in blue. See Figure 5-2 for the aquifer and bedrock material resistivity thresholds and stratigraphic codes.

5.3.3.1 Quaternary/Tertiary System beneath the PMRNRD

As indicated in the beginning of section 5.1.2, much of the east half of the project area is underlain by marginal aquifer with minimal principal aquifer deposits, most of which underlie thick sequences of aquitard materials. This trend is clearly present beneath much of the PMRNRD north of the Omaha metropolitan area. Along flight line 202001 (Figure 5-39), the Quaternary system ranges in thickness from approximately 100 to 400 ft, depending on location. Much of the Quaternary system in this profile is composed of marginal aquifer and aquitard material, with only isolated basal intervals of principal aquifer deposits that range in thickness from 50 to 100 ft. In some locations, the thickness of aquitard materials exceeds 200 ft, and along much of the profile, aquitard material comprises the upper 100 ft of the sequence. Along the southern one-third of profile 202001, two intervals of aquitard material are present, each exceeding 100 ft in places with marginal aquifer material between these two low permeability bodies. In the southern one-third of the profile 202001 and north of the Elkhorn River

valley (flat portion of profile), two intervals of basal principal aquifer are present beneath marginal and aquitard materials. Beneath the Elkhorn River valley, principal aquifer deposits comprise the majority of the underlying material, with thicknesses ranging from 25 to nearly 100 ft. Included beneath the valley is a small interval of sand-rich principal aquifer material (>50 ohm-m).

Perpendicular to flight line 202001, the eastern extent of profile 101701.1 (Figure 5-40) indicates a sequence of aquitard material exceeding 200 ft thick in many locations northeast of the city of Fremont. Some of this material overlies marginal aquifer material with small, isolated bodies of principal aquifer material. This trend demonstrates that the predominately marginal aquifer deposits overlain by thick sequences of aquitard material extends across much of the central section of the PMRNRD and are not limited to just the western edge of the district. Near the northern edge of flight line 202001 is a body of principal aquifer material that sits at the edge of the South Blackbird Creek drainage that dissects the hilly upland bluffs region along the Missouri River. This resistive feature extends beneath the uplands that are composed of marginal aquifer and aquitard materials.

In the northern one-fourth of the district, the Quaternary system ranges from 100 to over 200 ft in thickness, with a considerable portion of the deposits comprised of aquitard material that overlies marginal aquifer deposits. These deposits transition into an interval of principal aquifer material upwards of 200 ft in thickness near situated along the southern edge of the Missouri River valley west of South Sioux City, NE (Figure 5-40). In this area, the regional water table surface appears to be unconfined. Moving southward from this area, however, the regional water level surface is situated within or beneath the aquitard material, therefore it is likely that the aquifer is under confined conditions beyond the edge of the uplands that border the Missouri River valley. This feature of resistive material is similar to the body of resistive material at the northern edge of flight line 202001 along the edge of the upland bluffs that border the Nebraska side of the Missouri River valley, indicating that a trend of unconfined, resistive aquifer is present in this region of the PMRNRD.

South of the Omaha metropolitan area, an additional group of flight lines was acquired during the spring 2015 survey. The AEM data revealed that this area is underlain by extensive intervals of principal aquifer ranging from approximately 50 to 125 ft in thickness that are beneath marginal aquifer deposits and isolated intervals of aquitard material. The principal aquifer is above 50 ohm-m in the far southern PMRNRD beneath the Platte River valley, and ranges from 50 to 125 ft in thickness. Although the principal aquifer materials are present beneath most of the flight lines in the southern PMRNRD, the 1995 CSD water table surface is contained within these deposits at most locations, indicating that the entire sequence of principal aquifer materials may not be saturated at all locations. However, the lack of extensive aquitard deposits in this area indicates that potential for groundwater recharge can occur in this area.

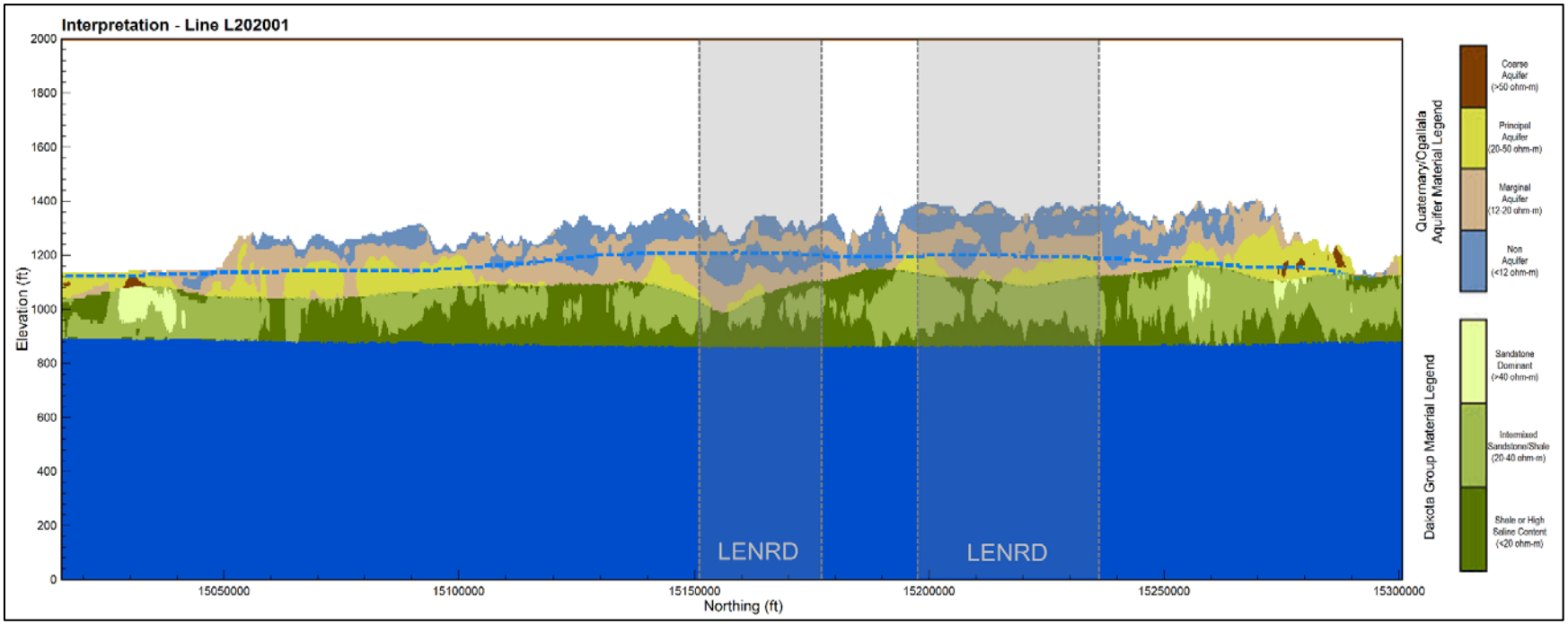


Figure 5-39: Interpreted profile for south-north flight line 202001 (left) that extends along the western side of the southern half of the PMRNRD. The CSD 1995 regional water table surface is indicated by dashed blue line. North is on the right, south to the left. The flight line intersects the LENRD in the following ranges: 15151000 - 15177635 ft Northing, 15198810 - 15235710 ft Northing. The stratigraphy color codes are listed in Figure 5-2.

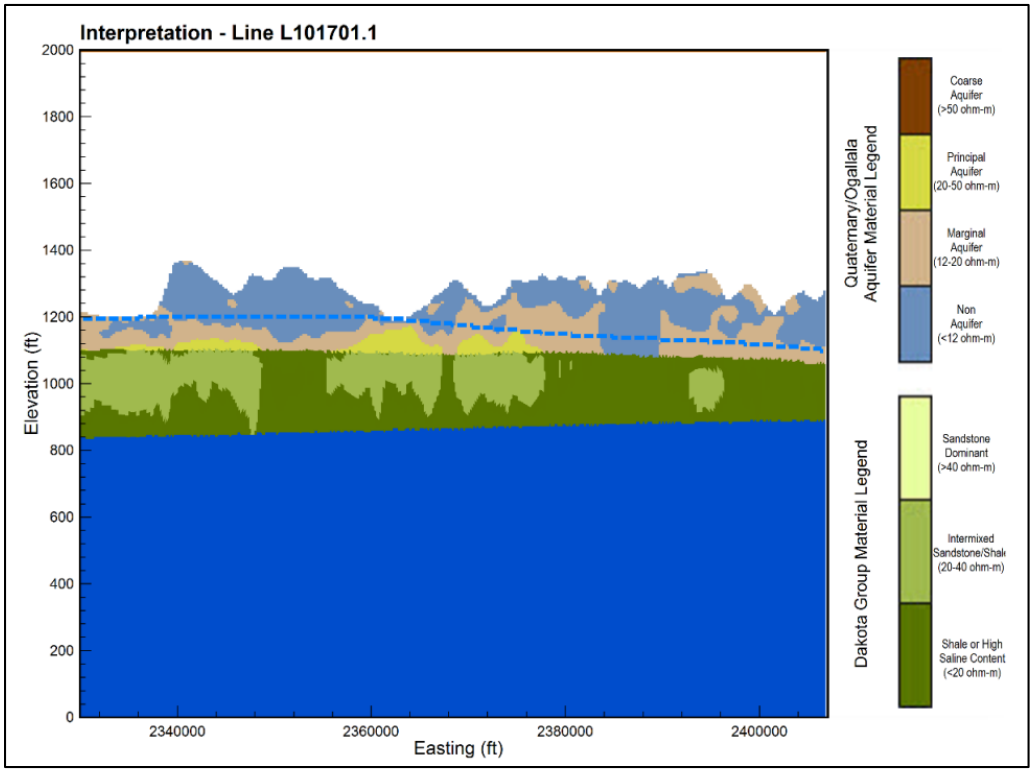


Figure 5-40: Interpreted profile for flight line 101701.1 (right) that extends west-east through the south-central section of the PMRNRD northwest of the Omaha metropolitan area. The CSD 1995 regional water table surface is indicated by dashed blue line. East is on the right, west to the left. The PMRNRD starts at 2339350 ft Easting. The stratigraphy color codes are listed in Figure 5-2.

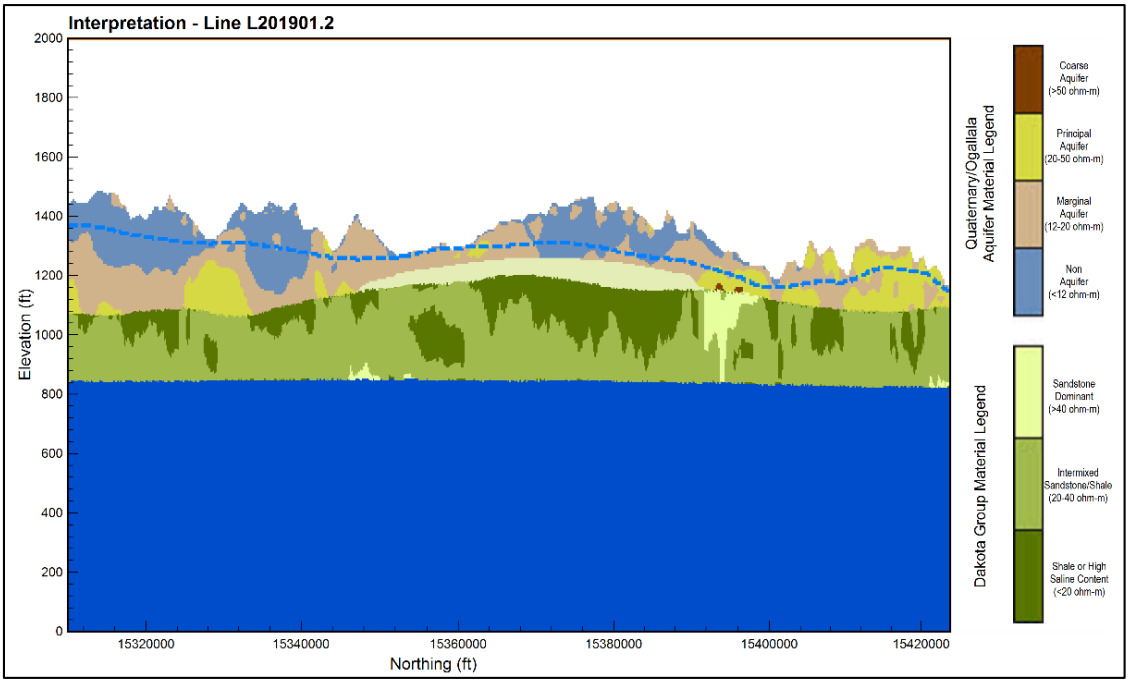


Figure 5-41: Interpreted profile for south-north flight line 201901.2 (left) that extends through the northern one-quarter of the PMRNRD. The CSD 1995 regional water table surface is indicated by dashed blue line. North is on the right, south to the left. The PMRNRD starts at 15313125 ft Northing. The stratigraphy color codes are listed in Figure 5-2.

5.3.3.1 *Cretaceous and Paleozoic Sequence beneath the PMRNRD*

The *Kd* is the uppermost bedrock unit beneath most of the PMRNRD north of the Omaha metropolitan area. The bedrock surface topography undulates north to south across the PMRNRD along flight line 201001, but is more subdued along flight line 201901. The thickness ranges from 150 to nearly 300 ft along flight line 201001, with the thickest area beneath northern Burt County and the thinnest area approximately 15 miles northeast of Fremont, NE in Washington County which appears to coincide with the area of the modern-day New York Creek surface drainage (Figure 5-39 and Figure 5-40). The *Kd* along flight lines 202001 and 201901 are predominately composed of material of 20 ohm-m or greater (light green intervals within *Kd* sequence of Figure 5-39 and Figure 5-40). The areas where basal principal aquifer material are present in the Quaternary system overly these 20 ohm-m or greater intervals of the *Kd*, These areas have potential for hydraulic communication between the unconsolidated and bedrock aquifers to occur.

In the northern one-fourth of the PMRNRD, a portion of the eastern terminus of the combined *KcKgg* is revealed along flight line 201901.2. This interval approaches 100 ft in thickness beneath northern Thurston and southern Dakota Counties. Beneath this *KcKgg* sequence, nearly the entire *Kd* thickness is above 20 ohm-m, indicating that potential for *Kd* aquifer development could still occur beneath the overlying limestone and shale of the *KcKgg*.

Beneath the southern PMRNRD flight lines acquired in the spring of 2015, the *Kd* is present in isolated bodies separate from the main body of the unit. However, these isolated bodies can range from 80 to 100 ft in thickness and contain some of the most abundant intervals of zones exceeding 40 ohm-m in the entire northern ENWRA project area. Some of these highly resistive zones are in direct contact with overlying principal and sand-rich principal aquifer deposits (Figure 5-42).

The Paleozoic sequence detected beneath the PMRNRD was undifferentiated in the interpretation. The Paleozoic surface beneath the southern PMRNRD is irregular (flight lines 300402, 401001), but is generally flat north of the Omaha metropolitan area (flight line 202001). Although the Paleozoic sequence is undifferentiated in the interpretation, the AEM profile of line 300402 reveals the Humboldt Fault zone (Figure 5-43). A considerable break in the resistivity occurs west of Easting value 2480000 ft, which is the location of the mapped fault that bounds the southern edge of the Thurston-Redfield Structural Zone. This fault area lies directly beneath Quaternary principal aquifer material of the Platte River valley. It is unclear, however, as to whether any hydrologic connection exists between the younger saturated alluvium beneath the Platte River and underlying faulted strata. Section 2.1.6 in Volume II of this report contains further discussion the structural geology beneath southeastern Nebraska.

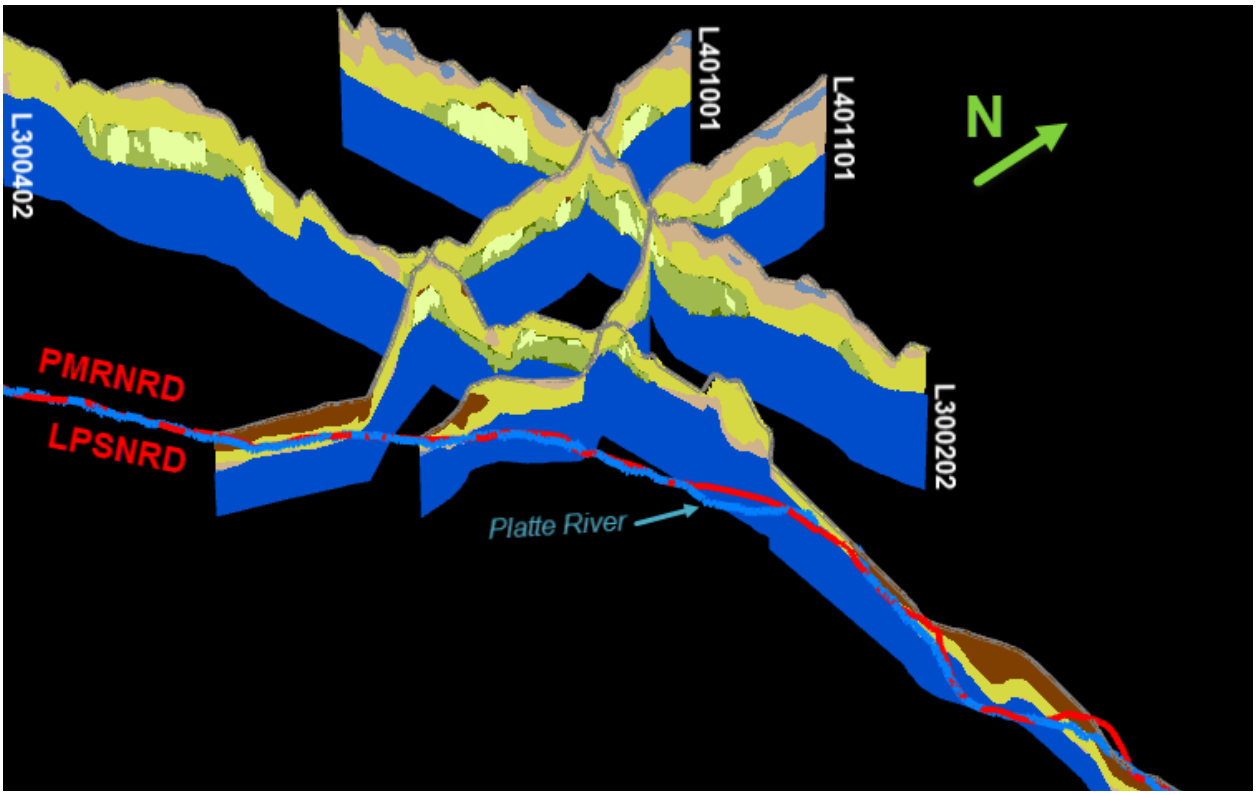


Figure 5-42: 3D framework of the southern PMRNRD flight lines (right) displaying the extent of the principal aquifer material and resistive intervals in the *Kd*. Vertical exaggeration is 30x. See Figure 5-2 for the resistivity threshold and stratigraphy legend.

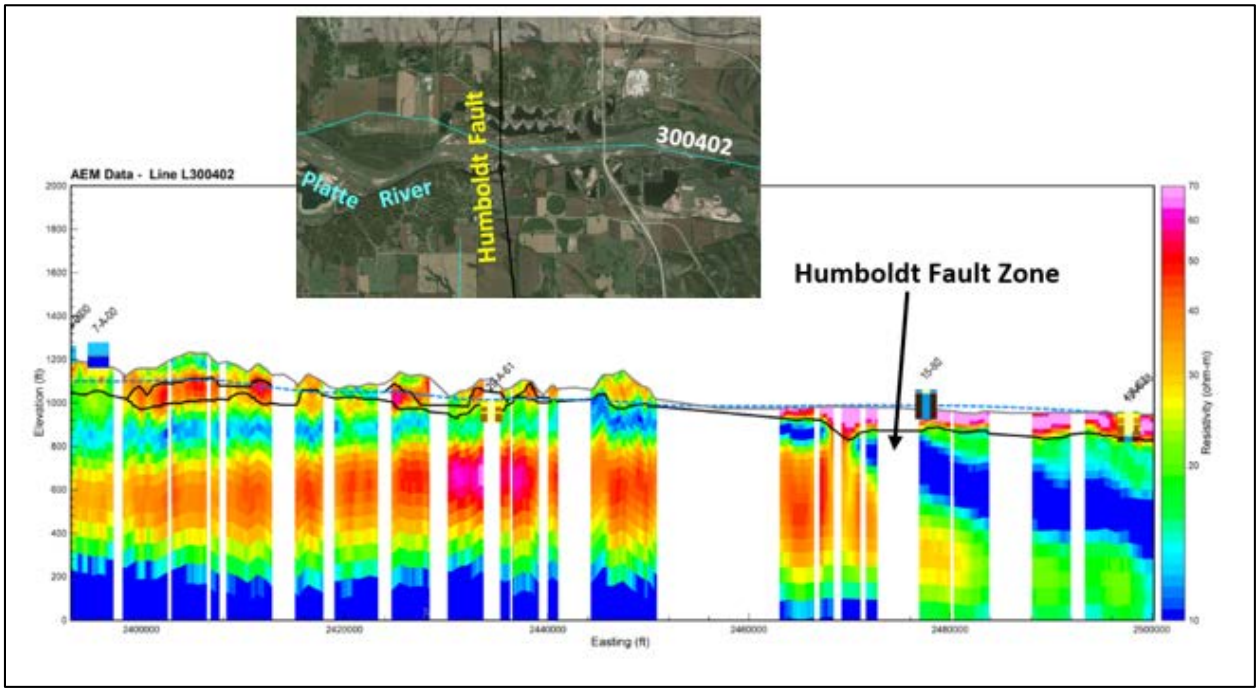


Figure 5-43: Resistivity profile of flight line 300402 (above) in the southern PMRNRD indicating the Humboldt Fault in the Paleozoic strata. The map to the left shows the location of the fault-flight line intersection.

5.3.4 Comparison of AEM Results with Previous Studies

Prior to the ENWRA project AEM surveys, smaller, local scale airborne geophysical surveys were conducted within the northern project area, including a survey in the Clarkson/Howells area of the LENRD (red area on Figure 5-44) conducted by XRI in 2013. Additionally, another survey in the eastern LENRD was completed near the town of Oakland (blue area on Figure 5-44 in 2007 by the USGS and another was completed by the CSD near Ashland, which also covered a small section of the southwestern PMRNRD (black area in Figure 5-44). Discussion and comparison of these surveys with the findings in this report are provided in the following subsections.

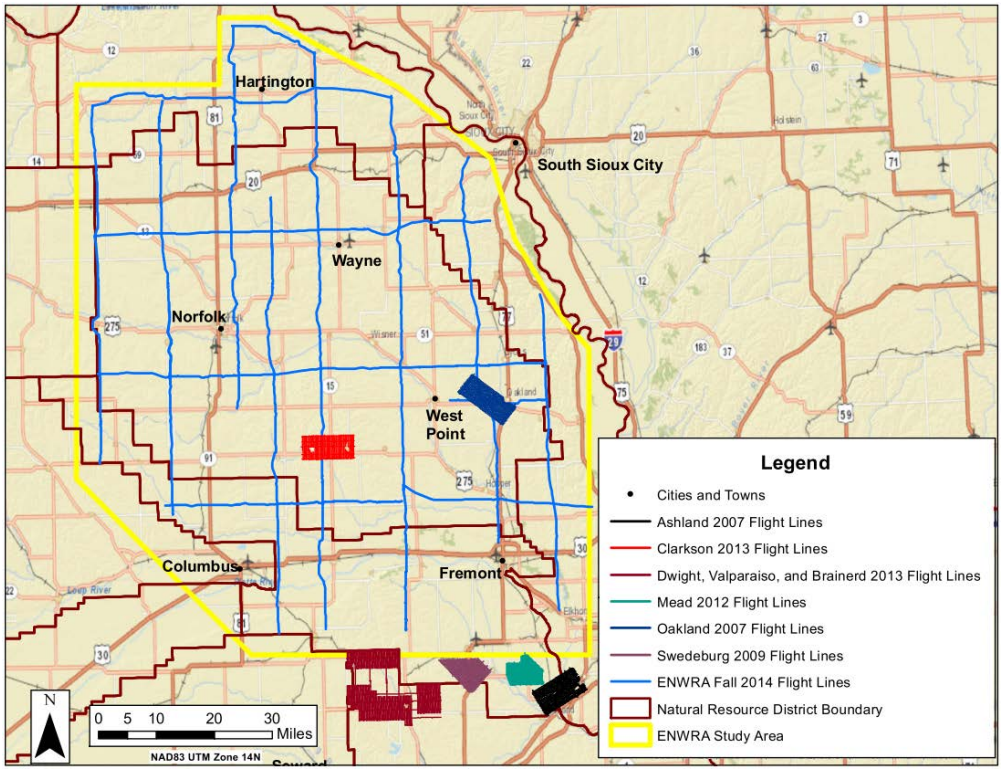


Figure 5-44: Locations of prior study airborne geophysical survey studies in the northern ENWRA project area.

5.3.4.1 Studies in the Lower Elkhorn NRD

Clarkson/Howells Area AEM Survey

To address water resource concerns of the LENRD in the area between the towns of Clarkson and Howells, an AEM project supporting development of a hydrogeologic framework was initiated by XRI Geophysics in August 2013 (Abraham et al., 2013). The LENRD area had experienced record groundwater declines in 2012 that prompted the district to look for additional information on the groundwater resources of the area. AEM survey results from a 36 mi^2 survey area were used to visualize the subsurface in 3D and to estimate various percentages of the aquifer materials and pore water volumes. The framework also provided insight into the connection of these aquifer materials and existing extraction wells, streams, and other aquifers. The survey was conducted with densely-spaced flight lines (approximately 1000 ft apart) to identify and characterize small and isolated bodies of Quaternary aquifer deposits. The primary aquifers in the area are small and of limited extent and are mostly confined

between the West and East Maple Creek drainages. There are numerous isolated deposits of aquifer materials that supply water to low yield wells across the project area as identified with the lower resistivity thresholds displayed in Abraham et al. (2013). It was estimated that over 106,200 ac-ft of recoverable water is available in the aquifer materials underlying the project area.

The limited volume of groundwater in the small, discontinuous intervals of aquifer beneath the project area, combined with the impact of the drought in 2012, which likely necessitated above normal extraction rates from wells in the area, resulted in the precipitous water level declines. The limited area identified in this study where aquifer recharge is expected to occur further restricts the sustainability of the aquifer during times of drought. The information provided herein can be used in determining the rate of withdrawal from the aquifer during varying climatic conditions. The estimate of the amount of groundwater in storage balanced with allowable withdrawals can lessen the impact of climate variations.

An additional result from this work was the identification of potential water supply in the sandstones of the *Kd*. It was recommended that additional work be conducted to determine the extent and character of this potential resource. The *Kd* is currently used for irrigation and water supply near the project area and it is possible for similar conditions to exist beneath the Clarkson/Howells area.

The locations where an ENWRA line intersects with the Clarkson flight lines are shown in Figure 5-45. The inverted models at each intersection marked are compared in Figure 5-46. The Clarkson survey data were

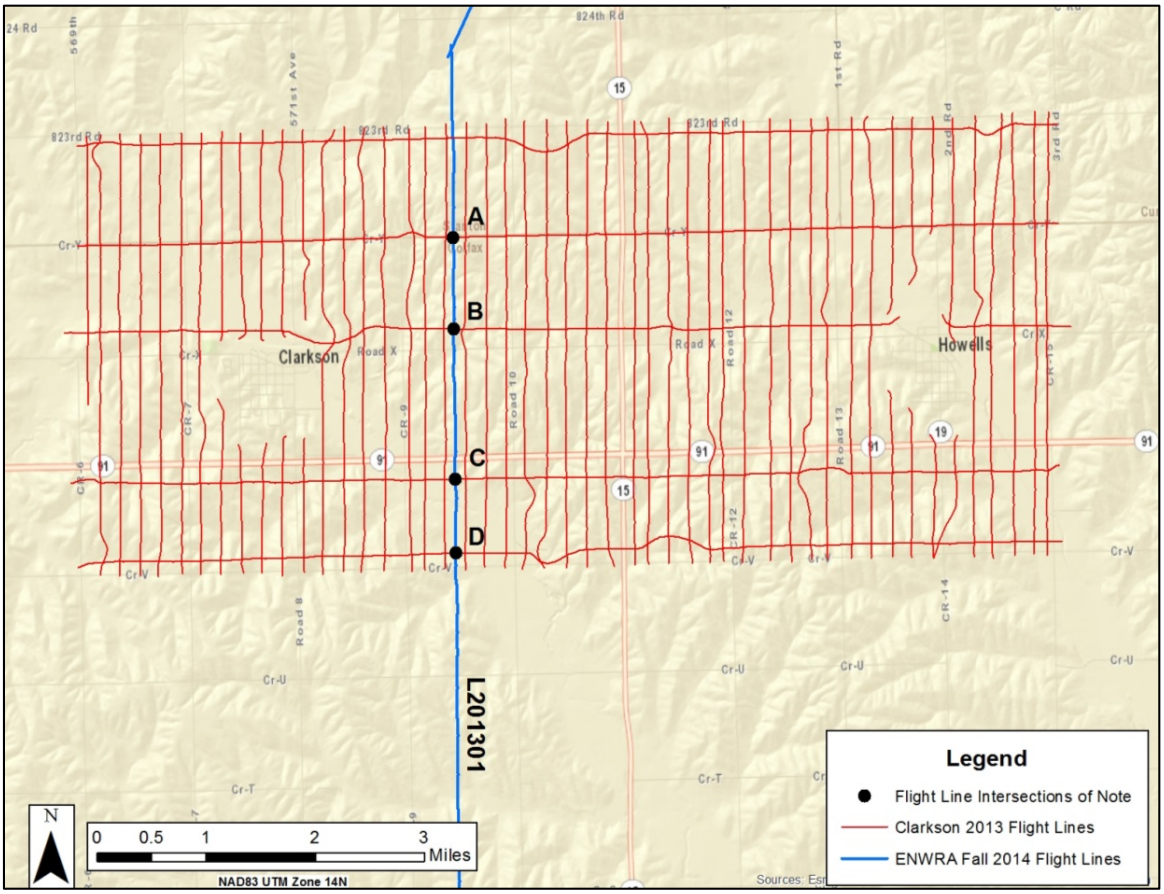


Figure 5-45: Clarkson flight lines shown with the ENWRA flight line in the area. Inverted models are compared at the marked locations.

acquired with the SkyTEM 304 system. The models from the different surveys match very well. The models diverge slightly at a depth of approximately 600 ft, which corresponds to the approximate depth of investigation of the 304 system.

This survey indicated that only local-scale flight line density provides adequately detailed in the subsurface information necessary to create 3D voxel models of aquifer features. Densely collected data provides the ability to estimate the aquifer material volume and estimates of groundwater in storage. Without closely spaced flight lines providing fine detail of the subsurface, it is not recommended that these volume and storage calculation be made. Figure 5-47 demonstrates how narrow intervals of aquifer deposits could be missed or not fully characterized if flight line spacing were increased from just 0.5 miles to 1.0 miles.

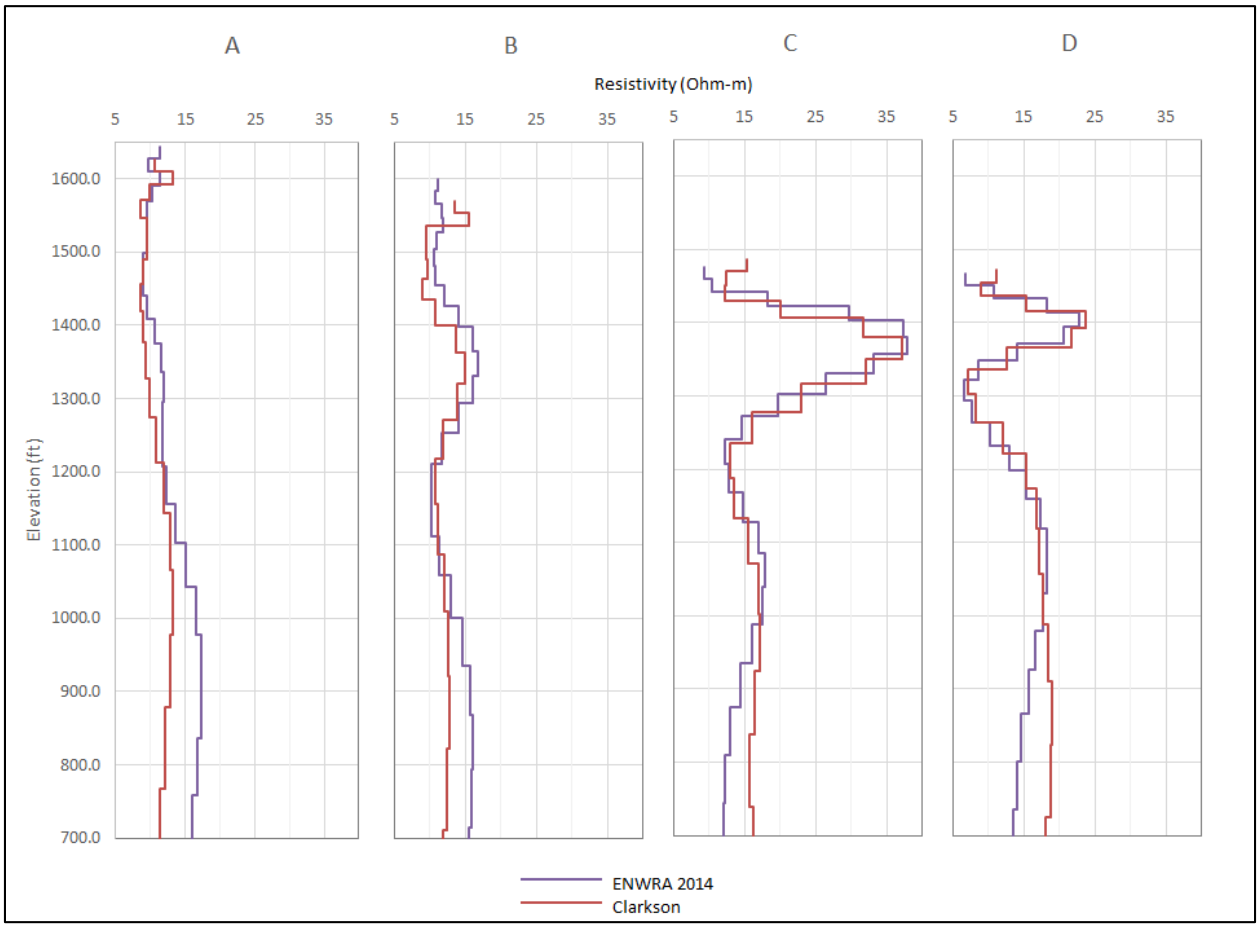


Figure 5-46: Comparison of inverted models between the Clarkson and ENWRA 2014 surveys. The models shown in panel A are 133 ft apart, panel B 53 ft, panel C 91 ft, and panel D 137 ft. The X-axes resistivities are linear.

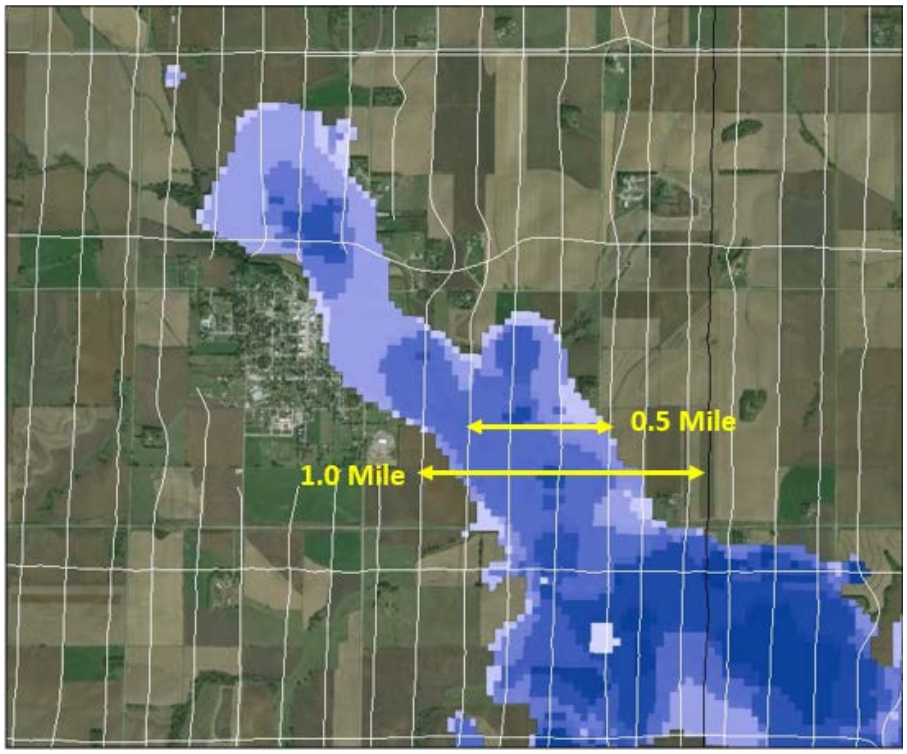


Figure 5-47: Display of aquifer material near Clarkson, NE with a 700 ft grid line spacing (white lines). The yellow lines demonstrate how some portion of the aquifer would have been missed if the AEM flight line spacing were set at 0.5 or 1.0 miles.

Oakland AEM Survey

Smith et al. (2008) presented a digital data release for a HEM and magnetic survey that was conducted during March 2007 in three areas (Firth, Ashland, Oakland) covering approximately 36 mi^2 (93 km^2) of eastern Nebraska as part of a joint CSD and USGS study. The objective of the survey was to improve the understanding of the relationship between surface water and aquifer systems critical to developing water resource management programs. The electromagnetic equipment consisted of six different coil-pair orientations that measured electrical resistivity at separate frequencies from approximately 400 hertz to near 115,000 hertz. The electromagnetic data were converted to electrical resistivity geo-referenced grids and maps, each representing different approximate depths of investigation for each area. The range of the subsurface investigation is comparable to the depth of shallow aquifers.

In early 2009, the USGS conducted a general assessment of the capabilities of several additional geophysical tools to delineate buried paleovalley aquifers in the glacial terrain of eastern Nebraska (Abraham et al., 2012). Mapping these paleovalleys was and remains an important objective for the ENWRA technical group. Previous attempts at mapping these buried valleys included a helicopter electromagnetic survey flown over an area near the town of Oakland, NE in March 2007 (Described above, Smith et al., 2008). This survey (blue area on Figure 5-44) had limited success in imaging the paleovalleys due to the restricted depth of investigation of the system in the clay-rich till overburden. The purpose of the 2009 study was to investigate whether other airborne electromagnetic or ground-based geophysical techniques, including audio-magnetotelluric, time-domain electromagnetic, gravity,

and magnetic methods could be used to image the paleovalleys within the clay-rich tills of eastern Nebraska.

Ground-surface audio-magnetotelluric and time-domain electromagnetic methods achieved sufficient depth of penetration and indicated that the paleochannel was much more complex than the original geological model. Simulated and observed gravity anomalies indicate that imaging the sand and gravel aquifers near Oakland would be difficult due to the complex basement density contrasts. Interpretation of the magnetic data indicated no magnetic sources from geologic units above the bedrock surface. Based upon the analysis and interpretation of the four methods evaluated, it was suggested that a large-scale survey using a high-powered time-domain airborne system be performed. This would be the most efficient and cost-effective path forward for the ENWRA group to map paleovalleys that lie beneath thick clay-rich glacial tills.

5.3.4.2 Studies in the Papio-Missouri River NRD

Ashland AEM Survey

As part of the ENWRA, a frequency-domain HEM geophysical investigation was conducted in conjunction with subsurface data to map the hydrostratigraphy of the Platte River valley and adjacent uplands near Ashland, NE. The HEM survey was performed over 36 square-mile study area, with the approximately eastern half within the PMRNRD. The western half of the survey was within the LPNNRD, and a small segment along the southern edge of the flight area in the LPSNRD, which is discussed in Volume II of this report. Specific data sets generated during the HEM survey at the Ashland site can be found in Smith et al. (2008). The survey was conducted in March 2007 on a flight line spacing of approximately 890 feet and the helicopter flew at a height of approximately 115 ft above the ground surface (flight area shown in black on Figure 5-44). Flight elevations were determined by onboard GPS and final ground elevations and were corrected using differential GPS. Ground surface elevation errors are expected to be on the order of ± 6.5 ft. The survey used six frequencies, ranging from 400 Hz to 114,000 Hz and individual soundings were taken at 11 ft intervals. The higher electromagnetic frequencies have shallow penetration depths whereas the lower frequencies can penetrate deeper into geological materials.

Following completion of the inversion, CSD compared the results of particle size analysis, borehole geophysics, and hydrochemistry from test holes and monitoring wells installed during the study to the inverted HEM profiles. In addition, CSD used registered groundwater wells, oil and gas borehole logs, and other pre-existing data that were not used in the inversion process. Hydrostratigraphic unit contacts were identified using subsurface data. Where these contacts correlated to contrasts in resistivity, the contacts were traced along HEM profiles. In some cases, there was no resistivity contrast at the unit contact (i.e. between sand/sandstone or sandstone/limestone). Therefore, only borehole data were used for correlation.

Hydrostratigraphic units were interpreted using earth resistivity models from the HEM survey and subsurface data, including CSD test holes, NGOCC deep oil and gas well logs, and registered well logs. Deposits of highly conductive materials (clay and silt) 80 to 100 ft thick limited the effectiveness of the HEM results for hydrostratigraphic mapping in the uplands. However, hydrostratigraphic units in recent and abandoned alluvial deposits of the Platte River, even where covered by 10-15 ft of fine sediments,

could be mapped in detail using the HEM survey results. The investigation showed that the Platte River and Quaternary aquifer materials are apparently connected hydrologically throughout the study area and that the Quaternary and *Kd* aquifers can be hydrologically connected except where the discontinuous aquitard strata in the *Kd* separates them.

Interpretive cross-sections drawn with the use of the available subsurface data and the HEM survey results show the relationships between subsurface hydrostratigraphic units. A cross-section drawn in the northern section of the Ashland HEM area shows up to approximately 175 feet (53 m) of Quaternary sediment and Cretaceous rock overlying Pennsylvanian bedrock. The area immediately adjacent to the modern day Elkhorn and Platte River channels is surrounded by Quaternary aquifer material. Quaternary fine material (aquitard) is found at the land surface along the edges of the Platte River valley, and within the Platte River valley Quaternary aquitard is comprised of overbank alluvium fines. The alluvium within the Platte River valley in most locations coarsens with depth. Throughout most of the Ashland HEM area, the Platte River valley alluvium directly overlies *Kd* except for a small area east of the active Platte River channel where K ad is present. Through most of this portion of the Platte River valley the Quaternary aquifer materials and the *Kd* units are hydrologically connected. Underlying the *Kd* units are low resistivity Pennsylvanian shales.

5.4 Summary and Recommendations

5.4.1 Key AEM Survey Findings

The AEM reconnaissance survey of the northern half of the ENWRA project area has provided a detailed interpretation of the subsurface hydrogeologic conditions at the 20 mile flight line spacing applied for this investigation. The AEM survey was able to detect strata as deep as the Paleozoic units beneath northeastern Nebraska, with the depth of investigation exceeding 1,200 ft in places. The following list summarizes the findings resulting from this survey:

- LCNRD - the aquifer resources beneath the LCNRD vary from thick sequences of principal and marginal aquifer materials beneath the western half of the district to minimal thickness in Quaternary deposits mantled atop Cretaceous bedrock in the north-central section of the district. Beneath the western half of the district is a continuous body of principal aquifer material interlayered with marginal aquifer material that sit atop basal aquitard material. The surficial deposits in this area range from 150 ft thick sequences of aquitard material to marginal aquifer material. The placement of the regional water table surface indicates that at least half of this sequence is unsaturated. The Quaternary sequence in this area sits above *Kp*. In the south central area of the district, the AEM survey revealed numerous locations of pronounced surface topography underlain by sand-rich principal aquifer material ranging from approximately 50 to 150 ft in thickness. Although many of these intervals are unsaturated, they do indicate locations where groundwater recharge is likely to occur. The eastern half of the district is underlain by predominately marginal aquifer and aquitard materials approaching 300 ft in thickness, with isolated pockets of principal and sand-rich principal aquifer materials. The *To* is present beneath nearly the western two-thirds of the district, with maximum thickness of approximately 100 ft. The full sequence of Cretaceous strata is present beneath the district, with each formation at

least 200 ft thick beneath the western half of the LCNRD. The westward dip of the Cretaceous units are clearly evident in the AEM data. The eastern terminus of the *Kp* and *Kn* are identified in the survey beneath the eastern half of the district. The *Kd* ranges from 400 to over 500 ft in thickness, with much of the eastern half of the district underlain by intervals with resistivities ranging from 20-40 ohm-m. The depth to the top of the *Kd* ranges from 1,000 ft near the LCNRD's western border to approximately 250 ft beneath the district's eastern edge. The undifferentiated Paleozoic strata ranges in depth from over 1,500 ft beneath the west side of the district to approximately 600 ft near the district's eastern boundary. The eastern half of the Paleozoic sequence hosts a considerable resistive interval, ranging from 35-45 ohm-m.

- LENRD - the LENRD hosts the most extensive sequences of continuous principal aquifer material in the northern half of the ENWRA project area, primarily in the western half of the district. Several distinct bodies of sand-rich principal aquifer (>50 ohm-m) ranging from 100-200 ft thick were identified in this area of the survey. The *To* is present beneath the western one-third of the LENRD and comprises nearly half of the principal aquifer at some locations in this area. East of flight lines 200801 and 201001, however, the Quaternary system is comprised primarily of marginal aquifer and aquitard materials. At some locations, the entire Quaternary sequence consists of aquitard materials, which can approach 400 ft in thickness. The contrast in subsurface conditions between the western and eastern halves of the district is evident in the distribution of irrigation wells. To the west/northwest of Norfolk, irrigation well density is over 3.6 per square mile, whereas in the eastern half of the LENRD in the area between flight line 201001 and the city of Wayne, the density is less than one well per square mile. Beyond the extensive aquifer resources of the district's western half, principal aquifer resources are also present in the southern LENRD, mostly associated with alluvium of the Elkhorn River and Morgan Creek valleys. In these areas, extensive sand-rich intervals of principal aquifer are present at thicknesses ranging from less than 100 ft to over 200 ft, depending on location. The entire Cretaceous sequence is present beneath the district, ranging in thickness from over 1,600 ft beneath the northern half of the district to approximately 1,000 ft below the southern half of the LENRD. The *Kp*, *Kn*, and *KcKgg* each terminate beneath the LENRD. The *Kd* is present beneath the entire district, ranging in thickness from nearly 600 ft in the west to approximately 100 ft in the far southeast corner of the LENRD. Beneath much of the eastern half of the LENRD, intervals of resistivity ranging from 20-40 ohm-m are common in the *Kd*, some approaching 400 ft in thickness, and at some isolated locations, intervals greater than 40 ohm-m are present.

- PMRND - the PMRNRD is underlain by predominately marginal aquifer and aquitard material, with discontinuous areas of principal and sand-rich principal aquifer material scattered across the district. This pattern of Quaternary material distribution is apparent along flight line 202001 that traces north to south along much of the district's extent. In this area, basal principal aquifer deposits area underlain by over 200 ft of marginal aquifer and aquitard deposits. In the northern area of the district southwest of South Sioux City, NE, most of the Quaternary sequence consists of aquitard material. South of the Omaha metropolitan area in Sarpy County, extensive sand-rich principal aquifer deposits are present beneath the Platte River valley, as well as in an

isolated corner of the district that includes a small section of the Platte River valley near Ashland, NE. *KcKgg* strata terminates in the northern corner of the PMRNRD, and *Kd* is present beneath the entirety of the district. Most of the *Kd* beneath the PMRNRD contains intervals ranging from 20-40 ohm-m that are typically 200 ft or greater in thickness. South of the Omaha metropolitan area, the *Kd* ranges from 100 to 200 ft in thickness, but consists primarily of strata with resistivity ranging from 20-40 ohm-m, with extensive intervals greater than 40 ohm-m. Along the district's southern edge, the AEM survey revealed the presence of the Humboldt Fault beneath the Platte River valley.

- Tertiary/*To* - The Tertiary *To* material under much of the western half of the northern ENWRA project area ranges in thickness from over 150 ft on the westernmost flight lines to near zero near flight line 200801. It is likely that these separate material types (Quaternary and Tertiary) act as one aquifer unit or are in close hydraulic communication. It is also possible that some siltstone layers common in the *To* could create local varying conditions in the vertical gradient between the two systems.

- Cretaceous Units - Although most units displayed unique resistivities in the Cretaceous sequence, identification of the individual *Kc* and *Kgg* units proved difficult due to their similarity in resistivity signatures. These units were combined as one unit in the hydrostratigraphic interpretation, which was considered appropriate since these formations are not known aquifer resources in eastern Nebraska and act as confining units to the underlying *Kd*.

- Paleozoic System - Underlying the Cretaceous sequence are Paleozoic strata. The Paleozoic system beneath the northern ENWRA project area had resistivities similar to the overlying Cretaceous deposits, but can were identified with comparison with NOGCC test holes at a few isolated locations. The Paleozoic sequence was undifferentiated in the interpretation of the AEM data for this project. None of the Paleozoic intervals are utilized for groundwater over widespread areas in eastern Nebraska.

The AEM survey flight line grid spacing of approximately twenty miles provided insight and information on a regional scale that allows for greater understanding of where future detailed work could occur. Denser grid spacing is required for smaller, specific water supply projects such as the survey conducted for the towns of Clarkson and Howells, NE in the southern portion of the LENRD in 2013 (Abraham et. al, 2013). This survey, in the southern LENRD, provides an example of the benefits of tightly spaced flight lines. A 1,000 ft line spacing was used during data acquisition in this 2013 survey conducted to detect and characterize limited aquifer resources in this area. This closely spaced flight path layout allowed for detection of the extent of the limited glacial outwash deposits surrounding these towns. Had a spacing of a one-half mile or one mile been used in this study, a considerable portion of the aquifer resources near Clarkson, NE would not have been detected (Section 5.3.2.3, Figure 5-47).

The flight line spacing necessary in eastern Nebraska for characterization of the bedrock strata is less stringent than the recommended spacing for delineating the Quaternary and Tertiary system. Review of the stratigraphic detail in the AEM data from an AEM Survey conducted in 2014 for the LENRD with

flight line spacing of three miles (Exploration Resources International, 2015) indicates that the character of the bedrock units in the project area has less variability than the overlying Quaternary deposits. At a spacing of three miles, the AEM survey reveals bedrock structure and features in detail. The features detailed in the subsurface profiles, however, are only appropriate for locations in close proximity to the flight lines, as remnant bodies of strata disconnected from the main extent of the unit may be missed with this three mile spacing distance. Evaluation of AEM data at the recon line spacing density (10-20 miles) also reveals the general trend in stratigraphic character (thickness, extent, structure) of the bedrock units beneath the project area. Although minor remnant or "pinch-out" features could be missed at a spacing of 10-20 miles, the flight line density is still considered adequate for district-scale surveys intended to characterize general trends in bedrock units that may host aquifers.

Just as recommended with smaller scale issues in the Quaternary system, closer grid spacing is required to map local bedrock features for water supply studies, particularly with identifying and characterizing resistive intervals within bedrock units such as the *To*, *Kd* (Maha aquifer), and in limited areas of fractured *Kn*. Additionally, closer grid spacing is recommended when using AEM for mapping bedrock features where known fault systems are present, such as in the southern PMRNRD and in the southern ENWRA flight area (Volume II). If characterization of the thickness and connection of units that are separated by a fault is an objective of an AEM survey, modification of the flight planning in the vicinity of such features is recommended. Because of the similarity in the lithologic character of the Quaternary system and the *To*, the three mile line spacing is appropriate for the Tertiary deposits as well.

5.4.2 Applicability and Recommendations Regarding Future Groundwater Investigations

The hydrostratigraphic framework resulting from the AEM reconnaissance survey provides a database of information on the structure of the groundwater resources available beneath the northern half the ENWRA area. The spacing of 10-20 miles between the survey flight lines allowed for hydrogeologic characterization of major features and trends in Quaternary, Tertiary, Cretaceous, and upper Paleozoic geology over an area greater than the size of the states of Connecticut and Rhode Island combined. The resulting datasets from this survey provide readily useable information for managers from multiple NRDs in northeast Nebraska. Although the distance between the flight lines undoubtedly misses some local subsurface features, the framework provided from the AEM survey identifies major subsurface trends, information from which can provide valuable insight with identifying areas where future, tighter-spaced surveys can be conducted to assess more localized hydrogeologic conditions. Such information can include the type of aquifer material present (if any), the depths to the aquifer top and base, as well as the thickness of the intervals of interest. Conversely, the extent and thickness of non-aquifer materials is also available, information that can assist in planning locations for managed groundwater recharge projects or developing groundwater quality protection plans (i.e. wellhead protection plans, best management practices for application of agri-chemicals). Additionally, for non-water development needs, the AEM survey data can be utilized to assess current or locate future sand and gravel mining operations in northeast Nebraska.

The lithologic character distributions based on resistivity as indicated in Figure 5-8 can also provide preliminary estimated ranges of hydraulic conductivity (*k*) for each of the aquifer materials. For the non-aquifer/aquitard category, which is predominately till, silt/loess, and clay, *k* values could range from 2.8

x 10^{-6} feet per day (ft/d) to 2.8 x 10^{-1} ft/d. For the marginal aquifer materials, much of the material distribution is similar to the aquitard material, with the exception of a larger interval of coarse material (nearly 15 percent). Thus, *k* values could be expected to increase in these areas toward the range of 1-3 ft/d where coarse materials are present. For the principal aquifer, more extensive areas of *k* values ranging from 30 to nearly 300 ft/d could be present. For areas of the principal aquifer with resistivity over 50 ohm-m, especially where well-sorted gravel is present, *k* values could exceed 1,000 ft/d. For this condition to occur, however, the gravel would need to be angular and well-sorted with a minimal component of sand or silt in the matrix (Fetter, 1994). Specific yield values in the sand-rich portion of the principal aquifer could range from 0.21 to 0.27, with values of the parameter ranging from 0.02 to 0.18 in clay, silt, and sandy clay deposits that are predominant in the marginal aquifer and aquitard materials (Johnson 1967). For the *To* portion of the principal aquifer, *k* values can range from 1 to 50 ft/d, with specific yield values ranging from less than 0.01 to 0.3 (Gutentag, et al. 1984).

Helgesen and others (1993) report transmissivity within the Maha aquifer beneath the project area ranging from approximately 7,500 to 75,000 gpd/ft (converted from reported values of 1,000 to 10,000 ft^2/d). With an assumed thickness of 500 ft, these transmissivity values would equate to a *k* range of 2 to 20 ft/d, with the higher values of this range likely occurring in the more resistive intervals of the *Kd* identified in the interpretive profiles of Appendix 1. These reported values are only estimates of the *k* that could be encountered in the *Kd*, and it is recommended that aquifer tests or other geophysical methods be implemented to specifically characterize local conditions in this bedrock aquifer source.

To more accurately characterize the physical parameters of the Quaternary aquifers and Cretaceous resistive intervals, as well as for further verification of the lithologic-resistivity relationship described in section 5.2.4, sonic cores of the subsurface materials are recommended to obtain specific lithologic samples undisturbed by drill bits or drilling mud. This would provide undisturbed core of the subsurface with only minimal disturbance of fine material that is normally lost during mud-rotary drilling. Following retrieval of the core, implementation of a calibrated, full-suite geophysical log would be recommended. The resulting data would provide specific resistivity and gamma log data that could be more reliably correlated with the lithology present at that interval. Additionally, nuclear magnetic resonance (NMR) technology could be utilized to characterize porosity and permeability of the materials encountered at the location of interest. It is possible that a sonic core could provide tighter constraints on the resistivity ranges, particularly with the maximum and minimum ranges for glacial till and sand. If the fines are lost in the mud rotary-based drill hole, it would be nearly impossible to accurately assess the quantity of fines in these intervals identified as till or sand, which would thus result in erroneous lithologic characterization, even if those intervals resulted in lower than expected resistivities from the geophysical log for that lithology type.

To further characterize the similarities and differences in the areas where Quaternary principal aquifer materials overlie *To* deposits, piezometer networks with short screened intervals (10 ft maximum) should be installed with several piezometers set and various depths to capture vertical flow gradients in the aquifer. Based on the density of irrigation wells in the western half of the project area, particularly north of the Elkhorn River, it is likely that both stratigraphic intervals are tapped. However, there is little understanding as to the specific connection of these two units and their productive capacities.

It is also recommended that sonic coring efforts focus on a location where bedrock resistors are present, particularly in the *Kd*, ideally with one in the northwest portion of the project area where less resistive intervals were detected in the AEM as well as higher resistive areas in the eastern half of the project area. Resistivities are typically below 20 ohm-m, and often below 15 ohm-m in the northwestern half of the northern ENWRA project area, and exceed 40 ohm-m at several locations in the eastern LENRD and the PMNRNRD. A core would provide beneficial insight into the understanding of the cause of the higher conductive areas in the *Kd*, which could be caused by lithologic or pore water characteristics. Sonic core data can also provide insight into the nature of the resistive intervals revealed in the *M* strata.

The hydrostratigraphic framework resulting from the AEM survey profiles can also be used as a guide to refine historic bedrock maps and cross sections, particularly in areas where uncertainty exists between CSD test hole locations. An example of this is where Burchett (1986) maps an isolated feature of *To* in the LENRD, but where little evidence of this feature is revealed in the AEM data or CSD test hole logs (see section 5.3.2.1 for further discussion).

Based on the experience and knowledge gained from this effort, the following preliminary recommendations are presented to guide future investigations in support of groundwater characterization and management in eastern Nebraska. They are as follows:

- **Additional AEM surveys can now be conducted in areas where the reconnaissance survey located potentially extensive zones of sand-rich, principal aquifer materials and/or resistive intervals in the *Kd*. Examples of these locations include, but are not limited to**:
    - The 200 ft thick interval of sand-rich material greater than 50 ohm-m between Maple Creek and the Elkhorn River in the southeast corner of the LENRD. It is likely that this feature extends northward from flight line 101701 and possibly southward into the LPNNRD;
    - A resistive feature in the northern PMRNRD that appears on the northern edge of flight line 202001, and to assess if it is connected to a similar resistive feature in flight line 201901;
    - Areas of the eastern LCNRD to determine the extent and character of resistive bodies identified in flight lines 201301 and 201801;
    - The character of the Elkhorn River valley aquifer materials where sand-rich intervals are present. A survey of this valley at a tightly-spaced flight line pattern could help identify and assess surface water-groundwater connection, and possibly assess where the bedrock fracture systems in the underlying *Kn* are in hydraulic connection with the overlying Quaternary system;
    - The area beneath Sarpy County in the PMRNRD (south of the Omaha metropolitan area) where extensive principal Quaternary aquifer material exceeding 100 ft in thickness and is sand-rich (>50 ohm-m) in places overlies resistive *Kd*, much of which was detected by the AEM with resistivities greater than 40 ohm-m. The area is generally undeveloped and would provide a greater understanding of the nature of the *Kd* and its hydrologic connection with the overlying Quaternary deposits. The Quaternary material in this area

is likely in hydrologic connection with the Platte River, and a densely-spaced grid of flight lines would provide a greater understanding of the connection of aquifer deposits and the Platte River in this area. In the far southeast area of Sarpy County, the Union Fault within the Paleozoic strata directly underlies the Platte River valley. A more refined grid of AEM data could provide greater detail in the nature of this fault beneath the area.

- **The connectivity between groundwater and surface water features along the streams and rivers within the project area is not well understood at all locations, particularly in areas where high densities of irrigation wells exist.** The addition of a near-surface, high resolution AEM streambed mapping program of the riparian area is recommended. This data would provide finer detail of the lithology of these critical areas, and more precisely characterize the extent and shape of the aquifers and aquitards that affect hydrologic connection to streams.

- **For locations where the topic of investigation involves localized aquifer features, denser grid spacing is recommended, on the order of 600 to 1,500 ft separation.** Surveys of this scale will allow for creation of 3D voxel models of aquifer materials, from which calculations of aquifer volume and groundwater in storage can be made, which can provide NRD managers greater insight into the quantity of groundwater available in the area of interest.

- **A CSD test hole program that includes penetration through the *Kd*, ideally in the areas where the most extensive resistors were detected in the AEM survey.** Following drilling and lithologic analysis, water quality testing and assessment of potential well yield via aquifer tests is recommended. It is suggested that future test hole sites be selected with knowledge gained from the AEM survey.

- **The AEM survey identified areas along the flight lines where a greater probability of groundwater recharge is likely to occur. A high resolution AEM survey of these areas would quantify the geographic extent of these areas and the hydrologic connection to the subsurface.** This information could then be applied to specifically site recharge studies in known locations that provide the greatest benefit to understanding the meteoric contribution to the water balance of locations of interest within the ENWRA area.

- **Utilize aquifer characterization techniques in conjunction with the AEM survey flight lines to improve the understanding of important changes in hydraulic conductivity, storage, and yield.** This information can then be used directly with future groundwater modeling endeavors to improve model calibration and predictive capability.

6 Description of Data Delivered

The geophysical and borehole electronic data are included as Appendix 4. Electronic interpretation results are also included.

Table 6-1 describes the data columns in the .xyz file 20141126_345_Nebraska_ENWRA1_XRI.xyz. This file contains the raw geophysical data, including magnetic, as supplied directly from SkyTEM. The result of the SCI is included in xyz files and ENWRA2014_SCIresults.xyz and the data columns of these databases are described in Table 6-2. The borehole data used to constrain the SCI inversion and to assist in the interpretation of the inversion results are included in the files listed in Table 6-3. Each type of borehole information has both a collar file containing the location of each of the wells, and a second file containing the borehole data for the individual wells. The data column descriptions for the collar files are listed in Table 6-4.

Table 6-5 describes the channels in all of the borehole data files as well as indicates which type of data contains each channel. The various interpretation results are included in data files ENWRA_north_AEMData_Interpretation.xyz. Table 6-6 describes the data columns of those files.

In addition to the data delivered in .xyz format, Google Earth .kmz files were created to view the geophysical AEM flight line locations, and interpreted geologic data. Unique .kmz files were created for each individual flight line, as well as a .kmz file for all flight lines. Within the .kmz file, the AEM flight line is shown, as well as place marks at each location where there are interpreted geologic results. The attribute data for each unique place mark contains information, including the top elevations of various geologic units, the presence of aquifer material, and the top elevation of the water table. These .kmz files are located within the "ENWRA_2014" folder. The file "read_me.txt" provides instructions in regards to the "Settings" changes that may need to be made in Google Earth, and how to use the .kmz files in Google Earth. A Microsoft Word document is also included, which serves as a legend for the attributes in the .kmz files.

Table 6-1: Channel name, description, and units for 20141126_345_Nebraska_ENWRA1_XRI.xyz with EM, mag, DGPS, Inclinometer, altitude, and associated data.

Parameter	Description	Unit
FID	Unique Fiducial Number	Seconds
LINE	Line Number	LLLLLL
FLIGHT	Name of Flight	yyyymmdd.ff
DATETIME	DateTime Format	Decimal days
DATE	DateTime Format	yyyymmdd
TIME	Time	hhmmss.sss
ANGLEX	Angle (in flight direction)	Degrees
ANGLEY	Angle (perpendicular to flight direction)	Degrees
HEIGHT	Filtered Height Measurement	Meters [m]
LON	Longitude, WGS84	Decimal Degrees
LAT	Latitude, WGS84	Decimal Degrees
E	Easting, NAD83 UTM Zone 13N	Meters [m]
N	Northing, NAD83 UTM Zone 13N	Meters [m]
DEM	Digital Elevation	Meters [m]
ALT	DGPS Altitude	Meters above sea level
GDSPEED	Ground Speed	Kilometers/hour [km/h]
CURR_2	Current, Low Moment	Amps
CURR_1	Current, High Moment	Amps
LMZ_G01	Normalized (PFC-Corrected) Low Moment Z-RxCoil value	pV/(m^4*A)
HMZ_G01	Normalized (PFC-Corrected) High Moment Z-RxCoil value	pV/(m^4*A)
LMX_G01	Normalized (PFC-Corrected) Low Moment X-RxCoil value	pV/(m^4*A)
HMX_G01	Normalized (PFC-Corrected) High Moment X-RxCoil value	pV/(m^4*A)
BMAG_RAW	Raw Base Station Mag Data	nanoTesla [nT]
DIURNAL	Diurnal Mag Data	nanoTesla [nT]
MAG_RAW	Raw Mag Data	nanoTesla [nT]
MAG_COR	Mag Data Corrected for Dirurnal Drift	nanoTesla [nT]
PLNI	Power Line Noise Intensity monitor	C*V/sqrt(Hz)
X_ft	Easting, NAD83 UTM Zone 13N	Feet [ft]
Y_ft	Northing, NAD83 UTM Zone 13N	Feet [ft]

Table 6-2: Channel name, description, and units for ENWRA2014_SCIresults.xyz with EM inversion results.

Parameter	Description	Unit
X_ft	Easting NAD83, UTM Zone 14	Feet [ft]
Y_ft	Northing NAD83, UTM Zone 14	Feet [ft]
X_m	Easting NAD83, UTM Zone 14	Meters [m]
Y_m	Northing NAD83, UTM Zone 14	Meters [m]
TOPO	Topography	Feet [ft]
FID	Unique Fiducial Number	
LINE	Line Number	
ALT	Altitude	Feet [ft]
INVALT	Inverted Altitude	Feet [ft]
INVALTSTD	Inverted Altitude Standard Deviation	
DELTAALT	Change in Altitude	Feet [ft]
NUMDATA	Number of data points	
RESDATA	Residual of individual sounding	
RESTOTAL	Total residual for inverted section	
DOI_LOWER	Less conservative estimate of DOI	Feet [ft]
DOI_UPPER	More conservative estimate of DOI	Feet [ft]
RHO_I_1 THROUGH RHO_I_30	Inverted resistivity of each later	Ohm-m
RHO_I_STD1 THROUGH RHO_I_STD2	Standard deviation of inverted resistivity	
SIGMA_I_1 THROUGH SIGMA_I_30	Conductivity	mS/m
DEP_BOT_1 THROUGH DEP_BOT_29	Depth to the bottom of individual layers	Feet [ft]
DEP_TOP_1 THROUGH DEP_TOP_30	Depth to the top of individual layers	Feet [ft]
THK_1 THROUGH THK_30	Thickness of individual layers	Feet [ft]

Table 6-3: Files containing borehole information.

Database	Description
CSD-E-logs_Collar.xyz CSD-E-logs_data.xyz	Electrical logs from CSD wells
CSD-GEO-logs_Collar.xyz CSD-GEO-logs_data.xyz	Geophysical logs from CSD wells
CSD-LITH_Collar.xyz CSD-LITH_from_to.xyz	Lithology logs from CSD wells
CSD-STRAT_Collar.xyz CSD-STRAT_from_to.xyz	Stratigraphy logs from CSD wells
GP-logs-inv-constrain_Collar.xyz GP-logs-inv-constrain_data.xyz	Geophysical logs used to constrain the SCIs
OandG-GP-logs_Collar.xyz OandG-GP-logs_data.xyz	Geophysical logs from the oil and gas wells
OandG-LITH_Collar.xyz OandG-LITH_from_to.xyz	Lithology logs from the oil and gas wells
OandG-STRAT_Collar.xyz OandG-STRAT_from_to.xyz	Stratigraphy logs from the oil and gas wells

Table 6-4: Channel name, description, and units for collar files.

Parameter	Description	Unit
DH_Hole	Name of individual boreholes	
DH_East	Easting of boreholes, NAD83, UTM Zone 14	Feet [ft]
DH_North	Northing of boreholes, NAD83, UTM Zone 14	Feet [ft]
DH_RL	Elevation of top of borehole	Feet [ft]
DH_Dip	Dip of borehole	Degrees
DH_Azimuth	Azimuth of borehole	Degrees
DH_Top	Depth to top of borehole	Feet [ft]
DH_Bottom	Depth to bottom of borehole	Feet [ft]
DH_ZMin	Minimum elevation in borehole	Feet [ft]
DH_ZMax	Maximum elevation in borehole	Feet [ft]

Table 6-5: Channel name description and units for borehole data.

Parameter	Description	Unit	Type of Log
DH_East	Easting of boreholes, NAD83, UTM Zone 14	Feet [ft]	All
DH_North	Northing of boreholes, NAD83, UTM Zone 14	Feet [ft]	All
DH_RL	Elevation of top of borehole	Feet [ft]	All
DH_From	End of interval	Feet[ft]	Strat, Lith
DH_To	Start of interval	Feet [ft]	Strat, Lith
DH_Strat_Code	Code used to indicate type of stratigraphy		Strat
DH_Soil_Code	Code used to indicate type of lithology		Lith
DH_Description	Description of stratigraphy or lithology		Strat, Lith
DH_Depth	Depth	Feet [ft]	GP
DH_SP	Self Potential	milliVolt [mV]	GP, E, Geo
DH_SN	Short Normal Resistivity	Ohm-m	GP
DH_SFL	Spherically Focus Log	Ohm-m]	GP
DH_ILD	Induction Log Deep	Siemens/m [S/m]	GP
DH_ILM	Induction Log Medium	Siemens/m [S/m]	GP
DH_LAT	Laterolog	Ohm-m	GP
DH_Res	Resistivity	Ohm-m	Constrain, E
DH_Nat_Gam	Natural Gamma	Counts	Geo
DH_Res_SnglPt	Resistivity Single Point	Ohm-m	Geo
DH_Res_16	Resistivity 16in	Ohm-m	Geo
DH_Res_64	Resistivity 65in	Ohm-m	Geo
DH_Res_Lat	Res Laterolog	Ohm-m	Geo
DH_SP_Cond	Self Potential Induction	milliVolt [mV]	Geo
DH_Res_FL	Resistivity of the fluid	Ohm-m	Geo
DH_Tmp_FL	Temperature of the fluid	Degrees F	Geo
DH_Del_Tmp	Change in temperature of the fluid	Degrees F	Geo

Table 6-6: Channel name description and units for the interpretation results file.

Parameter	Description	Unit
X_ft	Easting NAD83, UTM Zone 14	Feet [ft]
Y_ft	Northing NAD83, UTM Zone 14	Feet [ft]
Z_ft	Topography at 1000ft sampling (NAVD 1988)	Feet [ft]
Distance	Down line distance from start of flight line	Feet [ft]
RHO_I[1] through RHO_I[29]	Inverted resistivity of each later	Ohm-m
DEP_BOT[1] through DEP_BOT[29]	Depth to the bottom of individual layers	Feet [ft]
DEP_TOP[1] through DEP_TOP[29]	Depth to the top of individual layers	Feet [ft]
RESDATA	Residual of individual sounding	NA
RESTOTAL	Total residual for inverted section	NA
DOI_LOWER	Less conservative estimate of DOI	Feet [ft]
DOI_UPPER	More conservative estimate of DOI	Feet [ft]
WT_1995	Elevation of the top of the water table from the Nebraska School of Natural Resources Configuration Report, 1995.	Feet [ft]
Bedrock	Elevation of interpreted bedrock surface	Feet [ft]
PrincipalAquifer_Top	Elevation of top of principal aquifer material (>20 ohm-m)	Feet [ft]
CoarseAquifer_Top	Elevation of top of coarse aquifer material (>50 ohm-m)	Feet [ft]
PrincipalAquifer_Bot	Elevation of bottom of principal aquifer material (>20 ohm-m)	Feet [ft]
CoarseAquifer_Bot	Elevation of bottom of coarse aquifer material (>50 ohm-m)	Feet [ft]
To	Elevation of the top of the Tertiary Ogalla Group.	Feet [ft]
Kp	Elevation of the top of the Cretaceous Pierre shale.	Feet [ft]
Kn	Elevation of the top of the Cretaceous Niobrara Formation.	Feet [ft]
Kc_Kgg	Elevation of the top of the Cretaceous Carlile Shale.	Feet [ft]
Kd	Elevation of the top of the Cretaceous Dakota Formation.	Feet [ft]
P	Elevation of the top of the Paleozoic Strata.	Feet [ft]
*	No data or unit not detected	Feet [ft]

7 References

Abraham, J. D., Carney, C.P., and J. C. Cannia. 2013. Data Report on Mapping the Hydrogeology of the Clarkson Area within the Lower Elkhorn Natural Resources District Using an Airborne Electromagnetic Survey. Project findings report prepared for the Lower Elkhorn Natural Resources District.

Abraham, J. D., Bedrosian, P.A., Asch, T.H., Ball, L.B., Cannia, J. C., Phillips, J.D., and S. Olafsen-Lackey. 2011. Evaluation of Geophysical Techniques for the Detection of Paleochannels in the Oakland Area of Eastern Nebraska as Part of the Eastern Nebraska Water Resource Assessment. U.S. Geological Survey Scientific Investigations Report 2011-5228.

Bankey, V., Cuevas, A., David, D., Finn, C.A., Hernandez, I., Hill, P., Kucks, R., Miles, W., Pilkington, M., Roberts, C., Roest, W., Rystrom, V., Shearer, S., Snyder, S., Sweeney, R., Velez, J., Philips, J.D., and D. Ravat. 2002. Digital data grids for the magnetic anomaly map of North America. U.S. Geological Survey Open-File Report 02-414, Denver, CO: U.S. Geological Survey.

Bentall, R. 1971. Water supplies and the land, the ELkhorn River Basin of Nebraska; Lincoln. University of Nebraska-Lincoln Conservation and Survey Division Resource Atlas No. 1.

Burchett, R. R. 1986. Bedrock geology of Nebraska. University of Nebraska-Lincoln, School of Natural Resources. http://snr.unl.edu/data/geographygis/NebrGISgeology.asp#bedrock (accessed Jan 8, 2015).

Carney, C. P., Pierce, K.S., Abraham, J. D., Steele, G.V., Genco, A.G., and J. C. Cannia. 2014. Hydrogeologic Assessment and Framework Development of the Aquifers beneath the Brainard-Valparaiso Area of the Lower Platte South Natural Resources District in Eastern Nebraska. Available online at: http://www.enwra.org/downloads.html.

Christensen, N. B., Reid, J.E. and M. Halkjaer. 2009. Fast, laterally smooth inversion of airborne time-domain elecromagnetic data. Near Surface Geophysics, p. 599-612.

Christiansen, A. V., and E. Auken. 2012. A global measure for depth of investigation.. Geophysics.Vol. 77, No. 4, WB171-177.

Condra, G. E., and C. E. Reed. 1959. The geolgogical section of Nebraska with current revisions by C.E. Reed. Nebraska Geological Survey Bulletin, Lincoln, Nebraska: University of Nebraska-Lincoln, Consevation and Survey Division.

Diffendal, R. F. 1995. Geology of the Ogallala/High Plains regional aquifer system in Nebraska, field trip No.6 in Geological Society of America. Annual Meetings of the North-Central and South Central Sections.

Divine, D. P. 2012. Geologic cross section across eastern Nebraska from Pierce County to Dakota County. Correlations and Cross Sections, Conservation and Survey Division, School of Natural Resources, Institute of Agriculture and Natrual Resources, University of Nebraska-Lincoln.

Divine, D. P. and J. T. Korus. 2012. Eastern Water Resources Assessment. Three-dimensional Hydrostratigraphy of the Sprague Nebraska Area: Results from Helicopter Electromagnetic (HEM) Mapping in the Eastern Nebraska Water Resources Assessment (ENWRA), http://www.enwra.org/media/2012ENWRA_Sprague_final.pdf (accessed Jan 8, 2015).

Divine, D. P., Joeckel, R.M., Korus, J.T., Hanson, P.R., and S. Olafsen-Lackey. 2009. Eastern Nebraska Water Resources Assessment, Introduction to Hydrogeological Study. University of Nebraska-Lincoln, School of Natural Resources, Conservation and Survey Division.

Divine, D. P., Ross, S., and J. Korus. 2010. Compilation of Geologic Cross Sections of Eastern Nebraska. Open-File Report 109, Lincoln, Nebraska: School of Natural Resources, University of Nebraska-Lincoln.

Elder, J. A., Dreezen, V. H., and E. C. Weakly. 1951. University of Nebraska-Lincoln, School of Natural Resources. Topographic Regions of Nebraska. Available online at: http://snr.unl.edu/data/geographygis/NebrGISgeology.asp#topography

Ellis, M. J. 1984. Overview of the Dakota aquifer system in Nebraska, in Jorgensen, D.G. and Signor, D.C., eds., Geohydrology of the Dakota aquifer. National Water Well Association Proceedings, 48-55.

Exploration Resources International Geophysics, LLC. 2015. Airborne Electromagnetic Geophysical Surveys and Hydrogeologic Framework Development for Selected Sites in the Lower Elkhorn Natural Resources District. Project findings report prepared for the Lower Elkhorn Natural Resources District.

Flowerday, C. A., Kuzelka, R. D., and D. T. Pederson. 1998. The Groundwater Atlas of Nebraska. Resorce Atlas No. 4A, Lincoln, Nebraska: Conservation and Survey Division, School of Natural Resoirces, Institute of Agriculture and Natural Resoruces, University of Nebraska-Lincoln.

Foged, N., Auken, E., Christiansen, A.V., and K.I. Sorensen. 2013. Test-site calibration and validation of airborne and ground based TEM systems. Geophysics 78, No.2, E95-E106.

Fredrick, B. S., Linard, J.I., and J. L. Carpenter. 2006. Environmental setting of Maple Creek watershed Nebraska. Scientific Investigations Report 2006-5037, U.S. Geological Survey.

Gates, J. B., Steele, G.V., Nasta, P. and J. Szilagyi. 2014. Lithologic influenes on groundwater recharge through incised glacial till from profile to regional scales: Evidence from glaciated Eastern Nebraska. Water Resources 50, 466-481.

Gosselin, D. C., Harvey, F.E., and C. D. Frost. 2001. Geochemical evolution of groundwater in the Great Plains (Dakota) aquifer of Nebraska: implications for the management of a regional aquifer system. Ground Water 31, 98-108.

Gosselin, D. C., Headrick, J., Chen, X., Summerside, S., and R. Tremblay. 1996. Northeast glacial drift area hydrogeologic summary from domestic well-water quality in rural Nebraska. Lincoln, Nebraska: University of Nebraska-Lincoln, Conservation and Survey Division GIM.

Gutentag, E. D., Heilmes, F. J., Krothe, N.C., Luckey, R.R., and J. B. Weeks. 1984. Geohydrology of the High Plains aquifer in parts of Colorado, Kansas, Nebraska, New Mexico, Oklahoma, South Dakota, Texas, and Wyoming. Professional Paper 1400-B, U.S. Geological Survey .

Hanson, P. R., Korus, J.T., and D. P. Divine. 2012. Three-dimensional hydrostratigraphy of the Platte River Valley near Ashland, Nebraska: Results from Helicopter Electromagnetic mapping in the Eastern Nebraska Water Resources Assessment. Bulletin 2, Conservation and Survey Division, School of Natural Resources, Institute of Agricultutre and National Resources, University of Nebraska-Lincoln.

Helgesen, J. O., Leonard, R.B., and R. J. Wolf. 1993. Hydrology of the Great Plains aquifer system in Nebraska, Colorado, Kansas, and adjacent areas. Regional Aquifer-System Analysis—Central Midwest, Professional Paper 1414-E, U.S. Geological Survey.

HydroGeophysics Group Aarhus University. 2011. Guide for processing and inversion of SkyTEM data in Aarhus Workbench, Version 2.0.

HydroGeophysics Group Aarhus University. 2010. Validation of the SkyTEM system at the extended TEM test site.

Johnson, A. I. 1967. Specific yield- Compliation of specific yeilds for various materials. Water- Supply Paper 1662-D, U.S. Geological Survey.

Jorgensen, D. G., Helgesen, J.O, Signor, D.C., Leonard, R.B., Limes, J., and S. C. Christenson. 1993. Analysis of regional aquifers in the central Midwest of the United States in Kansas, Nebraska, and parts of Arkansas, Colorado, Missouri, New Mexico, Oklahoma, South Dakota, Texas, and Wyoming Geohydrologic framework. Professional Paper 1414-B, U.S. Geologic Survey.

Korus, J. T. 2012. Geologic cross section across eastern Nebraska from Thurston County to Pawnee County. Conservation and Survey Division, School of Natural Resources Institute of Agriculture and Natural Resources, University of Nebraska-Lincoln.

Korus, J. T., and R. M. Joeckel. 2011. Generalized geologic and hydrostratigraphic framework of Nebraska 2011, version 2. Conservation and Survey Division, University of Nebraska-Lincoln.

Korus, J. T., Divine, D. P., Hanson, P.R., and J. S. Dilion. 2012. Three geologic cross sections across portions of eastern Nebraska showing Quaternary lithologic units and stratigraphy of uppermost

bedrock. Correlations and Cross Sections, Conservation and Survey Division School of Natural Resources, University of Nebraska-Lincoln.

Korus, J.T., Joeckel, R.M. and Divine, D.P. 2013a. Three-dimensional hydrostratigraphy of the Firth, Nebraska Area: Results from Helicopter Electromagnetic (HEM) mapping in the Eastern Nebraska Water Resources Assessment (ENWRA). Conservation and Survey Division, School of Natural Resources, Institute of Agriculture and Natural Resources, University of Nebraska-Lincoln. Conservation Bulletin 3 (New Series), 100 p.

Korus, J.T., Howard, L.M., Young, A.R., Divine, D.P., Burbach, M.E., Jess, J.M., and D.R. Hallum (with contributions from Diffendal, R.F., and R.M. Joeckel). 2013b. The Groundwater Atlas of Nebraska. Conservation and Survey Division, School of Natural Resources, Institute of Agriculture and Natural Resources, University of Nebraska-Lincoln. 64 p.

Miller, J. A., and C. L. Appel. 1997. Ground water atlas of the United States; Segment 3 Kansas, Missouri, and Nebraska. Hydraulic Atlas 730D, U.S. Geological Survey.

Miller, R. D., Van Horn, R., Dobrovolny, E., and L. P. Buck. 1964. Geology of Franklin, Webster, and Nuckolls Counties, Nebraska Bulletin 1165, http://pubs.er.usgs.gov/publication/b1165 (accessed Mar 20, 2015).

Nebraska Oil and Gas Conservation Commision. 2008. Nebraska Oil and Gas Conservation Commission Data and Publications, http://www.nogcc.ne.gov/NOGCCPublications.aspx (accessed Jan 5, 2015).

Nolan, B. T., Healy, R.W., Taber, P. E., Perkins, K., Hitt, K.J., and D. M. Wolock. 2007. Factors influencing ground-water recharge in the eastern United States. Journal of Hydrology 332, 187-205.

Olafsen-Lackey, S. 2005a. Specific yield of principal aquifer Sioux City Quadrangle, Nebraska. Conservation and Survey Division, School of Natural Resources, University of Nebraska-Lincoln.

Olafsen-Lackey, S. 2005b. Transmissivity of principal aquifer Sioux City Quadrangle, Nebraska. Conservation and Survey Division, School of Natural Resources, University of Nebraska-Lincoln.

Olafsen-Lackey, S., and S. Summerside. 2005. Specific yeild of principal aquifer Fremont and Omaha Quadrangles, Nebraska. Conservation and Survey Division, School of Natural Resources, University of Nebraska-Lincoln.

Panday, S., Langevin, C.D., Niswonger, R.G., Ibaraki, M. and J. D. Hughes. 2013. MODFLOW–USG version 1: An unstructured grid version of MODFLOW for simulating groundwater flow and tightly coupled processes using a control volume finite-difference formulation. U.S. Geological Survey Techniques and Methods, book 6, chap. A45, 66 p.

Peterson, J. A. 1984. Stratigraphy and Sedimentary Facies of the Madison Limestone and Associated Rocks in Parts of Montana, Nebraska, North Dakota, South Dakota and Wyoming. Professional Paper 1273-A, U.S. Geological Survey.

Platt. 2014. Platts McGraw Hill Financial, http://www.platts.com (accessed Oct 2014).

Schamper, C., Auken, E., and K. Sorensen. 2014. Coil response inversion for very early time modelling of helicopter-borne time-domain electromagnetic data and mapping of near-surface Geologic Layers. European Association of Geoscientistis & Engineers, Geophysical Prospecting.

School of Natural Resources University of Nebraska-Lincoln. 2005. Delineation of 2005 land use patterns for the Sate of Nebraska Department of Natural Recorces. http://snr.unl.edu/data/geographygis/NebrGISland.asp#landuse05 (accessed Jan 12, 2015).

Signor, D. C., Helgesen, J.O., Jorgensen, D.G., and R. B. Leonard. 1996. Geohydrology and simulation of steady-state flow conditions in regional aquifer systems in Cretaceous and older rocks underlying Kansas, Nebraska, and parts of Arkansas, Colorado, Missouri, New Mexico, Oklahoma, South Dakota, Texas, and Wyoming. Professional Paper 1414-C, U.S. Geological Survey, http://pubs.usgs.gov/pp/1414c/report.pdf

SkyTEM Airborne Surveys Worldwide. 2012. SkyTEM survey: Mary Creek Canada data report.

SkyTem Airborne Surveys Worldwide. 2015. Appendix A, Specifications of the SkyTEM508 System 60 Hz, http://skytem.com/wp-content/uploads/2015/01/SkyTEM508-60-Hz.pdf (accessed March 18, 2015).

Smith, B.D., Abraham, J.A., Cannia, J.C., Steele, G.V., and P.L. Hill. 2008. Helicopter electromagnetic and magnetic geophysical survey data, Oakland, Ashland, and Firth study areas, Eastern Nebraska, March 2007: U.S. Geological Survey Open-File Report 2008-1018, 16 p.

Smith, B. D., Abraham, J.D., Cannia, J.C., Minsley, B. J., Ball, L. B., Steele, G. V., and M. Deszcz-Pan. 2009. Helicopter Electromagnetic Geophysical Survey Data, Swedeburg and Sprague Areas, Eastern Nebraska. U.S. Geological Survey Open-File Report 2010-1288.

Souders, V. L. 2000. Geologic maps and cross sections showing configurations of bedrock surfaces, Broken Bow 1° x 2° quadrangle, east-central Nebraska. Geologic Investigations Series I–2725, U.S. Geological Survey.

Stanton, J. S., Steele, G. V., and J. R. Vogel. 2007. Occurrence of agricultural chemicals in shallow ground water and the unstaturated zone, northeast Nebraska glacial till, Scientific Investigations Report 2002-04, U.S. Geological Survey.

Stanton, J. S., Peterson, S. M., and M. N. Fienen. 2010. Simulation of groundwater flow and effects of groundwater irrigation on stream base flow in the Elkhorn and Loup River Basins, Nebraska Phase Two. Scientific Investigations Report, U.S. Geological Survey, 78.

Summerside, S., Ponte, M., Dreezen, V.H., Harung, S. L., Khisty, M. J., and J. Szilagyi. 2001. Update and revision of regional 1x2 degree water-table configuration maps for the State of Nebraska. Lincoln, Nebraska: Conservation and Survey Division, Institute of Agriculture and Natural Resoruces University of Nebraska-Lincoln.

Szilagyi, J., and J. Jozsa. 2013. MODIS-Aided statewide net groundwater-recharge estimation in Nebraska. Ground Water 51, 735-744.

Szilagyi, J., Harvey, F. E., and I. F. Ayers. 2005. Regional estimation of total recharge to ground water in Nebraska. Ground Water 43, 63-69.

Tukey, J. W. 1977. Exploratory data analysis, Reading, PA. Addison-Weasley.

U.S. Census Bureau. 2013. Demographic profile, total population. http://factfinder.census.gov/faces/nav/jsf/pages/index.xhtml (accessed Jan 12, 2015).

U.S. Geological Survey, 2015, USGS surface-water data for Nebraska. http://waterdata.usgs.gov/ne/nwis/sw/ (accessed Jan 8, 2015).

United States Department of Agriculture, 2014. USDA Natural Resources Conservation Service. http://www.nrcs.usda.gov/wps/portal/nrcs/detail/oh/technical/dma/gis/?cid=nrcs144p2_029531 (accessed Oct 2014).

University of Nebraska-Lincoln School of Natural Resources. 2014. Nebraska statewide test-hole database. http://snr.unl.edu/data/geologysoils/NebraskaTestHole/NebraskaTestHoleIntro.asp (accessed October 15, 2014).

Viezzoli, A., Christiansen, A. V., Auken, E., and K. Sorensen. 2008. Quasi-3D modeling of airborne TEM data by spatially constrainted inversion.. Geophysics. Vol. 73 No. 3, F105-F113.

Witzke, B.J., and G.A. Ludvigson. 1994. The Dakota Formation in Iowa and the type area, Geological Society of America Special Paper 287.